ENGINEERING THE MORPHOLOGY OF CARBON MOLECULAR SIEVE (CMS) HOLLOW FIBER MEMBRANES

A Dissertation
Presented to
The Academic Faculty

By

Nitesh Bhuwania

In Partial Fulfillment
Of the Requirements for the Degree
Doctor of Philosophy in the
School of Chemical & Biomolecular Engineering

Georgia Institute of Technology

May 2014

ENGINEERING THE MORPHOLOGY OF CARBON MOLECULAR SIEVE (CMS) HOLLOW FIBER MEMBRANES

Approved by:

Dr. William J. Koros, Advisor
School of Chemical & Biomolecular Engineering
Georgia Institute of Technology

Dr. Pradeep K. Agrawal
School of Chemical & Biomolecular Engineering
Georgia Institute of Technology

Dr. Krista S. Walton
School of Chemical & Biomolecular Engineering
Georgia Institute of Technology

Dr. Anselm C. Griffin
School of Materials Science & Engineering
Georgia Institute of Technology

Dr. Paul J. Williams
Shell International Exploration and Production (US) Inc.
Shell Technology Center

Date Approved: December 18th 2013

Dedicated to those I love the most,

my parents, my sister and my wife Vineetha

ACKNOWLEDGEMENTS

The time spend at Georgia Tech has been a wonderful experience for me. There are innumerable people who made an impact during the past four years at GaTech.

I would like to start with my advisor and mentor, Dr. Bill Koros for his continuous support and guidance throughout my work. His energy, enthusiasm and strong work ethic were a great inspiration and a lot to learn from him. He took time in spite of his busy schedule to solve the most trivial problems and shape me both as a researcher and as a person.

I would also like to thank my committee members Dr. Pradeep Agrawal, Dr. Anselm Griffin and Dr. Krista Walton for their valuable comments and insights. I appreciate Dr. Jason Williams (from Shell) willingness to be a part of my thesis committee and share his valuable experience in CMS membranes. His guidance and fruitful discussions during our monthly telecons and update meetings were instrumental for this work. The financial support from Shell Global Solutions is greatly appreciated.

Several people have played a key role in completion of this work. I would like to thank Dr. Ying Labreche for the help in analyzing NMR characterization results. I appreciate the valuable time of Steven Burgess towards analyzing DMA results and also helping me towards the formulation of the thesis. Our squash session and coffee-breaks will be missed. I was fortunate to have a good friend and office mate in Dr. Carine Achoundong. Our technical discussions were important for developing the mechanism of the methods in this work. Special thanks to Dr. Jose Baltazar for not only being a good friend in need but also taking time to run and analyze the XPS data in this work. The time spend together in our discussion towards both technical and non-technical will be missed.

I acknowledge Anurag Rajagopal's time for proof-reading my thesis and also being a great apartment mate throughout my stay at Georgia Tech. His willingness to always lend a helping-hand whenever I needed is greatly appreciated.

Koros group members, past and present were not only helpful colleagues but also good friends as well. I would like to thank my collaborators under Shell funding Dr. Oguz Karvan, Ruben Kemmerlin and Shweta Karwa for their support. Dr. Dhaval Bhandari, Dr. Mayumi Kiyono, Dr. Liren Xu, Dr. Meha Rungta and Dr. Kuang Zhang have been wonderful senior students who taught me a lot of basics and patiently answered my questions. Dr. Brian Kraftschik, Xue Ning and Chen Zhang were excellent batchmates and bright researchers whom I will always admire. Lucy Lu, Shilu Fu, John Hesseler, Dr. Wulin, Danny Kim, Graham Wenz were all good colleagues and were always there to discuss research ideas. Thanks to Ms. Michelle Martin for being friendly and processing last minute supply orders.

I have always been fortunate to have good friends who have been present during good and more importantly tough times. I will always cherish and remember my friendship with Deepraj, Dr. Medina Ramos, Andac, Pramod, Prashant, Prabuddha, Dhaval Patel, Ambar, Tanu, Gautami, Rohan, Pradnya and Jaya. I can never return all the favors and sacrifices they have made for me.

I wish to thank my dearest parents for their unconditional love and support throughout my life. Despite being far away from me, their thoughts and prayers were always felt. My sister and brother-in-law are thanked for their love and encouragement.

Last but definitely not the least; I would also like to thank my wife Vineetha Bhuwania without whom this day would not have been possible. She has been my support system through the time I have known her and had constantly pushed me all these four years to do my best.

I am sure to have forgotten many names that have had a big impact and would whom this work was not possible. Thank you all!

TABLE OF CONTENTS

LIST OF TABLES

LIST OF FIGURES

SUMMARY

Carbon Molecular Sieve (CMS) membranes have a potential to achieve attractive gas separation properties. CMS membranes in dense film configuration have shown promising results. Hence, for industrial application it's important to translate this high performance in hollow fiber configuration. The key shortcoming in CMS hollow fiber fabrication has been the *collapse of porous suppor*t resulting in lower gas separation productivities.

Therefore, the goal of this study was to prevent the collapse in CMS hollow fibers by a process called as *V-Treatment.* The V-Treatment process uses the sol-gel reaction mechanism between organic-alkoxy silane (i.e. Vinyltrimethoxy Silane – VTMS) and moisture. The sol-gel reaction proposed in this study is a first-of-a-kind approach in asymmetric CMS membranes to create porous morphologies, and it can be easily integrated into the current asymmetric CMS membrane fabrication process. The V-treatment technique enables restricting the microscale morphology collapse in asymmetric CMS membranes without having a chemical reaction with the polymer precursor material. The effect of V-treatment is reported on two different polyimide precursors: Matrimid® and 6FDA:BPDA-DAM. Several characterization analyses are evaluated to understand the mechanism of V-treatment in restricting sub-structure collapse.

The optimization of the V-treatment process is crucial for obtaining better separation performance. The V-treatment optimization in terms of the VTMS concentration, and the final pyrolysis temperature for V-treated asymmetric Matrimid®

CMS hollow fiber membranes are performed. After evaluating the VTMS concentration for six different concentrations, an optimum amount for the *highest* increase in CMS gas permeance was found for the 10% VTMS in hexane. The preference for hexane as a non-solvent for the VTMS-hexane combination of V-treatment is due to the existing post spinning solvent exchange process. The novelty of using hexane for V-treatment allows direct "drop in" integration into current fiber precursor processing. The potential of optimized V-treatment for Matrimid® based CMS hollow fiber membrane is evaluated for industrially relevant mixed gas pairs (CO_2/CH_4, C_2H_4/C_2H_6 and C_3H_6/C_3H_8), which consistently showed an increase in gas permeances for all the gas separation pairs. In addition the importance of the pendant functional groups (vinyl and methoxy) for V-treatment are also discussed.

For the commercial application of 10% V-treated asymmetric CMS Matrimid® membranes, the separation performance stability under three different conditions (i) active mixed gas feed (ii) stored in pure gas CO_2 at 5-6 atm pressure and (iii) stored in ambient air is evaluated.

CHAPTER 1

INTRODUCTION

1.1 Membrane-based gas separation

Membrane-based separation processes have the ability to outperform thermally driven approaches by demonstrating significant reduction in energy consumption [1, 2]. Several key advantages for membrane processes include: small installation foot-print leading to low capital and operational cost, easy adaptability, low maintenance cost and environmental friendliness. Membranes in the liquid separation field have shown great benefits, as they reduce the energy costs by over an order of magnitude after displacing the traditional thermal separation units [1, 3]. The ability of membranes to selectively remove one component over other is being translated to large-scale gas separations. The membrane market for gas separation is envisioned to steadily increase at an average growth rate of 7-8% per year and expected to reach $760 million by year 2050 [2]. The projected market share is mainly dominated by the natural gas (29%) and refinery/petrochemical (24%) industries. Other membrane-based gas separation fields such as air (21%) and hydrogen (13%) separations are expected to continue their current demand.

The major separation in natural gas involves removal of condensable gases (such as carbon dioxide (CO_2) and hydrogen sulfide (H_2S)), nitrogen (N_2) and higher hydrocarbons (C_{3+})) from the methane (CH_4) stream [2, 4]. CO_2 is the most abundant impurity in raw natural gas and is expected to be less than 2% before it is pumped into the pipelines. The other emerging membrane-based separation market in

refinery/petrochemical field is the separation of olefins and paraffins [3, 5, 6]. Currently, these separation markets are dominated by energy intensive processes such as amine absorption [4] for natural gas (CO_2 removal from CH_4) and cryogenic distillation [7] for olefin/paraffin separation. A hybrid membrane separation unit can offer an attractive cost-reducing advantage as they are easy to integrate with the current process and requires a small foot print. A simplified hybrid membrane-current separation process plant for both the separations is shown in Figure 1.1.

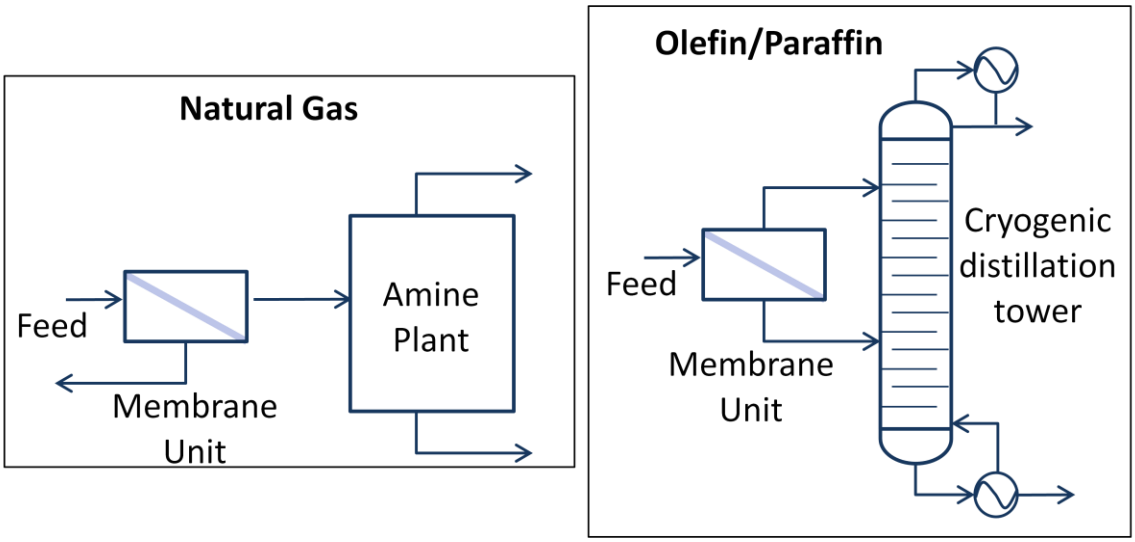

Figure 1.1: Schematic of hybrid membrane separation plants for natural gas and olefin/paraffin separations [4, 8].

The concept of hybrid membrane-amine absorption separation plant has already started to be applied in the natural gas industry by using polymer membranes [4]. The trade-off with polymer membranes are the performance limitations: being restricted only under certain natural gas feed conditions. Whereas for the case of olefin/paraffin separation, polymer membranes lack the ability to provide required minimum separation

efficiency [5, 9]. Hence it is important to develop advanced materials for these separations, which is the focus of this study.

1.2 Membrane technology

To develop membrane technologies for challenging separations, it is important to simultaneously consider four key elements [1]. Figure 1.2 summarizes the four enabling elements essential to develop a new or enhance an already existing membrane technology.

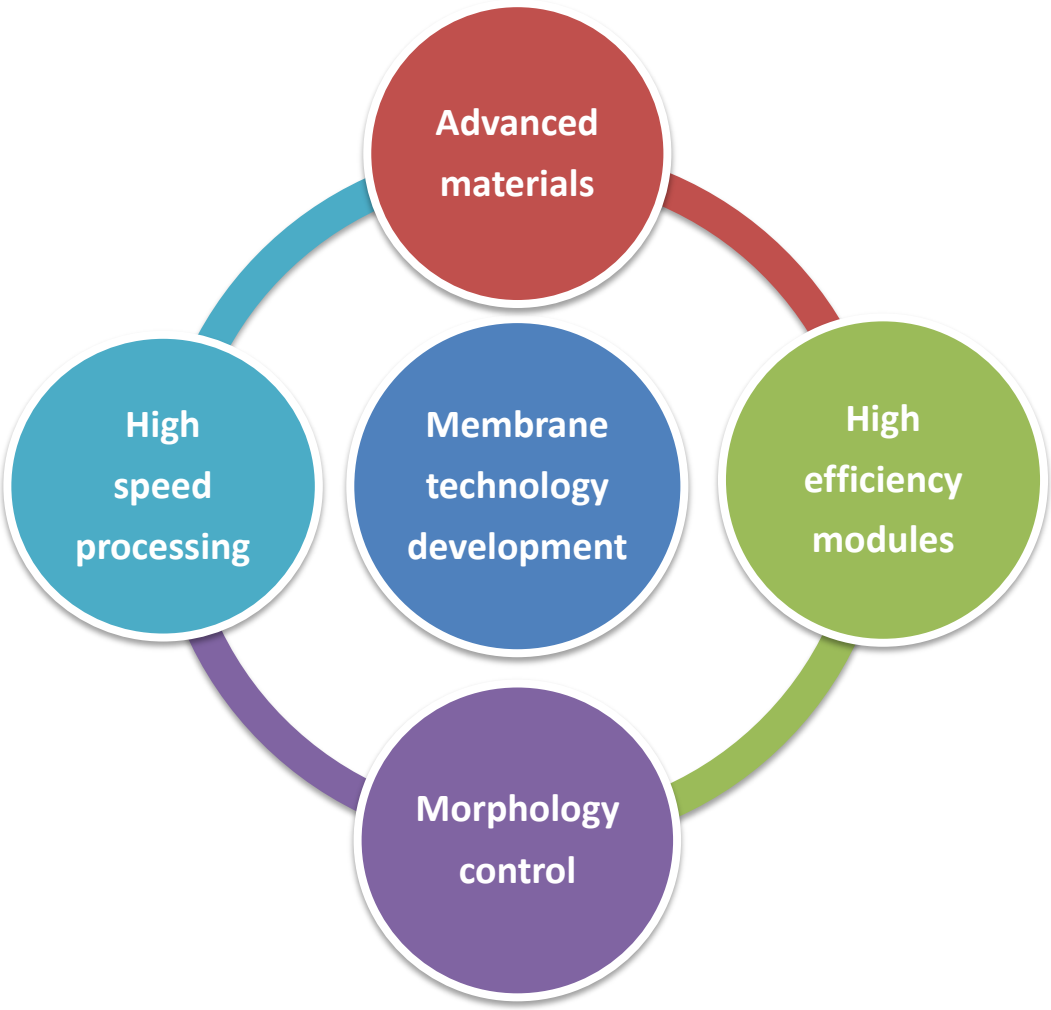

Figure 1.2: Enabling elements for membrane technology development [1].

1.2.1 Advanced materials

Development of advanced materials is a first stepping stone towards achieving the required separation performance. The class of membrane materials being utilized for gas separations can be broadly classified into polymer and inorganic membranes [1]. The separation limitation of polymer membranes arises due to a tradeoff between the productivity and the separation efficiency, as illustrated in Figure 1.3 [10]. The performance limitation of polymer membranes is observed to be much more pronounced for olefin/paraffin (like ethylene (C_2H_4)/ethane (C_2H_6), propylene (C_3H_6)/propane (C_3H_8) and more) compared to CO_2/CH_4 separation [5, 6]. Another draw-back of polymer membranes is the swelling-induced softening of the polymer chains ('plasticization') in presence of condensable gases (like CO_2, C_2H_4 and C_3H_6), which leads to a significant *decrease* in their separation efficiency. The advancement of polymer materials towards crosslinkable polymers is a major breakthrough towards preventing plasticization-induced efficiency loss [3]. Though the crosslinkable polymers are plasticization resistant, in terms of separation efficiency they are still limited by the trade-off curve.

To be cost-competitive with current efficient but energy-intensive amine absorption and cryogenic distillations, it is important to broaden the scope of membranes to inorganic porous materials. The class of inorganic materials which has gained significant importance are the carbon membranes, due to their gas-size sieving capability and relative ease of formation [11].

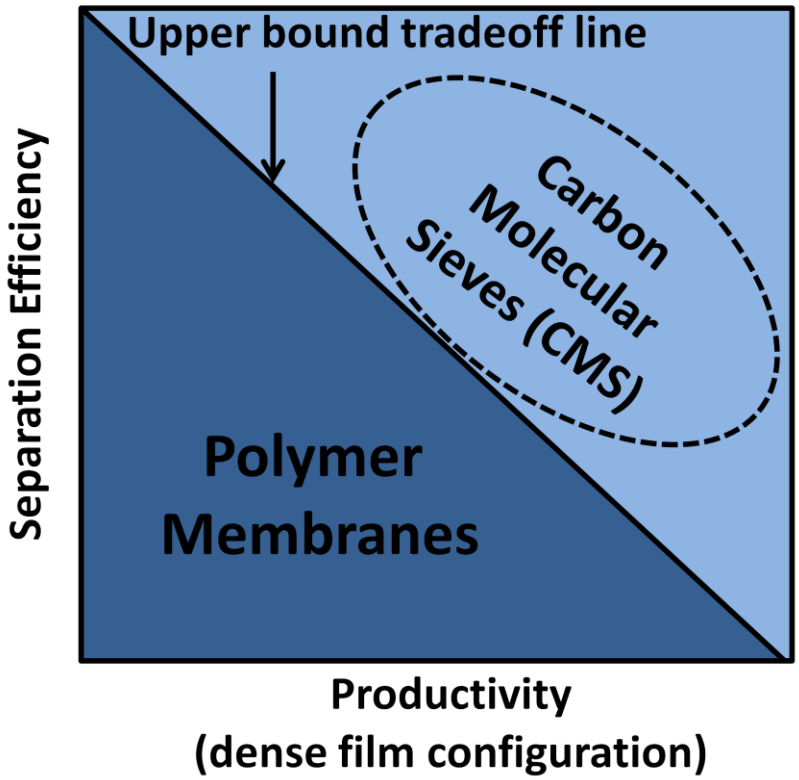

Figure 1.3: Hypothetical polymeric membrane performance trade-off and capability of CMS membranes to surpass that trade-off [6, 10].

1.2.1.1 Carbon molecular sieve (CMS) membranes

The carbon membranes are formed by thermal decomposition of polymer precursors and usually referred to as the carbon molecular sieve (CMS) membranes [11, 12]. CMS membranes have shown great potential in gas separation applications, such as O_2/N_2, CO_2/CH_4, C_2H_4/C_2H_6, C_3H_6/C_3H_8 by surpassing the "polymer upper bound trade-off line" for separation performance [8, 9, 13-15] as shown in Figure 1.3. Because of the rigid structure of CMS membranes unlike polymer membranes, they do not undergo any plasticization instability under condensable feeds [16]. Therefore to make the separation

capability of CMS membranes at an industrial level, the additional enabling elements in Figure 1.2, beyond advanced materials per se, become vital.

1.2.2 High efficiency modules

To meet the required separation productivities of large scale separations, it is essential to develop the membrane modules with large surface area to volume ratio. Different membrane module configurations have been investigated to meet these requirements, which include plate and frame, spiral wound, tubular and hollow fiber module [7, 17]. The hollow fiber membrane configuration is industrially preferred for large scale gas separation, as it can provide significantly higher surface area to volume ratio compared to other membrane configurations (i.e. >10 times compared to spiral wound). The advantage in hollow fiber membrane configuration comes from the asymmetric geometry consisting of thin separation selective layer on a microporous support [3]. The key feature in the asymmetric membrane geometry is the simultaneous formation of microporous and separation selective layer. Hence while developing advanced materials (like CMS), it is important to translate the attractive separation performance (as seen in Figure 1.3) to industrially relevant asymmetric hollow fiber configuration. Therefore, it leads to the third enabling element of membrane technology development, (Figure 1.2) i.e., *Morphology control.*

1.2.3 Morphology control

The engineering of asymmetric morphology in hollow fiber membrane is crucial for maintaining the high separation productivity through the modules [18]. The purpose of a microporous layer in asymmetric morphology (Figure 1.4) is to facilitate the gas

transport without performing any actual separation. They serve as a support for the thin dense separation layer where the actual gas separation happens. Therefore, if any resistance is developed in the microporous support layer, it will have a detrimental effect towards the gas productivity of membrane module.

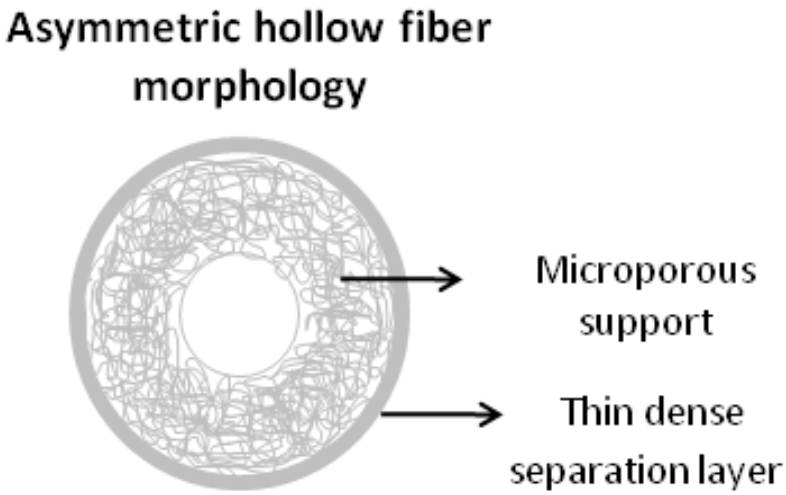

Figure 1.4: Asymmetric hollow fiber morphology illustrating thin dense separation and a microporous support layer [18].

The shortcoming in asymmetric CMS hollow fiber membranes has been the densification of microporous support during the fabrication of asymmetric CMS membranes [19]. Though the CMS hollow fiber membranes can show encouraging separation efficiencies, the gas transport flux (i.e. membrane productivity) has been much lower than expected of the productivity increase in corresponding dense membranes [16, 19] as seen in Figure 1.3. Lower productivity is a major concern for the industrial scalability of CMS hollow fiber membranes, as it will *increase* the net membrane surface area to meet the separation requirement. The *increase* in membrane surface area will also

increase the effective membrane module cost. This off-set in cost advantage of asymmetric CMS hollow fiber membranes is not good if morphology collapse occurs, especially when one of the major advantages of membranes is the desire to reduce the cost of separation.

1.2.4 High speed processing

For the effective development of membrane technology, it is crucial to synchronize all the above elements simultaneously. It is important for achieving the economical feasibility of the membrane process for large-scale separation applications. The cost of industrial-scale CMS hollow fiber membrane module is estimated to be ~$50-100 per m^2 [20]. Inspite of the prediction being 5 times higher than the polymer state-of-art modules [3] (~$10-20/$m^2$), the separation efficiency gain in CMS membranes is still significant and the membrane module cost can be further reduced. The major cost drivers for CMS membrane modules are the fabrication process and the requirement of higher membrane surface area.

Hence, the current hurdle which needs to be addressed is the low membrane productivity of asymmetric CMS hollow fiber membranes. In order to address the commercial viability of asymmetric CMS hollow fiber membranes, the focus of this study is to restrict the densification of porous support (also termed as sub structure collapse) and obtain superior separation performance in terms of gas productivity and separation efficiency.

1.3 Research objectives

The overarching goal of this thesis dissertation is to "Establish a framework to engineer the morphology of the microporous support layer in asymmetric membranes undergoing thermal processing above the glass transition of the intrinsic polymer precursor." In order to achieve this goal, the three objectives of this work are:

Research Objective 1: Methodology to restrict sub-structure collapse in asymmetric CMS hollow fiber membranes (Chapter 4)

This chapter will focus on the mechanism of sub-structure collapse and various methodologies used in an attempt to restrict the collapse. A novel pre-pyrolysis treatment is developed to restrict the morphology collapse in asymmetric carbon molecular sieve (CMS) hollow fiber membranes. The technique is referred to as V-treatment due to the use of a sol-gel crosslinking reaction between an organic-alkoxy silane (vinyltrimethoxysilane) and moisture. The V-treatment technique enables restricting the microscale morphology collapse in asymmetric CMS membranes without having a chemical reaction with the polymer precursor material. The sol-gel reaction proposed in this study is a first-of-a-kind approach in asymmetric CMS membranes to create porous morphologies, and it can be easily integrated into the current asymmetric CMS membrane fabrication process. Several characterization analyses are used to verify the proposed mechanism and obtain insights for further optimization. The effect of V-treatment are presented for two different polyimide precursors Matrimid® and 6FDA:BPDA-DAM.

Research objective 2: Optimization of V-treatment and pyrolysis parameters for superior separation performance in asymmetric CMS hollow fiber membranes (Chapter 5)

This chapter will describe the results of optimization conditions in terms of different VTMS concentration and pyrolysis conditions (varying final pyrolysis temperature and oxygen doping) to obtain superior separation performance. In addition, the importance of both organic and alkoxy functional groups are also explored. The control of VTMS concentration is crucial for V-treatment, as the excessive silica can hamper the intrinsic CMS separation properties. For reducing the VTMS concentration, different polymer non-solvents (Toluene, n-heptane and hexane) are used. VTMS-hexane combination in V-treatment is preferred due to the existing post-spinning solvent exchange process. 10 wt% VTMS in hexane is found to be the optimum amount which maintains both the asymmetric CMS morphology and gives higher gas productivities. Moreover, the novelty of using hexane for V-treatment allows direct "drop in" integration into current fiber precursor processing.

The optimization results are evaluated in terms of separation performance for both pure gas feed and industry relevant mixed-gas pairs (i.e. CO_2/CH_4, C_2H_4/C_2H_6 and C_3H_6/C_3H_8) at 35°C.

Research Objective 3: Realistic evaluation of V-treated CMS hollow fiber membrane for natural gas separation (Chapter 6)

This chapter will evaluate some critical points for the commercial viability of CMS membranes for industrial scale-ups. In the pyrolysis process, when untreated polymer precursor fibers are pyrolysed in bundles they adhere to each other making them

unusable as CMS membranes. Individually separating each fiber during pyrolysis can add additional processing and labor cost. In addition to improved permeances, V-treatment offers a key advantage of 'anti-stickiness' to the asymmetric CMS fibers from V-Treated Matrimid® precursor. Presence of silica on the outer layer of V-Treated fibers assists in the 'anti-stickiness' property. This offset of 'stickiness' do not arise for 6FDA based precursors, as even the untreated 6FDA precursor fibers were seen to be separable after pyrolysis.

Recent studies on CMS hollow fiber membranes have observed similar aging phenomena as seen in glassy polymer membranes. The predicted mechanism for aging in CMS membranes is complex; it varies from each gas pair and has a strong relationship with storage/testing conditions. This section will include time-dependent separation performance tests for V-Treated CMS membranes from Matrimid® precursor. The stability of the membranes is evaluated for aggressive feed gas conditions containing 50% CO_2/50% CH_4. The aging study is performed under three different conditions (i) active mixed gas feed (ii) stored in ambient air and (iii) dry CO_2.

1.4 Dissertation organization

This dissertation is organized into seven chapters including this chapter. Chapter 2 contains background information pertaining to gas transport in CMS membranes. The chapter also includes a literature review on CMS membranes. Chapter 3 covers the materials, equipments and characterization techniques used in this study. Chapter 4 describes the mechanism of sub-structure collapse in asymmetric CMS membranes and various methodologies which attempt to restrict collapse. The chapter will introduce a

novel pre-pyrolysis approach termed as 'V-treatment' to improve the sub-structure pore morphology of CMS hollow fiber membranes from Matrimid® and 6FDA:BPDA-DAM precursor material. Chapter 5 presents the effect of different fabrication parameters on the separation performance of CMS hollow fiber membrane from V-treated precursors. Chapter 6 evaluates the performance stability of CMS V-treated hollow fiber membrane from Matrimid® precursor under different conditions (i) active mixed gas feed, (ii) stored in dry CO_2, and (iii) in ambient air. Chapter 7 summarizes the key results of this work, along with the recommendations for further study.

For the commercial application of 10% V-treated asymmetric CMS Matrimid® membranes, the separation performance stability under three different conditions (i) active mixed gas feed (ii) stored in pure gas CO_2 at 5-6 atm pressure and (iii) stored in ambient air is evaluated.

1.5 References

1. Koros, W.J., Evolving beyond the thermat age of separation processes: Membranes can lead the way. Aiche Journal, 2004. **50**(10): p. 2326-2334.
2. Baker, R.W., Future Directions of Membrane Gas Separation Technology. Industrial & Engineering Chemistry Research, 2002. **41**(6): p. 1393-1411.
3. Koros, W.J. and R.P. Lively, Water and beyond: Expanding the spectrum of large-scale energy efficient separation processes. Aiche Journal, 2012. **58**(9): p. 2624-2633.
4. Baker, R.W. and K. Lokhandwala, Natural Gas Processing with Membranes: An Overview. Industrial & Engineering Chemistry Research, 2008. **47**(7): p. 2109-2121.
5. Burns, R.L. and W.J. Koros, Defining the challenges for C3H6/C3H8 separation using polymeric membranes. Journal of Membrane Science, 2003. **211**(2): p. 299-309.
6. Rungta, M.; Zhang, C.; Koros, W. J.; Xu, L., Membrane-based ethylene/ethane separation: The upper bound and beyond. Aiche J **2013,** 59 (9), 3475-3489.
7. Robinson S, Jubin R, and C. B., Materials for Separation Technology: Energy and Emission Reduction Opportunities. 2005, US Dept. Of Energy: Washington DC.
8. Xu, L.; Rungta, M.; Brayden, M. K.; Martinez, M. V.; Stears, B. A.; Barbay, G. A.; Koros, W. J., Olefins-selective asymmetric carbon molecular sieve hollow fiber membranes for hybrid membrane-distillation processes for olefin/paraffin separations. J Membrane Sci **2012,** 423–424 (0), 314-323.
9. Rungta, M., L. Xu, and W.J. Koros, Carbon molecular sieve dense film membranes derived from Matrimid® for ethylene/ethane separation. Carbon, 2012. **50**(4): p. 1488-1502.
10. Robeson, L.M., The upper bound revisited. Journal of Membrane Science, 2008. **320**(1-2): p. 390-400.
11. Williams, P.J. and W.J. Koros, Gas separation by carbon membranes. Advanced Membrane Technology and Applications, 2008: p. 599-631.
12. Saufi, S. and A. Ismail, Fabrication of carbon membranes for gas separation—a review. Carbon, 2004. **42**(2): p. 241-259.
13. Steel, K.M. and W.J. Koros, An investigation of the effects of pyrolysis parameters on gas separation properties of carbon materials. Carbon, 2005. **43**(9): p. 1843-1856.
14. Jones, C.W. and W.J. Koros, Carbon molecular sieve gas separation membranes-I. Preparation and characterization based on polyimide precursors. Carbon, 1994. **32**(8): p. 1419-1425.
15. Kiyono, M., P.J. Williams, and W.J. Koros, Effect of polymer precursors on carbon molecular sieve structure and separation performance properties. Carbon, 2010. **48**(15): p. 4432-4441.
16. Vu, D.Q., W.J. Koros, and S.J. Miller, High pressure CO2/CH4 separation using carbon molecular sieve hollow fiber membranes. Industrial & Engineering Chemistry Research, 2002. **41**(3): p. 367-380.
17. Koros, W.J. and G.K. Fleming, Membrane-based gas separation. Journal of Membrane Science, 1993. **83**(1): p. 1-80.

18. Carruthers, S.B., G.L. Ramos, and W.J. Koros, Morphology of integral-skin layers in hollow-fiber gas-separation membranes. Journal of Applied Polymer Science, 2003. **90**(2): p. 399-411.
19. Xu, L., M. Rungta, and W.J. Koros, Matrimid® derived carbon molecular sieve hollow fiber membranes for ethylene/ethane separation. Journal of Membrane Science, 2011. **380**(1-2): p. 138-147.
20. Kiyono, M., Carbon molecular sieve membranes for natural gas separations. Doctor of Philosophy, Georgia Institute of Technology, 2010.
21. Kiyono, M., W.J. Koros, and P.J. Williams, Correlation between pyrolysis atmosphere and carbon molecular sieve membrane performance properties. Vol. 14. 2011: Elsevier: Amsterdam.

CHAPTER 2

BACKGROUND AND THEORY

2.1 Overview

The first half of this chapter explains the fundamentals and gas transport of CMS membranes. The second half of the chapter gives an insight into the fabrication parameters and their effects on the separation performance of asymmetric CMS hollow fiber membranes.

2.2 Structure of CMS membranes

CMS membranes can be formed by the thermal decomposition of polymeric precursor materials under controlled atmospheric conditions. CMS membranes produced by pyrolysis are mostly char, with a turbostatic structure (Figure 2.1(a)) [1, 2]. These materials are amorphous, consisting of disordered sp^2 hybridized condensed hexagonal sheets with pores formed from packing imperfections and an idealized pore structure that can be represented as "slit-like" (Figure 2.1(b)). The pore size distribution has a bi-modal character, with two major divisions: (i) "Micropores" ranging between 7–20 Å and (ii) "Ultramicropores" which are <7 Å (Figure 2.1(c)).

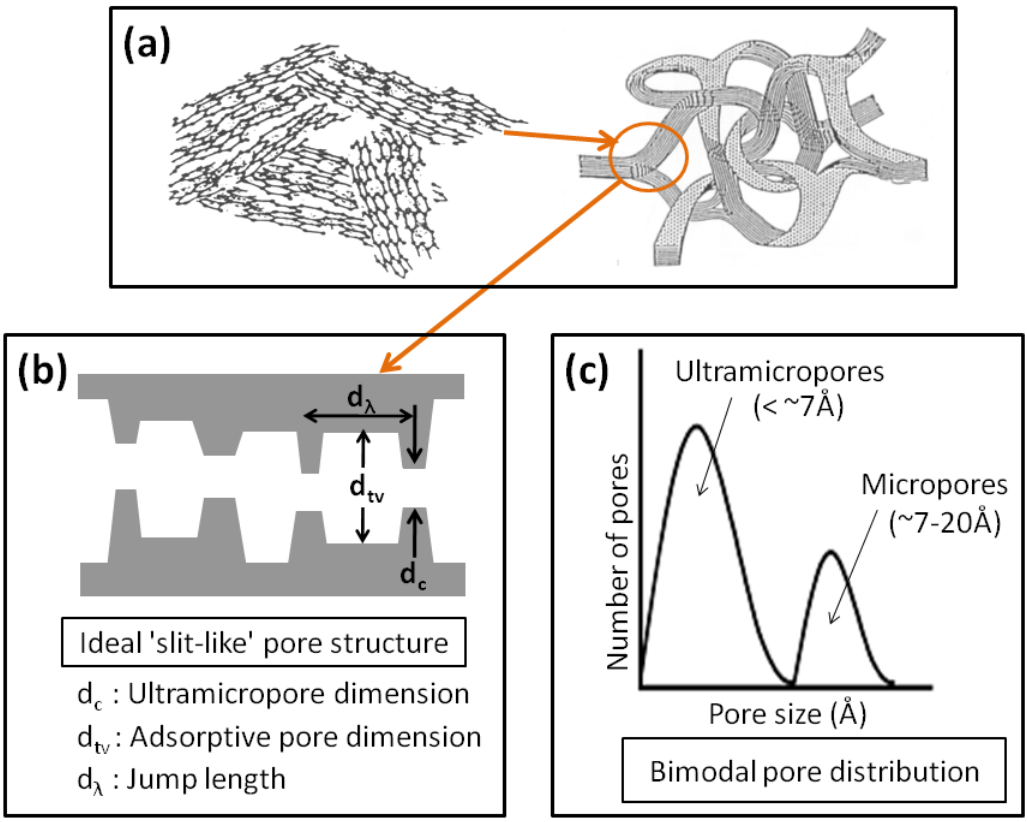

Figure 2.1: (a) Structure of pyrolytic carbon material [1, 2] (b) Idealized pore structure of CMS membrane [3] with (c) Idealized bimodal pore size distribution of CMS membrane [3].

2.3 Transport in CMS membranes

2.3.1 Permeation

Gas transport through carbon molecular sieve membranes occurs by a sorption-diffusion mechanism [4]. Gas molecules sorb into the membrane from upstream side, diffuse through the membrane under a chemical potential gradient and finally desorb on downstream side of the membrane as illustrated in Figure 2.2.

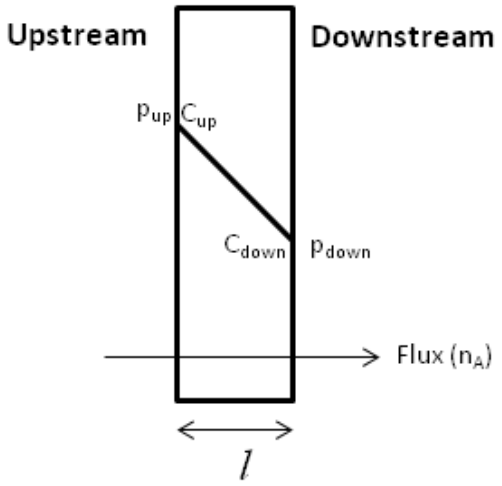

Figure 2.2: Schematic of gas transport through a dense membrane [4].

The performance of membranes is evaluated using two key intrinsic properties, "permeability" and "selectivity". Permeability is a measure of the productivity of a dense film membrane, and is given as the pressure and thickness normalized flux (Equation 2.1) below:

$$P_A = \frac{[n_A][l]}{[\Delta p_A]} \tag{2.1}$$

In equation (2.1), P_A is the permeability of component A through the membrane, n_A is the flux, l is the membrane thickness and Δp_A is the partial pressure difference between the upstream and downstream faces. For mixed gas feed, Δp_A is best replaced by the transmembrane component fugacity difference to account for thermodynamic non-idealities.

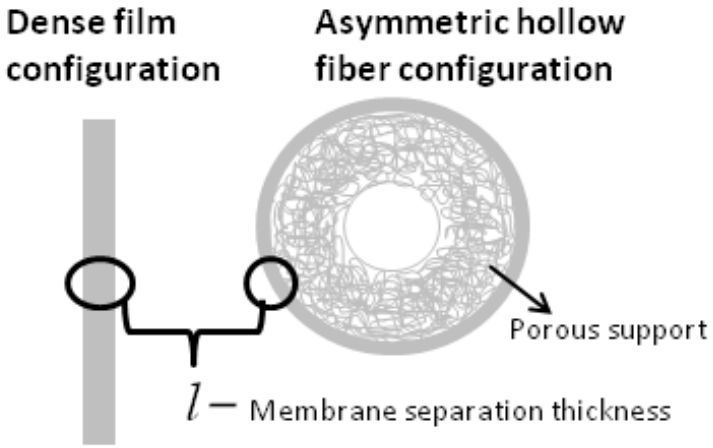

Figure 2.3: Illustration of CMS dense film and asymmetric hollow fiber configuration

For the case of asymmetric hollow fibers (illustrated in Figure 2.3), the actual membrane skin thickness is hard to determine; hence, the productivity is described by the permeance which is the partial pressure (fugacity) normalized flux, viz.:

$$\left(\frac{P_A}{l}\right) = \frac{n_A}{\Delta p_A} \tag{2.2}$$

The units for permeability and permeance are Barrer and GPU (gas permeance unit), respectively:

$$1\,\text{Barrer} = 10^{-10}\,\frac{\left[\text{cm}^3(\text{STP})\right][\text{cm}]}{\left[\text{cm}^3\right][\text{s}][\text{cmHg}]} \qquad 1\,\text{GPU} = 10^{-6}\,\frac{\left[\text{cm}^3(\text{STP})\right]}{\left[\text{cm}^3\right][\text{s}][\text{cmHg}]}$$

The separation efficiency or ideal permselectivity of a membrane with negligible downstream pressure is defined as the ratio of the component permeabilities or permeances i.e.,

$$\alpha_{A/B} = \frac{P_A}{P_B} = \frac{(P/l)_A}{(P/l)_B} \tag{2.3}$$

For mixed gas feeds, when the downstream pressure is negligible compared to the upstream as it is in this study, the selectivity is defined as the separation factor which is the ratio of permeate (y) and feed-side mole fractions (x) corresponding to the components A and B:

$$\alpha_{A/B} = \frac{(y_A / y_B)}{(x_A / x_B)} \tag{2.4}$$

2.3.2 Sorption and Diffusion

Gas permeability can further be represented as the product of kinetic and thermodynamic parameters i.e., the diffusion coefficient (D_A) and the sorption coefficient (S_A):

$$P_A = \left[D_A\right]\left[S_A\right] \tag{2.5}$$

For molecular sieving material like CMS, the sorption coefficient is the pressure normalized uptake membrane concentration of gas at an equilibrium pressure. Sorption coefficients primarily depend on the gas condensability and its interaction with the membrane material. The isotherm can be represented using a Langmuir isotherm, i.e.,

$$S_A = \frac{C_A}{p_A} = \frac{\left[C'_{HA}\right]\left[b_A\right]}{1 + b_A \; p_A} \tag{2.6}$$

In equation (2.6), C_A is the equilibrium uptake of penetrant A by the sorbent, p_A is the partial pressure, C'_{HA} is the Langmuir hole filling capacity and b_A Langmuir affinity constant for component A.

Selective diffusion of gases in CMS material ("slit-like" pore structure-Figure 2.1(b)) involves molecular size sieving. The similar size gas molecules can be effectively separated based on considerable differences in their activation energy for diffusion termed as 'energetic selectivity'. In addition unlike the conventional polymers, CMS membranes can provide additional high 'entropic selectivity' because of the rigid ultramicropores windows (Figure 2.1(b)). These can effectively restrict the degrees of freedom for the rotation and internal vibration of the gas molecules [5, 6].

2.4 Formation of asymmetric CMS hollow fiber membranes

The focus of this study is on asymmetric hollow fiber configuration due to its industrial scale-up advantage as explained in Chapter 1. To form the asymmetric CMS hollow fiber membranes, the first step is to obtain an asymmetric polymeric hollow fiber membrane. The second step is the pyrolysis of the polymer hollow fiber membrane.

2.4.1 Polymer precursor hollow fiber membranes

Asymmetric polymer hollow fiber membranes comprise an ultra-thin dense skin layer supported by a porous substructure as illustrated in Figure 2.3. Such membranes are formed via a dry-jet/wet quench spinning process [7-11] illustrated in Figure 2.4. The polymer solution used for spinning is referred to as "dope". Dope composition can be described in terms of a ternary phase diagram as shown in Figure 2.5.

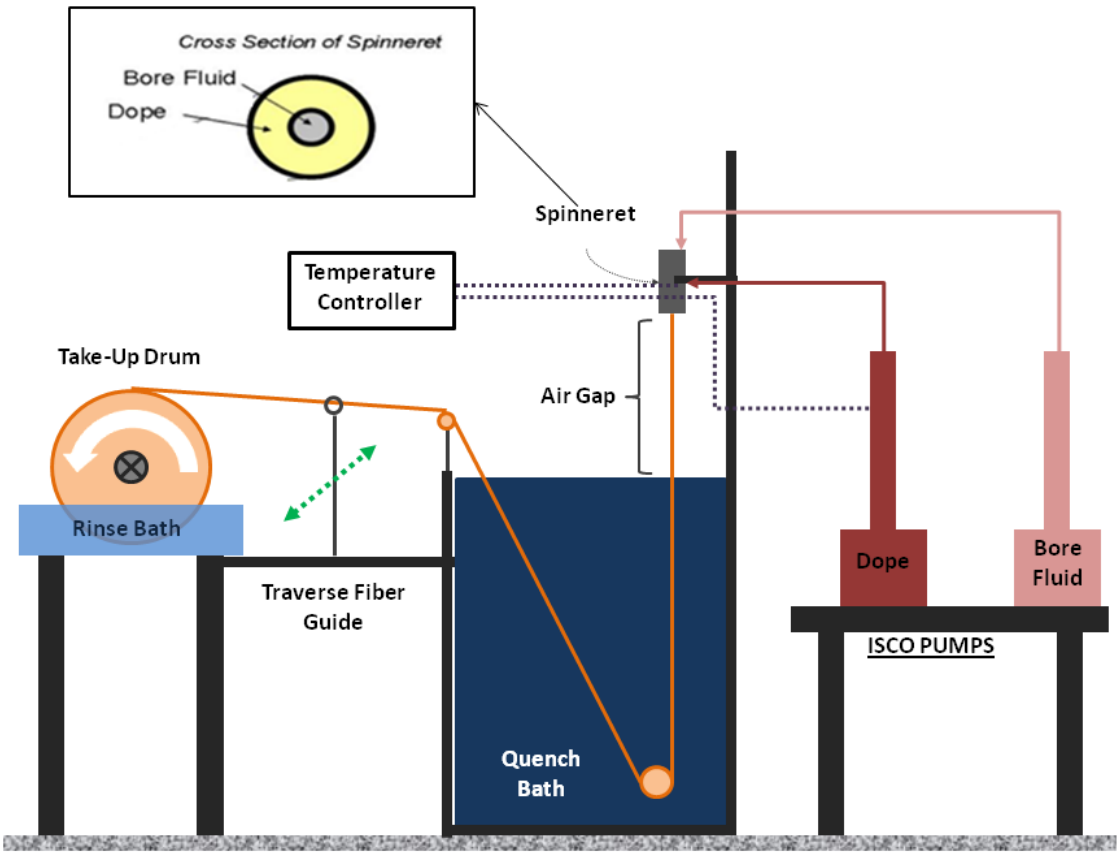

Figure 2.4: Dry-jet/wet-quench spinning process for polymer precursor hollow fiber membrane fabrication.

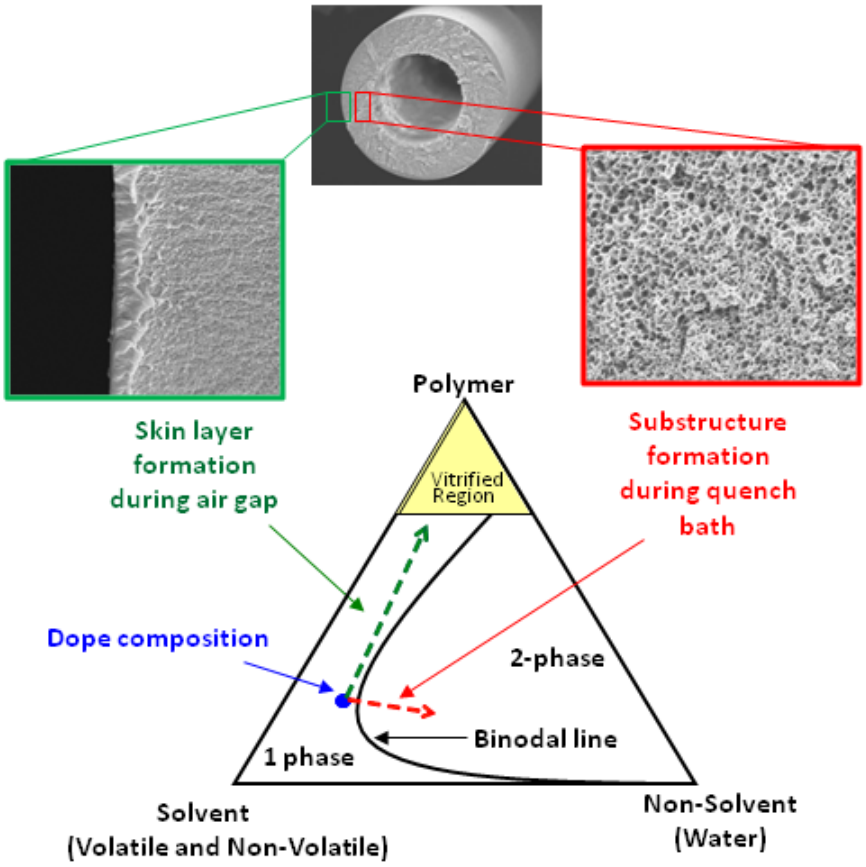

Figure 2.5: Ternary phase diagram showing the asymmetric polymer membrane formation process adapted from [11].

Polymer molecular weight and concentration are closely correlated to viscosity and rheology of the dope, which affects the overall morphology of hollow fibers [12]. The ratio of solvents to that of non-solvents should be adjusted in order to keep the dope in the 1-phase region close to the binodal line in Figure 2.5. Several key factors go into the formation of successful defect-free skin layer [9] as illustrated in Table 2.1.

Table 2.1: Key parameters in the fiber spinning process [9] (Figure 2.5)

Spinning Parameters		
Dope Composition	Air gap height	Quench bath temperature
Bore fluid composition	Take-up rate	Quench bath composition
Dope/bore fluid flow rate	Spinning temperature	Humidity

In the spinning process of Figure 2.5, the dope and bore fluid are coextruded through a spinneret into an air gap ("dry-jet"), where a dense skin layer is formed and then immersed into an aqueous quench bath ("wet-quench"), where the dope phase separates to form a porous substructure and can support the vitrified dense skin layer. The dense skin layer is formed by evaporation of volatile solvents which drives the dope composition toward the vitrified region (indicated by the green dashed line indicated by the "Skin Layer Formation" arrow in Figure 2.5). The porous substructure is formed when the dope phase separates in the quench bath and enters into a 2-phase region (indicated by red dashed line indicated by the "Substructure Formation" arrow in Figure 2.5). In this way, a desirable asymmetric morphology comprising a dense selective skin layer with a porous support structure is formed.

After phase separation in the quench bath, fibers are collected by a take-up drum and kept for solvent exchange. The solvent exchange process is an extremely important step in the membrane fabrication process [13, 14]. If the porous precursor fibers contain water at the time they are subjected to high temperatures, for instance during drying or pyrolysis, removal of the water causes significant changes to the structure and properties of the fiber, and of the resulting CMS membrane. The high capillary forces associated

with removal of water within the small radii of the pores close to the skin can cause densification of the structure in this region, which will result in a less permeable membrane [14]. To prevent this, the solvent exchange process replaces the water that is present in the porous substructure of the precursor fiber with a fluid having a lower surface tension.

2.4.2 Pyrolysis process for asymmetric CMS hollow fiber membranes

CMS membranes are fabricated upon controlled pyrolysis of polymer precursors [15]. As illustrated in Figure 2.3 for asymmetric CMS hollow fiber, gas separation occurs primarily in the intrinsic CMS dense skin. The dense layer of asymmetric CMS corresponds to a molecular sieving structure having a bimodal pore distribution (illustrated in Figure. 2.1). The nano-size pore structure and distribution can be altered using several parameters [15], such as: (2.4.2.1) choice of polymer precursor, (2.4.2.2) pre-pyrolysis treatment of polymer precursor, (2.4.2.3) pyrolysis temperature protocol, (2.4.2.4) pyrolysis atmosphere, and (2.4.2.5) post-pyrolysis treatment. The details for these key parameters are given below:

2.4.2.1 Polymer precursor

Precursor selection for the CMS membrane should satisfy a number of criteria: having a high aromatic carbon content, high glass transition temperature (T_g), chemical stability and superior starting separation properties [15]**.** Several classes of polymers have been investigated for CMS membrane formation viz. cellulose derivatives [16], phenolic resins [17, 18], poly (vinyldene) – based polymers [19], polyacrylonitrile (PAN) [20] and polyimides [21-27]. Polyimide precursors are preferred over other polymer precursors based on the separation performance and mechanical strength [21].

Various gas-pair separations have been done in the past using commercially available polyimide Matrimid® and co-polyimide 6FDA:BPDA-DAM in both the CMS dense film and asymmetric CMS hollow fiber membrane configurations [24, 26-31]. Matrimid® based CMS dense films have shown to give higher selectivity with lower permeability for O_2/N_2, CO_2/CH_4 and C_2H_4/C_2H_6 when compared to the 6FDA:BPDA-DAM based CMS membranes [27, 28, 32]. The case of C_3H_6/C_3H_8 separation is different, as Steel & Koros[28] have demonstrated that 6FDA:BPDA-DAM based CMS dense film have both higher selectivity and permeability when compared to Matrimid® based CMS. These performance trends were explained by the difference in fractional free volume for both the precursors, leading to a shift on the hypothetical CMS bimodal pore size distribution [32]. Additionally, Williams [23] showed that while Matrimid® pyrolysis evolved volatile products such as aniline, toluene, CO_2, and CO, 6FDA based precursors gave off significant amounts of $–CF_3$ related compounds in addition to these products which contributed to the higher permeability of 6FDA based CMS membranes.

A similar relation of precursor-CMS separation performance is seen in the asymmetric CMS hollow fiber configuration too [26, 31]. Recent studies by Xu [33] have compared the asymmetric CMS hollow fiber separation performance for Matrimid® and 6FDA:BPDA-DAM precursors as shown in the Figure 2.6(a) and (b).

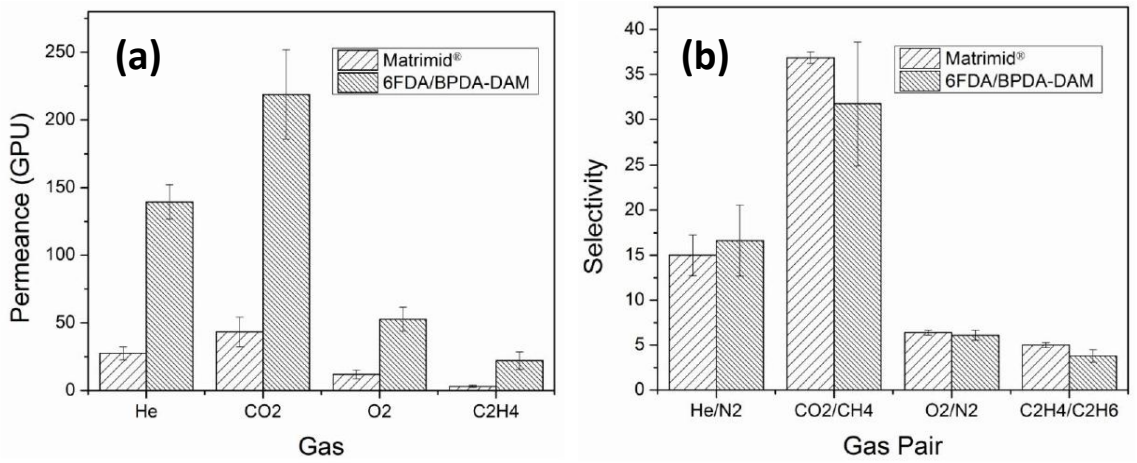

Figure 2.6: Comparison of asymmetric CMS hollow fiber membranes (a) Permeance and (b) Selectivity from Matrimid® and 6FDA:BPDA-DAM precursors, prepared under same fabrication conditions by Xu [33].

The differences in asymmetric CMS hollow fiber permeance formed from Matrimid® and 6FDA:BPDA-DAM (Figure 2.6(a)) can be accounted for as being due to two important factors viz., higher intrinsic CMS permeability of 6FDA:BPDA-DAM and differences in resultant asymmetric CMS hollow fiber substructure morphology. A detailed explanation for the effect of asymmetric CMS substructure morphology on gas permeance is given in section 2.5.

For the purpose of this study, asymmetric CMS hollow fiber from both Matrimid® and 6FDA:BPDA-DAM precursors are considered. Due to their ability to achieve high intrinsic CMS selectivities, any improvement in the permeances of asymmetric CMS hollow fiber membranes would be desirable.

2.4.2.2 Pre-pyrolysis treatment of polymer precursor

The purpose of precursor pre-treatment is to pre-arrange and stabilize the polymer material before undergoing the high-temperature pyrolysis. Pre-treatment can alter the chain segmental mobility and morphology of the precursor material, which can translate

to a change in the resulting CMS structure [34]. Precursor pre-treatment techniques can be broadly classified into primarily thermal vs. primarily chemical pre-treatment [34].

Typical thermal stabilization techniques are carried out either in oxidative or non-oxidative atmospheres at elevated temperatures, but below the carbonization temperatures (i.e. decomposition temperatures of polymers). By pre-oxidation of the asymmetric precursor hollow fibers, Kusuki *et al*. [35] and Okamoto *et al.* [36] prevented complete morphology loss of their asymmetric precursors. The pre-treatment avoided the excessive volatilization of carbon-containing fragments and resulted in a high carbon yield. Centeno & Fuertes [18] observed that the pyrolysis of phenolic resin precursor after pre-oxidation results in a more open pore structure with a drastic decrease in separation selectivity. On the other hand, by the pre-oxidation of poly vinyldene chloride-co-vinyl chloride (PVDC-VC) precursors, the same authors observed the resultant CMS membrane to be much less permeable [19]. Xu [33] performed pre-oxidation studies on asymmetric hollow fibers from Matrimid®, 6FDA:BPDA-DAM and 6FDA-DAM polyimide precursors. It was observed that only the 6FDA:BPDA-DAM precursor had improvement in resultant asymmetric CMS substructure morphology with no effect on other polyimides. Therefore, stabilization studies using pre-oxidation on CMS membrane should be carefully chosen as it appears to be favorable only for a specific polymer precursor material and to be only partially understood.

Chemical modification of polymer precursors is another technique that can be used for tailoring the resultant CMS separation properties. Some of the techniques that have been studied includes chemical modifications by polymer cross-linking [37], non-

solvent treatment [38] , and grafting of functional groups [39-41] on polyimides to enhance the separation capabilities of CMS dense film membranes.

Tin *et al.* [37] carried out chemical crosslinking on Matrimid® dense film precursor using 10 w/v% solution of p-xylenediamine for different time intervals. The chemical crosslinking mechanism involved diamine-imide reaction with the opening of imide rings. Upon the pyrolysis of different time interval crosslinked Matrimid® precursors, a decrease in CMS permeability for all the cases was observed. Only the 1-day crosslinked Matrimid® precursor, showed an improvement in CO_2/CH_4 CMS selectivity. For the purpose of this study, the diamine crosslinking reaction of Matrimid® precursor was evaluated for asymmetric hollow fiber configuration. It was observed to not offer improvements in asymmetric CMS substructure morphology. The details for the study are provided in Chapter 4.

Tin *et al.* [38] have also studied an extended non-solvent soaking effect of Matrimid® and P84 precursor dense films in different non-solvents (methanol, ethanol, propanol and butanol for 1 day). The resulting CMS membranes showed an increase in selectivity due to increased structural re-organization of solvent treated precursors, leading to smaller pores during pyrolysis. However, the fundamental causes of the improvement were not explored.

Xiao *et al.* [39] have investigated the effect of bromination on Matrimid® precursor for CMS dense film separation. Some researchers have also attempted to improve the CMS transport properties by sulfonation of the polyimide precursors [40, 41]**.** As both studies change the molecular structure of polymer precursor, the resultant

modified precursor properties for membrane formation can be much different from the original precursor. Also, most of the chemical pre-treatment stabilizations studies have been limited to dense film configuration. Very few studies have attempted to translate the affect to asymmetric hollow fiber configuration.

In this study, some of the above techniques are tested for asymmetric Matrimid® hollow fiber precursor and were found to have limitations when applied for asymmetric precursors. Therefore, the focus of this study is to develop a novel pre-pyrolysis treatment for asymmetric precursor hollow fibers which will lead to an improvement in the final CMS separation performance.

2.4.2.3 Pyrolysis temperature protocol

Several parameters in the pyrolysis process such as final pyrolysis temperature, heating ramp rate and thermal soak time at the final pyrolysis temperature can play a critical role in tuning the molecular sieving pore structure of CMS membranes [15].

The final pyrolysis temperature is defined as the temperature to which the polymer precursors are heated for the formation of carbon membranes. CMS membranes posses an ability to tune their separation performance based on the final pyrolysis temperature [27-30, 42]. Typically, an increase in final pyrolysis temperature translates to a change in CMS structure, leading towards smaller average pore size [3] as illustrated schematically in Figure 2.7.

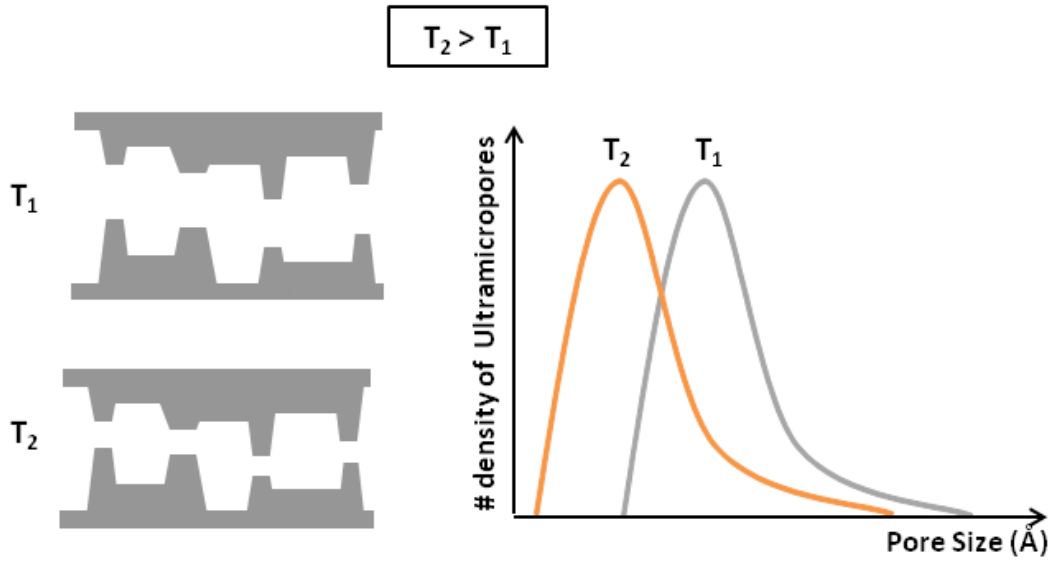

Figure 2.7: Illustration of final pyrolysis temperature (T) effect on the intrinsic molecular sieving structure of CMS membrane adapted from Steel and Koros [3].

By increasing the final pyrolysis temperature for Matrimid® & 6FDA:BPDA-DAM dense film precursors, Steel & Koros [28] observed an increase in selectivity with decrease in permeability for O_2/N_2 and CO_2/CH_4 separations. Rungta *et al.* [27, 30] have observed similar permeation trend for C_2H_4/C_2H_6 separation.

Jones & Koros [21] pyrolysed 6FDA precursor based asymmetric CMS hollow fibers at 500°C and 550°C. The higher temperature pyrolysed (550°C) CMS fibers showed a slight increase in O_2/N_2 selectivity accompanied with a decrease in O_2 permeance. Xu *et al.* [29] observed the same trend in C_2H_4/C_2H_6 separation from Matrimid® based CMS fibers by extensively studying different final pyrolysis temperature as shown in Figure 2.8.

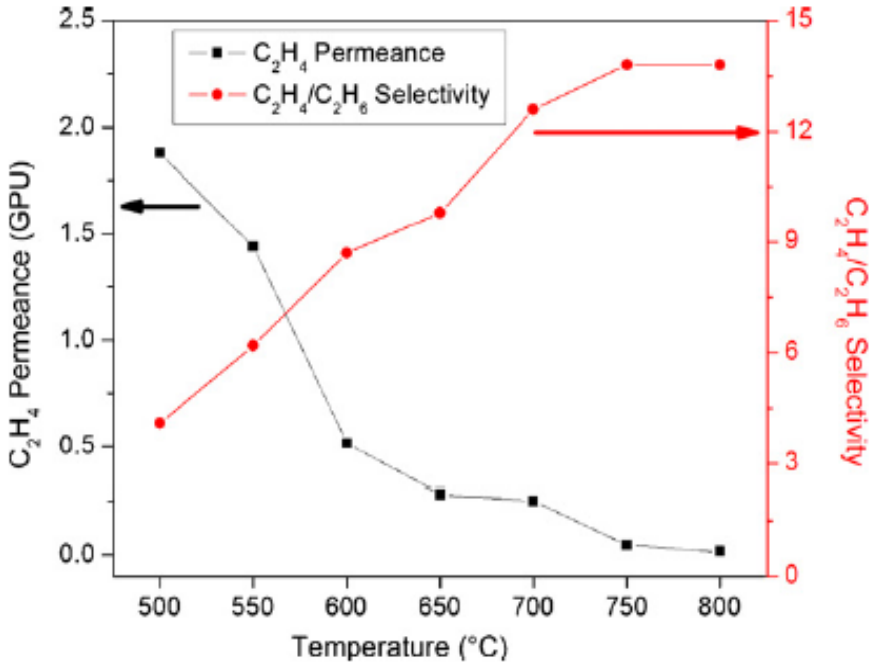

Figure 2.8: Role of final pyrolysis temperature on asymmetric CMS hollow fiber separation performance from Matrimid® precursor by Xu *et al.* [29].

Researchers have also studied the role of different heating ramp-rates [42] and thermal soak times [28, 31] for tuning the CMS separation performance. For the purpose of this study, mainly optimization of final pyrolysis temperature is considered for achieving the 'sweet spot' for particular separation.

2.4.2.4 Pyrolysis atmosphere

Pyrolysis atmosphere is critical in controlling the intrinsic CMS structure and its resulting separation performance. Geiszler & Koros [43], and Xu [33] have both separately compared the asymmetric CMS hollow fiber separation performance under vacuum and inert atmospheres. It is observed that pyrolysis under vacuum atmosphere produces high selective but less permeable CMS membranes compared to the inert gas atmospheres. A comparison of CMS separation performance for vacuum and argon inert

gas pyrolysis using 6FDA:BPDA-DAM precursor fibers is performed by Xu [33] and is shown in Figure 2.9.

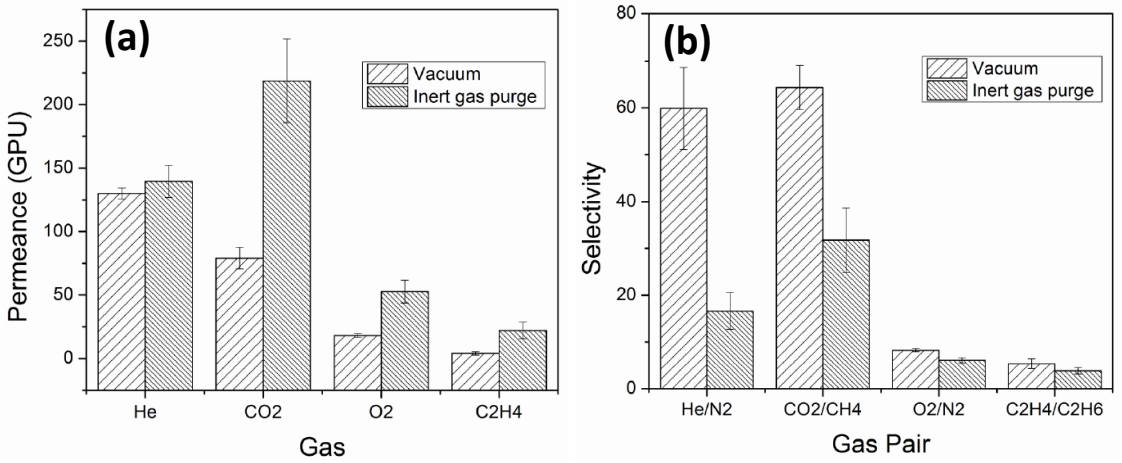

Figure 2.9: Comparison of asymmetric CMS hollow fiber membrane (a) Permeance and (b) Selectivity from 6FDA:BPDA-DAM precursor, pyrolysed under vacuum and inert gas atmospheres by Xu [33].

To understand the difference between vacuum and inert pyrolysis, Williams [23] hypothesized that the amount of oxygen present in the inert purge gas can affect the resulting CMS separation performance. Kiyono *et al.* [32, 44] studied the hypothesis by investigating the importance of 'oxygen doping' on Matrimid® and 6FDA:BPDA-DAM precursors for CO_2/CH_4 separation which is illustrated in figure 2.10.

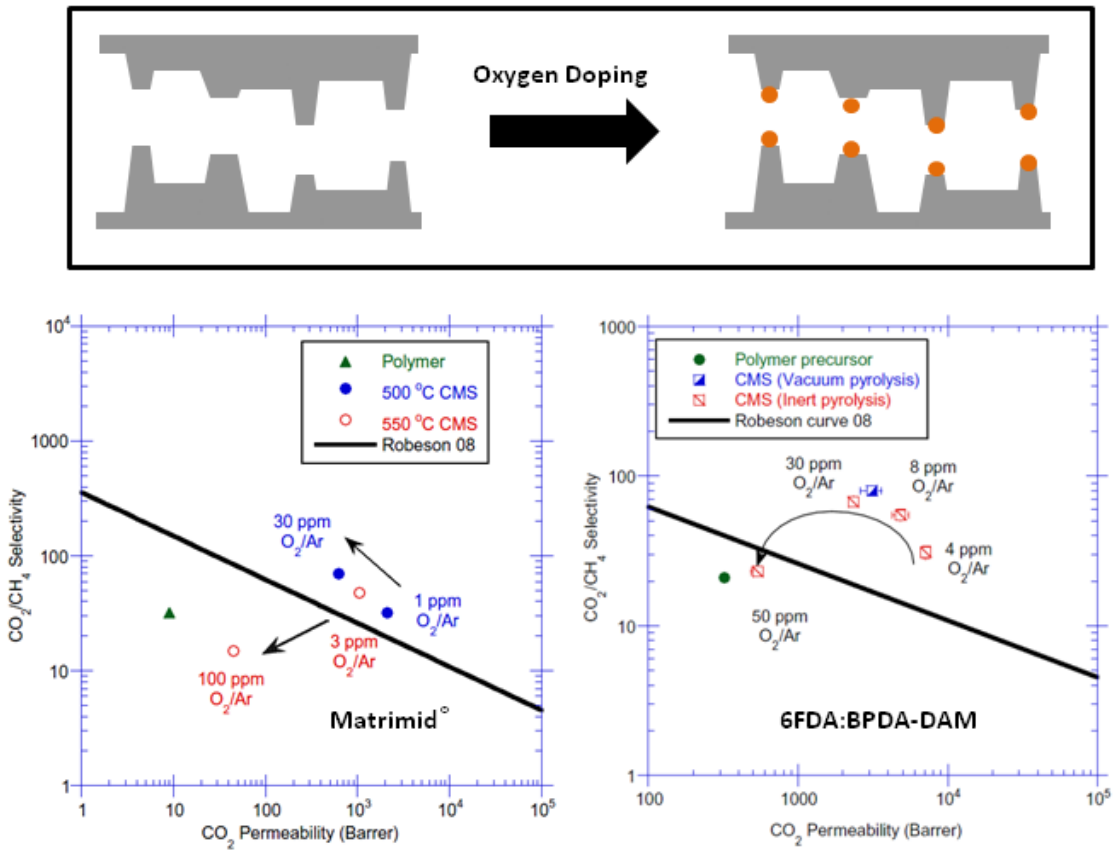

Figure 2.10: Oxygen doping effect on CO_2/CH_4 separation performance for CMS dense film from Matrimid® & 6FD:BPDA-DAM precursor [32, 45].

Rungta *et al.* [27] observed slight improvement in CMS selectivities for C_2H_4/C_2H_6 separation by applying the oxygen doping concept on 6FDA:BPDA-DAM based CMS dense films.

Hence by utilizing the oxygen doping concept during pyrolysis, the need for vacuum atmosphere to achieve high selectivities can be avoided, thereby preserving higher permeabilities. The concept of oxygen doping to tune the separation performance is mainly applied for intrinsically open morphology precursors [27]. In the current study, the oxygen doping concept is applied to engineer the separation performance of asymmetric CMS hollow fibers.

2.4.2.5 Post-pyrolysis treatment

Thermochemical post-treatments have been studied by researchers to finely tune the pore dimensions and distributions of CMS membranes. Some of the common techniques used are chemical vapor depositions (CVD), post-pyrolysis thermal treatment and coating of CMS membranes [15]. Post-oxidation has been the favorite method; where CMS membranes after pyrolysis are again heated in oxidative atmosphere to *increase* the pore volume, which typically increases the permeability of CMS membrane [46]. Post-oxidation and chemical vapor depositions techniques have also been extensively investigated by Soffer *et al.* [47] for cellulose derived CMS fibers. Unlike oxygen doping where the pyrolysis is conducted in trace amounts of oxygen, post-oxidation is performed after the pyrolysis. Hence the difficulty arises in maintaining the high selectivity.

Recently, Singh & Koros [48] developed a post-pyrolysis oxygen doping concept referred as 'Dual Temperature Secondary Oxygen Doping (DTSOD)' where the CMS membranes are exposed to trace amounts of oxygen by briefly taking it to a temperature higher than the final pyrolysis temperature. The reaction mechanism is similar to the primary oxygen doping, difference being in selective doping of the ultramicropores edges resulting to a favorable pore size distribution. The DTSOD concept has been applied on 6FDA:BPDA-DAM based CMS for O_2/N_2 [48] and C_2H_4/C_2H_6 [27] separation.

2.5 Transition of asymmetric polymer precursor fiber to asymmetric CMS hollow fiber

The advantage of CMS membrane in dense film configuration has been the ability to surpass the polymer membranes separation performance by an increase in both permeability and selectivity [49]. For the industrial use of CMS membranes, this intrinsic advantage must be translated to the hollow fiber configuration. Vu & Koros [31] studied the performance of CMS hollow fiber membranes for both Matrimid® and 6FDA:BPDA-DAM precursors. In spite of achieving attractive selectivities for CO_2/CH_4, the productivity (i.e., permeance) in CMS hollow fiber membranes was much lower than the anticipated value from CMS dense films. In fact, the CMS permeances were even lower than the precursor fiber permeances.

Similar reduction in CMS hollow fiber permeance was observed by Xu *et al.* for C_2H_4/C_2H_6 separation [26, 29]. The cause for lower CMS permeances are related to the densification of substructure pores during pyrolysis, referred to as 'substructure collapse'. The advantage of asymmetric hollow fiber configuration is ideally due to the high transport fluxes obtained through ultra thin membrane skin thickness ((l)<1 μm) [50]. Unfortunately the substructure collapse in CMS hollow fibers caused the membrane skin thickness (l) to increase which caused the CMS permeance (i.e. P/l – permeability normalized thickness) to decrease. The extent of collapse is seen to be a property of the precursor [26], Matrimid® based precursors shows the highest degree of collapse. Xu *et al.* [29] attempted some engineering techniques to restrict the collapse in CMS hollow fibers by reducing the 'apparent' separation layer thickness (i.e thin wall precursor fibers) and having a dual layer precursor fiber by incorporating zeolite (13X) in the core polymer

matrix. Even though both techniques had slight improvement in resultant CMS permeance, the issue of collapse in asymmetric CMS hollow fibers from Matrimid® precursor still remained to be addressed. Xu [33] also applied the pre-oxidation technique to stabilize the asymmetric polymer substructure morphology prior to pyrolysis. Even though no improvement was observed in case for Matrimid® and 6FDA-DAM precursor, 6FDA:BPDA-DAM precursor fibers after pre-oxidation showed an improvement in final asymmetric CMS substructure morphology. The transport performance of the pre-oxidized asymmetric CMS hollow fiber membranes still require optimization, as changing the intrinsic properties of precursor will change the resultant intrinsic CMS properties too.

The main focus of this study is to restrict the substructure morphology collapse in asymmetric CMS hollow fiber membranes, by developing a common pre-treatment technique which can be applied to any asymmetric polymer precursor. The mechanism and details of this phenomenon will be explained in the subsequent chapters.

2.6 References

1. Jenkins, G.M., Polymeric carbons: carbon fibre, glass and char. 1976: Cambridge University Press.
2. Pierson, H.O., Handbook of carbon, graphite, diamond, and fullerenes: properties, processing, and applications. 1993: Noyes Publications Park Ridge, NJ.
3. Steel, K.M. and W.J. Koros, Investigation of porosity of carbon materials and related effects on gas separation properties. Carbon, 2003. 41(2): p. 253-266.
4. Koros, W.J. and G.K. Fleming, Membrane-based gas separation. Journal of Membrane Science, 1993. 83(1): p. 1-80.
5. Singh-Ghosal, A. and W.J. Koros, Air separation properties of flat sheet homogeneous pyrolytic carbon membranes. Journal of Membrane Science, 2000. 174(2): p. 177-188.
6. Singh, A. and W.J. Koros, Significance of entropic selectivity for advanced gas separation membranes. Industrial & Engineering Chemistry Research, 1996. 35(4): p. 1231-1234.
7. Clausi, D.T., S.A. McKelvey, and W.J. Koros, Characterization of substructure resistance in asymmetric gas separation membranes. Journal of Membrane Science, 1999. 160(1): p. 51-64.
8. Clausi, D.T. and W.J. Koros, Formation of defect-free polyimide hollow fiber membranes for gas separations. Journal of Membrane Science, 2000. 167(1): p. 79-89.
9. McKelvey, S.A., D.T. Clausi, and W.J. Koros, A guide to establishing hollow fiber macroscopic properties for membrane applications. Journal of Membrane Science, 1997. 124(2): p. 223-232.
10. Carruthers, S.B., G.L. Ramos, and W.J. Koros, Morphology of integral-skin layers in hollow-fiber gas-separation membranes. Journal of Applied Polymer Science, 2003. 90(2): p. 399-411.
11. Chen, C.-C., Thermally crosslinked polyimide hollow fiber membranes for natural gas purification. Doctor of Philosophy, Georgia Institute of Technology, 2011.
12. Omole, I.C., S.J. Miller, and W.J. Koros, Increased molecular weight of a cross-linkable polyimide for spinning plasticization resistant hollow fiber membranes. Macromolecules, 2008. 41(17): p. 6367-6375.
13. Pinnau, I. and W.J. Koros, Influence of quench medium on the structures and gas permeation properties of polysulfone membranes made by wet and dry/wet phase inversion. Journal of Membrane Science, 1992. 71(1): p. 81-96.
14. Clausi, D.T., Formation and characterization of asymmetric polyimide hollow fiber membranes for gas separations. 1998: Doctor of Philosophy, The University of Texas at Austin.
15. Saufi, S. and A. Ismail, Fabrication of carbon membranes for gas separation—a review. Carbon, 2004. 42(2): p. 241-259.
16. Koresh, J.E. and A. Sofer, Molecular Sieve Carbon Permselective Membrane. Part I. Presentation of a New Device for Gas Mixture Separation. Separation Science and Technology, 1983. 18(8): p. 723-734.
17. Shusen, W., Z. Meiyun, and W. Zhizhong, Asymmetric molecular sieve carbon membranes. Journal of Membrane Science, 1996. 109(2): p. 267-270.

18. Centeno, T.A., J.L. Vilas, and A.B. Fuertes, Effects of phenolic resin pyrolysis conditions on carbon membrane performance for gas separation. Journal of Membrane Science, 2004. 228(1): p. 45-54.
19. Centeno, T.A. and A.B. Fuertes, Carbon molecular sieve gas separation membranes based on poly (vinylidene chloride-co-vinyl chloride). Carbon, 2000. 38(7): p. 1067-1073.
20. David, L. and A. Ismail, Influence of the thermastabilization process and soak time during pyrolysis process on the polyacrylonitrile carbon membranes for O2/N2 separation. Journal of Membrane Science, 2003. 213(1): p. 285-291.
21. Jones, C.W. and W.J. Koros, Carbon molecular sieve gas separation membranes-I. Preparation and characterization based on polyimide precursors. Carbon, 1994. 32(8): p. 1419-1425.
22. Ma, X.; Swaidan, R.; Teng, B.; Tan, H.; Salinas, O.; Litwiller, E.; Han, Y.; Pinnau, I., Carbon molecular sieve gas separation membranes based on an intrinsically microporous polyimide precursor. Carbon 2013.
23. Williams, P.J., Analysis of factors influencing the performance of CMS membranes for gas separation. Doctor of Philosophy, Georgia Institute of Technology, 2006.
24. Kiyono, M., W.J. Koros, and P.J. Williams, Correlation between pyrolysis atmosphere and carbon molecular sieve membrane performance properties. Vol. 14. 2011: Elsevier: Amsterdam.
25. Tin, P. S.; Chung, T.-S.; Liu, Y.; Wang, R., Separation of CO2/CH4 through carbon molecular sieve membranes derived from P84 polyimide. Carbon 2004, 42 (15), 3123-3131.
26. Xu, L.; Rungta, M.; Brayden, M. K.; Martinez, M. V.; Stears, B. A.; Barbay, G. A.; Koros, W. J., Olefins-Selective Asymmetric Carbon Molecular Sieve Hollow Fiber Membranes for Hybrid Membrane-Distillation Processes for Olefin/Paraffin Separations. J Membrane Sci 2012.
27. Rungta, M.; Zhang, C.; Xu, L.; Koros, W. J., Membrane-based ethylene/ethane separation: The upper bound and beyond. Aiche J 2013.
28. Steel, K.M. and W.J. Koros, An investigation of the effects of pyrolysis parameters on gas separation properties of carbon materials. Carbon, 2005. 43(9): p. 1843-1856.
29. Xu, L., M. Rungta, and W.J. Koros, Matrimid® derived carbon molecular sieve hollow fiber membranes for ethylene/ethane separation. Journal of Membrane Science, 2011. 380(1-2): p. 138-147.
30. Rungta, M., L. Xu, and W.J. Koros, Carbon molecular sieve dense film membranes derived from Matrimid® for ethylene/ethane separation. Carbon, 2012. 50(4): p. 1488-1502.
31. Vu, D.Q., W.J. Koros, and S.J. Miller, High pressure CO2/CH4 separation using carbon molecular sieve hollow fiber membranes. Industrial & Engineering Chemistry Research, 2002. 41(3): p. 367-380.
32. Kiyono, M., P.J. Williams, and W.J. Koros, Effect of polymer precursors on carbon molecular sieve structure and separation performance properties. Carbon, 2010. 48(15): p. 4432-4441.

33. Xu, L., Carbon Molecular Sieve Hollow Fiber Membranes For Olefin/Paraffin Separations. Doctor of Philospohy, Georgia Institute of Technology, 2012.
34. Tin, P.S., Y. Xiao, and T.S. Chung, Polyimide-Carbonized Membranes for Gas Separation: Structural, Composition, and Morphological Control of Precursors. Separation & Purification Reviews, 2006. 35(4): p. 285-318.
35. Kusuki, Y.; Shimazaki, H.; Tanihara, N.; Nakanishi, S.; Yoshinaga, T., Gas permeation properties and characterization of asymmetric carbon membranes prepared by pyrolyzing asymmetric polyimide hollow fiber membrane. J Membrane Sci 1997, 134 (2), 245-253.
36. Okamoto, K.-i.; Kawamura, S.; Yoshino, M.; Kita, H.; Hirayama, Y.; Tanihara, N.; Kusuki, Y., Olefin/paraffin separation through carbonized membranes derived from an asymmetric polyimide hollow fiber membrane. Industrial & Engineering Chemistry Research 1999, 38 (11), 4424-4432.
37. Tin, P. S.; Chung, T.-S.; Kawi, S.; Guiver, M. D., Novel approaches to fabricate carbon molecular sieve membranes based on chemical modified and solvent treated polyimides. Micropor Mesopor Mat 2004, 73 (3), 151-160.
38. Tin, P.S., T.-S. Chung, and A.J. Hill, Advanced fabrication of carbon molecular sieve membranes by nonsolvent pretreatment of precursor polymers. Industrial & Engineering Chemistry Research, 2004. 43(20): p. 6476-6483.
39. Xiao, Y.; Dai, Y.; Chung, T.-S.; Guiver, M. D., Effects of Brominating Matrimid Polyimide on the Physical and Gas Transport Properties of Derived Carbon Membranes. Macromolecules 2005, 38 (24), 10042-10049.
40. Kim, Y.K., H.B. Park, and Y.M. Lee, Carbon molecular sieve membranes derived from metal-substituted sulfonated polyimide and their gas separation properties. Journal of Membrane Science, 2003. 226(1-2): p. 145-158.
41. Islam, M. N.; Zhou, W.; Honda, T.; Tanaka, K.; Kita, H.; Okamoto, K.-i., Preparation and gas separation performance of flexible pyrolytic membranes by low-temperature pyrolysis of sulfonated polyimides. J Membrane Sci 2005, 261 (1-2), 17-26.
42. Suda, H. and K. Haraya, Gas permeation through micropores of carbon molecular sieve membranes derived from Kapton polyimide. The Journal of Physical Chemistry B, 1997. 101(20): p. 3988-3994.
43. Geiszler, V.C. and W.J. Koros, Effects of polyimide pyrolysis conditions on carbon molecular sieve membrane properties. Industrial & Engineering Chemistry Research, 1996. 35(9): p. 2999-3003.
44. Kiyono, M., P.J. Williams, and W.J. Koros, Generalization of effect of oxygen exposure on formation and performance of carbon molecular sieve membranes. Carbon, 2010. 48(15): p. 4442-4449.
45. Kiyono, M., P.J. Williams, and W.J. Koros, Effect of pyrolysis atmosphere on separation performance of carbon molecular sieve membranes. Journal of Membrane Science, 2010. 359(1): p. 2-10.
46. Fuertes, A.B., Effect of air oxidation on gas separation properties of adsorption-selective carbon membranes. Carbon, 2001. 39(5): p. 697-706.
47. Soffer, A.; Azariah, M.; Amar, A.; Cohen, H.; Golub, D.; Saguee, S.; Tobias, H., Method of improving the selectivity of carbon membranes by chemical carbon vapor deposition. U.S. Patent No. 5,695,818.: 1997.

48. Singh, R. and W.J. Koros, Carbon molecular sieve membrane performance tuning by dual temperature secondary oxygen doping (DTSOD). Journal of Membrane Science, 2012. 427: p. 472-478.
49. Robeson, L.M., The upper bound revisited. Journal of Membrane Science, 2008. 320(1-2): p. 390-400.
50. Koros, W.J. and R.P. Lively, Water and beyond: Expanding the spectrum of large-scale energy efficient separation processes. Aiche Journal, 2012. 58(9): p. 2624-2633.

CHAPTER 3

MATERIALS AND EXPERIMENTAL METHODS

3.1 Overview

This chapter describes the materials and experimental methods used in this study. The chapter lists all materials including polymers, solvents, non-solvents, silane agents and gases. The asymmetric polymer precursor and CMS hollow fiber membrane formation is discussed along with the methods for permeation, sorption and various other characterization techniques used. However, the detailed protocol for 'silane' pre-pyrolysis treatment on asymmetric polymer hollow fibers will be discussed in the next chapter because it is a new technique and is used for the first time in CMS membrane application.

3.2 Materials

3.2.1 Polymer precursor

As discussed in Chapter 2, polyimides are favored as polymer precursors for the formation of CMS membranes [1, 2]. Two polyimides Matrimid® 5218 (BTDA-DAPI) and 6FDA:BPDA-DAM were used in this study. The molecular structure, glass transition temperature (T_g), fraction free volume (FFV) for both the polyimide precursors are shown in Table 3.1. Matrimid® 5218 is a commercially available polyimide and was obtained from Huntsman International LLC. 6FDA:BPDA-DAM was lab custom synthesized using standard procedure [3]. All the polymers were dried under vacuum at 150°C overnight before use.

Table 3.1: Properties and molecular structure of polyimide precursors Matrimid® 5218 and 6FDA:BPDA-DAM [4-6]

Polymer	Chemical structure
Matrimid® 5218 T_g ~305°C FFV – 0.110	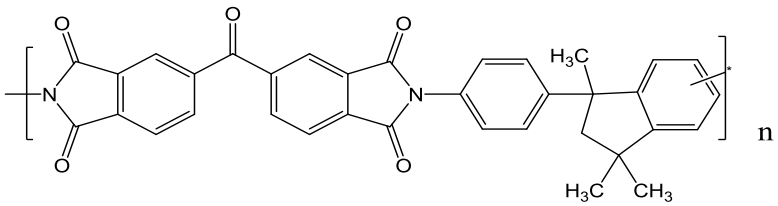
6FDA:BPDA-DAM T_g ~424°C FFV – 0.145	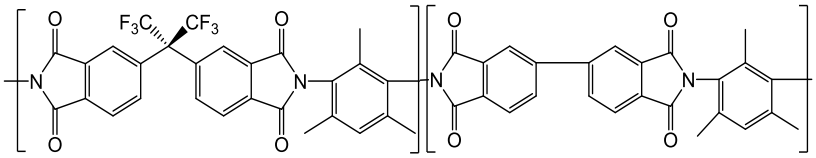

3.2.2 Solvents and non-solvents

For the asymmetric polymer precursor hollow fiber spinning, n-methylpyrrolidone (NMP), ethanol, tetrahydrofuran (THF), and lithium nitrate ($LiNO_3$) were all purchased from Sigma Aldrich. For the solvent exchange of precursor fibers, methanol, and hexane were purchased from VWR.

3.2.3 Silane agents

The molecular structure and physical properties of different silane agents used in this study are summarized in Table 3.2. Vinyltrimethoxysilane (VTMS), trimethoxysilane, and vinyltrimethylsilane were purchased by Sigma Aldrich and ethyltrimethoxysilane (ETMS) from Gelest Inc. They were all liquid at room temperature.

Table 3.2: Physical properties and molecular structure of silane agents

Silane agent	Boiling point (B.P.) (°C)	Density (g/cc)	Chemical structure
Vinyltrimethoxysilane (VTMS)	123°C	0.97	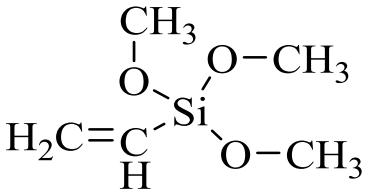
Trimethoxysilane	81°C	0.96	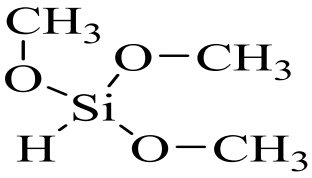
Vinyltrimethylsilane	55°C	0.68	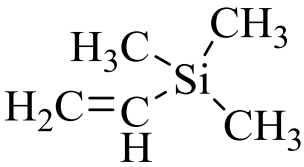
Ethyltrimethoxysilane (ETMS)	125°C	0.95	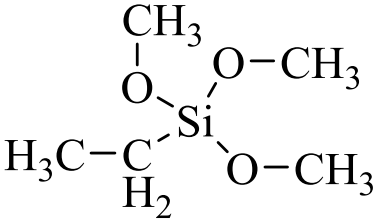

3.2.4 Gases

For permeation and sorption experiments, all the pure gases (He, O_2, CO_2, N_2 and CH_4) were obtained from Airgas. For the mixed gas permeation experiments, binary mixtures of 50 mol% CO_2 and 50 mol% CH_4, 63.2 mol% C_2H_4 and 36.8 mol% C_2H_6, and 50 mol% C_3H_6 and 50 mol% C_3H_8 were obtained from Praxair.

For pyrolysis experiments, argon gas with varied amount of oxygen level (in ppm) was used. Ultra High Purity (UHP) argon was purchased from Airgas and specialty gases containing 1.08, 10.1, 28.8 and 49.1 ppm of O_2 in Ar were purchased from Praxair.

3.3 Membrane formation

The formation of asymmetric CMS hollow fiber membranes is a two-step process: where first the polymeric precursor hollow fibers are formed and then pyrolysed to form the CMS hollow fiber membrane.

3.3.1 Asymmetric polymer precursor hollow fiber membranes

3.3.1.1 Dope formulation

The dope compositions for both the polymer precursors Matrimid® and 6FDA:BPDA-DAM have been well studied in the past [4, 7, 8]. Similar dope composition were adapted in this study as shown in Table 3.3, as it yielded good mechanical and defect-free precursor hollow fibers. Typical dope compositions consist of polymer, solvents and non-solvents. NMP was chosen as non-volatile solvent due to its relatively benign nature towards the environment, and THF was selected as the volatile solvent for defect-free skin formation. Ethanol was the non-solvent for both polymer dopes. For 6FDA:BPDA-DAM dopes, $LiNO_3$ was added for assisting phase separation and controlling the viscosity of the dope. Once the dope was formed, it was allowed to roll for 2-4 weeks to obtain a homogenous solution.

Table 3.3: Dope composition and spinning conditions for Matrimid® and 6FDA:BPDA-DAM polymer precursor hollow fibers [7, 9, 10]

		Matrimid®	6FDA:BPDA-DAM
Dope composition (wt %)	Polymer	26.2	20.0
	NMP	53.0	47.5
	Ethanol	14.9	16.0
	THF	5.9	10.0
	$LiNO_3$	---	6.5
Bore Fluid composition (wt %)	NMP/Water	96/4	90/10
Dope/Bore fluid flow-rate (mL/hr)		180/60	180/60
Air gap (cm)		5-10	5-10
Take-up rate (m/min)		20	15
Dope temperature (°C)		60	60
Quench bath temperature (°C)		50	50
Precursor fiber O.D. (μm)		450	300

3.3.1.2 Asymmetric polymer hollow-fiber spinning

The polymer hollow fiber spinning was done by dry jet/ wet quench spinning process, which results in asymmetric morphology comprising a defect-free skin and a porous substructure. The schematic for hollow fiber spinning set-up has been shown in figure 2.4 and the optimized spinning conditions are summarized in Table 3.2. The prepared dope was loaded into 500-mL syringe pump (ISCO Inc., Lincoln, NE) and allowed to degas overnight. Bore fluid was loaded into a separate 100-mL syringe pump. The dope and bore fluid were co-extruded through a custom spinneret with in-line filtration between the delivery pumps and the spinneret with 20 μm and 2 μm metal filters, respectively. Spinning was temperature-controlled; with thermocouples placed on the spinneret, dope line and dope pump. The co-extruded dope solution with bore fluid passed through an air gap and was immersed into a water quench bath. The phase-

separated hollow fiber spin line was then collected on a 0.32 m diameter rotating polyethylene drum after passing over Teflon® guide. The hollow fibers were cut-off the take-up drum and immersed into water baths for solvent exchange for 48 hrs with occasional exchange of deionized water (D.I.) water. The fibers were solvent exchanged in glass containers with three separate 20 min methanol baths followed by 3 separate 20 min hexane baths and dried under vacuum at 75°C for 2 hrs.

3.3.2 Pre-pyrolysis treatment on polymer precursor hollow fiber membranes

The major part of this study involved exploring looking into several thermal and chemical pre-treatment techniques carried out prior to pyrolysis. These treatments were essential for restricting substructure collapse in asymmetric CMS membranes. The detail mechanism and treatment conditions are explained in the subsequent chapters.

For the purpose of characterizing the new pre-treatment techniques, the same procedure of pre-treatment for precursor fibers were carried on polymer powders too. The procedure helped in understanding the effects of pre-treatment on chemical molecular structure of precursor by eliminating any mass-transport limitations. The details of the pre-treatments are provided in their respective sections.

3.3.3 Asymmetric CMS hollow fiber membrane formation

3.3.3.1 Pyrolysis set-up

Both the untreated and pre-treated precursor hollow fiber membranes were pyrolysed in the presence of an inert gas to form a CMS membrane. The pyrolysis set-up

used for the study was similar to the previously reported system [7, 11] and also shown in Figure 3.1.

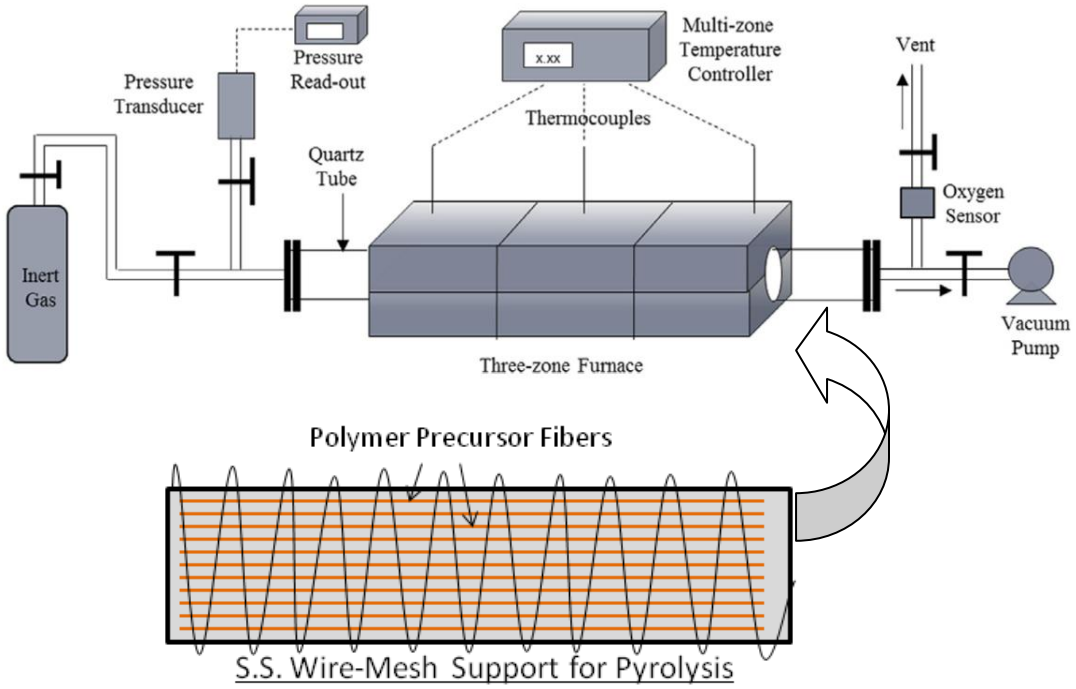

Figure 3.1: Schematic for pyrolysis set-up [11, 12].

The precursor fibers were placed on a stainless steel wire mesh plate (McMaster Carr, Robbinsville, NJ) and loosely bound separately with thin stainless steel wires, and loaded into a pyrolysis setup as shown in Figure 3.1. The setup consisting of a three-zone furnace (Thermocraft, Inc., model # XST-3-0-24-3C, Winston-Salem, NC) connected to a multichannel temperature controller (Omega Engineering Inc., Stamford, CT). A quartz tube (National Scientific Co., 55 mm ID and 4 ft long, Quakertown, PA) was used to hold the fibers in the furnace. An assembly of a metal flange with silicon O-rings (MTI Corporation, model EQ-FI-60, Richmond, CA) was used on both ends of the quartz tube. An oxygen analyzer (Cambridge Sensotec Ltd., Rapidox 2100 series, Cambridge,

England) was integrated to monitor oxygen concentration during the pyrolysis process. The flow rate of the purge gas was controlled with a mass flow controller (Alicat Scientific, part number MC-500 SCCM-D). Between experiments, the quartz tube and wire mesh were rinsed with acetone and baked in air at 800 °C to remove any residue which could affect subsequent runs.

3.3.3.2 Pyrolysis protocol

The pyrolysis process was carried out under constant inert or oxygen doped inert gas flow rate of 200 sccm (standard cubic centimeter per minute). Different grades of argon gas were used namely Ultra High Purity (UHP), 1.08, 10.1, 28.8 and 49.1 ppm of O_2 in argon. The oxygen level in the pyrolysis was ensured to be stable and close to the cylinder value before starting the pyrolysis. The entire set-up was purged for greater than 8 hrs to maintain uniform oxygen concentration. After the initial purging, a heating protocol was started depending on the final pyrolysis temperature. Several final pyrolysis temperatures were investigated in this study, ranging from 500°C to 650°C. For the sake of convenience, all the different transport results at different pyrolysis temperatures are referred to as '*final pyrolysis temperature–argon gas grade'* (for e.g., 550°C-UHP). The same heating ramp-rate was employed for all the different final pyrolysis temperatures, as shown in Table 3.4.

Table 3.4: Heating protocol followed for pyrolysis at different final temperatures.

$T_{initial}$ (°C)	T_{final} (°C)	Ramp rate (°C/min)
50	250	13.3
250	T_{max} - 15	3.85
T_{max} - 15	T_{max}	0.25
T_{max}	T_{max}	2 hrs soak

Once the heating cycle was completed, the furnace was allowed to cool down to room temperature. The resultant CMS fibers were removed from the furnace and used for further characterization.

3.3.3.3 Hollow fiber module formation

The separation properties for the asymmetric CMS hollow fibers were evaluated using small lab scale fiber modules as described earlier [12]. A typical module is shown in Figure 3.2. For accuracy, CMS fibers were potted into replicate single fiber and multiple fiber (4-5) modules. 3M (DP-100) epoxy, commonly referred as '5-min epoxy' was used to pot the module ends.

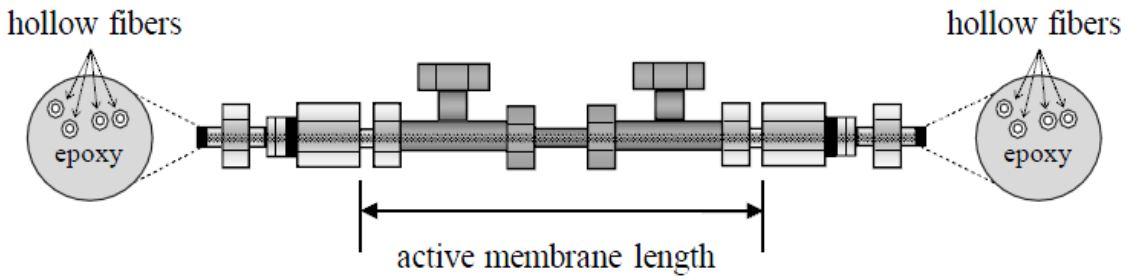

Figure 3.2: Schematic of a lab-scale hollow fiber membrane module [12].

3.4 Membrane characterization techniques

3.4.1 Transport properties

3.4.1.1 Pure gas permeation

For pure gas testing of asymmetric CMS hollow fiber modules, constant volume-variable pressure permeation system was used [12, 13]. The schematic of the constant volume-variable pressure permeation system is shown in Figure 3.3.

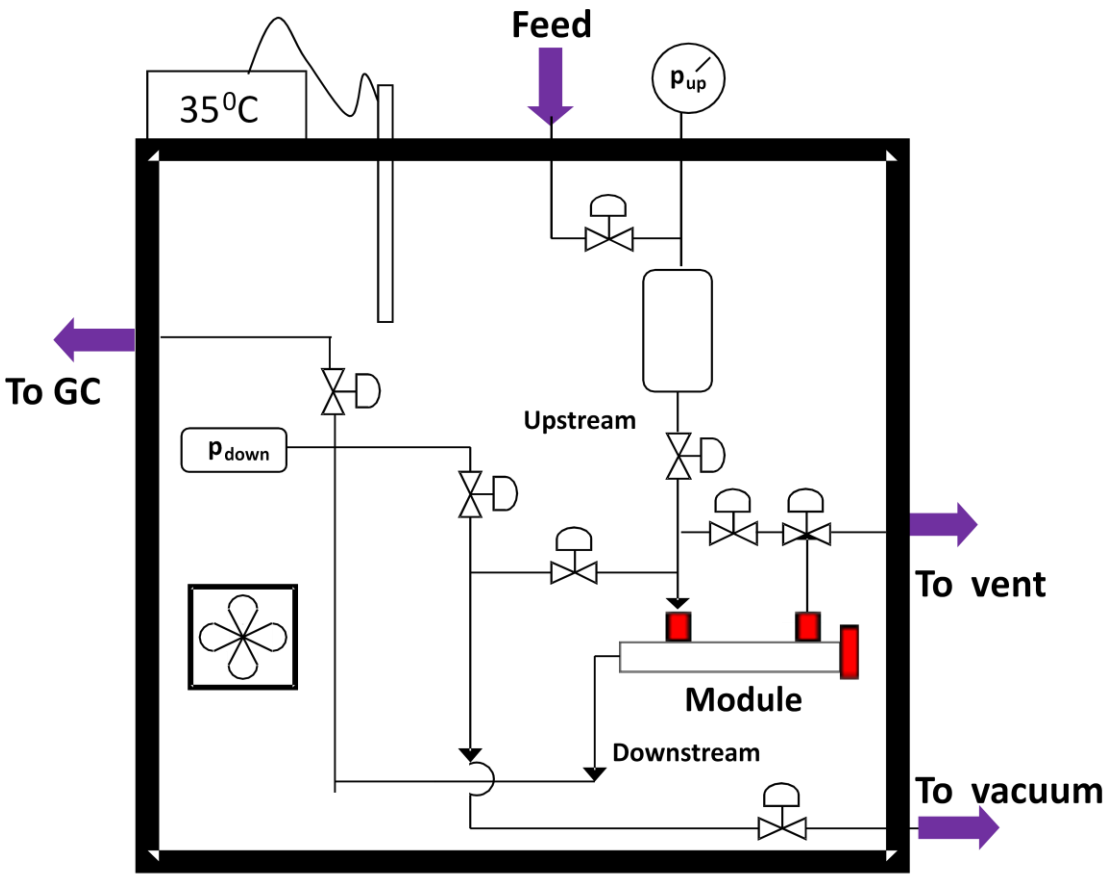

Figure 3.3: Schematic of a constant volume-variable pressure permeation set-up

Both the upstream and downstream of the permeation system were evacuated under vacuum for at least 12 hrs and a leak rate was measured, which was always less than 1% of the permeate rate of the slowest gas. Once the whole system was evacuated, the upstream (shell side) was pressurized with the test gas while the downstream was maintained at vacuum, but isolated from the vacuum pump. The pressure rise in a standard volume on the downstream was monitored over time by LabView (National Instruments, Austin, TX) and permeance was calculated using Equation (2.2) in Chapter 2. The system was evacuated for at least 12 hrs before experiments with different gases.

The pure gas permeation properties for CMS membranes were primarily evaluated for feed gases He, CO_2, O_2, N_2 and CH_4. For all the measurements, constant upstream feed pressure (shell-side feed) of 100 psi was maintained. The permeation temperature was constant at 35°C for all the runs.

3.4.1.2 Mixed gas permeation

For practical applications of asymmetric CMS membrane, it is important to evaluate the mixed gas separation performance, which is of course the real situation in any application. Similar to pure gas permeation, even for mixed gas measurements constant volume-variable pressure permeation systems (shell-side feed) was used. The stage cut (ratio of permeate flow rate to feed flow rate) was maintained less than 1% to avoid concentration polarization. The selectivity was calculated from the GC (gas chromatography) analysis of permeate composition, while permeance was obtained from the pressure rise in downstream. Due to high feed pressures (up to 800 psi at times) and non-ideality of the gas, fugacity coefficients were calculated using virial equation of state and taken into permeance calculation.

The binary mixture of 50 mol % CO_2/50 mol % CH_4 up to 800 psi total feed pressures is most commonly used. This aggressive natural gas feed condition was chosen in order to evaluate the most realistic separation performance of asymmetric CMS membranes and also to make a comparison with previous related studies [12, 14]. In addition to CO_2/CH_4, mixed gas performance evaluation for C_2H_4/C_2H_6 and C_3H_6/C_3H_8 was also performed in this study. The purpose of the olefin-paraffin separation evaluation was a 'proof-of-concept' study to show the broad application of the current work. The separation performance of this study extends the potential of asymmetric CMS

membranes for olefin-paraffin separation, studied recently by Xu [10]. For olefin-paraffin separation comparison, similar mixed gas feed compositions were followed, i.e., 63.2 mol% C_2H_4 and 36.8 mol% C_2H_6, and 50 mol% C_3H_6 and 50 mol% C_3H_8.

3.4.1.3 Sorption

A pressure-decay sorption set-up [14, 15] was used for measuring the equilibrium sorption of asymmetric CMS hollow fiber samples. The schematic of the sorption set-up is shown in Figure 3.4.

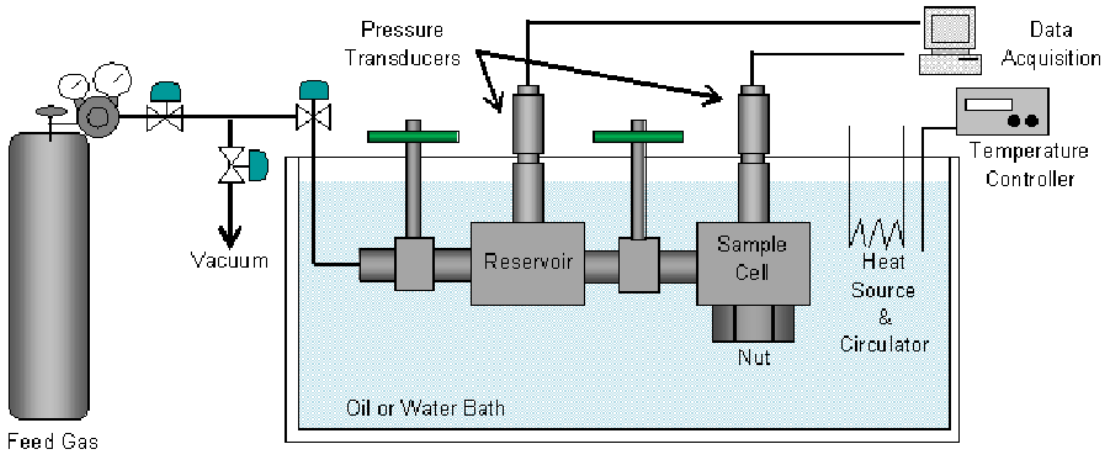

Figure 3.4: Schematic of pressure-decay sorption set-up for asymmetric CMS fiber samples [14].

The CMS hollow fiber samples was broken into small pieces, loaded into a porous stainless steel filter element (0.5 micron, Swagelok) and wrapped using aluminum foil to ensure that the sample does not fall out. The sample cell (with CMS fiber sample) was dried to 150°C in vacuum overnight to remove any sorbed moisture. After drying, the samples were loaded into the sample cell chamber, and the sorption cell was placed in an oil bath with a circulator and temperature controller to maintain uniform temperature at

35°C. The entire system was evacuated for 24 hrs prior to testing. The reservoir chamber was then charged with feed gas and the temperature was allowed to equilibrate for about 15 min. The valve between the reservoir and sample cell was then cracked to quickly introduce gas into the sample cell. The pressure in both the reservoir and sample chamber was monitored using pressure transducers and recorded over time using LabView (National Instruments, Austin, TX) until the pressure became constant.

A mole balance approach was used to obtain the amount of gas taken up by the samples as per equation (3.1) below:

$$n_{total} = n_{res}^{ini} + n_{sam}^{ini} + n_{mem}^{ini} = n_{res}^{fin} + n_{sam}^{fin} + n_{mem}^{fin} \quad (3.1)$$

Where 'n' representing the number of moles. The volume of both the reservoir (res) and sample cell (sam) is known, along with the mass and density of the sample (mem). The initial (ini) and final (fin) pressure data was recorded via Lab-View and the compressibility factors of the gases was calculated using equations listed in Appendix B. For the CMS samples, Langmuir model was issued to obtain the sorption isotherms.

3.4.2 Scanning electron microscopy (SEM)

SEM was used to characterize the morphology of both asymmetric precursor, and CMS hollow fiber membranes. The SEM LEO 1530 and 1550 was used, equipped with a thermally assisted field emission gun and operating voltage 5 kV. All fibers were coated with gold before SEM.

3.4.3 Dynamic mechanical analysis (DMA)

DMA measurements were performed on asymmetric polymeric fibers to evaluate the effect of pre-pyrolysis treatment on polymer fiber bulk-flow. The measurement was performed on single hollow fiber precursors loaded in tensile mode using a TA Q800 DMA. A frequency of 1 Hz and temperature ramp rate of 3 °C/min between 50 °C to 400 °C was used for all measurements. Since accurate estimation of the annular sample dimensions proved difficult, modulus values were estimated using diameter measurements and a solid cylindrical geometry.

3.4.4 ^{13}C solution nuclear magnetic resonance (NMR)

^{13}C solution NMR spectrum was performed at Shell Global Solutions (US) Inc. The spectrum was obtained using a Bruker Avance 500 spectrometer equipped with a 10 mm auto tune/auto shim probe. The spectra were recorded at 2000 scans under 45 degree pulse standard inverse gated quantitative carbon experiment with composite pulse decoupling. Approximately 500 mg of sample (precursor fibers and powder) was dissolved in dimethyl sulfoxide containing (0.1M) TEMPO as a free radical agent. A 1000 scan J-modulated spin echo experiment was also acquired to help in peak assignments. The solution NMR was helpful to probe the differences in chemical structure (if any) and the results are explained in Chapter 4.

3.4.5 Solid-state NMR

Solid-state NMR spectra were measured at the Georgia Tech NMR center by Johannes Leisen using a high resolution Bruker AV3-400 solid-state spectrometer. The spectrometer operated at ^{1}H frequency of 400 MHz. Both the ^{13}C and ^{29}Si solid-state

NMR spectrum were important for understanding the mechanism of pre-treatment methods explained in Chapter 4.

3.4.5.1 ^{13}C NMR spectrum

^{13}C solid state NMR spectra were recorded at Cross Polarization – Magic Angle Spinning (CP-MAS) with ^{1}H 90 degree pulse length 5 µs, MAS at 12 kHz, repetition delay of 4 s and 2000 µs contact time. The data points were recorded over 2048 points over during 24 millisecond time period, along with high power ^{1}H decoupling. Due to the conductive nature in CMS samples, some samples had to be measured using Direct Polarization (DP)-MAS. The spectrum from CP-MAS technique was averaged between 2000-8000 scans and for DP-MAS was averaged around 8000 scans. The other parameters for DP-MAS were similar to the CP-MAS technique.

3.4.5.2 ^{29}Si NMR spectrum

^{29}Si solid state NMR studies were carried out using CP-MAS with ^{1}H 90 degree pulse length 5 µs, MAS at 10 kHz contact time of 3000 µs and repetition delay of 5s. The data points were recorded over 2048 points over during 24 millisecond time period, along with high power ^{1}H decoupling. The spectrum was recorded for the data averaged between 1000-8000 scans. The referencing in ^{29}Si NMR is mostly done relative to tetramethylsilane (TMS) due to their lower boiling point, inert nature, and short relaxation time [16]. Negative values of the ^{29}Si shift are due to low frequency and high field compared to TMS.

3.4.6 Thermo gravimetric analysis (TGA)

TGA curves were obtained from STA 409PC Luxx from NETZCH. The heating protocol for TGA was maintained the same as the pyrolysis temperature profile in Table 3.4 with respective final pyrolysis temperatures under UHP Argon flow at 30 mL/min.

3.4.7 Fourier transform infrared (FTIR) spectrum

IR spectra were measured using a Bruker Tensor 27 FT-IR spectrometer equipped with a Harrick MVP 2 Series^{TM} ATR. Each sample was analyzed using 128 scans with a scanner velocity of 10 kHz with a resolution of 4 cm^{-1} and 6 mm aperture setting. The spectrum data was recorded for a scan range from 370 to 4000 cm^{-1}.

3.4.8 Elemental analysis

Elemental analysis of both the precursor and CMS samples was performed by ALS labs, Tuscon, AZ. The samples were dried a 150°C and bench ground into fine powder before the analysis. C, H and N wt% were obtained using combustion/IR explained in Appendix C. For O wt% similar pyrolysis/IR was used. Si wt% was obtained using total dissolution method and F wt% was carried out oxygen flask/bomb technique [17] analyzed by ion chromatography (IC). A more detailed procedure for each of this analysis is provided in Appendix C.

3.4.9 X-ray photoelectron spectroscopy (XPS) and sputter argon-ion etching

XPS with sputter argon-ion etching was performed to obtain the silicon depth profile in asymmetric CMS hollow fiber membranes. The spectra were acquired using a Thermo K-Alpha XPS (Thermoscientific) with a monochromatic Al Kα line, operating

under ultra-high vacuum conditions and a 100 μm spot size. Survey XPS scans were obtained over the B.E. range (0-800 eV) with a step size of 1 eV and high resolution scans typically at 20 eV pass energy. Calibration of spectra was done with the Si2p peak set to Binding Energy (BE) = 104.9 eV. Sputter depth profiling was performed using an argon ion gun operating at 3000 eV. More details of XPS-ion etching are provided in the chapters 4 and 5.

3.5 References

1. David, L. and A. Ismail, Influence of the thermastabilization process and soak time during pyrolysis process on the polyacrylonitrile carbon membranes for O_2/N_2 separation. Journal of Membrane Science, 2003. 213(1): p. 285-291.
2. Jones, C.W. and W.J. Koros, Carbon molecular sieve gas separation membranes-I. Preparation and characterization based on polyimide precursors. Carbon, 1994. 32(8): p. 1419-1425.
3. Chen, C.-C., Thermally crosslinked polyimide hollow fiber membranes for natural gas purification. Doctor of Philosophy, Georgia Institute of Technology, 2011.
4. Xu, L.; Rungta, M.; Brayden, M. K.; Martinez, M. V.; Stears, B. A.; Barbay, G. A.; Koros, W. J., Olefins-Selective Asymmetric Carbon Molecular Sieve Hollow Fiber Membranes for Hybrid Membrane-Distillation Processes for Olefin/Paraffin Separations. J Membrane Sci 2012.
5. Williams, P.J., Analysis of factors influencing the performance of CMS membranes for gas separation. Doctor of Philosophy, Georgia Institute of Technology, 2006.
6. Guiver, M. D.; Robertson, G. P.; Dai, Y.; Bilodeau, F.; Kang, Y. S.; Lee, K. J.; Jho, J. Y.; Won, J., Structural characterization and gas-transport properties of brominated matrimid polyimide. Journal of Polymer Science Part A: Polymer Chemistry 2002, 40 (23), 4193-4204.
7. Singh, R. and W.J. Koros, Carbon molecular sieve membrane performance tuning by dual temperature secondary oxygen doping (DTSOD). Journal of Membrane Science, 2012. 427: p. 472-478.
8. Clausi, D.T., Formation and characterization of asymmetric polyimide hollow fiber membranes for gas separations. 1998: Doctor of Philosophy, The University of Texas at Austin.
9. Xu, L., M. Rungta, and W.J. Koros, Matrimid® derived carbon molecular sieve hollow fiber membranes for ethylene/ethane separation. Journal of Membrane Science, 2011. 380(1-2): p. 138-147.
10. Xu, L., Carbon Molecular Sieve Hollow Fiber Membranes For Olefin/Paraffin Separations. Doctor of Philospohy, Georgia Institute of Technology, 2012.
11. Rungta, M., L. Xu, and W.J. Koros, Carbon molecular sieve dense film membranes derived from Matrimid® for ethylene/ethane separation. Carbon, 2012. 50(4): p. 1488-1502.
12. Vu, D.Q., W.J. Koros, and S.J. Miller, High pressure CO2/CH4 separation using carbon molecular sieve hollow fiber membranes. Industrial & Engineering Chemistry Research, 2002. 41(3): p. 367-380.
13. Pye, D.G., H.H. Hoehn, and M. Panar, Measurement of gas permeability of polymers. I. Permeabilities in constant volume/variable pressure apparatus. Journal of Applied Polymer Science, 1976. 20(7): p. 1921-1931.
14. Kiyono, M., Carbon molecular sieve membranes for natural gas separations. Doctor of Philosophy, Georgia Institute of Technology, 2010.

15. Koros, W.J. and D. Paul, Design considerations for measurement of gas sorption in polymers by pressure decay. Journal of Polymer Science: Polymer Physics Edition, 1976. 14(10): p. 1903-1907.
16. Uhlig, F. and H.C. Marsmann, 29 Si NMR Some Practical Aspects. Gelest Inc.,.
17. Third Supplement to the Fourth Edition of The International Pharmacopoeia.; http://apps.who.int/phint/en/p/docf/].

CHAPTER 4

METHODOLOGY TO RESTRICT SUB-STRUCTURE COLLAPSE IN ASYMMETRIC CMS HOLLOW FIBER MEMBRANES

4.1 Overview

This chapter will focus on the mechanism of sub-structure collapse and various methodologies used in an attempt to restrict the collapse. A novel pre-pyrolysis treatment is developed to restrict the morphology collapse in asymmetric carbon molecular sieve (CMS) hollow fiber membranes. The technique is referred to as V-treatment due to the use of a sol-gel crosslinking reaction between an organic-alkoxy silane (vinyltrimethoxysilane) and moisture. V-treatment results in significant improvement of asymmetric CMS microscale morphology, increasing the gas productivities of CMS V-treated membranes. Several characterization analyses are presented to verify the proposed mechanism of stabilization and obtain insights for further optimization. The effect of V-treatment are presented for two different polyimide precursors Matrimid® and 6FDA:BPDA-DAM.

4.2 Methodologies investigated for restricting sub-structure collapse

Low permeances are an area of concern for the industrial scale-up of CMS hollow fiber membranes. The permeance decrease in CMS hollow fibers is observed due to the densification of the porous support during the pyrolysis process [1]. The magnitudes of sub-structure collapse and selective layer thickening in asymmetric CMS hollow fibers from Matrimid® (~40x) and 6FDA:BPDA-DAM (~16x) precursors are shown in Figure 4.1 and 4.2 respectively.

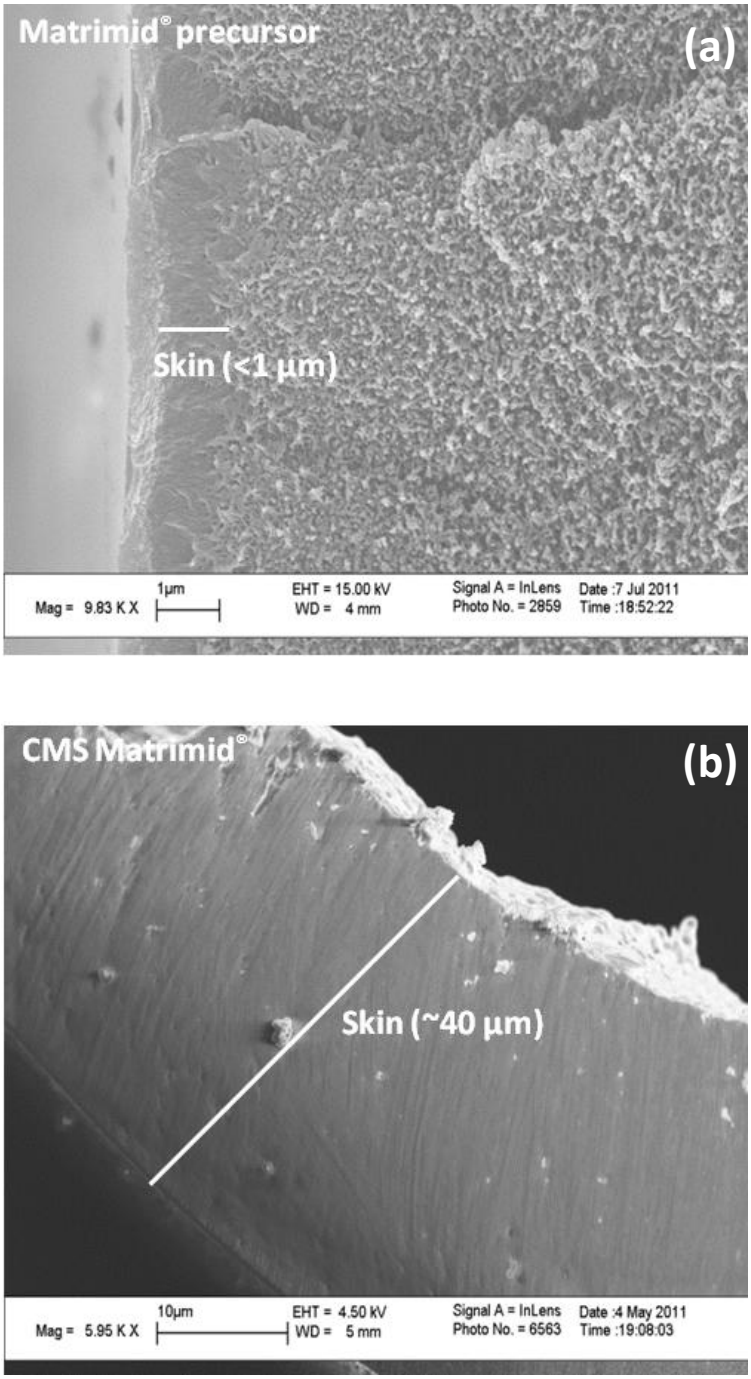

Figure 4.1 SEM images of (a) Matrimid® precursor hollow fiber and (b) CMS hollow fiber from Matrimid® precursor.

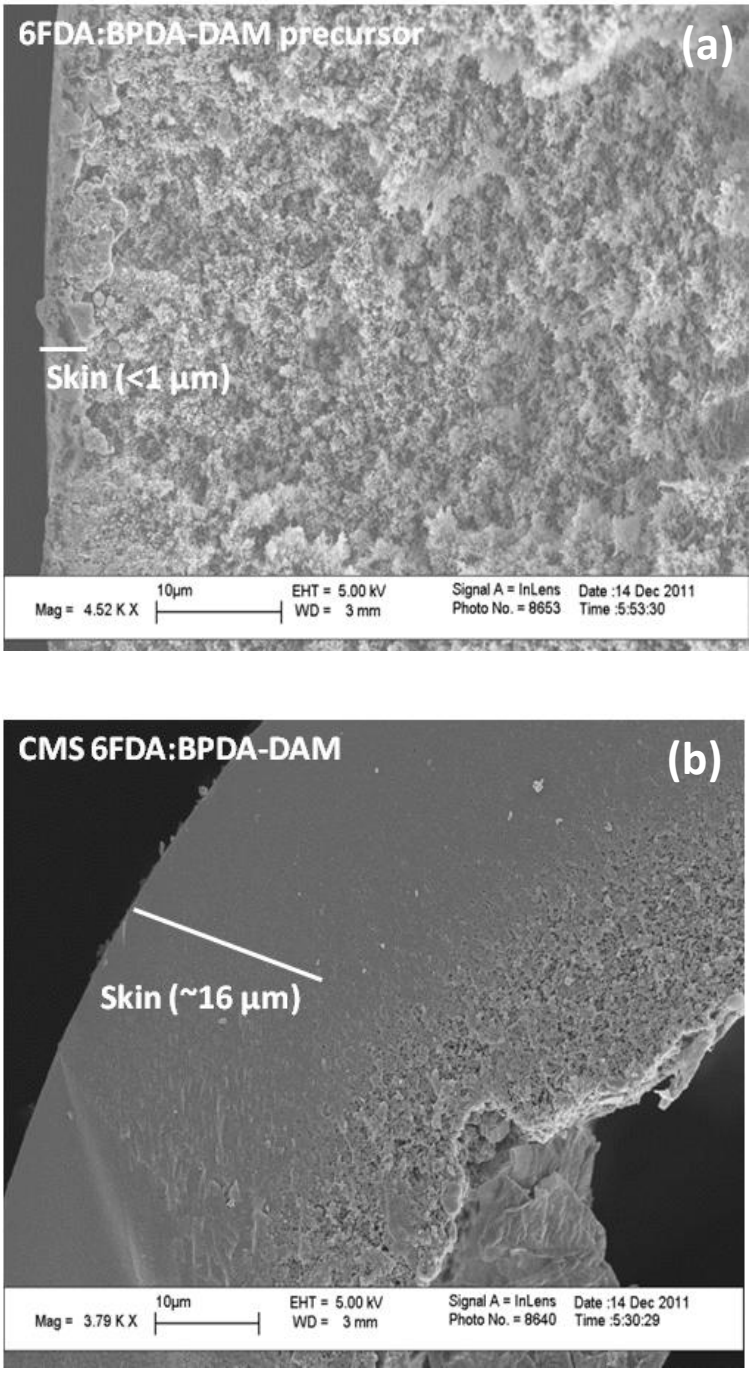

Figure 4.2 SEM images of (a) 6FDA:BPDA-DAM precursor hollow fiber and (b) CMS hollow fiber from 6FDA:BPDA-DAM precursor.

The spinning process that was described earlier is designed in such a way that the resultant polymer precursor hollow fiber has an asymmetric structure with a nano-scale separation skin. The substructure pores formed during spinning do not allow a uniform well-packed distribution of polymer chains in the precursor morphology. During heat treatment (pyrolysis) when temperature crosses the glass-rubber transition (T_g) of the polymer precursor, the un-oriented polymer chains enter into a soft and viscous zone which increases the chain mobility, thereby enabling segments to move closer to each other. This heat treatment above T_g increases the chain packing density, resulting in the substructure morphology collapse. The chain mobility of Matrimid® precursor at T_g characterized by a DMA plot of storage modulus vs. temperature [2] is shown in Figure 4.3(a). SEM image of a Matrimid® precursor fiber wall after being heated slightly above T_g i.e., up to 350 °C (isothermal for 30 mins) is shown in Figure 4.3(b). Essentially the entire Matrimid® precursor fiber wall which had a separation skin (<1 μm) as shown in Figure 4.1(a) is completely collapsed at T_g.

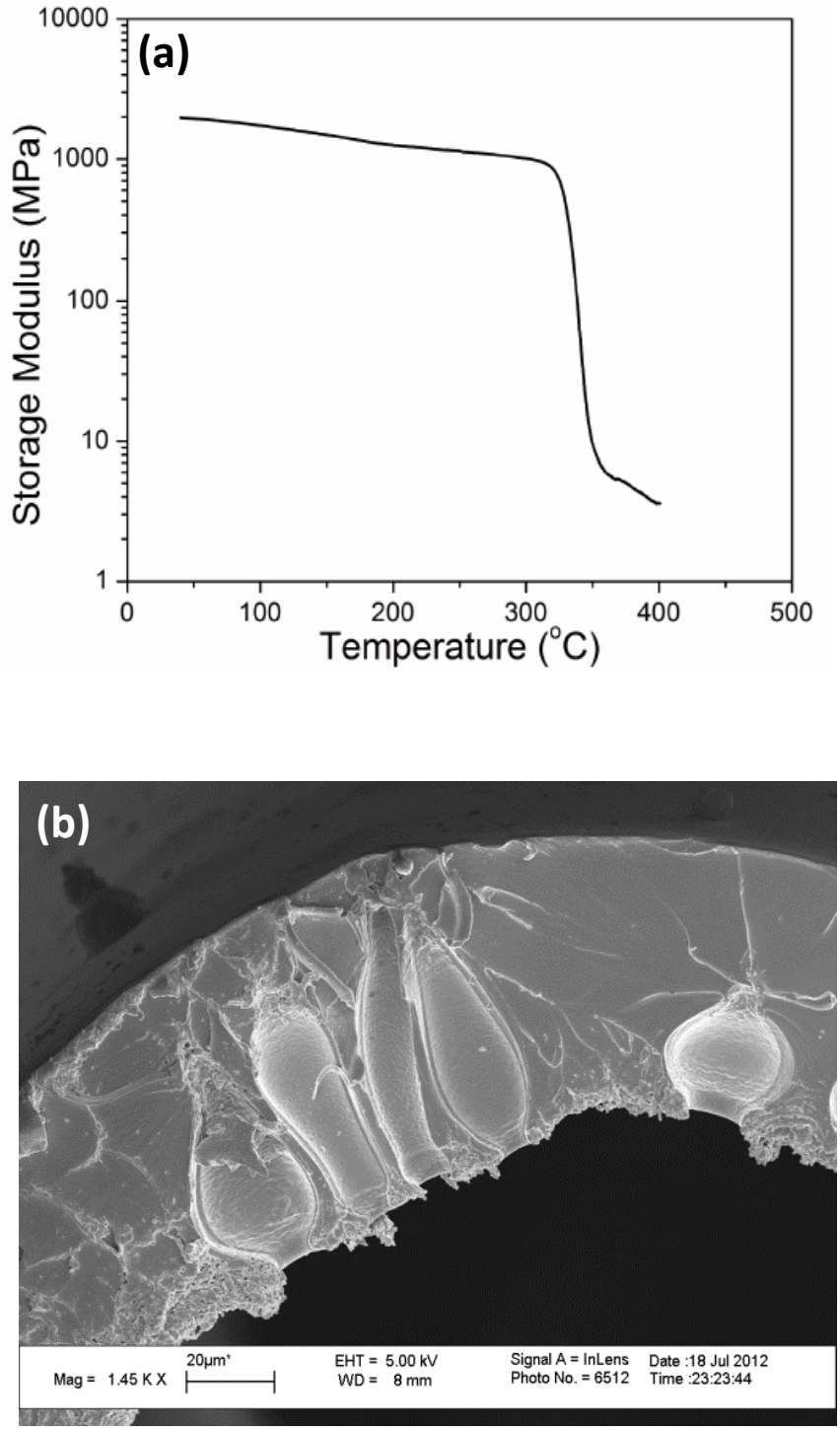

Figure 4.3: (a) DMA plot of an untreated Matrimid® polymer precursor dense film as reported previously [2] (b) SEM image of a untreated Matrimid® hollow fiber heated up to 350 °C for 30 mins.

In spite of an increase in permeability (P) of the intrinsic CMS dense skin (compared to the polymer precursor permeability), the final CMS permeance (i.e., P/*l*) still remained low because of the pronounced increase in separation membrane skin thickness (*l*) at T_g (~40x densification as shown in Figure 4.1(b)). For the case of Matrimid® precursor which has the highest degree of collapse, a comparison of precursor and CMS CO_2 productivities in dense film and hollow fiber is shown in Table 4.1.

Table 4.1: Comparison of precursor and CMS CO_2 productivities in dense film and hollow fiber membrane ([a]dense film permeation data from Kiyono *et al.* [3], [b]CMS untreated hollow fiber – This study).

	Untreated Matrimid® precursor	CMS from untreated Matrimid® precursor
Dense film membrane[a] (CO_2 Permeability)	**10 Barrers**	**1049 Barrers**
Hollow Fiber membrane[b] (CO_2 Permeance)	**42 GPU**	**25 GPU**

Xu *et al.* [4] observed that the 6FDA based polymer precursors exhibited a lower degree of substructure collapse in comparison with Matrimid® precursor because of the rigid structure and higher T_g. SEM images for both CMS hollow fiber membranes from untreated Matrimid® and 6FDA:BPDA-DAM are shown in Figures. 4.1 and 4.2. CMS hollow fibers from 6FDA:BPDA-DAM exhibited a lower degree of collapse, but still a significant amount of densification (~16x) in membrane skin thickness (*l*) was observed as shown in Figure 4.2.

4.2.1 Pre-pyrolysis treatment on polymer precursor hollow fiber

As shown for the Matrimid® precursor in Figure 4.3(a), the primary cause for morphology collapse during pyrolysis is the order of magnitude drop in storage modulus

at T_g,. To restrict collapse it is important to stabilize the polymer precursor before the glass-rubber transition to suppress the bulk flow mobility of polymer chains. Some different approaches were investigated in an earlier part of the work, which can be broadly classified into:

(i) Chemical and thermal pre-pyrolysis treatment on polymer precursors

For stabilizing the polymer precursors, 'puffing agents' (like polyethylene glycol–PEG) were filled in precursor pores prior to pyrolysis [5], chemical crosslinking using diamine linkers: reaction mechanism involves opening of imide rings to form amides [6-8], thermal stabilization below T_g to induce charge transfer complexes in the precursor structure [9, 10], and hydrogen abstraction grafting-crosslinking reaction using peroxide and silanes [11]. The pre-treatment procedures and results for each of the treatments are provided in Appendix C.

Though none of the above pre-treatments were favorable in terms of restricting collapse, they were essential for establishing the platform for the effect of pre-treatment on asymmetric CMS substructure morphology. The control of pre-treatment studies leads to the ultimate advantageous technique, explained in section 4.3.

(ii) Tuning of pyrolysis temperature profile (i.e. high ramp-rates)

Some researchers have achieved slightly increased gas permeabilities of CMS dense films by pyrolysing precursors at higher ramp-rates [12]. The subtle change in CMS permeability by using higher ramp-rate was not sufficient to give a significant improvement in terms of gas permeances. The details for the ramp-rates used and the resultant CMS hollow fiber performance are given in Appendix C.

4.3 Sol-gel approach to restrict substructure collapse in asymmetric CMS membranes (V-treatment)

After exploring several other engineering routes, hydrogen abstraction crosslinking using VTMS [11] was applied for Matrimid® polymer precursor. Even though the extreme peroxide reaction conditions were found to be unsuitable for polymer fibers, the actual sol-gel reaction of VTMS was beneficial for restricting collapse. Hence, VTMS here was used as a starting 'morphology stabilizer'.

For the treatment, precursor fibers were exposed to an organic-alkoxy silane and moisture to undergo a sol-gel reaction which proceeds via hydrolysis and condensation of methoxy groups as shown in Figure 4.4 [13-15]. The sol-gel reaction of organic-alkoxy silanes is commonly used in the paint and adhesives industry, where the silanes act as 'moisture scavengers' to improve adhesives strength [16, 17]. A related reaction mechanism has been commonly used to prepare silica membranes for high temperature separation applications [18, 19].

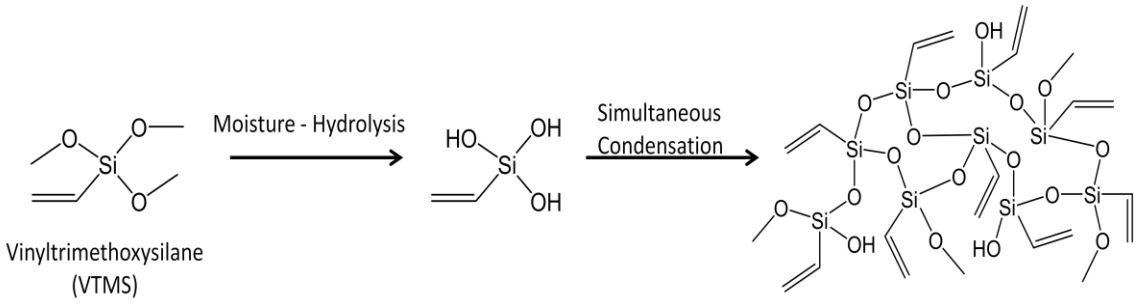

Figure 4.4: Sol-gel crosslinking reaction of VTMS in presence of moisture at 25 °C.

The precursor fibers after the spinning process were saturated with VTMS liquid first and then exposed to ambient moisture at 25 °C. The purpose of saturating the fibers with silane-moisture was to create organic crosslinked silica on the fiber pore walls via

the sol-gel crosslinking reaction between VTMS and moisture [14]. Since the reaction process was a pre-pyrolysis step carried out using VTMS, for convenience it is referred to as “V-treatment”.

The above reaction was carried out at ambient conditions (i.e., room temperature 25 °C and different relative humidity conditions). The VTMS saturated fibers were kept in ambient conditions for about 24 hours to create the crosslinked silica. Before starting the pyrolysis, silane treated fibers were heated to 150 °C for 12 hours in vacuum to remove unreacted VTMS and moisture (B.P. of VTMS: 123 °C).

4.3.1 V-treatment reaction condition selection

For V-treatment, different temperatures (up to 200°C) and reaction times were also explored in both ambient (~30-40 %RH), and 100% RH humidity. The reason to keep the treatment condition closer to ambient conditions was for process simplification and easy scalability for industrial purposes, such as post spin solvent exchange treatment.

Both functional groups in VTMS were crucial for V-treatment. The alkoxy (methoxy) group was important for creating sol-gel and reactive organic (vinyl) group for mechanical properties and rearrangement of silica residue during pyrolysis. For testing the effect of both functional groups separately, three different silanes i.e., vinyl trimethyl silane, trimethoxy silane (TMS), and ethyl trimethoxy silane (ETMS) were explored. The details for each of the non-VTMS silane treatment are provided in the Chapter 5.

Another important condition for V-treatment was the use of 100% VTMS. The results for 100% VTMS are shown in this chapter to illustrate the actual treatment

mechanism. Various other concentrations of VTMS (in different non-solvents) are also studied and are discussed in Chapter 5.

4.3.2 Mechanism of V-treatment in restricting sub-structure collapse

The mechanism of V-treatment substructure protection in CMS membrane formation appears to restrict the bulk polymer precursor chain mobilization during pyrolysis. By performing V-treatment, crosslinked silica was formed at the surface of micropores in the hollow fiber support via a sol-gel reaction of VTMS and moisture (Figure 4.4). The schematic representation of V-treatment in the overall CMS fabrication process is shown in Figure 4.5.

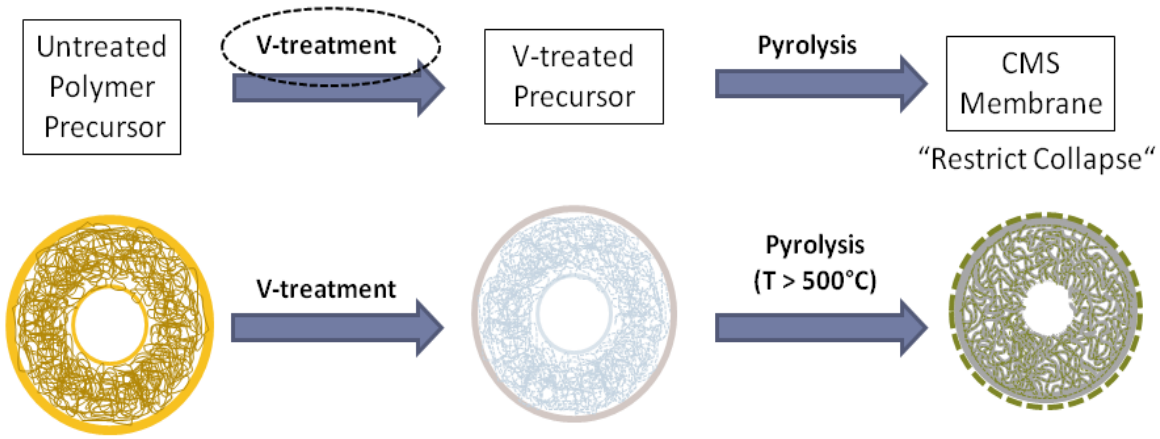

Figure 4.5: Schematic representation of V-treatment process in the overall CMS formation

The first step in Figure 4.5 is the V-treatment process, where the sol-gel reaction occurs when the VTMS molecule comes into contact with moisture to form the vinyl-crosslinked silica layer. The sol-gel reaction mostly occurred at two places i.e., on the substructure pore walls and on the outer-most surface of the precursor fiber. This is confirmed by the presence of siloxane chains (Si-O-Si) in the polymer precursor as

characterized by ^{29}Si solid-state NMR as discussed in section 4.4.5. The step 2 in Figure 4.5 is pyrolysis of V-treated precursor to form the final asymmetric CMS hollow fiber membrane. The majority of silica remained in the V-treated Matrimid® based CMS sample, which was confirmed through ^{29}Si solid-sate NMR (section 4.4.5), TGA (section 4.4.7) and elemental analysis (section 4.4.8) characterizations.

In order to illustrate the silicon distribution in the final asymmetric CMS V-treated membrane, a schematic representation is shown in Figure 4.6. As analyzed by XPS in section 4.4.9, the majority of silicon was observed on the outermost surface of the intrinsic CMS skin as a combination of SiO_2, silica carbide (Si-C), and siloxane bridges (Si-O-Si). SiO_2 was mostly present on the outermost surface of silica and as etching proceeded into the silica-CMS surface, the percentage of silicon decreased and the silicon chemical moieties changed to Si-C and Si-O-Si bridges. More detail into the surface characterization of asymmetric CMS V-treated Matrimid® hollow fiber membrane through XPS is discussed in section 4.4.9.

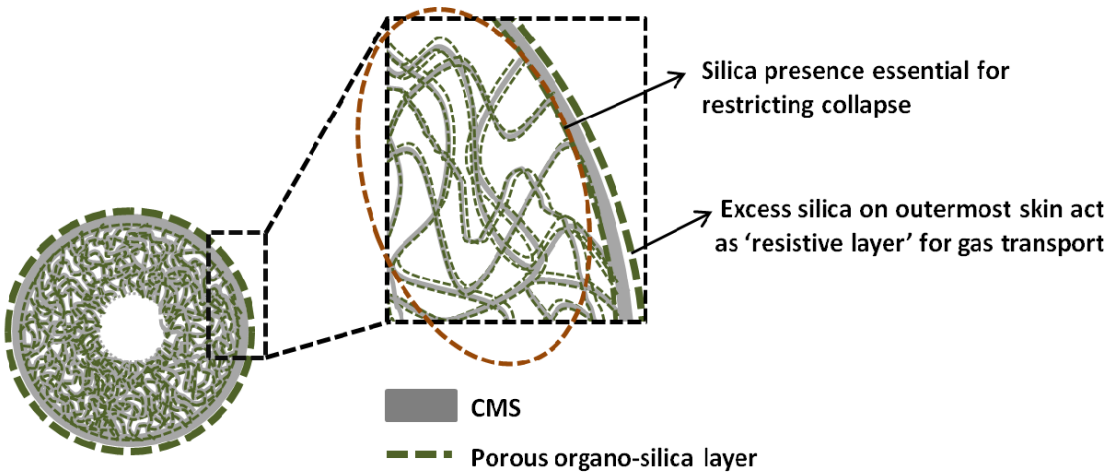

Figure 4.6: Schematic representation of silicon distribution on the asymmetric CMS V-treated structure

Even though the silica in CMS substructure pores is essential for preventing the collapse, excess silica on the outermost surface of intrinsic CMS skin is not desirable. The silica layer on CMS skin act as an additional resistive layer which limits gas separation properties. Hence optimization studies for V-treatment to circumvent the excess silica are required. The VTMS concentration in V-treatment plays a significant role in reducing the excess silica and even further enhancing the transport properties. The optimization study is presented in Chapter 5. Nevertheless, the enhancement with 100% VTMS V-treatment for both Matrimid® and 6FDA:BPDA-DAM precursors shown here are important advances compared to any other current technology and hence been focused in this chapter to show the fundamental effect of V-treatment.

4.4 Characterization of V-treatment

4.4.1 SEM characterization of asymmetric CMS hollow fiber membranes

Asymmetric CMS hollow fiber membranes from both V-treatment Matrimid® and 6FDA:BPDA-DAM showed an improvement in substructure morphology. As shown in the SEM image in Figure 4.1(b), the CMS membrane skin thickness (*l*) from untreated Matrimid® precursor is close to the entire membrane wall (~40 μm). For the case of CMS hollow fiber from untreated 6FDA:BPDA-DAM precursor (Figure 4.2(b)), the collapse is less compared to Matrimid® precursor; however, there is still a significant increase in membrane skin thickness (*l*) to ~16 μm. After pyrolysis of both the V-treated precursor fibers, a reduction of 5-6x was observed in CMS membrane skin thickness (*l*) versus untreated precursor, as shown in the SEM images Figures 4.7 and 4.8. SEM analysis is summarized in Table 4.2.

Table 4.2: Comparison of asymmetric CMS membrane skin thickness from untreated and V-treated precursors (SEM)

	Asymmetric membrane skin thickness in hollow fiber (*l*) from SEM		
	Membrane precursor skin before any treatment	CMS membrane from untreated precursor	CMS membrane from V-treated precursor
Matrimid®	< 1 μm	~40 μm	~5-6 μm
6FDA:BPDA-DAM		~16 μm	~3-4 μm

This comparison is a semi-quantitative approach to determine the membrane skin thickness, and the more accurate way to determine the skin thickness in asymmetric membranes is to take the ratio of the dense film permeability and hollow fiber permeance. Since the V-treatment is more of a substructure morphology treatment, it is hard to determine the exact permeability of CMS dense film from the V-treated precursor (as no micropore support morphology exists in dense film). A less selective silica membrane would get deposited on the dense film surface acting as a resistive layer. Nevertheless, the improvement of V-treatment in CMS membrane skin thickness was accompanied by a very large increase in final asymmetric CMS permeance as discussed in section 4.5.

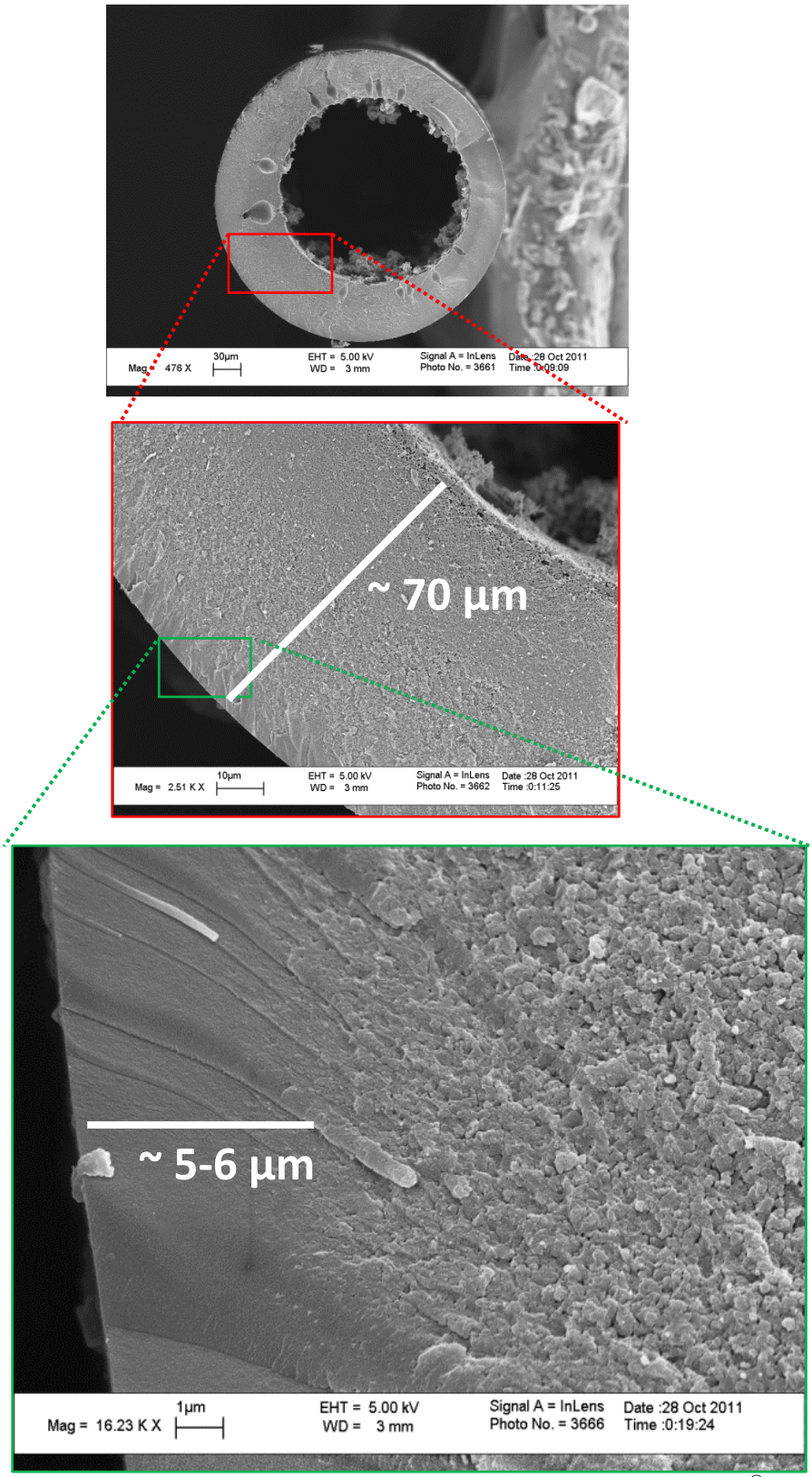

Figure 4.7: SEM images of CMS hollow fiber from V-treated Matrimid® precursor showing improved substructure morphology.

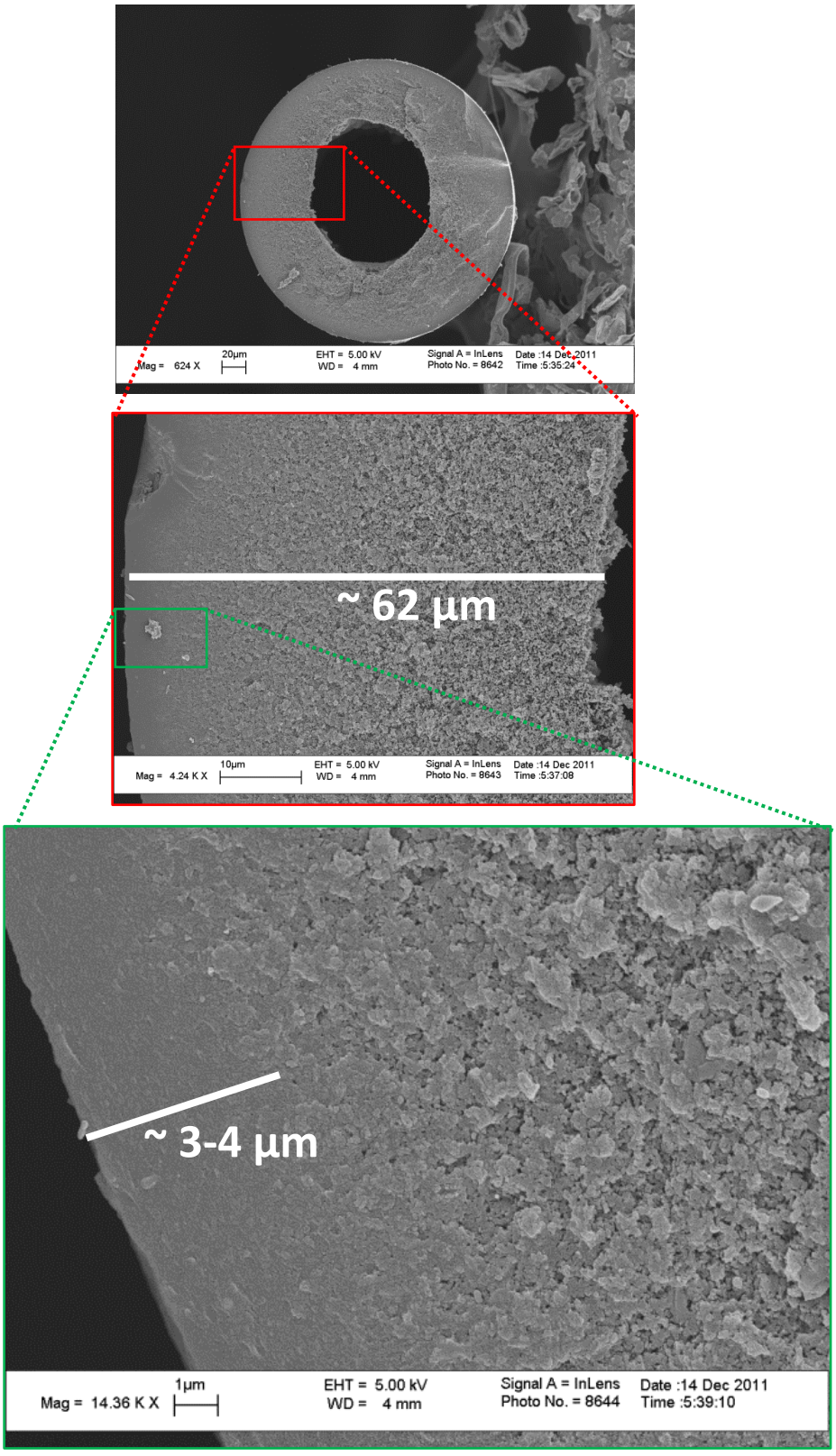

Figure 4.8: SEM images of CMS hollow fiber from V-treated 6FDA:BPDA-DAM precursor showing the improved morphology.

4.4.2 DMA on untreated and V-treated Matrimid® precursor hollow fiber membranes

Dynamic mechanical analysis (DMA) study was performed on both the untreated and V-treated Matrimid® polymer precursor hollow fibers. The mechanism of sub-structure collapse in untreated Matrimid® polymer hollow fiber is enabled by the decrease in storage modulus by several orders of magnitude at T_g as shown in Figure 4.3(a). The study in Figure 4.3(a) was done on a polymer precursor dense film [2], the modulus value at 25°C was reported to be around 2000 MPa. In this section, DMA study was extended to polymer precursor hollow fibers and plotted as storage modulus vs. temperature as shown in Figure 4.9. Because of the asymmetric structure with porous micro-support, the storage modulus at 25°C was around 350 MPa which was lower than the precursor dense film modulus. The details on the DMA experimental conditions are illustrated in Chapter 3.

In Figure 4.9, the untreated Matrimid® polymer fiber (purple curve) starts losing storage modulus significantly at T_g and continues to decrease until the sample shape is lost at ~365 °C. In comparison, V-treated Matrimid® polymer fibers (green curve) have a significantly better thermal stability at T_g. Interestingly, the storage modulus goes through a minimum at ~365 °C before increasing again throughout the remainder of the test. The modulus vs. temperature behavior is attributed to the silica forming a reinforcing glass throughout the porous substructure, thus imparting increased rigidity and preventing further sample deformation.

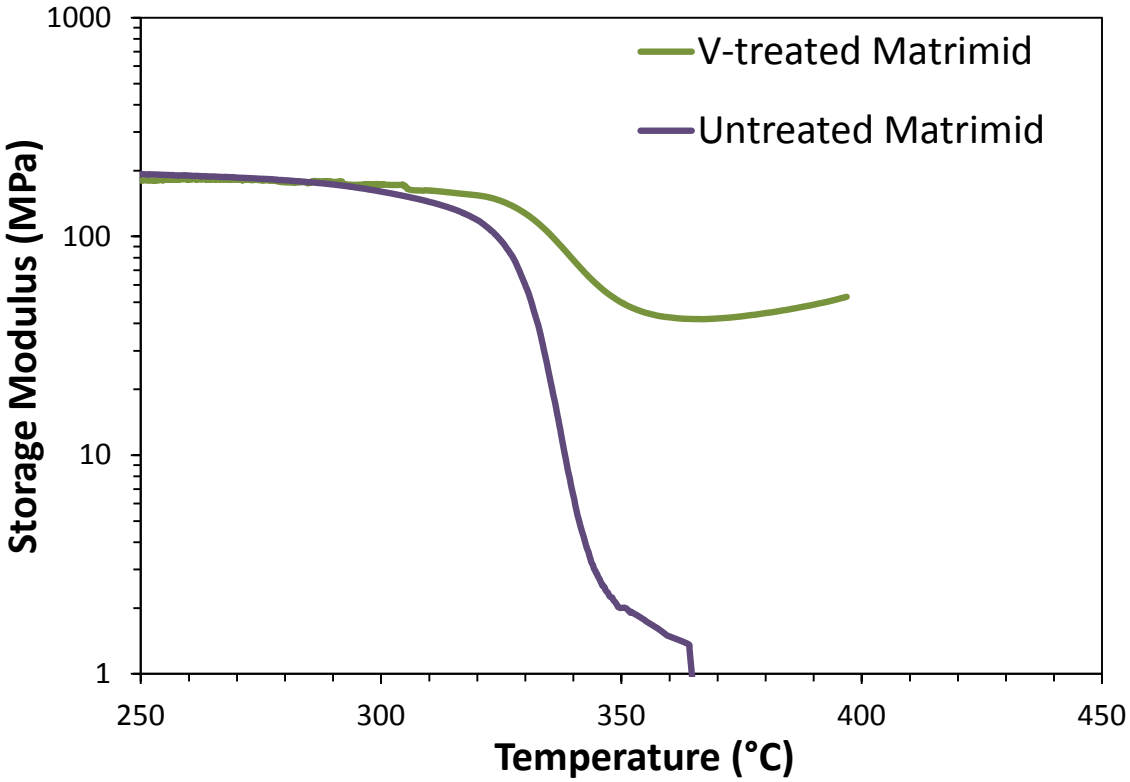

Figure 4.9: DMA for the untreated and V-treated Matrimid® precursor hollow fibers (storage modulus).

Aside from storage modulus, the tan delta also reveals an interesting aspect of the V-treatment process specific to the beta relaxation. Matrimid® is known to exhibit two sub-T_g relaxation processes, both of which correspond to short-range motion and are less cooperative than the T_g [2]. Smoothed tan delta values corresponding to the T_g for the untreated and V-treated precursor fibers are shown in Figure 4.10, with the beta relaxation shown in the inset. Of special inset in Figure 4.10 is the fact that the beta relaxation amplitude for the V-treated fiber is significantly depressed when compared to the untreated precursor fiber. As the beta relaxation reflects a combination of underlying complex interactions, understanding which motions are suppressed as a result of the V-treatment remains a challenge. Multi-frequency DMA studies could be used to measure

the beta peak activation energy and to further investigate the effect of V-treatment, but are outside the scope of the current work.

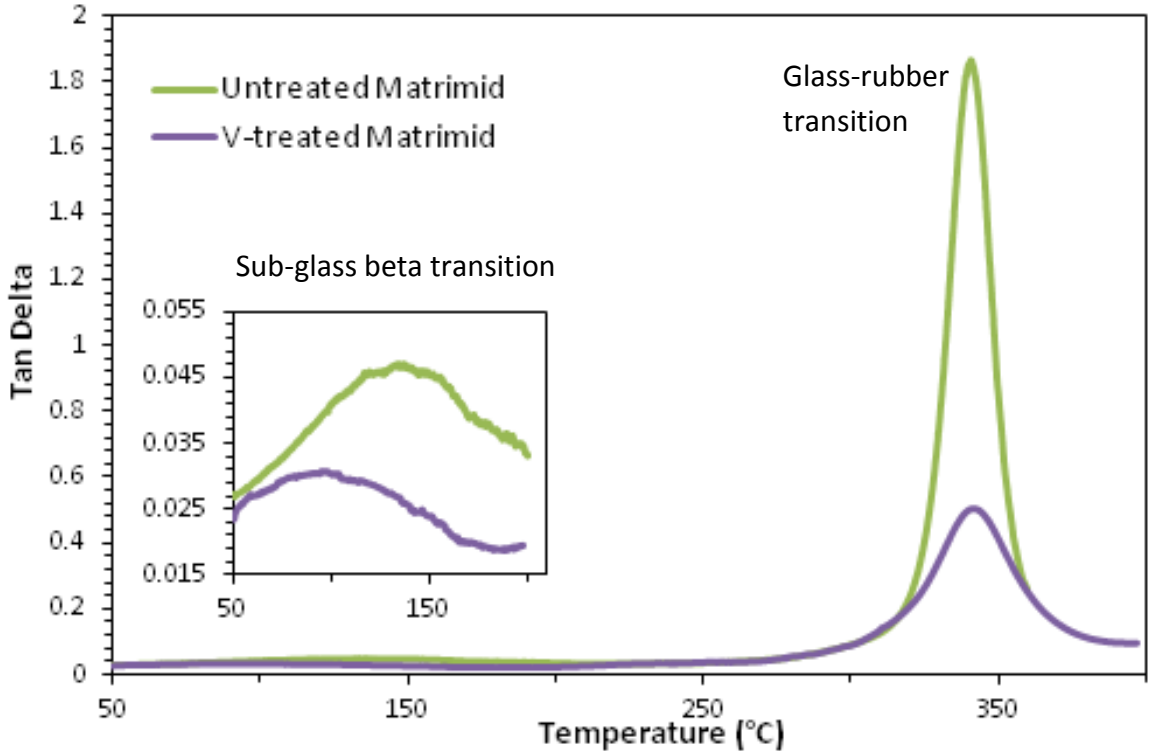

Figure 4.10: DMA for the untreated and V-treated Matrimid® precursor hollow fibers (Tan delta).

4.4.3 ^{13}C Solution NMR on untreated and V-treated Matrimid® precursors

^{13}C solution NMR spectra were obtained for both the untreated and V-treated Matrimid® polymer precursor as shown in Figure 4.11. No sign of chemical reaction between vinyl crosslinked silica and Matrimid® molecular structure could be observed. The V-treated Matrimid® precursor showed exactly the same ^{13}C NMR spectra as untreated Matrimid® precursor with all the corresponding precursor structure carbon peaks [20]. This verifies the hypothesis that V-treatment is mainly a 'substructure morphology' treatment on the polymer precursor without having any significant chemical

reaction with the polymer molecular structure. The list of all the carbon numbers in Matrimid® repeat unit and corresponding peaks (ppm) can be found in reported studies [20].

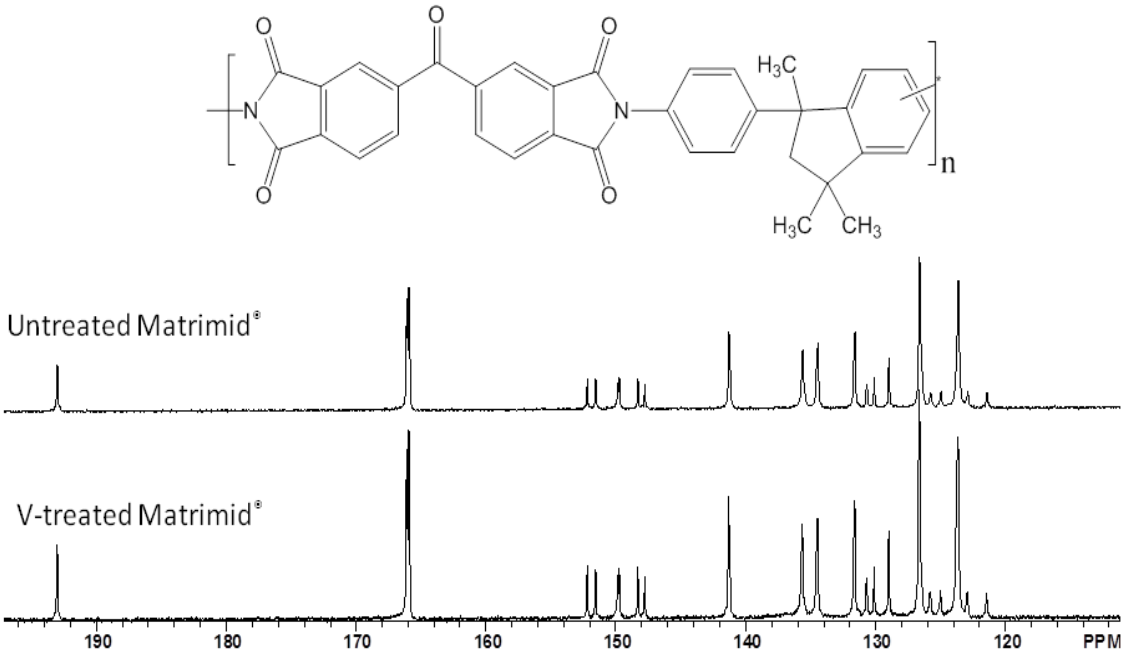

Figure 4.11: ^{13}C solution NMR spectrum of untreated and V-treated Matrimid® precursor.

The presence of vinyl carbons in V-treated Matrimid® precursor was not evident in ^{13}C solution NMR spectrum. The lower amounts and overlapping of olefinic carbon in crosslinked silica (Figure 3) compared to the carbons in Matrimid® structure makes detection difficult in solution NMR. Some slight evidence of olefinic carbon in V-treated polymer sample could be observed from solid-state ^{13}C NMR as shown in Figure 4.12.

4.4.4 Solid-state NMR (^{13}C) on untreated and V-treated Matrimid® precursors

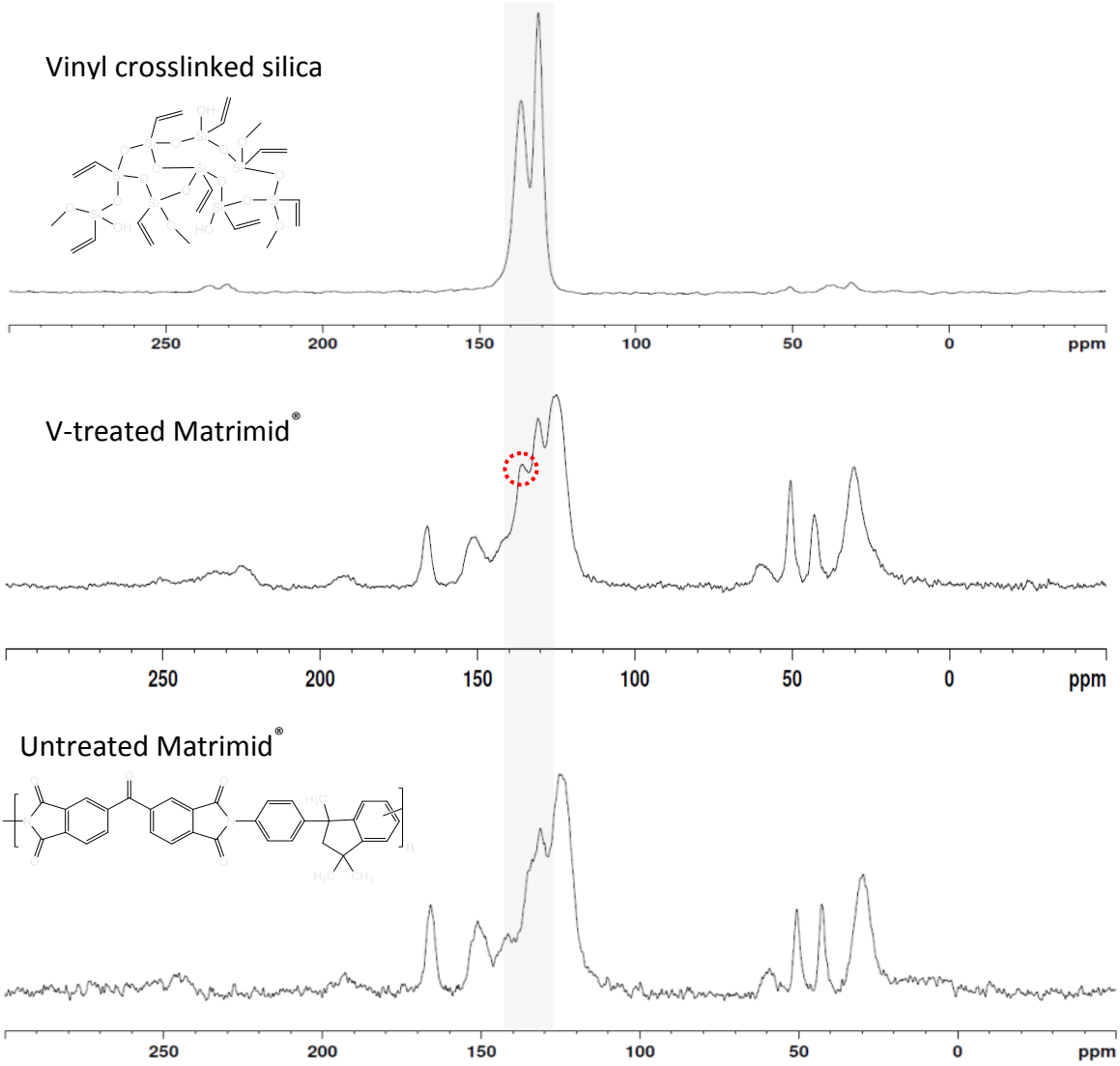

Figure 4.12: ^{13}C solid state NMR spectrum (top) vinyl crosslinked silica film (middle) V-treated Matrimid® and (bottom) untreated Matrimid® precursors.

The (top) ^{13}C NMR spectrum in Figure 4.12 is from a vinyl crosslinked silica film. The film was formed by exposing the VTMS liquid to a humid atmosphere (RH 100%) for 24 hours, giving a silica film upon methanol evaporation. Similar to solution NMR, even in solid-state NMR most of the carbon peaks for V-treated (middle) and

untreated (bottom) Matrimid® precursor correlate with each other. In Figure 4.12 (middle) the spectrum of V-treated Matrimid®, a small peak ~140 ppm in the range of olefinic carbon from vinyl group (top spectrum) was observed. This indicates the presence of the vinyl dispersed in the polymer precursor sample.

4.4.5 Solid-state NMR (^{29}Si) on V-treated Matrimid® precursor and CMS V-treated Matrimid®

In addition to ^{13}C solid-state NMR, ^{29}Si solid-state NMR was also performed on the V-treated Matrimid® precursor shown in Figure 4.13(top). ^{29}Si NMR was also performed on the CMS from V-treated Matrimid® pyrolysed at 550°C and shown in Figure 4.13(bottom). The chemical shifts in ^{29}Si NMR are based on tetra methyl silane ($(CH_3)_4Si$) as a reference at 0 ppm [21].

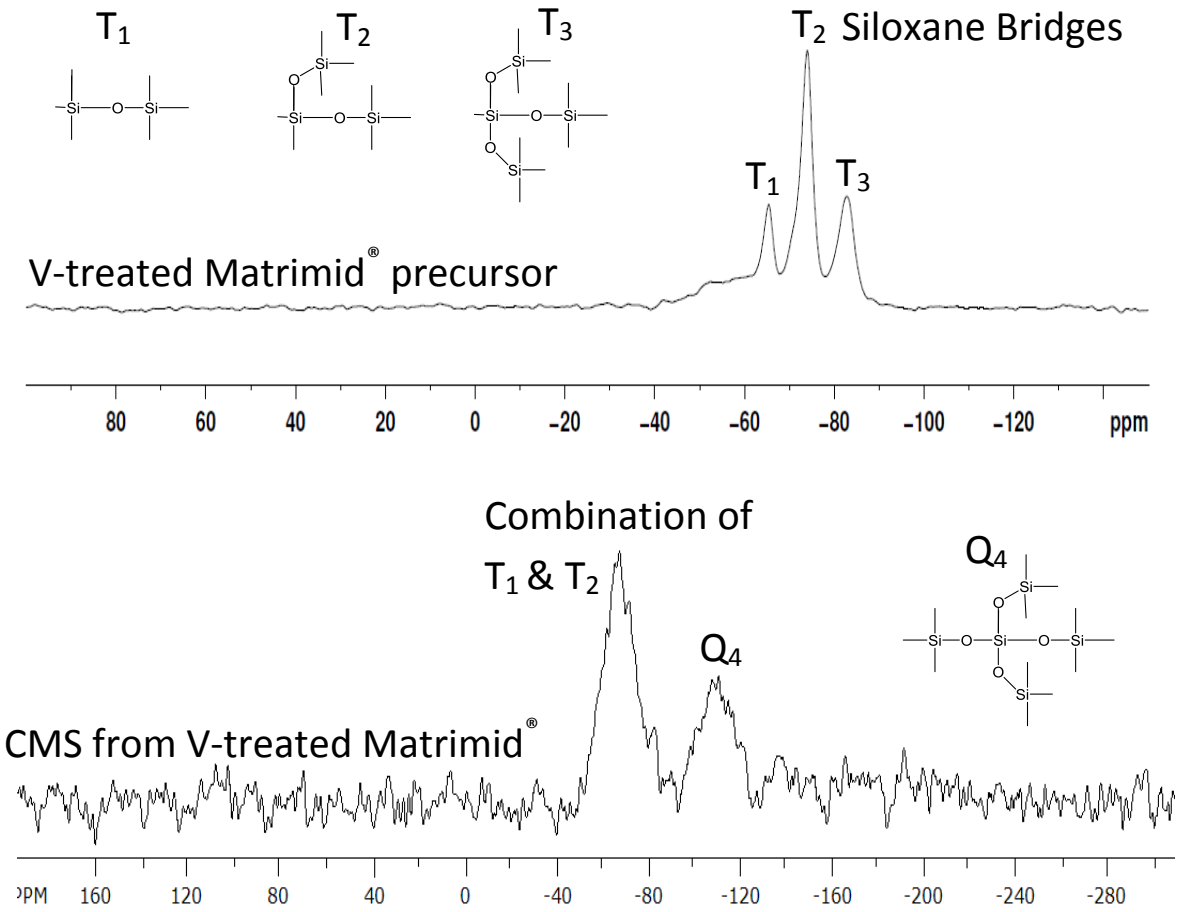

Figure 4.13: ^{29}Si solid state NMR spectrum V-treated Matrimid® precursor (top), and CMS V-treated Matrimid® pyrolysed at 550°C (bottom).

The presence of siloxane bridges (Si-O-Si) was observed in both V-treated Matrimid® precursor and CMS from V-treated Matrimid® (Figure 4.13). The single VTMS molecule should show a peak at -55 ppm and the peaks get shifted upon hydrolysis and condensation of methoxy groups [14]. After the sol-gel reaction of VTMS at current V-treatment conditions (i.e., 25°C and 30-40% RH for 24 hours), a distribution of siloxane bridges was observed for the V-treated Matrimid® precursor as shown in Figure 4.13(top). The tri-functional (T) siloxane bridges in V-treated precursor are

bonded to vinyl at one end and hydroxide (-OH) or another siloxane on other ends. The tri-functional siloxane distribution can be denoted by the following notation i.e., T_n = -Si(OSi)$_n$OH$_{(3-n)}$ [22]. The peaks for T_1 are observed at -65 ppm, T_2 at -73 ppm and T_3 at -81 ppm.

After pyrolysis, the CMS V-treated Matrimid® spectrum in Figure 4.13(bottom) indicated the change in silica structure. The T_3 peak at -81 ppm (Fig 13(bottom)) shifted to -110 ppm corresponding to a Q_4 (i.e., tetra siloxane bridges –Si-(O-Si-)$_4$) structure. The Q_4 peak results from to the loss of vinyl group at temperatures greater than 500 °C [23]. The remaining siloxane bridges (T1 and T2) in Fig 4.13(bottom), merges into a single broad peak at ~-68 ppm.

4.4.6 FTIR-ATR on untreated and V-treated Matrimid® precursors

In addition to the above NMR data-set, FTIR-ATR spectra were also obtained for untreated and V-treated Matrimid® precursor. The FTIR spectra correlate well with the NMR results, and the proposed hypothesis of no reaction between silica and the polymer precursor. The FTIR spectrum in Figure 4.14 shows the (red) V-treated precursor to have an additional peak ~1050 cm^{-1} which corresponds to siloxane bridges (Si-O-Si) [23].

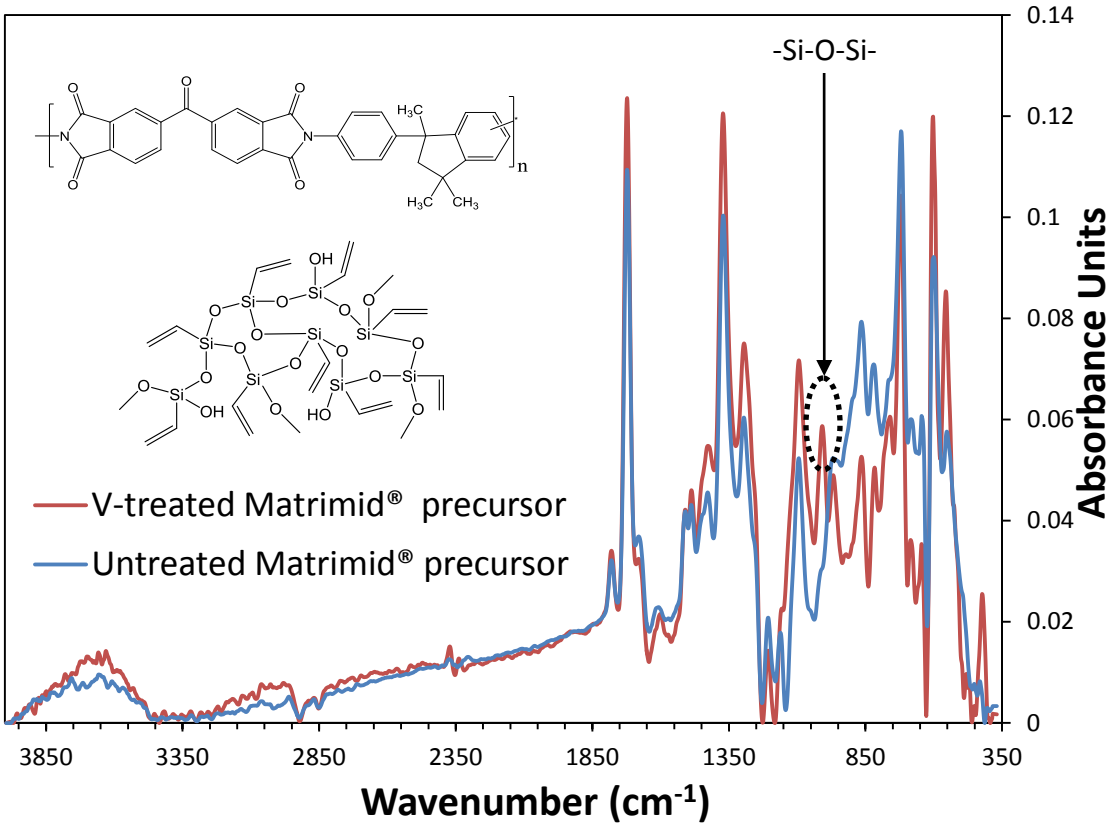

Figure 4.14: FTIR spectrum (ATR) for Untreated and V-treated Matrimid® polymer precursor.

4.4.7 TGA on untreated and V-treated Matrimid® precursors

The thermal stability of V-treated Matrimid® was evaluated by performing TGA on three different samples: vinyl crosslinked silica film (Figure 4.15), untreated and V-treated Matrimid® precursors (Figure 4.16) at the same pyrolysis temperature profile of 550°C.

The TGA plot of vinyl crosslinked silica film in Figure 4.15 has two distinctive weight losses. The first loss started immediately above 100°C indicating loss of moisture and any unreacted VTMS molecule, and the second loss was at temperatures above 500°C, showing the reaction of vinyl group in silica. The two losses suggest the

hypothesis of Q_4 structure formation (^{29}Si NMR in Figure 4.13(bottom)). The majority of the silica remained as a porous amorphous material (~87 wt%) in the CMS sample even after 550 °C.

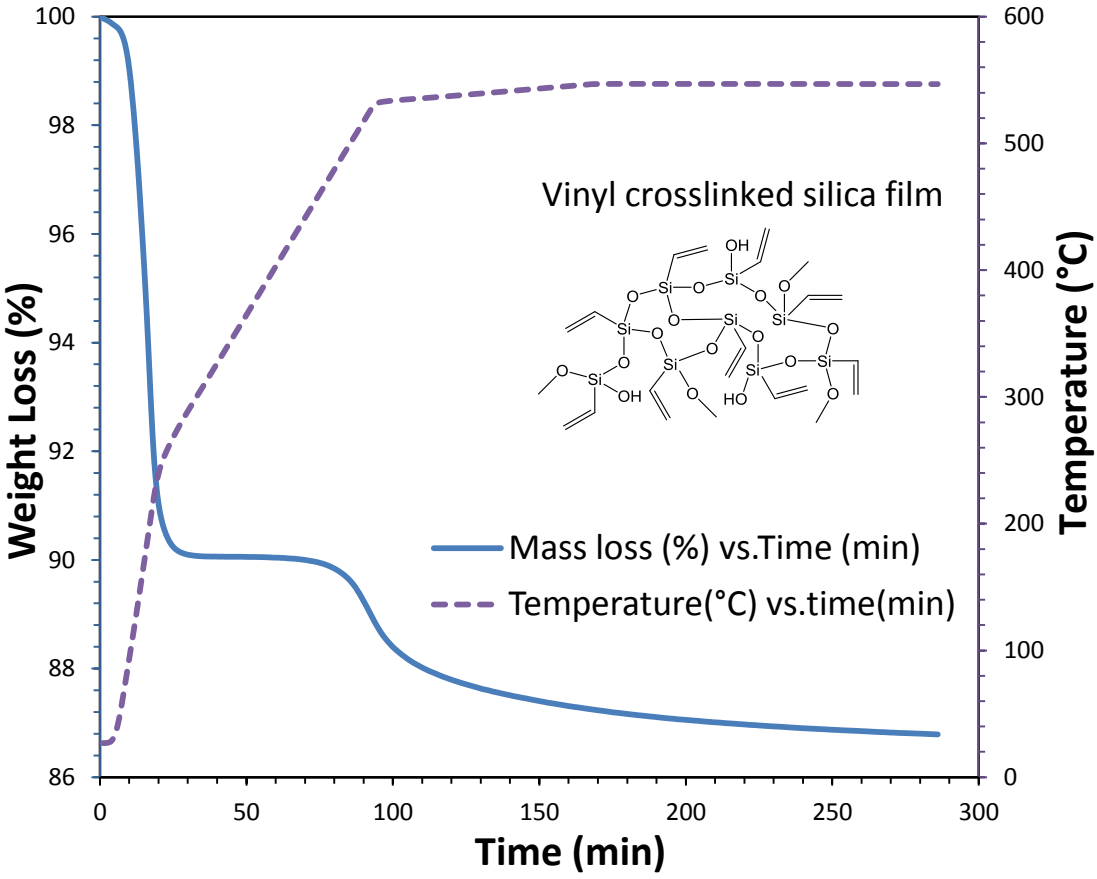

Figure 4.15: TGA plot of vinyl crosslinked silica film pyrolysed at 550 °C (Table 2a) in Argon UHP.

The TGA plots of untreated and V-treated Matrimid® pyrolysed are shown in Figure 4.16. The (blue) untreated Matrimid® had a weight loss of ~38 wt% after primarily evolving CO, CO_2 and CH_4 at ~450 °C [24], whereas the (red) V-treated Matrimid® had slightly lower weight loss i.e., ~35 wt%, which also indicates that silica remains in the final CMS sample. In addition, the early onset weight loss above 100 °C is for the

residual moisture and methanol due to the continued hydrolysis and condensation sol-gel reactions (Figure 4.4).

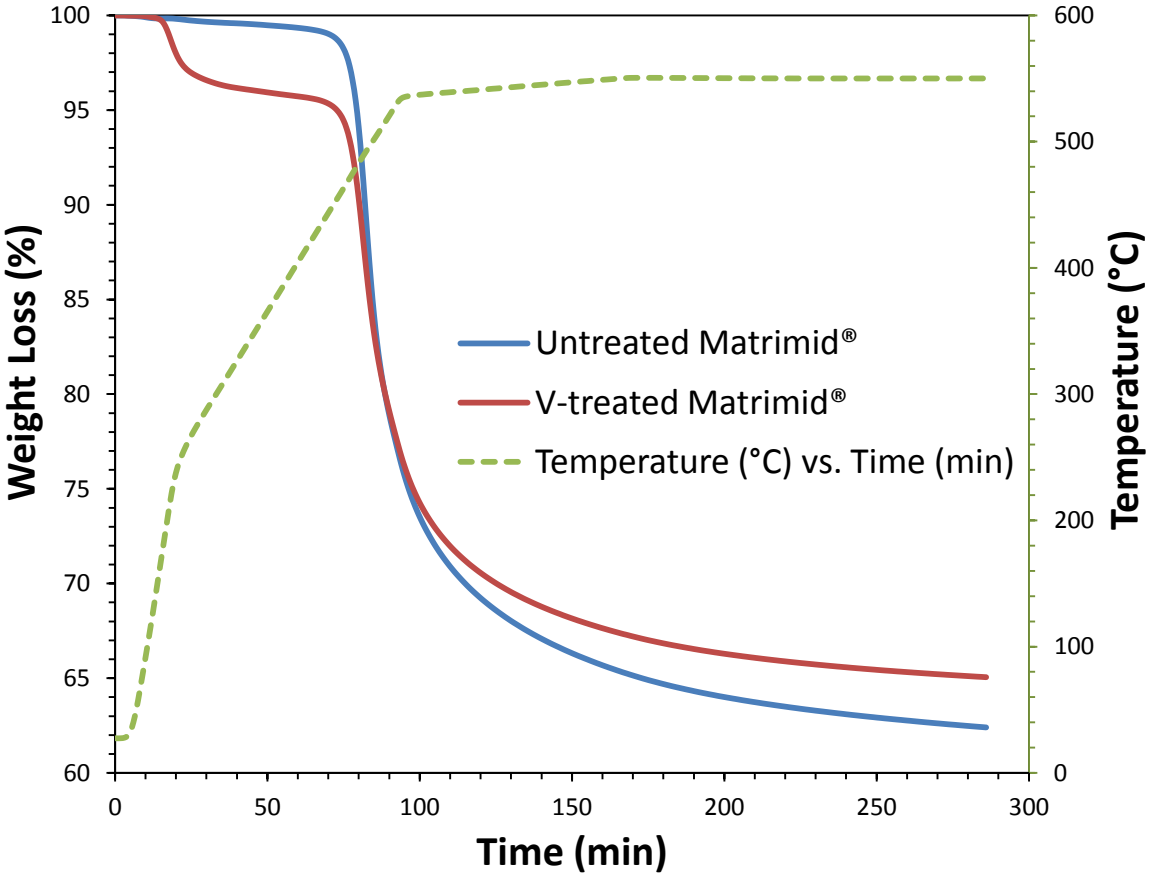

Figure 4.16: TGA plot of Untreated and V-treated Matrimid® at temperature profile of 550 °C and Argon UHP atmosphere.

4.4.8 Elemental analysis of untreated and V-treated Matrimid® precursor, and CMS.

The above characterization analysis provides a comprehensive proof of crosslinked silica in the V-treated Matrimid® precursor and CMS V-treated Matrimid®.

To determine the Atomic (At) % of each element in the sample, elemental analysis was performed on both the untreated and V-treated Matrimid® and 6FDA:BPDA-DAM precursor. The results are summarized for both wt% and At% in Table 4.3.

Table 4.3: Elemental analysis for untreated and V-treated Matrimid®, and 6FDA:BPDA-DAM *precursor*.

		Carbon	Hydrogen	Nitrogen	Oxygen	Fluorine	Silicon
Untreated Matrimid® precursor	(wt %)	75.4	4.4	5.3	14.5	---	---
	(At %)	52.4	36.9	3.2	7.5	---	---
V-treated Matrimid® precursor	(wt %)	73.2	4.9	4.5	13.2	---	4.2
	(At %)	49.8	39.6	2.6	6.7	---	1.2
Untreated 6FDA:BPDA-DAM precursor	(wt %)	64.2	3.3	5.8	15.4	11.4	---
	(At %)	47.1	29.1	3.6	8.5	5.3	---
V-treated 6FDA:BPDA-DAM precursor	(wt %)	63.9	4.0	5.2	12.6	10.2	4.1
	(At %)	47.8	35.6	3.4	7.1	4.8	1.3

In order to determine the accuracy of the obtained elemental analysis, the experimental composition for the untreated polymer precursors were compared to the theoretical composition as per the molecular structure shown in the Table 4.4. Both the experimental and theoretical values match with an uncertainty range of +/- 1%. The theoretical calculations were based on the precursor molecular structure as shown in Figure 4.17.

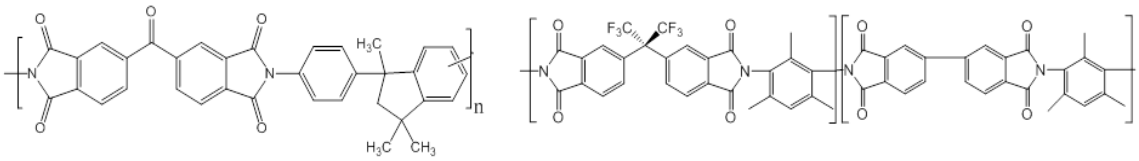

(a) (b)

Figure 4.17: Molecular structure of (a) Matrimid® and (b) 6FDA:BPDA-DAM

Table 4.4: Comparison of the theoretical and experimental elemental analysis for untreated Matrimid®, and 6FDA:BPDA-DAM *precursor*.

		Carbon	Hydrogen	Nitrogen	Oxygen	Fluorine
Matrimid® (experimental)	(wt%)	75.4	4.4	5.3	14.5	---
	(At%)	52.4	36.9	3.2	7.5	---
Matrimid® (Theoretical[1])	(wt%)	75.9	4.5	5.1	14.4	---
	(At%)	52.2	37.3	3.0	7.5	
6FDA:BPDA-DAM (experimental)	(wt%)	64.2	3.3	5.8	15.4	11.4
	(At%)	47.1	29.1	3.6	8.5	5.3
6FDA:BPDA-DAM (Theoretical)	(wt%)	65.8	3.3	5.8	13.3	11.8
	(At%)	48.3	29.2	3.6	7.3	5.5

For the elemental analysis of the CMS sample, CMS fibers were first ground into fine powder and then analyzed for each element as per the procedure in Chapter 3. It is important to note that the results in Table 4.5 are represented for the bulk CMS sample.

[1]The sample calculation of carbon wt% in Matrimid® monomer molecule: the monomer's molecular weight is around 553 grams per mole and has 35 carbon atoms as shown in the structure (Figure 4.17(a)). The carbon wt% per mole of Matrimid® monomer would be ((35*12)/553)*100 = *75.9 wt%*)

Table 4.5: Elemental analysis for untreated and V-treated CMS Matrimid® and 6FDA:BPDA-DAM *(Pyrolysed at 550°C)*

		Carbon	Hydrogen	Nitrogen	Oxygen	Fluorine	Silicon
CMS Untreated Matrimid®	(wt%)	87.4	3.1	4.8	4.8	---	---
	(At%)	66.1	28.1	3.1	2.7	---	---
CMS V-treated Matrimid®	(wt%)	76.1	3.2	4.0	5.2	---	11.6
	(At%)	56.2	35.6	2.3	2.4	---	3.6
CMS Untreated 6FDA:BPDA-DAM	(wt%)	82.5	3.1	7.4	7.0	---	---
	(At%)	60.6	27.0	4.7	3.9	---	---
CMS V-treated 6FDA:BPDA-DAM	(wt%)	78.9	2.8	6.9	8.8	0.2	2.4
	(At%)	62.4	26.8	4.7	5.2	0.1	0.8

The elemental analysis on V-treated precursor samples in Table 4.3 indicates the presence of silica. The elemental analysis for final V-treated CMS samples also confirmed the presence of silicon (in Table 4.5) as seen in other characterization analysis. Interestingly, the percentage of silicon for CMS V-treated 6FDA:BPDA-DAM was found to be much lower when compared with the CMS V-treated Matrimid® sample. One of the reasons for this difference could be the etching behavior of fluorine species (like CHF_3, HF), which are the by-product gases evolved during the pyrolysis of 6FDA based precursors [24]. CHF_3, HF are strong etching agents shown to etch away the silica chemical moieties (SiO_2, Si-O-Si and Si-C) in other applications [25-27]. Though the elemental analysis results in Table 4.5 indicate that the similar etching behavior might be taking place during the pyrolysis of V-treated 6FDA:BPDA-DAM precursor, further

characterization analyses would be required to quantitatively confirm this hypothesis. The potential of this study in future, is been discussed in Chapter 7. The reduction of silica in the final CMS V-treated 6FDA:BPDA-DAM can be desirable when related to an improvement in separation properties as explained in section 4.5.2.

4.4.9 XPS on asymmetric CMS V-treated Matrimid® hollow fiber membrane

The silicon distribution on the outer surface of asymmetric CMS V-treated Matrimid® hollow fiber membrane (pyrolysed at 550°C) was confirmed through XPS and sputter Ar ion etching, performed as per the procedure explained in Chapter 3. Figure 4.18(a) shows the shallow, and deep etch[2] distribution profile for silicon (Si2p) and carbon (C1s) at the outer surface of CMS V-treated Matrimid® hollow fiber as a function of the sputter depth profiling time. The initial Si At% was approximately 35 % for both shallow and deep etch sample and decreased to as low as 5% for the deep etch sample. It is important to note that the surface elemental composition via XPS analysis cannot estimate the hydrogen, whereas hydrogen's are significantly present in the CMS samples (Table 4.5).

[2] Due to the variety of bonds present on the CMS V-treated sample, it is challenging to estimate an accurate etch rate. Taking the different bond etch rates for Si-O-Si, Si-C, and C-C the rough estimate would be ~0.2-0.25 nm/s.

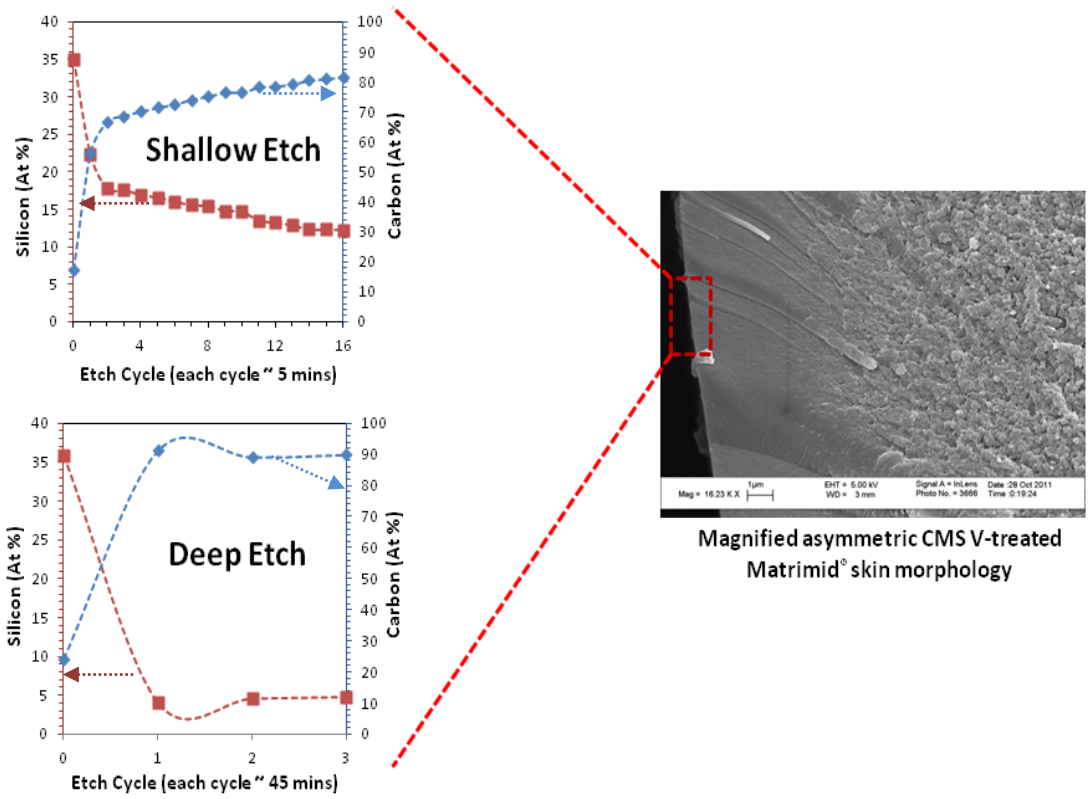

Figure 4.18(a) XPS surface composition profile (Si2p and C1s) as a function of sputter etch depth profiling time

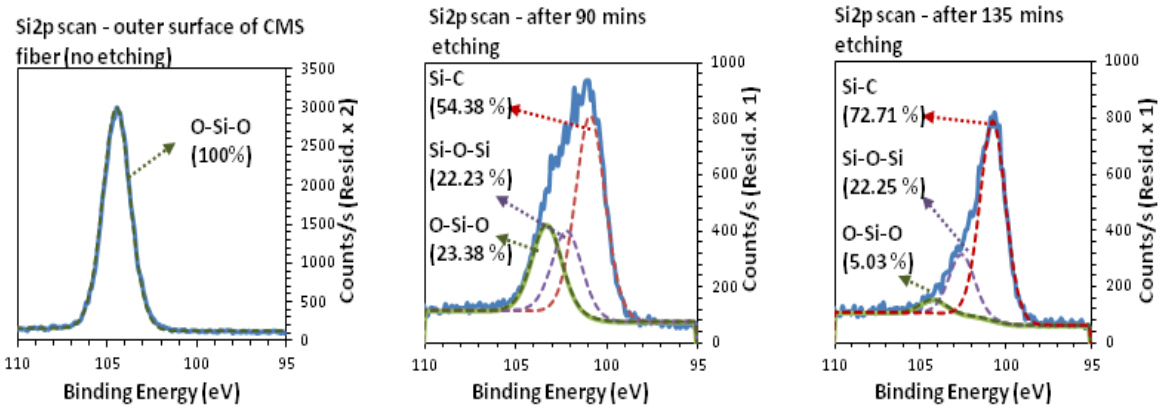

(i) (ii) (iii)

Figure 4.18(b) XPS spectra representing the Si2p B.E. region as a function of sputter etch depth profiling time

In order to understand the chemical bonding of the silicon as a function of the sputter etch depth profiling, high resolution Si2p spectra were obtained. Figure 4.18(b) shows the chemical shifts in the high resolution Si2p spectra for (i) outermost surface of

the CMS V-treated Matrimid® fiber (no etching), (ii) 90 mins etching[3] and (iii) 135 mins etching[4] into the surface. It was observed that for the surface of the fiber (i), the Si2p peak maximum occurs with a bond energy (B.E.) of 104.5 eV which is a characteristic of SiO_2 [28]. For 90 mins etch (ii), the Si2p peak can be deconvulated and fit with three peaks centered at 100.9 eV (representing 54.38% of the total Si2p peak area), at 102.2 eV (representing 22.23% of the total Si2p peak area) and 103.3 eV (representing 23.38% of the total Si2p peak area), which can be assigned to O-Si-O (SiO_2), Si-O-Si and Si-C respectively [28] . For the 135 mins etch, the Si2p peak maximum occurs with at bonding energy (B.E.) of 100.8 eV, which can be assigned to Si-O-Si and Si-C (representing 72.71% and 22.25% of the total Si2p peak area respectively.

The trend on Si2p profile indicated that most of the silica is present on the outer surface of CMS V-treated fibers, which agrees with the excess silica hypothesis discussed in section 4.2. As we etched deeper into the surface, the transformation of O-Si-O to Si-O-Si and Si-C moieties can be observed (Figure 4.18(b)).

4.5 Permeation properties

4.5.1 Pure gas feed (Matrimid®)

Pure gas permeation was carried out on CMS untreated and V-treated Matrimid® hollow fibers pyrolysed at two different pyrolysis temperatures 550 °C and 650 °C, and under Argon UHP inert atmosphere. CMS V-treated fibers at both pyrolysis temperatures

[3] Due to the variety of bonds present on the CMS V-treated sample, it is challenging to estimate an accurate etch rate. Taking the different bond etch rates for Si-O-Si, Si-C, and C-C the rough estimate would be ~0.2-0.25 nm/s.

550°C and 650°C showed greater than 3x increase in gas permeance for the pure gases shown in Figures. 4.19(a) and 4.20(a). The increase in permeance after pyrolysis of the V-treated precursor results from restricting sub-structure collapse in asymmetric CMS hollow fiber membranes. As seen in the SEM image in Figure 4.7, V-treatment reduced the CMS separation membrane skin thickness (*l*) by 5-6x which directly resulted in an increase of gas permeance (P/*l*). The effect of additional silica layer on the intrinsic CMS skin (as discussed in section 4.3.2) can be seen with a limited increase in CO_2 permeance (3x instead of 5x) and slight decrease in selectivities for CMS V-treated Matrimid® compared to untreated CMS Matrimid® fibers as shown in Figures. 4.19-4.20. The optimization of VTMS concentration can show an even further improvement in permeation properties of the resulted CMS V-treated membranes and is discussed in Chapter 5. Nevertheless as noted earlier, the standard V-treatment as shown here shows a substantial improvement in permeance compared to untreated fibers.

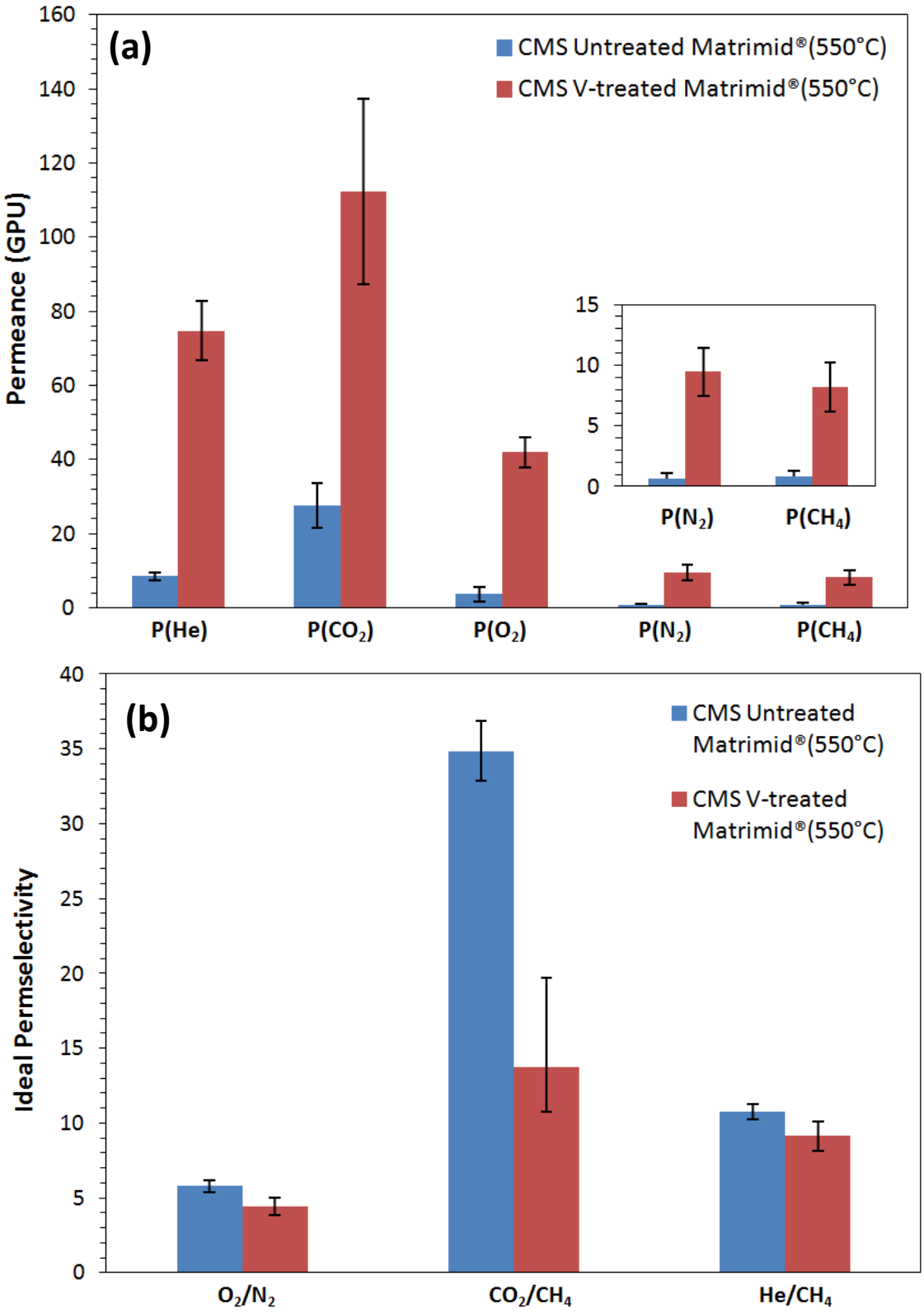

Figure 4.19: Pure-Gas (a) permeances and (b) permselectivities for CMS untreated (blue) and V-treated (red) Matrimid® hollow fiber membranes pyrolysed at 550 °C under argon UHP, feed pressure 100 psi and testing temperature 35 °C.

The molecular sieving structure of intrinsic CMS (shown in Chapter 2) strongly depends upon the final pyrolysis temperature and atmosphere. By increasing the final pyrolysis temperature from 550 °C to 650 °C, CMS V-treated Matrimid® hollow fibers showed similar permeation trend (Figures. 4.20(a) and (b)) as was observed in the case of intrinsic CMS dense films [29]. Such an improvement in gas permeances for CMS V-treated Matrimid® compared to the untreated CMS Matrimid® hollow fiber membranes is quite attractive and can have broad separation applications.

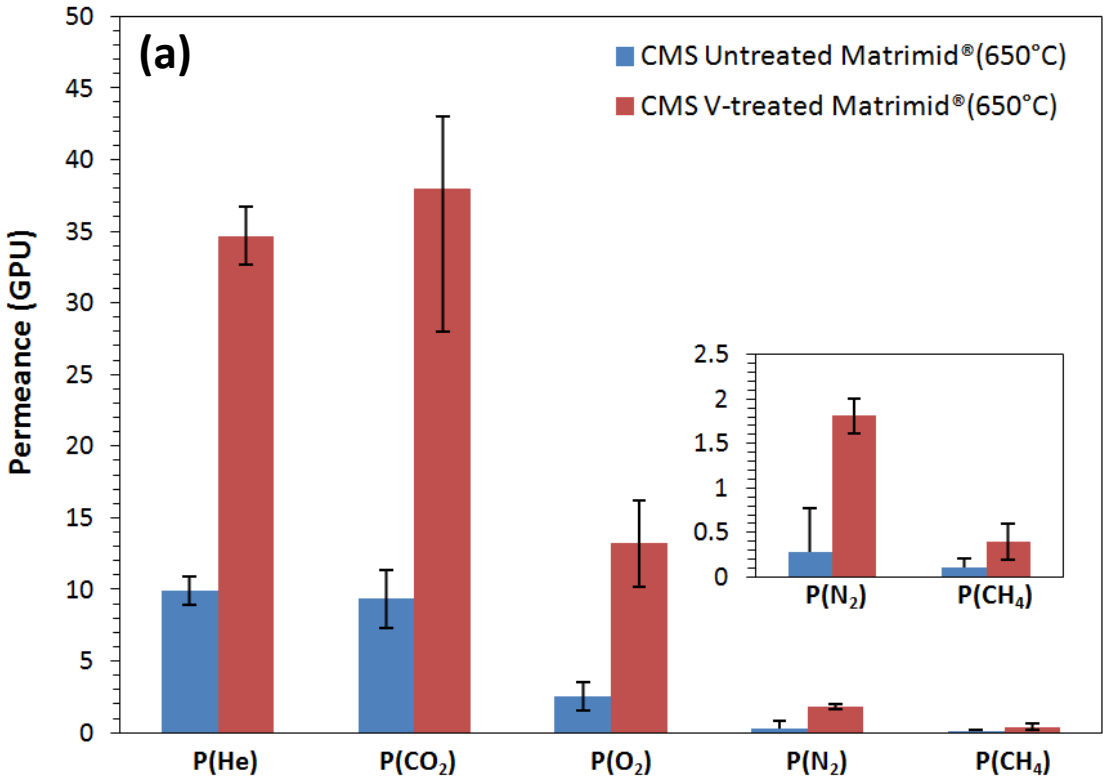

Figure 4.20(a): Pure-Gas permeances for CMS untreated (blue) and V-treated (red) Matrimid® hollow fiber membranes pyrolysed at 650 °C under argon UHP, feed pressure 100 psi and testing temperature 35 °C.

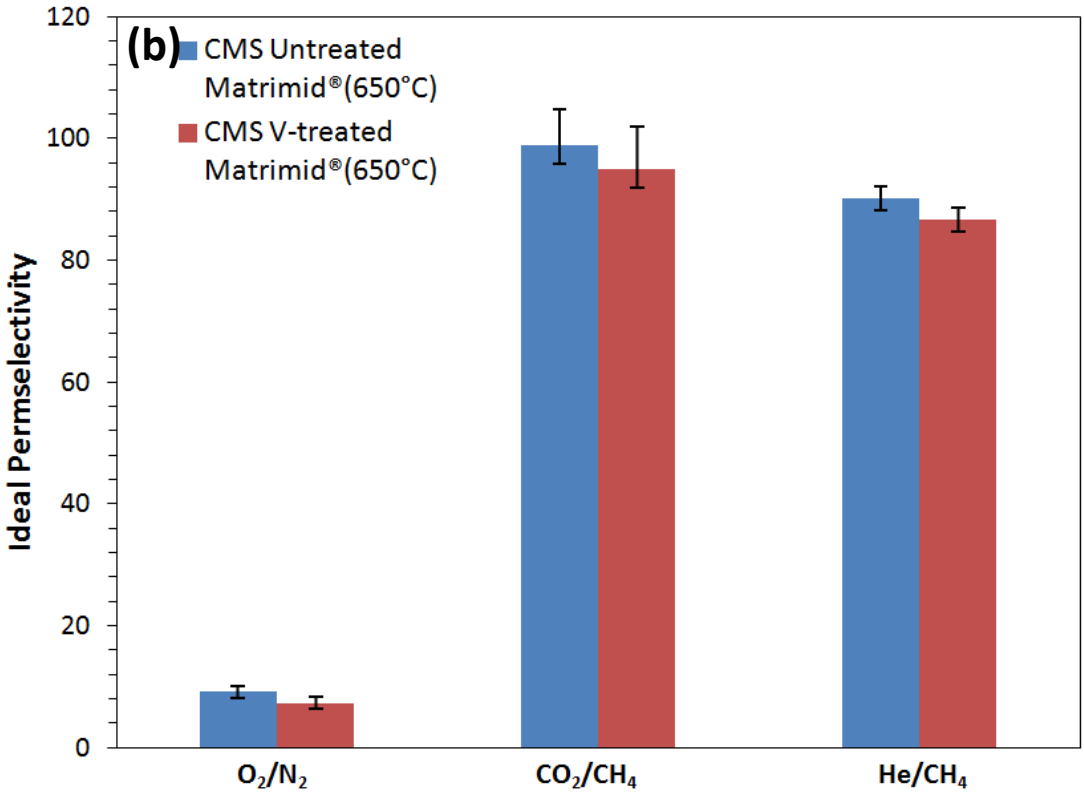

Figure 4.20(b): Pure-gas permselectivity for CMS untreated (blue) and V-treated (red) Matrimid® hollow fibers pyrolysed at 650 °C under argon UHP, feed pressure 100 psi and testing temperature 35 °C.

4.5.2 Pure gas feed (6FDA:BPDA-DAM)

As a proof of concept study, CMS untreated and V-treated 6FDA:BPDA-DAM hollow fibers were tested for pure gas CO_2 and CH_4. Both the untreated and V-treated 6FDA:BPDA-DAM precursor fibers were pyrolysed at 550 °C and 30 ppm of oxygen level in Argon. These conditions were chosen based on a CMS dense film study carried out in the earlier work [3]. As discussed earlier, 6FDA based precursor's showed a lower degree of substructure collapse when compared with the Matrimid® precursors, but there was still ~16x increase in membrane skin thickness *(l)* for CMS untreated 6FDA:BPDA-DAM (Figure 4.2(b)) . After the pyrolysis of V-treated 6FDA:BPDA-DAM precursor,

similar reduction (~5-6x) in asymmetric membrane skin thickness (*l*) was observed as shown in Figure 4.8. The decrease in membrane skin thickness caused a permeance increase of greater than 4x in asymmetric CMS V-treated 6FDA:BPDA-DAM hollow fiber membranes shown in Figure 4.21(a).

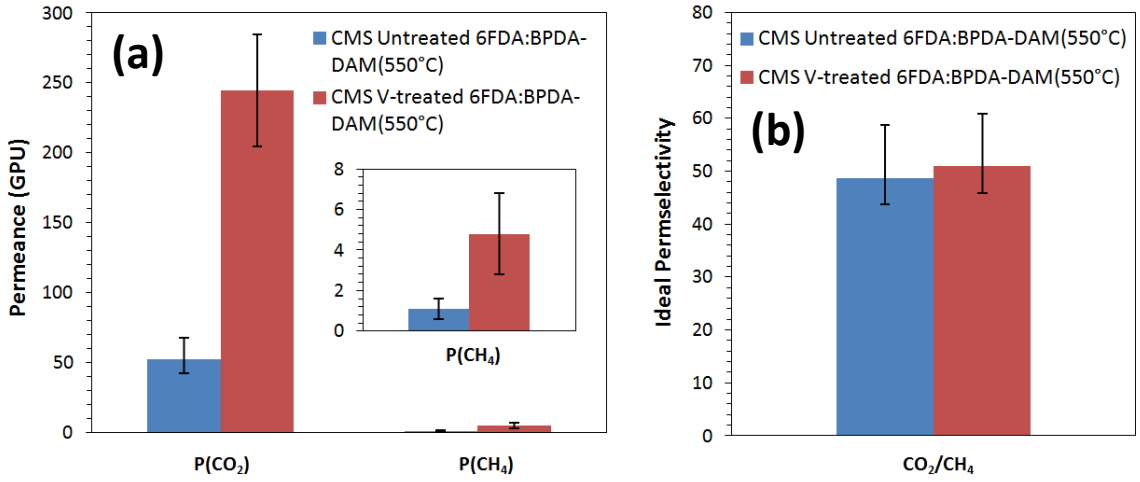

Figure 4.21: Pure gas (a) permeances and (b) permselectivities for CMS untreated and V-treated 6FDA:BPDA-DAM hollow fibers pyrolysed at 550 °C, under argon with 30 ppm of O_2, feed pressure 100 psi and testing temperature 35 °C.

Even though the V-treatment reduced final CMS membrane skin thickness by similar order (~5-6x), the change in transport properties of CMS V-treated Matrimid® and 6FDA:BPDA-DAM fibers pyrolysed at 550°C were different (Figures. 4.19 and 4.21). The increase in CO_2 permeance for CMS V-treated 6FDA:BPDA-DAM (4x) was higher compared to the increase in CMS V-treated Matrimid® (3x) without any drop in CO_2/CH_4 intrinsic CMS selectivity. The hypothesis for the difference can be explained in terms of the excess silica layer formed on the outer surface of intrinsic V-treated CMS (as explained in section 4.3). One main difference between 6FDA based precursors and Matrimid® is the evolution of fluorine based by-products as volatile gases during

pyrolysis [24]. Therefore as discussed in the elemental analysis section 4.4.8, it is possible that CHF_3/HF evolved during the pyrolysis of V-treated 6FDA:BPDA-DAM etches the silica surface on intrinsic CMS skin as observed by the decrease in the Si% on the elemental analysis (Table 4.5). Nevertheless, this hypothesis would need to be further tested with more detailed analysis on V-treated 6FDA based precursors and is a point of future study.

4.5.3 Mixed-gas permeation

For practical application of CMS V-treated membranes, it is important to evaluate the mixed gas separation performance, which is of course the real situation in any application. An aggressive natural gas feed composition of 50% CO_2/50% CH_4 was used up to a total feed pressure of 800 psi. Due to non-ideality of mixed gas at high feed pressures, fugacity coefficients were calculated to obtain accurate gas permeance values.

The mixed gas separation performance of CMS untreated and V-treated Matrimid® hollow fibers pyrolysed at 650°C and Argon UHP are shown in Figure 4.21. CMS V-treated Matrimid® maintained the increased permeance trend along with attractive selectivities for CO_2/CH_4 even under aggressive feed conditions (high concentrations of CO_2 and feed pressures). A similar mixed gas test comparison for CMS untreated and V-treated 6FDA:BPDA-DAM pyrolysed at 550°C and 30ppm O_2 in Argon was also carried out. The results are shown in the Figure 4.22.

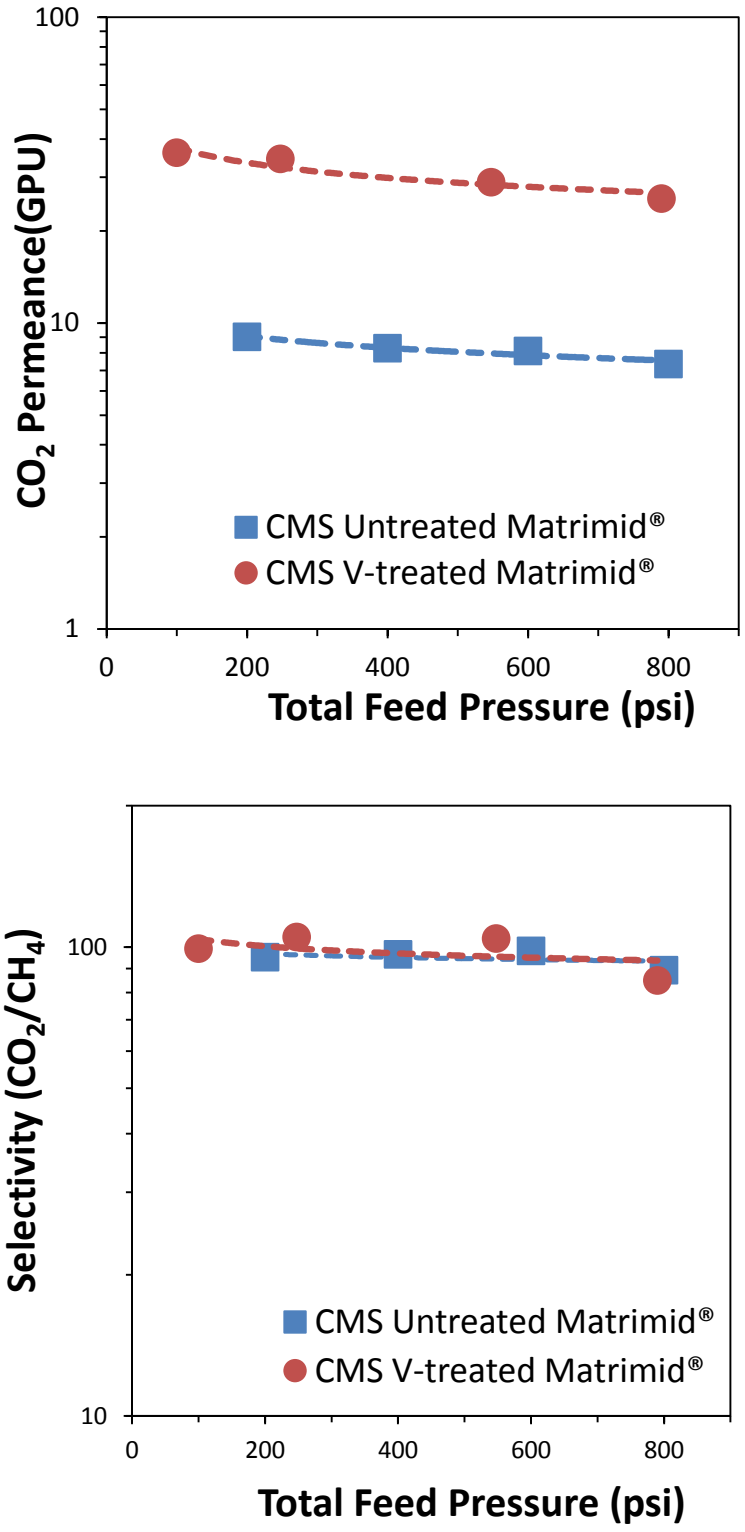

Figure 4.21: Mixed-Gas feed separation performance (50%CO_2/50%CH_4) for CMS untreated and V-treated Matrimid® hollow fiber membranes pyrolysed at 650 °C, Argon UHP and tested at 35 °C.

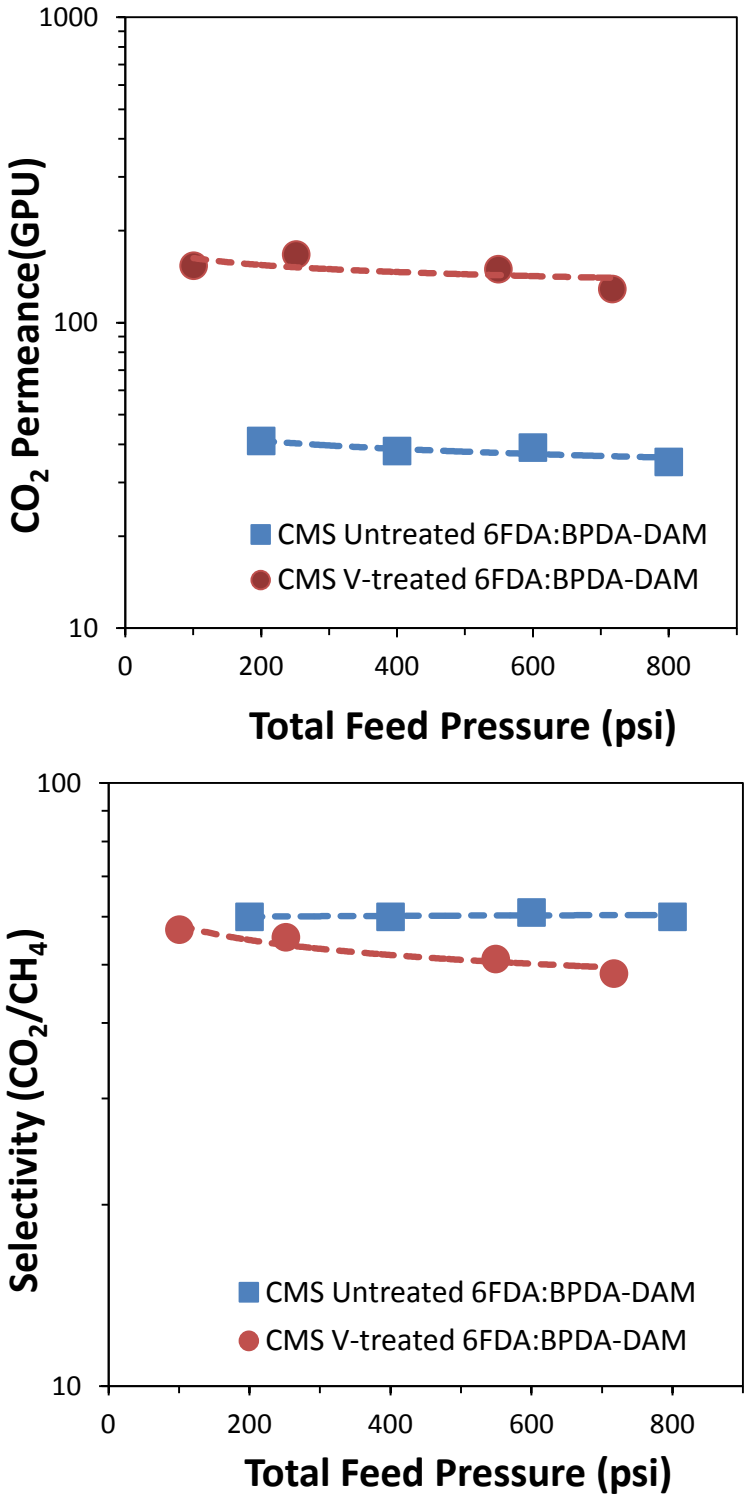

Figure 4.22: Mixed-gas feed separation performance (50%CO_2/50%CH_4) for CMS untreated and V-treated 6FDA:BPDA-DAM hollow fiber membranes pyrolysed at 550 °C and 30 ppm O_2 in Argon, tested at 35 °C.

4.6 Summary

This chapter has presented a novel pre-pyrolysis treatment (V-treatment) approach to restrict substructure morphology collapse in asymmetric CMS hollow fiber membranes. The V-treatment technique uses a sol-gel crosslinking reaction to induce vinyl crosslinked silica on precursor fiber pore walls, which restricts the ability of the porous support to collapse during pyrolysis. The effect of V-treatment was applied on two widely studied polyimide precursors: Matrimid® and 6FDA:BPDA-DAM. The fact that the V-treatment does not involve any chemical reaction with precursor molecular structure makes it a simple integral approach to restrict morphology collapse on any class of asymmetric CMS polymer precursors. This will enable low-cost facile integration into practical membrane production.

A significant reduction of approximately 5-6x in membrane skin thickness (l) for asymmetric CMS hollow fibers from both the V-treated precursors was found. This improvement in membrane skin thickness (l) directly translated to an increase in gas permeance (P/l) by more than 3x for asymmetric CMS V-treated Matrimid® hollow fibers tested for both pure gases (He, CO_2, O_2, N_2 ,CH_4) and aggressive high pressure (CO_2/CH_4) mixed gas feeds. Similar improvement in permeance for asymmetric CMS V-treated 6FDA:BPDA-DAM hollow fibers by more than 4x for both pure and mixed gas (CO_2/CH_4) feed was observed. The separation performance of asymmetric CMS membranes from both the V-treated precursors showed attractive separation performance even under aggressive natural gas feed conditions at high pressures (800 psi). Further optimization of this treatment process is crucial for obtaining even better separation performance and hence presented in Chapter 5.

4.7 References

1. Xu, L., M. Rungta, and W.J. Koros, Matrimid® derived carbon molecular sieve hollow fiber membranes for ethylene/ethane separation. Journal of Membrane Science, 2011. **380**(1-2): p. 138-147.
2. Comer, A. C.; Kalika, D. S.; Rowe, B. W.; Freeman, B. D.; Paul, D. R., Dynamic relaxation characteristics of Matrimid® polyimide. Polymer 2009, 50 (3), 891-897.
3. Kiyono, M., P.J. Williams, and W.J. Koros, Effect of pyrolysis atmosphere on separation performance of carbon molecular sieve membranes. Journal of Membrane Science, 2010. **359**(1-2): p. 2-10.
4. Xu, L.; Rungta, M.; Brayden, M. K.; Martinez, M. V.; Stears, B. A.; Barbay, G. A.; Koros, W. J., Olefins-Selective Asymmetric Carbon Molecular Sieve Hollow Fiber Membranes for Hybrid Membrane-Distillation Processes for Olefin/Paraffin Separations. J Membrane Sci 2012.
5. Lafyatis, D.S., J. Tung, and H.C. Foley, Poly(furfuryl alcohol)-derived carbon molecular sieves: dependence of adsorptive properties on carbonization temperature, time, and poly(ethylene glycol) additives. Industrial & Engineering Chemistry Research, 1991. **30**(5): p. 865-873.
6. Zhao, H.-Y.; Cao, Y.-M.; Ding, X.-L.; Zhou, M.-Q.; Yuan, Q., Effects of cross-linkers with different molecular weights in cross-linked Matrimid 5218 and test temperature on gas transport properties. J Membrane Sci **2008,** 323 (1), 176-184.
7. Tin, P. S.; Chung, T.-S.; Kawi, S.; Guiver, M. D., Novel approaches to fabricate carbon molecular sieve membranes based on chemical modified and solvent treated polyimides. Micropor Mesopor Mat **2004,** 73 (3), 151-160.
8. Tin, P. S.; Chung, T. S.; Liu, Y.; Wang, R.; Liu, S. L.; Pramoda, K. P., Effects of cross-linking modification on gas separation performance of Matrimid membranes. J Membrane Sci **2003,** 225 (1–2), 77-90.
9. Krol, J.J., M. Boerrigter, and G.H. Koops, Polyimide hollow fiber gas separation membranes: preparation and the suppression of plasticization in propane/propylene environments. Journal of Membrane Science, 2001. **184**(2): p. 275-286.
10. Barsema, J. N.; Klijnstra, S. D.; Balster, J. H.; van der Vegt, N. F. A.; Koops, G. H.; Wessling, M., Intermediate polymer to carbon gas separation membranes based on Matrimid PI. J Membrane Sci **2004,** 238 (1–2), 93-102.
11. Barzin, J., H. Azizi, and J. Morshedian, Preparation of silane-grafted and moisture cross-linked low density polyethylene: Part I: Factors affecting performance of grafting and cross-linking. Polymer-Plastics Technology and Engineering, 2006. **45**(8): p. 979-983.
12. Suda, H. and K. Haraya, Gas Permeation through Micropores of Carbon Molecular Sieve Membranes Derived from Kapton Polyimide. The Journal of Physical Chemistry B, 1997. **101**(20): p. 3988-3994.
13. Baney, R. H.; Itoh, M.; Sakakibara, A.; Suzuki, T., Silsesquioxanes. Chemical Reviews 1995, 95 (5), 1409-1430.

14. Douskey, M.; Gebhard, M.; McCormick, A.; Lange, B.; Whitman, D.; Schure, M.; Beshah, K., Spectroscopic studies of a novel cyclic oligomer with pendant alkoxysilane groups, Progress in organic coatings 2002, 45 (2), 145-157.
15. Achoundong, C. S.; Bhuwania, N.; Burgess, S. K.; Karvan, O.; Johnson, J. R.; Koros, W. J., Silane Modification of Cellulose Acetate Dense Films as Materials for Acid Gas Removal. Macromolecules 2013, 46 (14), 5584-5594.
16. Wang, D. and G.P. Bierwagen, Sol–gel coatings on metals for corrosion protection. Progress in organic coatings, 2009. **64**(4): p. 327-338.
17. Ishida, H., A review of recent progress in the studies of molecular and microstructure of coupling agents and their functions in composites, coatings and adhesive joints. Polymer Composites, 1984. **5**(2): p. 101-123.
18. Kanezashi, M.; Yada, K.; Yoshioka, T.; Tsuru, T., Organic–inorganic hybrid silica membranes with controlled silica network size: preparation and gas permeation characteristics. J Membrane Sci **2010,** 348 (1), 310-318.
19. Duke, M. C.; Diniz da Costa, J. C.; Lu, G. Q.; Petch, M.; Gray, P., Carbonised template molecular sieve silica membranes in fuel processing systems: permeation, hydrostability and regeneration. J Membrane Sci **2004,** 241 (2), 325-333.
20. Guiver, M. D.; Robertson, G. P.; Dai, Y.; Bilodeau, F.; Kang, Y. S.; Lee, K. J.; Jho, J. Y.; Won, J., Structural characterization and gas-transport properties of brominated matrimid polyimide. Journal of Polymer Science Part A: Polymer Chemistry 2002, 40 (23), 4193-4204.
21. Uhlig, F. and H.C. Marsmann, 29 Si NMR Some Practical Aspects. Gelest Inc.,.
22. Zhou, H.; Su, Y.; Chen, X.; Yi, S.; Wan, Y., Modification of silicalite-1 by vinyltrimethoxysilane (VTMS) and preparation of silicalite-1 filled polydimethylsiloxane (PDMS) hybrid pervaporation membranes. Sep Purif Technol 2010, 75 (3), 286-294.
23. Abe, Y.; Kagayama, K.; Takamura, N.; Gunji, T.; Yoshihara, T.; Takahashi, N., Preparation and properties of polysilsesquioxanes. Function and characterization of coating agents and films, Journal of non-crystalline solids 2000, 261 (1), 39-51.
24. Kiyono, M., P.J. Williams, and W.J. Koros, Effect of polymer precursors on carbon molecular sieve structure and separation performance properties. Carbon, 2010. **48**(15): p. 4432-4441.
25. Coburn, J. and H.F. Winters, Plasma etching—A discussion of mechanisms. Journal of vacuum Science and Technology, 1979. **16**(2): p. 391-403.
26. Pan, W.S. and A. Steckl, Reactive ion etching of SiC thin films by mixtures of fluorinated gases and oxygen. Journal of the Electrochemical Society, 1990. **137**(1): p. 212-220.
27. Dhar, S.; Seitz, O.; Halls, M. D.; Choi, S.; Chabal, Y. J.; Feldman, L. C., Chemical properties of oxidized silicon carbide surfaces upon etching in hydrofluoric acid. J Am Chem Soc 2009, 131 (46), 16808-16813.
28. Watanabe, H. and T. Hosoi, Fundamental Aspects of Silicon Carbide Oxidation. Physics and Technology of Silicon Carbide Devices. 2012.

29. Steel, K.M. and W.J. Koros, An investigation of the effects of pyrolysis parameters on gas separation properties of carbon materials. Carbon, 2005. **43**(9): p. 1843-1856.

CHAPTER 5
OPTIMIZATION OF V-TREATMENT AND PYROLYSIS PARAMETERS FOR SUPERIOR SEPARATION PERFORMANCE IN ASYMMETRIC CMS HOLLOW FIBER MEMBRANES

5.1 Overview

This chapter presents the results of optimization conditions for different VTMS concentrations and final pyrolysis temperatures. In addition, the importance of both organic and alkoxy functional groups are presented. The optimization results is evaluated in terms of separation performance for both pure gas feed and industry relevant mixed-gas pairs (i.e. CO_2/CH_4, C_2H_4/C_2H_6 and C_3H_6/C_3H_8) at 35°C. Several characterization analyses such as SEM, XPS and elemental analysis for optimized V-treated CMS membranes are also presented.

5.2 Mechanism for V-treatment optimization

As discussed in Chapter 4, the majority of silica in an asymmetric CMS V-treated hollow fiber (using 100% VTMS) was concentrated on the outermost surface of the fiber as shown in Figure 5.1. Even though the porous organo-silica components in the sub-structure support were essential for restricting collapse, the additional undesirable silica layer formed outside the intrinsic CMS skin acted as an additional resistive layer for gas transport. Due to the excess silica deposition on the outermost CMS skin, limited increase in gas permeances were observed.

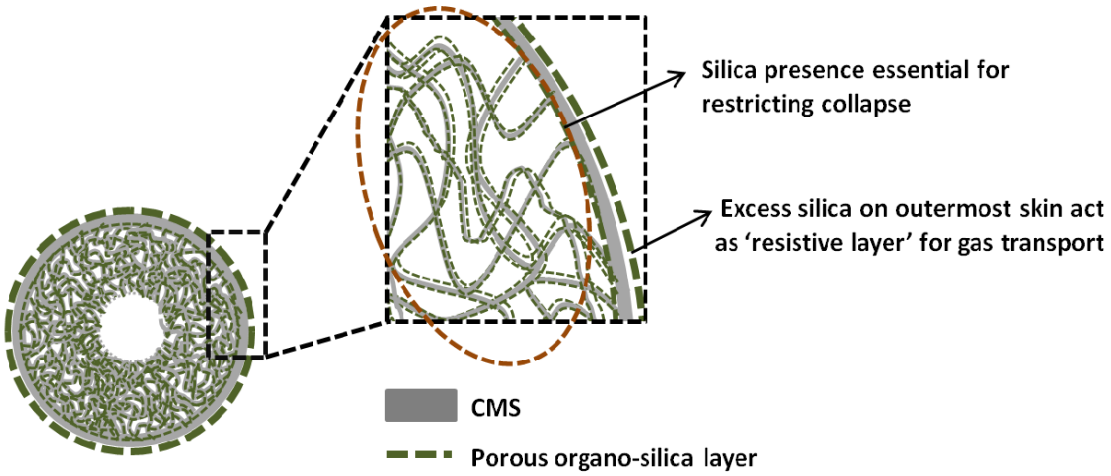

Figure 5.1: Schematic illustration of excessive silica deposition on outermost intrinsic CMS skin.

Optimization of the VTMS concentration in V-treatment is essential for reducing the excess silica. In the initial studies (discussed in Chapter 4), V-treatment was started with 100% VTMS as a proof-of-concept method to see if it had the capability to restrict sub-structure collapse. The potential was clearly indicated in Chapter 4, so the next step was the optimization of VTMS in V-treatment. To reduce the concentration of VTMS, different polymer non-solvents such as toluene, n-heptane and hexane were used. Though in principle any of the three non-solvents could be used, hexane as a non-solvent was preferred due to the existing post-spinning solvent exchange process. The V-treatment optimization results for different concentrations of VTMS in hexane were evaluated through SEM and CO_2/CH_4 transport properties, as discussed in section 5.3.1. The step by step procedure shown in Figure 5.2 was adapted in all the V-treatment optimization studies.

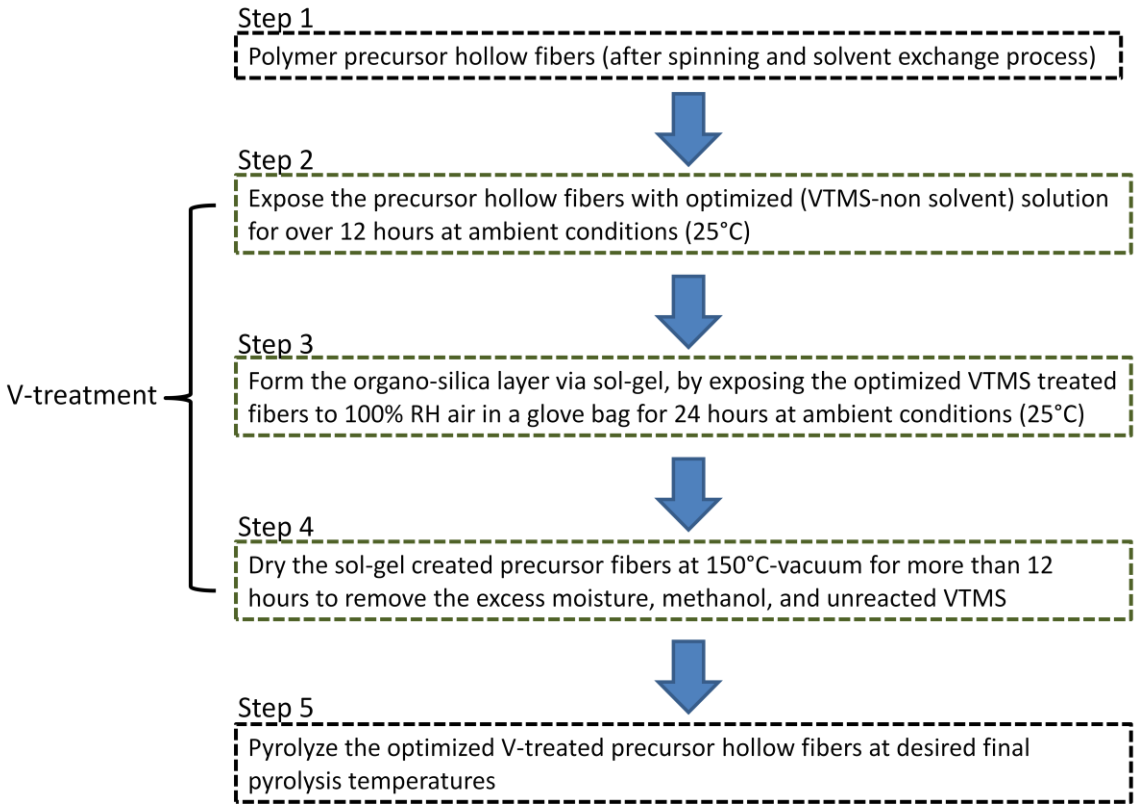

Figure 5.2: Illustration of the step by step V-treatment optimization protocol.

After evaluating different concentrations of VTMS (i.e. 75%, 50%, 25%, 10%, 5% and 1%) in hexane, *10%* VTMS was observed to be the optimum level, which restricted the collapse and also translated to an equivalent improvement in CMS permeance. The results for the separation performance of CMS hollow fiber after the optimized V-treatment on Matrimid® precursor are discussed in sections 5.3.1, 5.5 and 5.6. In addition to the enhancement in separation performance, optimized V-treated CMS hollow fibers also exhibited lower silicon percentages throughout the CMS sample and most importantly, on the outermost CMS skin. This observation was made through elemental analysis and XPS, and is discussed in sections 5.4.1 and 5.4.2, respectively.

For future studies of V-treatment, one critical objective will be to explore various silanes with different pendant groups. Hence, it is important to establish the role of vinyl (organic) and methoxy (alkoxy) functional groups in V-treatment. Three different silanes were tested under the same V-treatment procedure as shown in Figure 5.2 and are mentioned below:

(a) Trimethoxy silane (TMS) treatment – showed the importance of the vinyl (organic) group towards flexibility of V-treated precursor fibers. The TMS treated precursor fibers were found to have much higher silicon content compared to V-treated and were too brittle to use in any further studies. The results are discussed in the section 5.3.2.1

(b) Vinyl trimethyl silane treatment – showed the importance of methoxy (alkoxy) group for the formation of sol-gel, as the vinyl trimethyl silane treated CMS hollow fibers showed a collapsed morphology after pyrolysis. The results are discussed in the section 5.3.2.2.

(c) Ethyl trimethoxy silane (ETMS) treatment – was crucial for testing the effect of an unsaturated hydrocarbon (vinyl) vs. a saturated hydrocarbon (ethyl). The TGA, XPS, NMR and elemental analysis characterizations in Chapter 4 suggested the possibility of a reaction between the vinyl and silica during pyrolysis. To evaluate the need of reactive hydrocarbon group (like vinyl), a relatively unreactive group ‘ethyl’ was evaluated. The ETMS treated CMS hollow fiber does not show the similar permeance increase, as it showed for V-treated CMS hollow fibers. Further details are discussed in the section 5.3.2.3.

5.3 Optimization parameters for V-treatment

5.3.1 Different concentrations of VTMS in hexane

The least amount of silica deposited on the outermost layer of the asymmetric V-treated CMS skin (Figure 5.1) is desirable for improved gas transport properties. To reduce the silica in the V-treatment step, six different concentrations of VTMS in hexane (i.e. 75%, 50%, 25%, 10%, 5% and 1%) using a Matrimid® precursor were used. Sub-structure morphology of all the different VTMS-hexane treated and untreated CMS fibers were analyzed using SEM as shown in Figures 5.3(a) to 5.3(h).

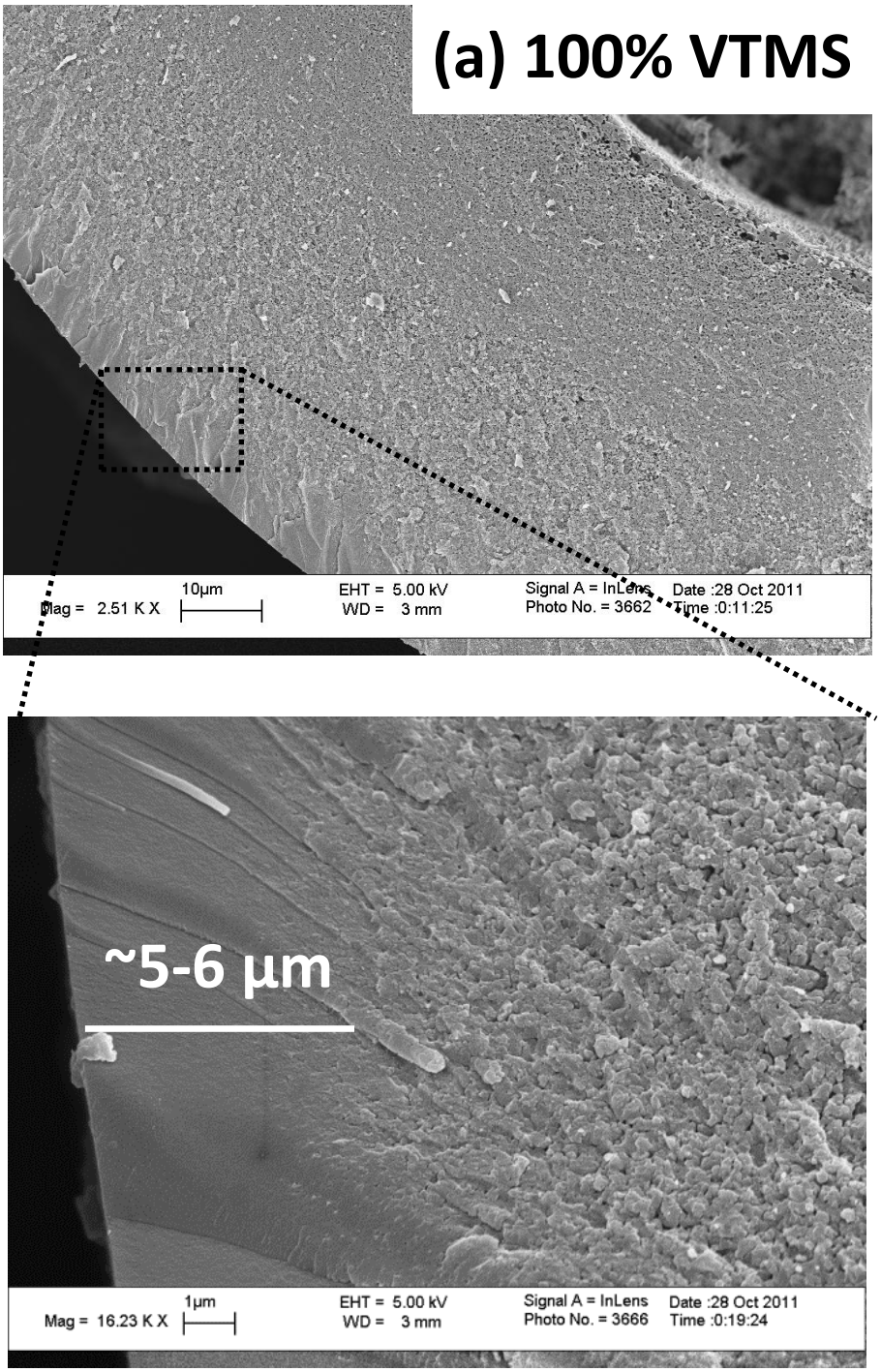

Figure 5.3(a): SEM images of 100% V-treated Matrimid® CMS hollow fibers pyrolyzed at 650°C under argon UHP atmosphere.

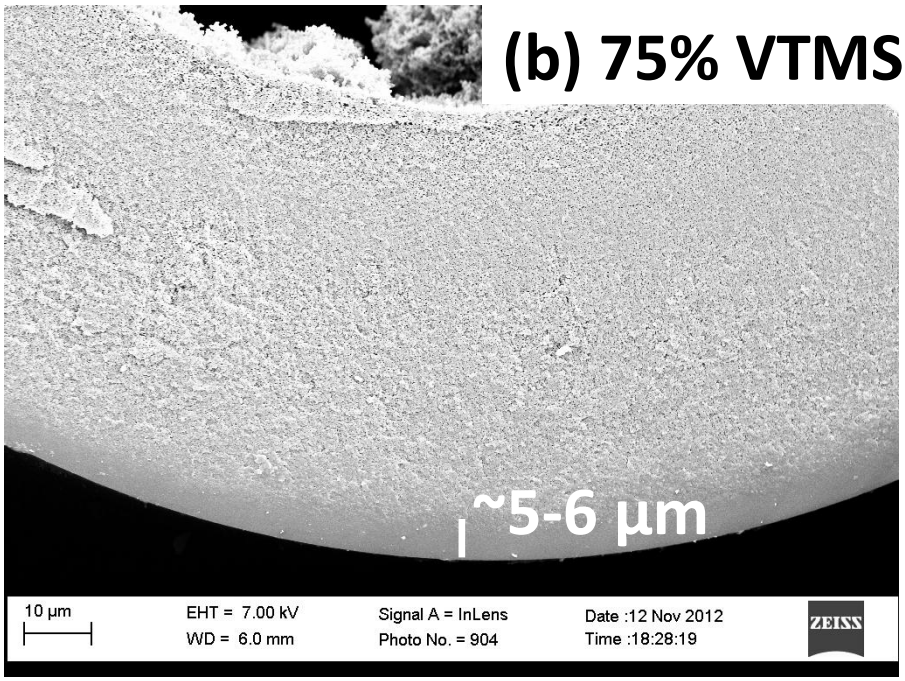

Figure 5.3(b): SEM images of 75% V-treated Matrimid® CMS hollow fibers pyrolyzed at 650°C under argon UHP atmosphere.

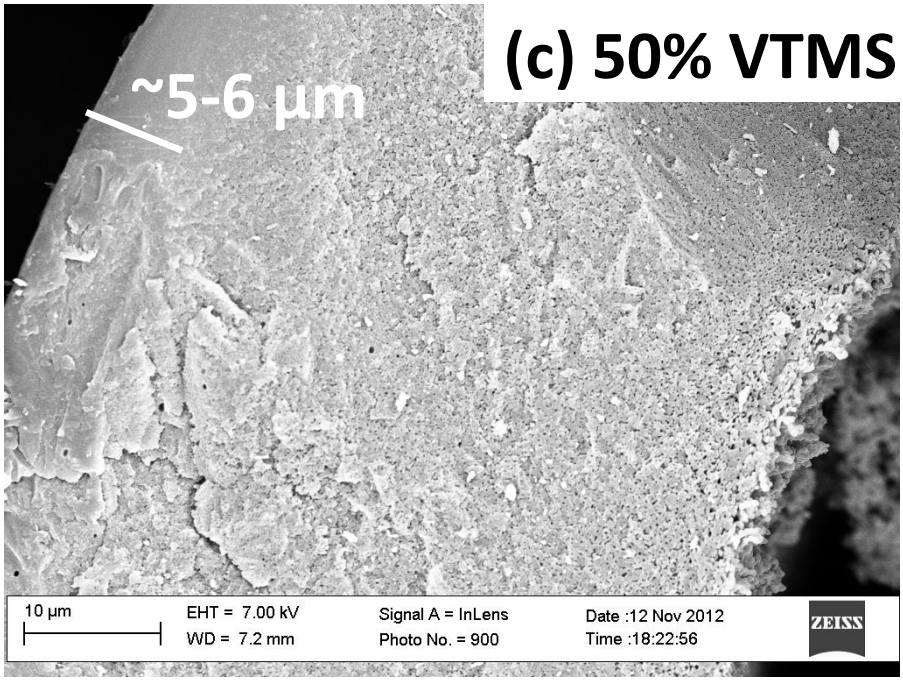

Figure 5.3(c): SEM images of 50% V-treated Matrimid® CMS hollow fibers pyrolyzed at 650°C under argon UHP atmosphere.

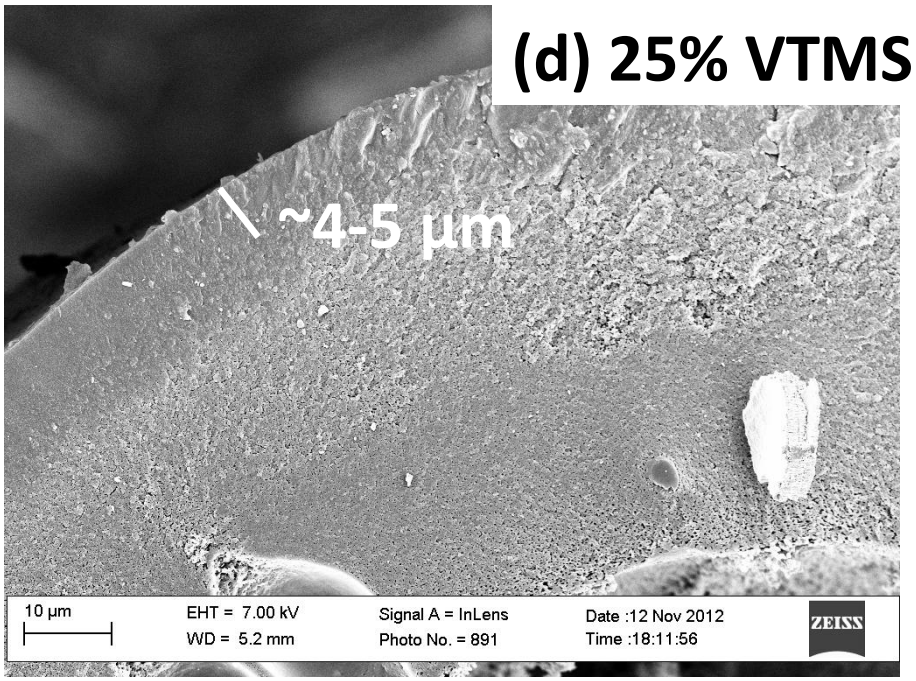

Figure 5.3(d): SEM images of 25% V-treated Matrimid® CMS hollow fibers pyrolyzed at 650°C under argon UHP atmosphere.

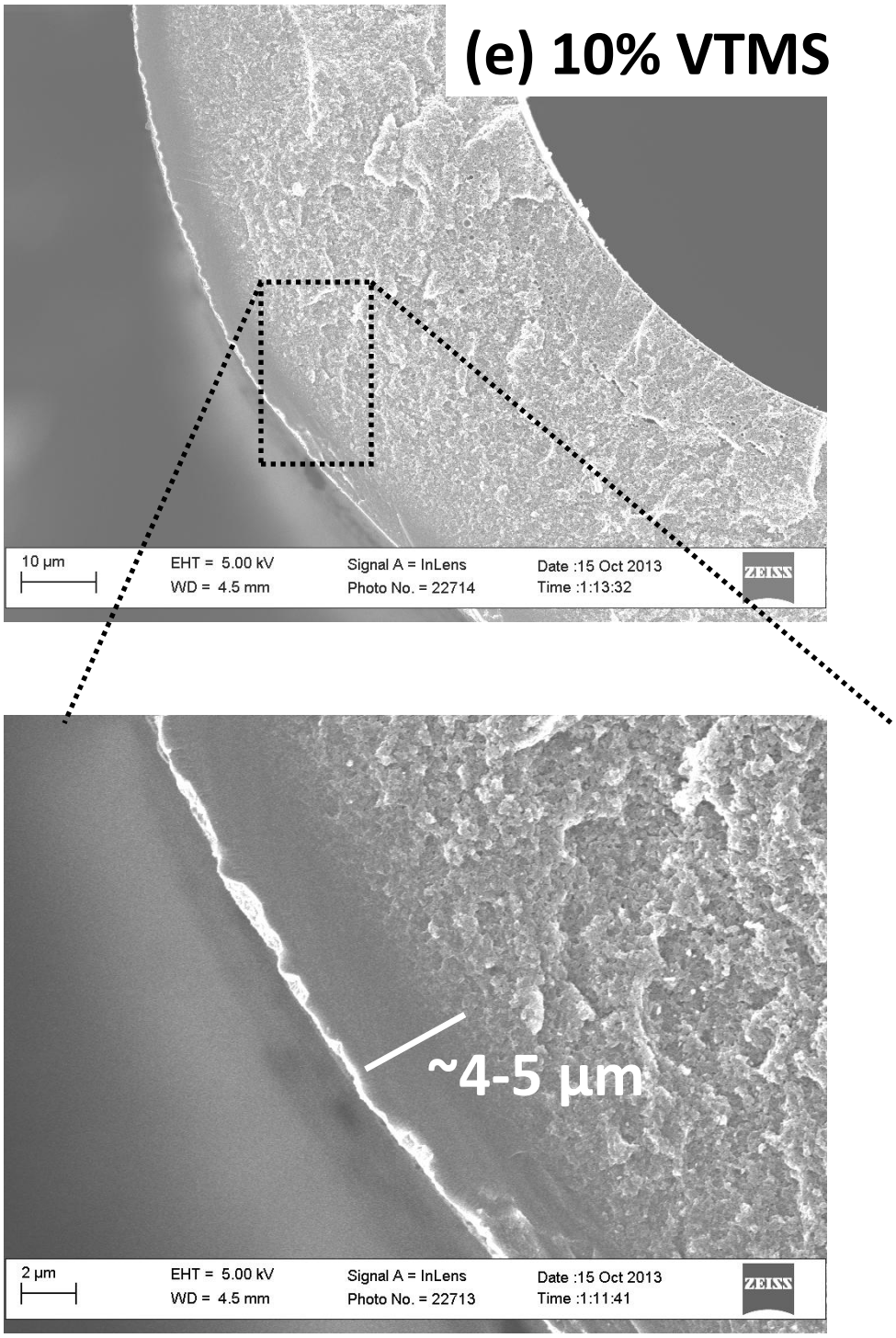

Figure 5.3(e): SEM images of 10% V-treated Matrimid® CMS hollow fibers pyrolyzed at 650°C under argon UHP atmosphere (*Optimum* VTMS% based on the permeation results in Figure 5.4).

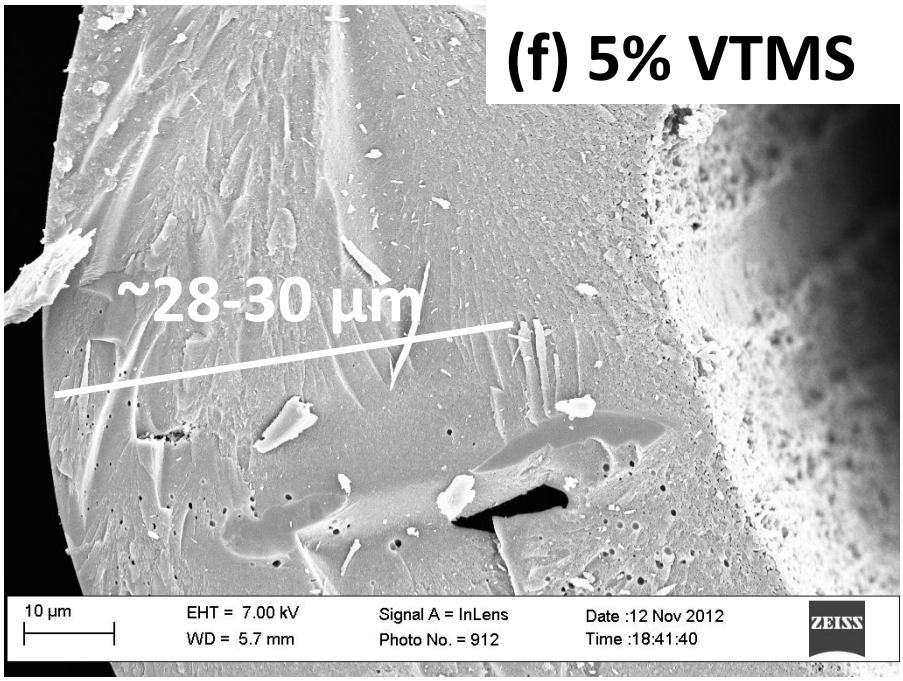

Figure 5.3(f): SEM images of 5% V-treated (VTMS-hexane) Matrimid® CMS hollow fibers pyrolyzed at 650°C under argon UHP atmosphere

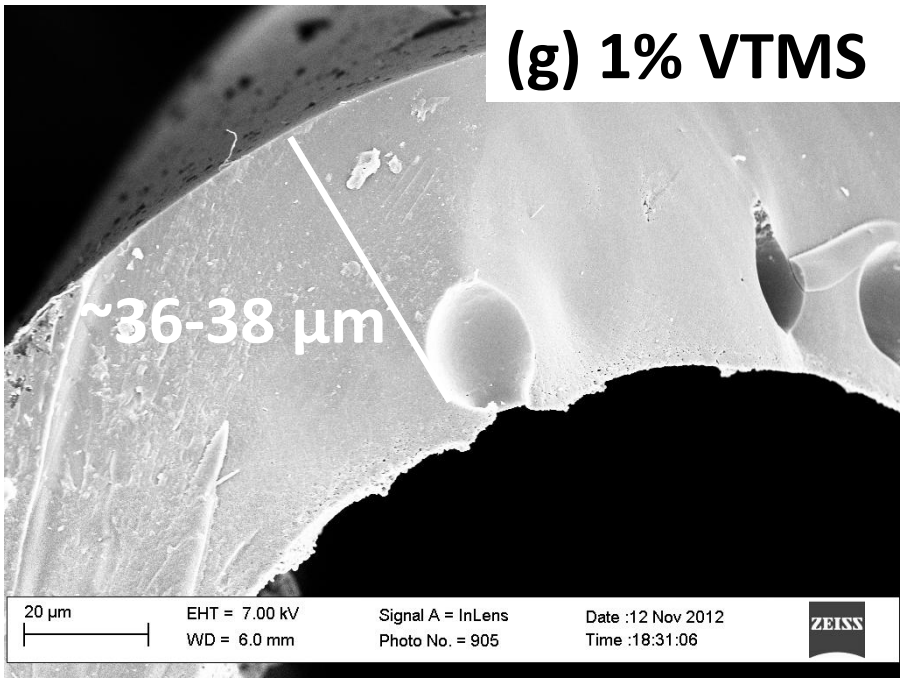

Figure 5.3(g): SEM images of 1% V-treated (VTMS-hexane) Matrimid® CMS hollow fibers pyrolyzed at 650°C under argon UHP atmosphere

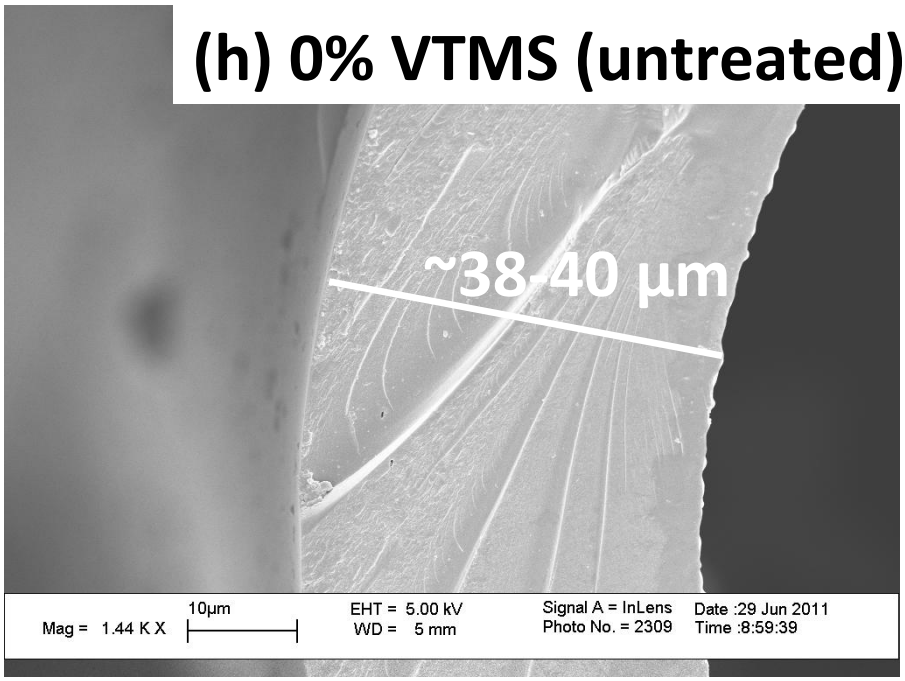

Figure 5.3(h): SEM images of *untreated* Matrimid® CMS hollow fibers pyrolyzed at 650°C under argon UHP atmosphere

All SEM images in Figure 5.3(b) to Figure 5.3(e) showed a similar asymmetric CMS sub-structure morphology like that of the 100% VTMS V-treated (Figure 5.3(a)). The 10% VTMS in hexane is the *lowest* concentration of VTMS which gives the improved asymmetric CMS morphology and also have the reduced silica content. The separation skin thickness of the 10% V-treated[4] fiber in Figure 5.3(e) is around 4-5 µm, which is significantly lower by *~9-10x* when compared the original untreated CMS Matrimid® (~38-40 µm as shown in Figure 5.3(h)).

In order to quantitatively evaluate the optimization of V-treatment, pure gas CO_2/CH_4 permeation was performed on the different VTMS% (V-treated) CMS hollow

[4]This notation will be used for the remainder of the chapter to refer to the 10% VTMS in hexane as the optimized solution for V-treatment.

fibers pyrolysed at 650°C under argon UHP. The permeation results from using the various V-treatment solutions are shown in Figure 5.4. The 10% V-treated CMS Matrimid® hollow fiber showed the *highest* permeance increase compared to any other VTMS% and untreated CMS hollow fiber. The CO_2/CH_4 selectivity for all the cases remained attractive at ~100. In Figure 5.4, the CO_2 permeance for the 10% V-treated CMS hollow fiber from the Matrimid® precursor is approximately 85-90 GPU, in comparison to the 8-9 GPU gas permeance for the untreated CMS hollow fiber. The permeance enhancement correlates well with the *9-10x* decrease in separation skin thickness for the asymmetric 10% V-treated CMS Matrimid® hollow fiber (Figure 5.3(e)). Further analysis using XPS discussed in section 5.4.2, showed later that the 10% V-treated CMS also exhibited lower silicon content on the outermost CMS skin when compared to the 100% V-treated CMS. The permeation results correlate well with the hypothesis of lowering the silica on the outermost CMS skin for superior separation performance as proposed in section 5.2.

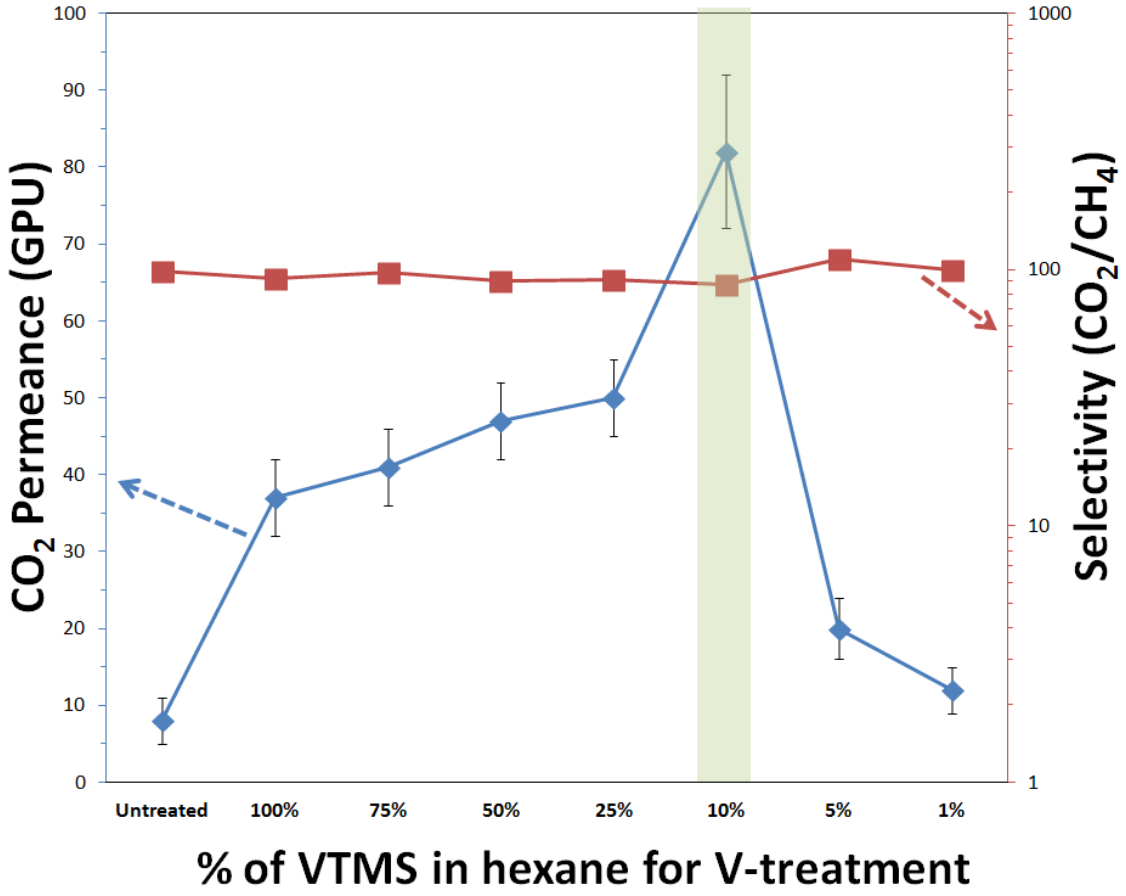

Figure 5.4: Separation performance evaluation for different (VTMS-hexane) V-treated Matrimid® CMS hollow fibers pyrolyzed at 650°C under argon UHP, pure gas feed was used for testing at 100 psi and 35°C.

5.3.2 Role of organic and alkoxy functional groups towards V-treatment

5.3.2.1 Trimethoxy silane (TMS) treatment

The difference in the molecular structure of VTMS and TMS is the absence of the 'vinyl' group in TMS, as shown in Figure 5.5. The 100% TMS treatment on Matrimid® precursor fibers was carried out using the same procedure as indicated in Figure 5.2. The reason to do 100% TMS treatment was to perform a proof-of-concept study, comparing only the effect of silane functional groups in the pre-treatment.

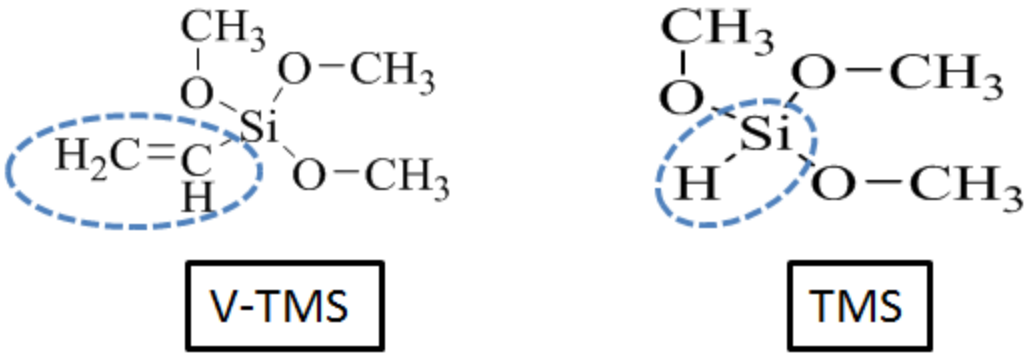

Figure 5.5: Molecular structure for Vinyl trimethoxy silane (V-TMS) and Trimethoxy silane (TMS).

After pyrolysis the TMS-treated CMS hollow fibers were found to be extremely brittle and also exhibited a thick silica layer on the outermost CMS skin as shown in the SEM images in Figure 5.6. Even though the TMS treated CMS hollow fiber had the improved asymmetric sub-structure morphology, the silicon loading in the TMS treated polymer precursor was found to be ~8.5 wt%, which was twice the amount found in 100% VTMS treated precursors (i.e. 4.23 wt% as discussed in Chapter 4). The increased silica layer in Figure 5.6 can be due to the increase in silicon content for the TMS treated polymer hollow fibers and the lack of 'vinyl' functional group, which made the TMS treated precursor hollow fibers exhibit the characteristics of silica glass (i.e. Si-O-Si) rather than silica-carbide (Si-C) or silica oxy-carbide (Si-O-C). The XPS results for the 100% V-treated CMS in Chapter 4 had indicated that the majority of organo-silica domains are bonded as Si-C (except on the outermost of surface which is primarily O-Si-O (SiO_2)).

Therefore, the 'vinyl' (organic) pendant group is essential for the pre-treatment approach to maintain the mechanical properties of the polymer precursor and resulting

CMS hollow fiber. VTMS gives the flexibility in the V-treatment process, allowing the organo-silica film to form on polymer chains but at the same time avoiding formation of excess silica (i.e. Si-O-Si). The importance of the 'vinyl' group in providing flexibility to the silane-treated polymers is also observed in VTMS-grafting related studies for cellulose acetate polymers [1].

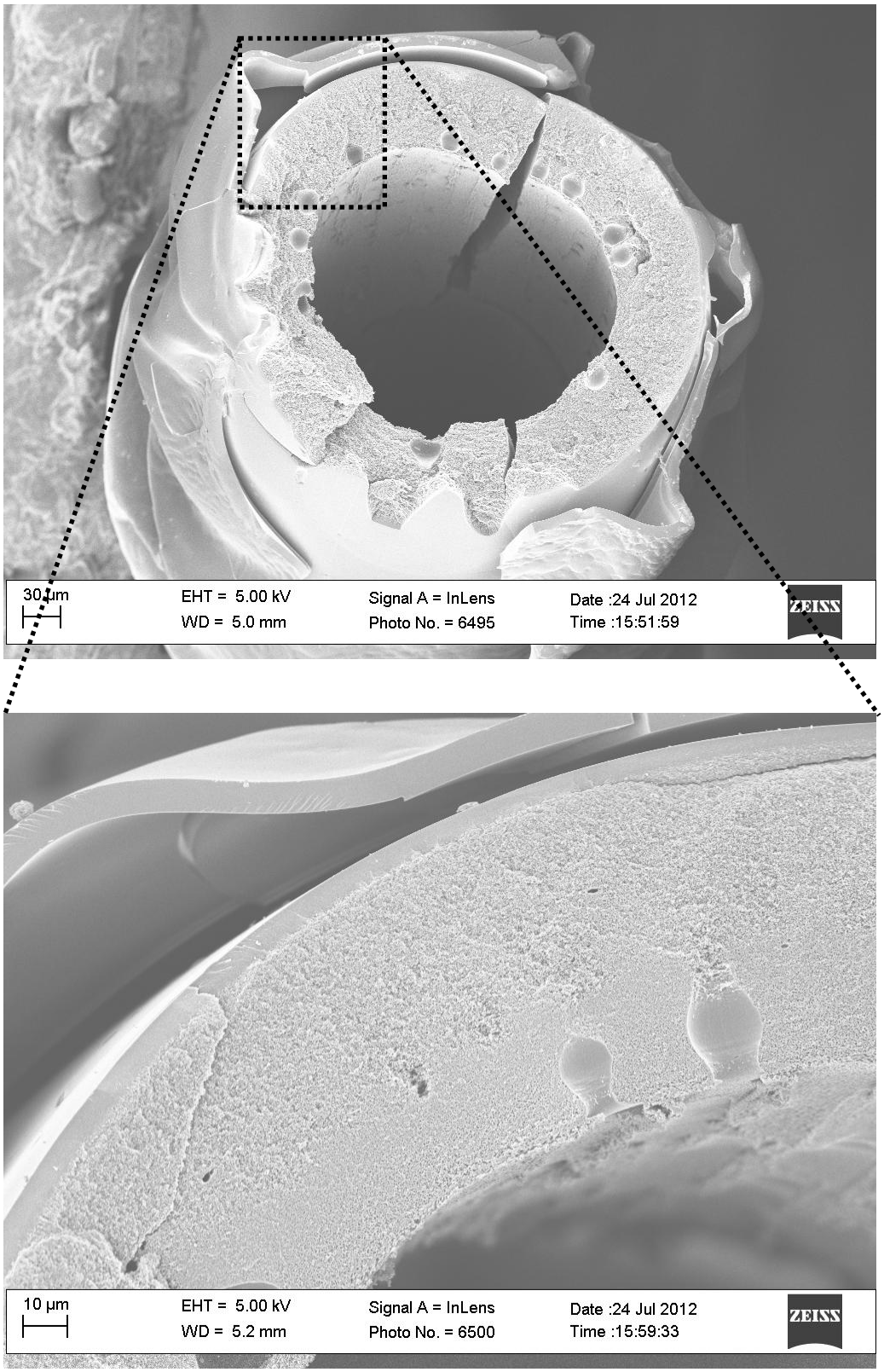

Figure 5.6: SEM images of CMS hollow fiber after the 100% TMS treatment on Matrimid® precursor, pyrolysed at 550°C under argon UHP.

5.3.2.2 Vinyl trimethyl silane treatment

The importance of the alkoxy functional groups in V-treatment is to create the sol-gel which restricts the morphology collapse during pyrolysis. To test the alkoxy sol-gel hypothesis, a vinyl silane *without* the methoxy groups but instead attached to methyl functional group was used. The molecular structures are shown in Figure 5.7.

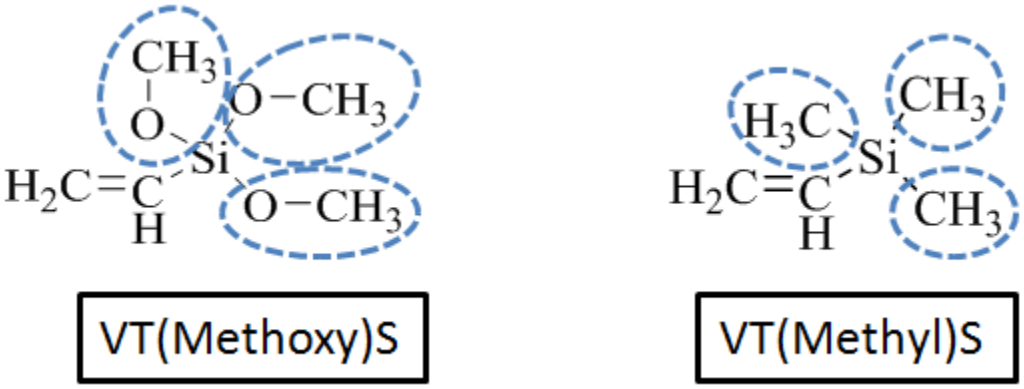

Figure 5.7: Molecular structure for Vinyl tri(methoxy) silane and Vinyl tri(methyl) silane.

Similar to the TMS treatment, the 100% vinyl trimethyl silane was used for the treatment according to the procedure in Figure 5.2. Unlike the TMS treatment, the precursor and CMS hollow fibers after vinyl trimethyl treatment had the mechanical properties to conduct further transport studies but showed a collapsed morphology after pyrolysis as shown in Figure 5.8. The lack of the organo-silica domain in the precursor hollow fibers prior to the pyrolysis allowed the polymer chains to mobilize, thus resulting in a collapsed morphology.

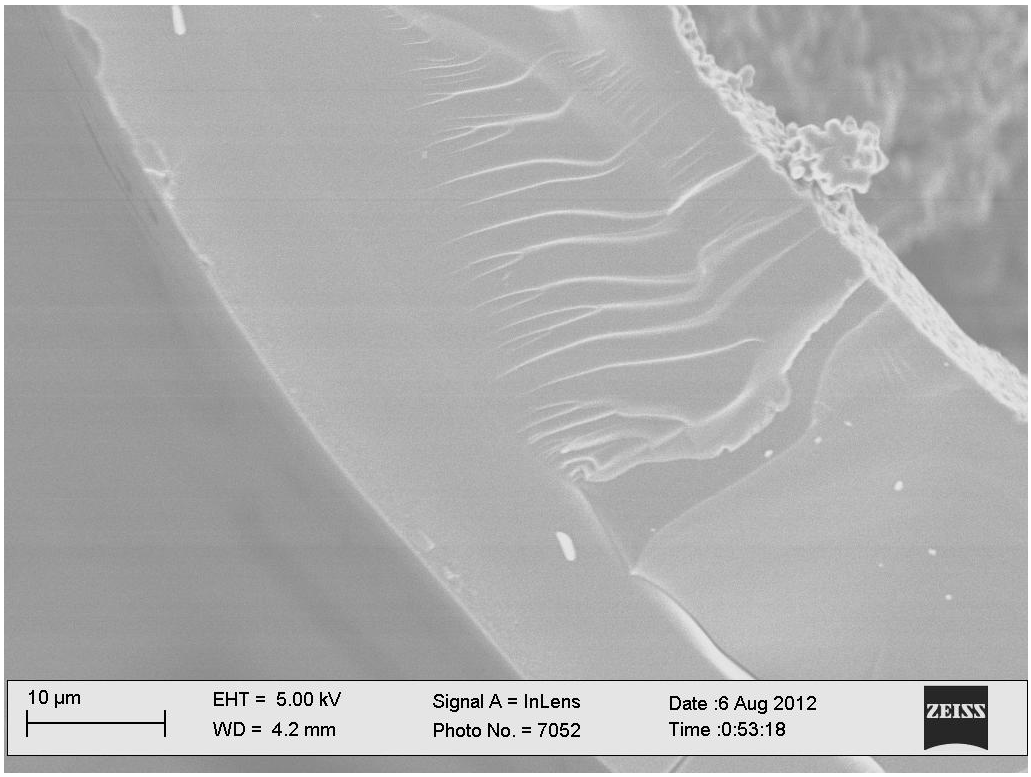

Figure 5.8: SEM images of CMS hollow fiber after the 100% vinyl trimethyl silane treatment on Matrimid® precursor, pyrolysed at 550°C under argon UHP.

5.3.2.3 Ethyl trimethoxy silane treatment

The XPS results for the 100% V-treated CMS in Chapter 4, indicated the presence of three different chemical bonding structures for the silicon atom (i.e., Si-C (majority), Si-O-Si, O-Si-O (outermost skin)). The Si-C bonding arises from two different chemical structures, one is from the existing vinyl-silicon bond and the second arises during the pyrolysis process when some of the vinyl reacts at higher temperatures (greater than 500°C) within the silica domain to form new Si-C bonds. The reaction of vinyl at higher temperatures was indicated in the TGA and NMR analyses discussed in Chapter 4 and also in the literature [2]. The importance of having a reactive hydrocarbon pendant group

(like vinyl) compared to a less reactive hydrocarbon group was verified using ethyl trimethoxy silane (ETMS). The molecular structures are shown in Figure 5.9.

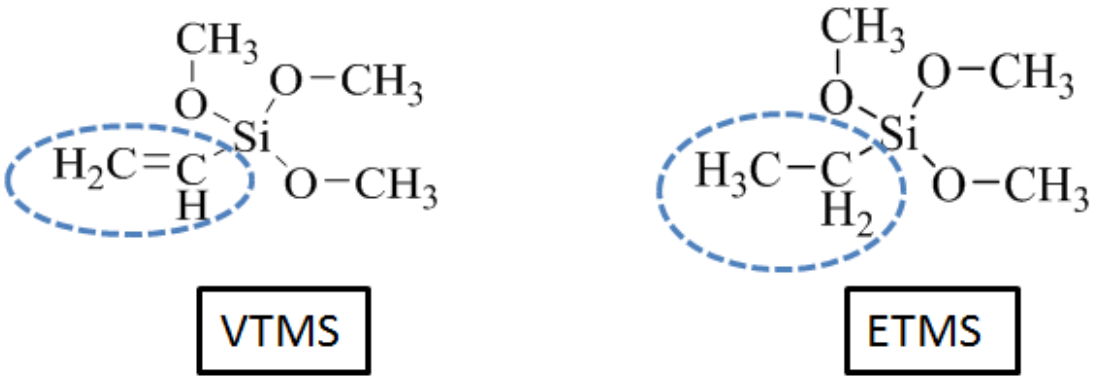

Figure 5.9: Molecular structure for Vinyl trimethoxy silane (VTMS) and Ethyl trimethoxy silane (ETMS).

The ETMS control treatment was done using 10% ETMS in hexane following the similar procedure in Figure 5.2. After pyrolysis at 650°C under argon UHP, the ETMS treated CMS hollow fiber sub-structure morphology was porous, similar to the 10% VTMS treated, but the CMS separation skin was thicker (~8-10 µm) for the ETMS treated compared to the (~4-5 µm) VTMS treated fibers. The SEM image comparison of the CMS sub-structure morphology for both 10% ETMS and 10% VTMS treated is shown in Figure 5.10 (a) and (b). The mechanical properties of the ETMS treated precursor and CMS hollow fibers were similar to the VTMS treated fibers, further modulus testing would be required to conclusively compare the difference. As the transport results shown in Table 5.1 where less attractive for ETMS treated hollow fibers, mechanical properties characterization for were not pursued.

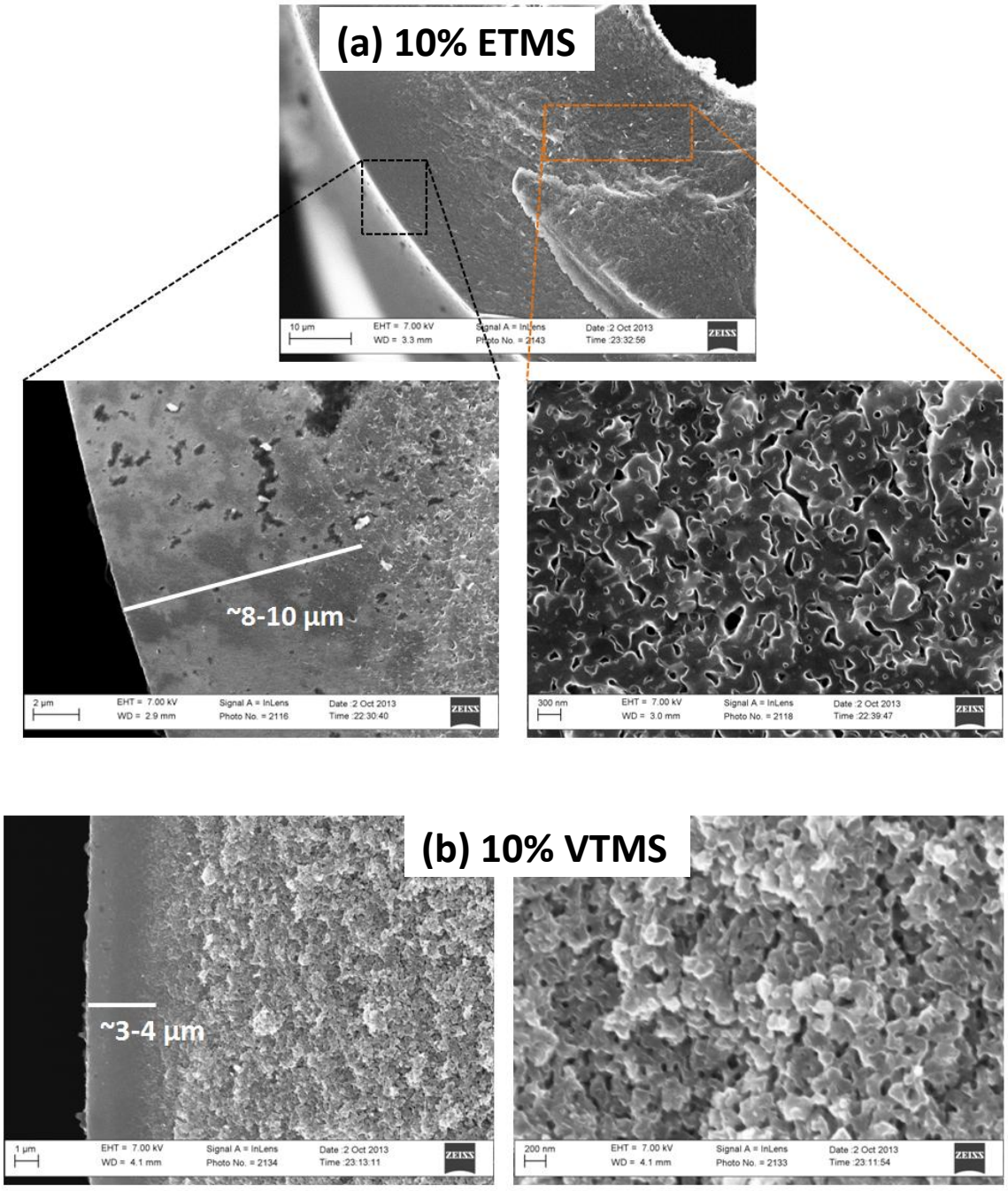

Figure 5.10: SEM image comparison of asymmetric CMS sub-structure morphology after (a) 10% ETMS treatment and (b) 10% VTMS treatment on Matrimid® precursor, pyrolysed at 650°C under argon UHP.

CO_2/CH_4 permeation was performed on the 10% ETMS treated CMS hollow fiber from Matrimid® precursor and compared with the 10% VTMS treated CMS hollow fiber

results, and are listed in Table 5.1. The 10% ETMS treated CMS hollow fiber showed lower CO_2 permeance due to the increased separation CMS skin as shown in Figure 5.10(a).

Table 5.1: Separation performance comparison for 10% ETMS and VTMS treated CMS hollow fibers from Matrimid® precursors pyrolyzed at 650°C under argon UHP, pure gas feed was used for testing at 100 psi and 35°C.

State	$P(CO_2)$ (GPU)	CO_2/CH_4
10% ETMS treated CMS	17	95
10% VTMS treated CMS	85	93

The results from the ETMS treatment are a further indication that, along with an alkoxy group, a reactive hydrocarbon pendant group (e.g., unsaturated compounds) is useful for restricting collapse and achieving enhanced separation performance. The study using various silanes with different reactive pendant groups can be a future path for optimization.

5.4 Characterization of optimized (10%) V-treated precursor and CMS hollow fiber membranes

5.4.1 Elemental analysis

The bulk elemental composition for both 10% V-treated Matrimid® precursor and CMS sample was obtained similar to the procedure mentioned in Chapter 3. For the elemental analysis of the CMS sample, CMS fibers were first ground into fine powder

and then analyzed for each element. To verify the accuracy[2] of the lab results, a comparison of the untreated polymer precursor (experimental values) with the theoretical composition (according to molecular structure) was obtained and found to agree to within *+/- 1%*. The comparison of untreated, 100% V-treated, 10% V-treated precursor and respective CMS fibers are listed in Table 5.2 and 5.3, respectively.

Table 5.2: Combined elemental analyses for untreated, 100% VTMS and 10% VTMS treated Matrimid® *precursor*.

		Carbon	Hydrogen	Nitrogen	Oxygen	Silicon
Untreated[5]	(wt %)	75.4	4.4	5.3	14.5	---
	(At %)	52.4	36.9	3.2	7.6	---
V-treated (100% VTMS)	(wt %)	73.2	4.9	4.5	13.2	4.2
	(At %)	49.8	39.6	2.6	6.7	1.2
V-treated (10% VTMS)	(wt %)	74.4	4.6	4.9	13.8	2.3
	(At %)	51.3	37.9	2.9	7.1	0.7

By reducing the 100% VTMS to the 10% VTMS for V-treatment, a decrease in silicon% for both the V-treated precursor (Table 5.2) and the resultant CMS samples (Table 5.3) were observed. The decrease is desirable for the optimization of V-treatment and translation to the CMS permeance increase as shown in Figure 5.4 and section 5.5.

[5]In terms of the accuracy of the technique, untreated precursor samples were also obtained and the results closely matched with the precursor molecular structures as discussed in Chapter 4.

Table 5.3: Combined elemental analyses for untreated, 100% VTMS and 10% VTMS treated CMS Matrimid® sample (Pyrolysed at 550°C under argon UHP).

		Carbon	Hydrogen	Nitrogen	Oxygen	Silicon
Untreated	(wt %)	87.4	3.1	4.8	4.8	---
	(At %)	66.1	28.1	3.1	2.7	---
V-treated (100% VTMS)	(wt %)	76.1	3.2	4.0	5.2	11.6
	(At %)	56.2	35.6	2.3	2.4	3.6
V-treated (10% VTMS)	(wt %)	85.6	3.4	3.9	3.0	4.2
	(At %)	64.2	30.3	2.5	1.7	1.3

In addition to the VTMS concentration optimization, tuning of final pyrolysis temperature is also important for obtaining superior separation performance as discussed in section 5.6. Elemental analyses for the CMS samples pyrolysed at different final pyrolysis temperatures with and without V-treatment are shown in Table 5.4. As we increase the pyrolysis temperatures, both the carbon and silicon percentages in Table 5.4 increase due to the re-arrangement of carbon sheets in the CMS and probably the reaction of vinyl groups within the organo-silica domain at higher temperatures as discussed in XPS and TGA characterization sections in Chapter 4.

Table 5.4: Comparison of elemental analyses for untreated, 100% VTMS and 10% VTMS treated CMS Matrimid® at different final pyrolysis temperatures under argon UHP.

		Carbon	Hydrogen	Nitrogen	Oxygen	Silicon
CMS Untreated Matrimid®						
550°C	wt%	87.4	3.1	4.8	4.8	
	mol%	66.1	28.1	3.1	2.7	---
650°C	wt%	91.2	1.3	3.8	2.7	
	mol%	81.7	13.7	2.9	1.8	---
CMS V-Treated Matrimid® (100% VTMS)						
550°C	wt%	76.1	3.2	4.0	5.2	11.6
	mol%	56.2	35.6	2.3	2.4	3.6
650°C	wt%	76.3	2.4	2.7	3.0	15.6
	mol%	66.0	24.3	2.0	1.9	5.8
CMS V-Treated Matrimid® (10% VTMS)						
550°C	wt%	85.6	3.4	3.9	3.0	4.2
	mol%	64.2	30.3	2.5	1.7	1.3
600°C	wt%	87.6	2.7	3.4	2.0	4.3
	mol%	69.2	25.9	2.3	1.2	1.5
650°C	wt%	86.1	2.5	3.1	2.6	5.8
	mol%	70.1	24.2	2.2	1.6	2.0

5.4.2 XPS with sputter-ion etch

The elemental analysis result in section 5.4.1 gives the bulk composition of the CMS V-treated samples, analyzed as described in Chapter 3. To characterize the V-treatment optimization, it is important to obtain the silicon depth profile in the CMS sample, especially in the intrinsic CMS skin and outermost skin layer. XPS with sputter-ion etch was performed on the outermost skin of 10% V-treated CMS, according the procedure mentioned in Chapter 3. XPS with sputter-ion etch helps in obtaining the Si2p

and C1s depth profile by a shallow and deep etch[6] distribution as a function of the sputter depth profiling time. A comparison of shallow etch XPS distribution profile for Si2p and C1s on the outer surface of the 10% V-treated CMS with 100% V-treated CMS hollow fiber is shown in Figure 5.11. For 10% V-treatment, the silicon (At%) on the outermost skin[3] (which is approximately less than 1 μm) drops down to ~17% compared to ~35% in 100% V-treated CMS. For the 10% V-treated intrinsic CMS skin, the surface composition for silicon% drops down to less than 2%, further indicating that the majority of silica is present on the outermost CMS skin.

[6]Due to the variety of bonds present on the CMS V-treated sample, it is challenging to estimate an accurate rate. Taking the different bond etch rates for Si-O-Si, Si-C and C-C the rough estimate would be ~0.2-0.25 nm/s.

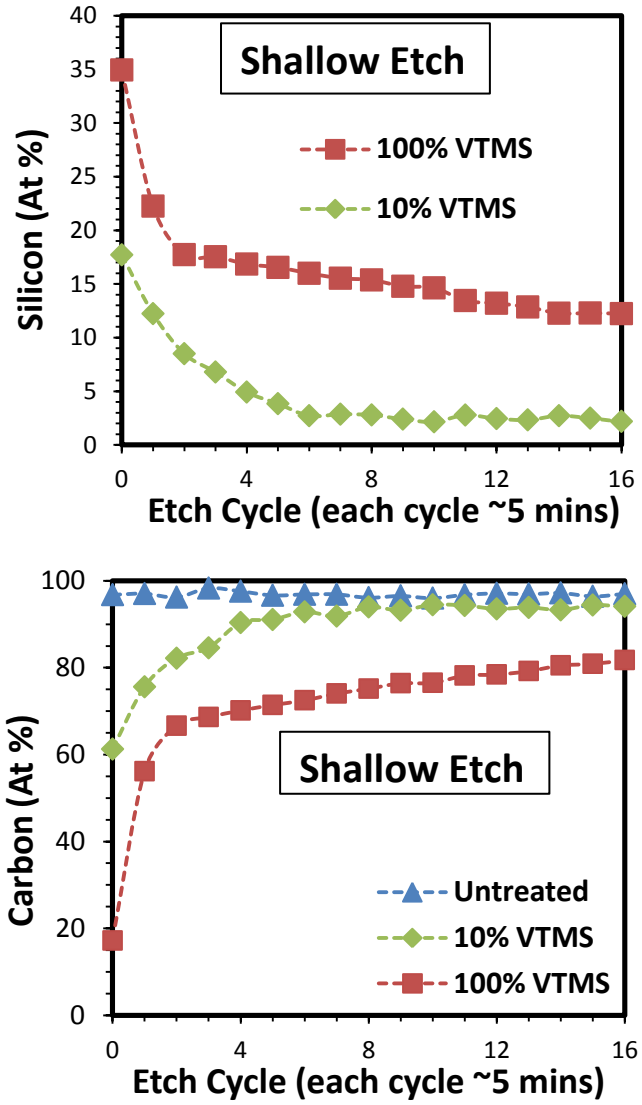

Figure 5.11: XPS surface composition profile for Si2p and C1s as a function of sputter etch depth profiling time for CMS hollow fibers pyrolysed at 550°C under argon UHP.

The Si2p and C1s shallow etch distribution profile in Figure 5.11 shows that the 10% V-treated CMS is closer to the untreated intrinsic CMS with much lower silicon% (compared to 100% V-treated CMS). It is important to note that At% estimated from XPS cannot estimate hydrogen, therefore the XPS percentages are much higher compared to the actual bulk CMS sample as shown in Table 5.4 (which includes the hydrogen%).

The shallow etch-XPS distribution is accurate to estimate only the outermost surface analysis. For the depth profile in Figure 5.11, the etching depth would be approximately *less than* 1μm depending upon the etch rate[7]. To obtain an increased depth profile, the duration of sputter-ion etching was increased to 45 mins per cycle and tested for three etching cycles as shown in Figure 5.12. After looking at the SEM image of the etched surface for outermost 10% V-treated CMS skin (top view), a distribution of smaller pores could be observed. It is difficult to accurately predict the exact depth at which XPS cycle was estimated because of the complexity of various bond etch-rates. After the third sputter-ion etch cycle, the etched area in Figure 5.12 could be somewhere between the transition and microstructure regions.

[7] Due to the variety of bonds present on the CMS V-treated sample, it is challenging to estimate an accurate rate. Taking the different bond etch rates for Si-O-Si, Si-C and C-C the rough estimate would be ~0.2-0.25 nm/s.

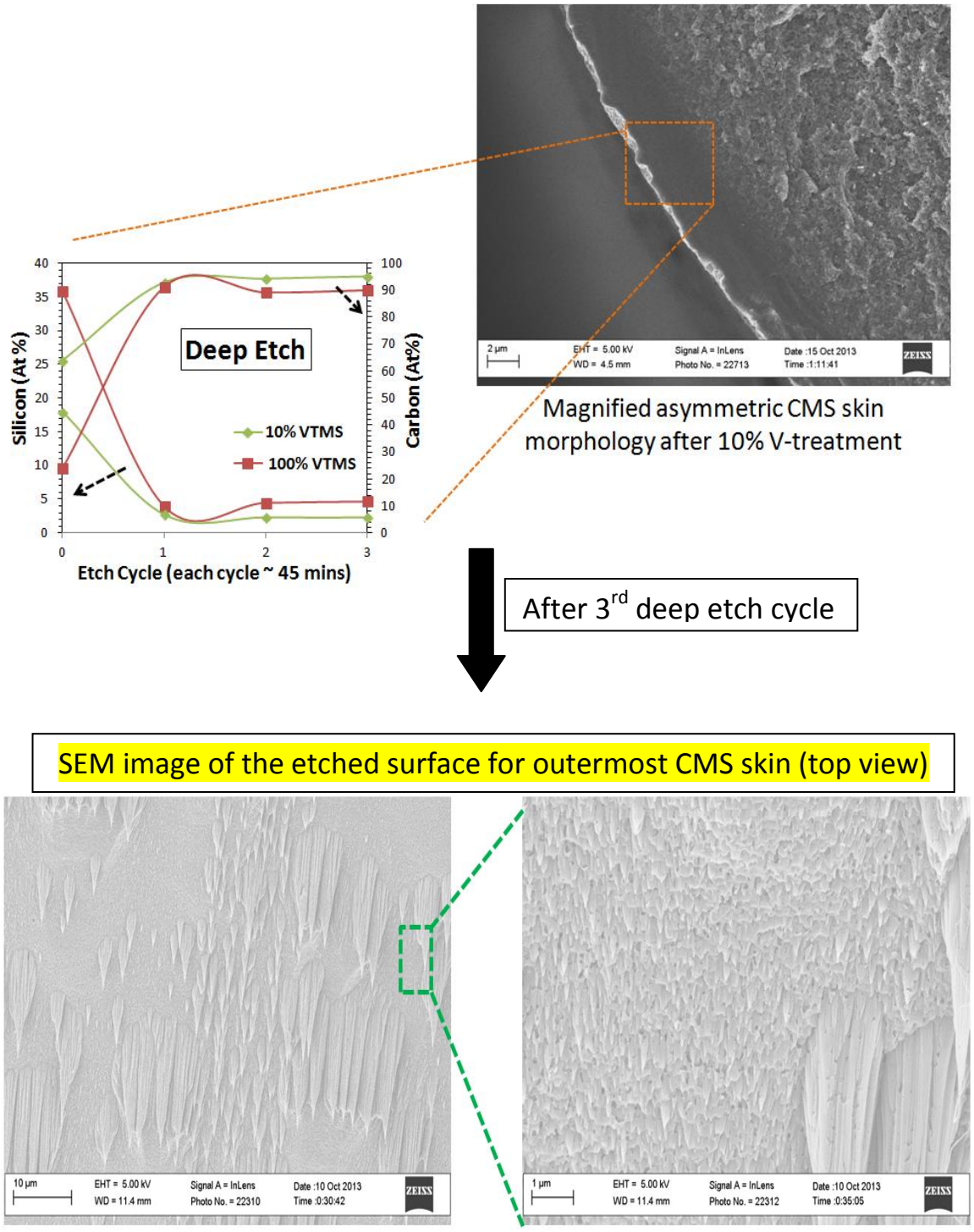

Figure 5.12: Combination of Si2p and C1s deep-etch XPS profile as a function of depth profiling time, and SEM images of the top view (from CMS skin side) for 10% V-treated CMS surface after 3rd cycle of etching, pyrolysed at 550°C under argon UHP.

5.4.3 DMA on the different VTMS % treated Matrimid® precursor hollow fibers

As discussed in Chapter 4, the mechanism behind the sub-structure collapse during pyrolysis is the bulk re-arrangement of polymer chains at the glass-rubber transition. The mobilization of polymer chains at T_g is observed by a significant decrease in storage modulus as seen by the qualitative DMA study (Figure 5.13), where the blue solid curve denotes the untreated Matrimid® precursor hollow fiber. The storage modulus of precursor hollow fiber in Figure 5.13 is around 200 MPa, which is lower than the reported precursor dense film storage modulus (around 2000 MPa), the lower value is due to the asymmetric porous micro-support structure, also discussed in Chapter 4. In comparison, the V-treated precursor fibers exhibit better thermal stability at T_g. Due to the presence of silica in the porous sub-structure, the fiber rigidity is increased and severe sample deformation is avoided above T_g. It is also apparent from Figure 5.13 that higher silica loadings provide increasing resistance to sample deformation above T_g.

The different VTMS% treated fibers exhibit different silica loading as seen from the elemental analysis results (Table 5.2), and the highest silica content for the 100% V-treated sample results in the least drop in modulus as shown in Figure 5.13. The 10% V-treated showed a similar trend as the 100% sample, but with a slightly larger drop in storage modulus because of lower silica content (Table 5.2). The 10% V-treated fiber after reaching the minima at ~365°C showed a similar increasing trend in storage modulus, signifying the ability to restrict the collapse. The 5% V-treated asymmetric CMS sub-structure morphology (Figure 5.3(f)) exhibited a higher degree of collapse because of the insufficient silica domains in the porous sub-structure.

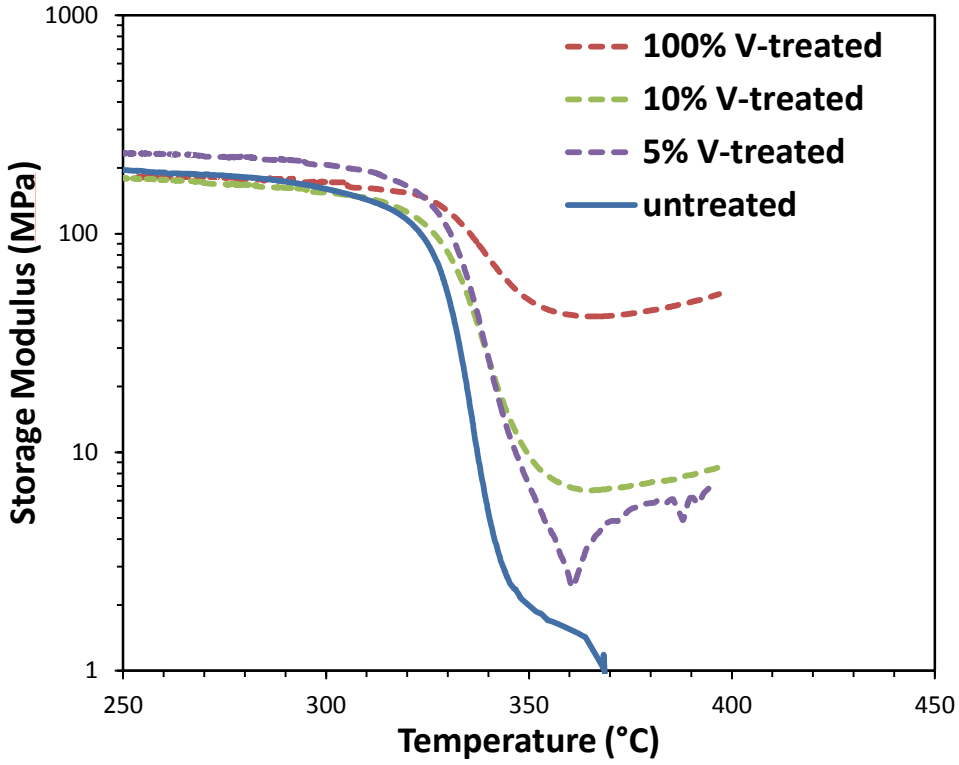

Figure 5.13: DMA for the untreated and different VTMS % (V-treated) Matrimid® precursor hollow fibers (storage modulus).

5.5 Permeation and sorption measurements for the optimized (10%) V-treated CMS from Matrimid® precursor

5.5.1 Permeation results for pure gas feed

Pure gas permeation was carried out on the 10% V-treated CMS hollow fibers pyrolysed at two different pyrolysis temperatures, 550°C and 650°C, under argon UHP. At both pyrolysis temperatures, the 10% V-treated CMS hollow fibers showed at least as high as or higher than *9x* increase in gas permeance as shown in Figure 5.14(a) and 5.15(a). By optimizing the V-treatment, the 10% V-treated CMS permeance increased by

at least *9x*, which is even higher when compared to the 100% V-treated CMS permeance increase (i.e. at least 3x). The higher increase in CMS permeance resulted due to the optimization of VTMS concentration (10%), which reduced the excess silica on the outermost V-treated CMS skin as discussed in sections 5.3 and 5.4. The increase in gas permeance for 10% V-treated CMS hollow fiber (at least *9x*) correlated with the reduced CMS separation skin (i.e. *9-10x*) as shown in the SEM image Figure 5.3(e).

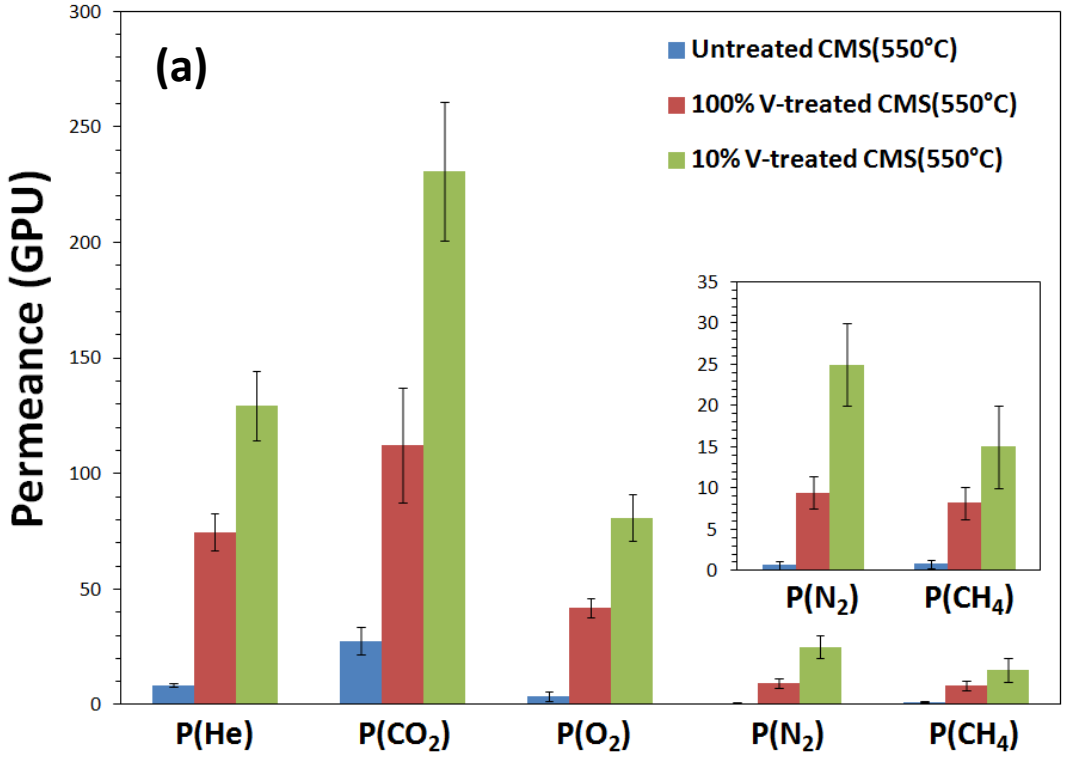

Figure 5.14(a): Comparison of gas permeance for the optimized (10%) V-treated, 100% V-treated and untreated CMS hollow fibers from Matrimid® precursor pyrolysed at 550°C under argon UHP, pure-gas feed pressure of 100 psi and at testing temperature 35°C.

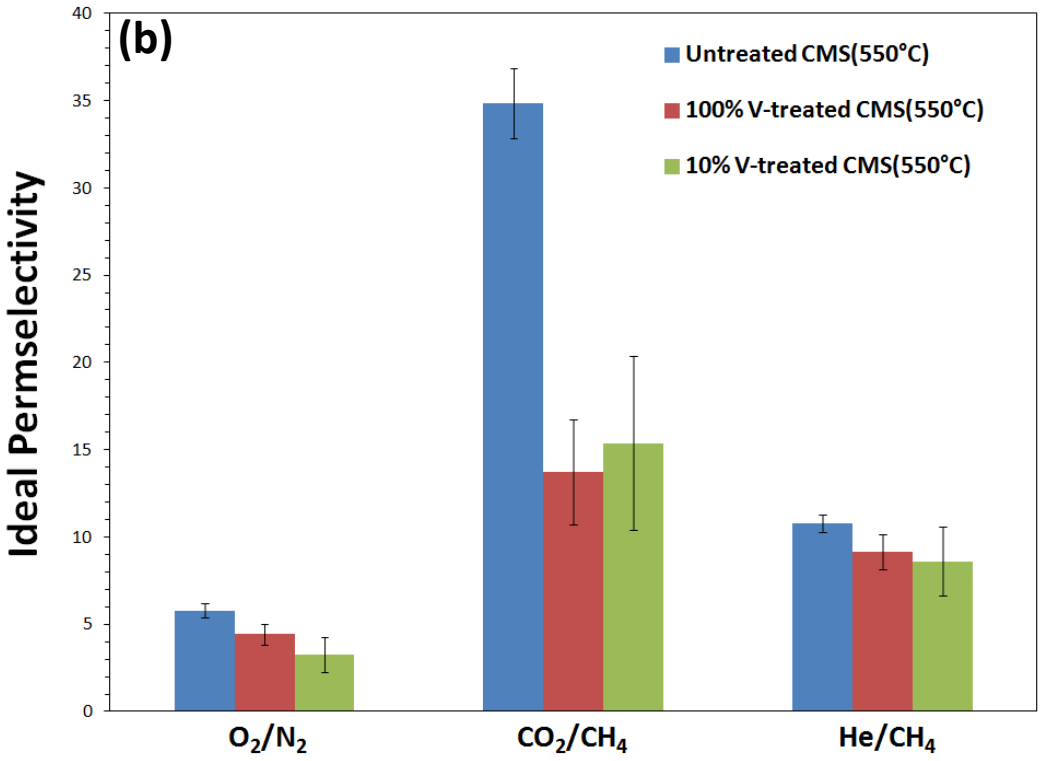

Figure 5.14(b): Comparison of permselectivity for the optimized (10%) V-treated, 100% V-treated and untreated CMS hollow fibers from Matrimid® precursor pyrolysed at 550°C under argon UHP, pure-gas feed pressure of 100 psi and at testing temperature 35°C.

The desirable gas permeance increase for both 10% and 100% V-treated CMS hollow fibers pyrolysed at 550°C in Figure 5.14(a) resulted in slightly lower permselectivities when compared with untreated CMS membranes, shown in Figure 5.14(b). For the case of CO_2/CH_4, the V-treated CMS membranes showed significantly lower selectivity (by a factor of 2) compared to untreated CMS membranes. To understand this behavior, equilibrium sorption measurements were carried out on both untreated and 10% V-treated CMS samples, discussed in section 5.5.2. The equilibrium sorption isotherms discussed in section 5.5.2, showed some effect of the glassy domains (i.e. organo-silica layer) on the properties of the optimized V-treated CMS membranes;

however, the thin sheath silica layering on the skin and porous micro structure ("struts") illustrated in Fig 5.1 have relatively small effects on sorption in most cases.

To address the lower gas permselectivities of the optimized V-treated CMS membranes, the final pyrolysis temperature can be tuned to change the molecular sieving structure of the intrinsic CMS. By increasing the pyrolysis temperature from 550°C to 650°C, attractive permselectivities with permeance increase (approximately 9x) for the 10% V-treated CMS hollow fiber from Matrimid® were observed, as shown in the Figures 5.15 (a) and (b).

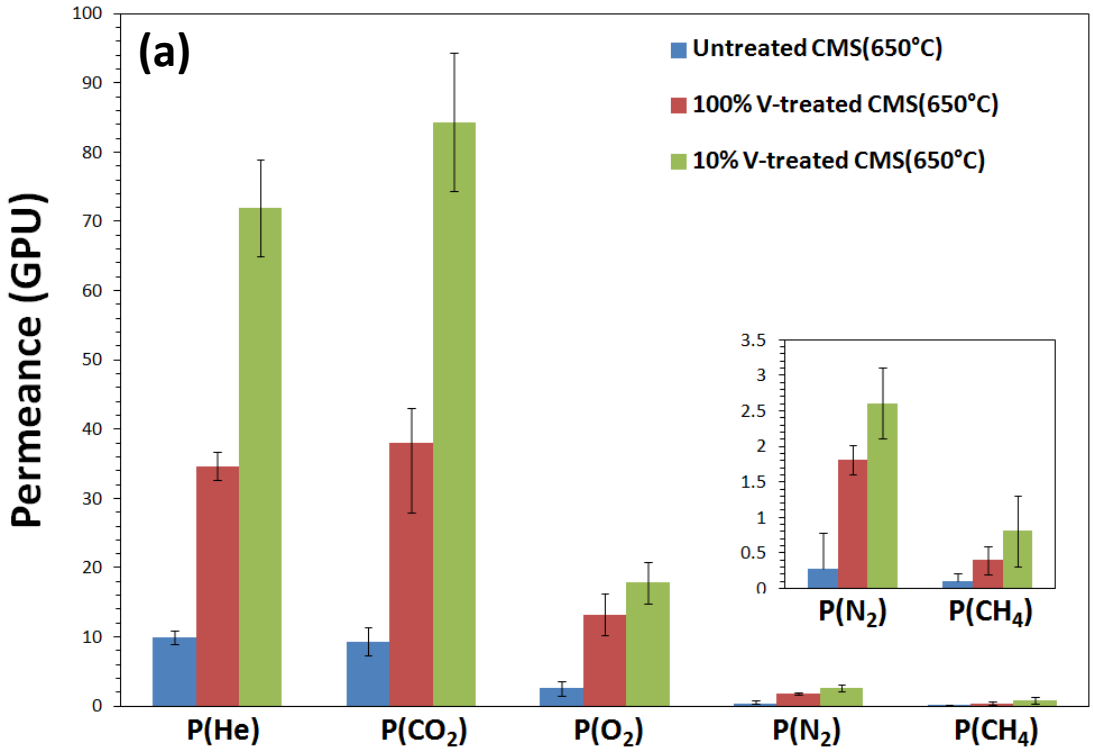

Figure 5.15(a): Comparison of gas permeance for the optimized (10%) V-treated, 100% V-treated and untreated CMS hollow fibers from Matrimid® precursor pyrolysed at 650°C under argon UHP, pure-gas feed pressure of 100 psi and at testing temperature 35°C.

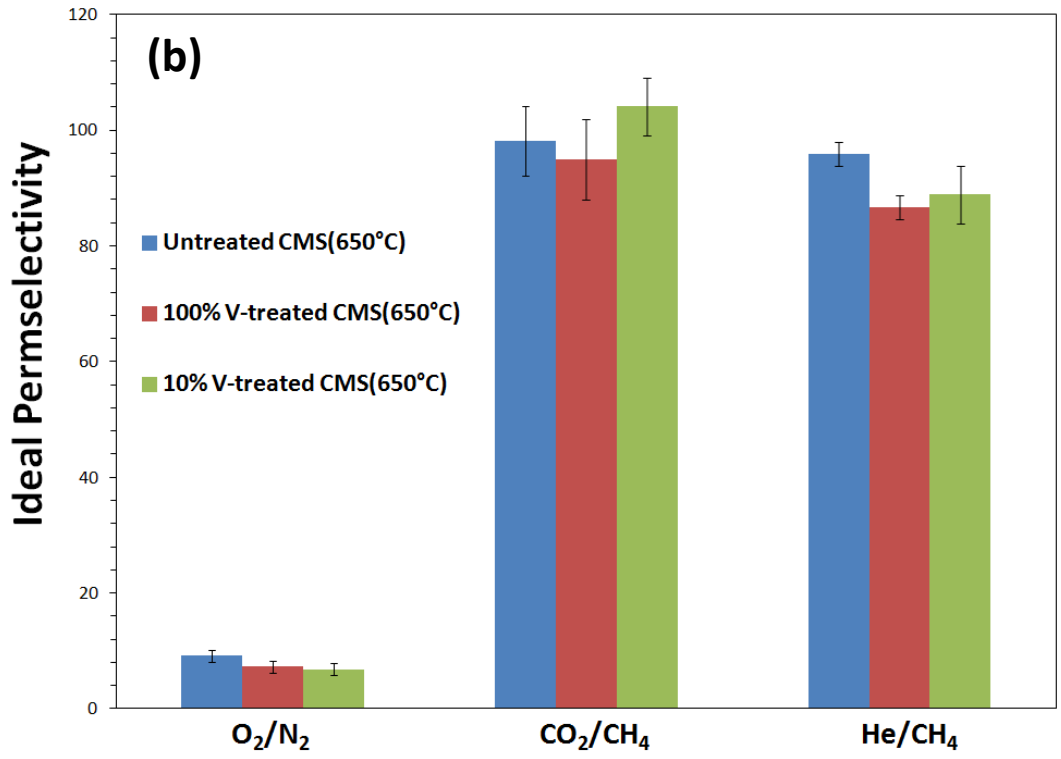

Figure 5.15(b): Comparison of permselectivity for the optimized (10%) V-treated, 100% V-treated and untreated CMS hollow fibers from Matrimid® precursor pyrolysed at 650°C under argon UHP, pure-gas feed pressure of 100 psi and at testing temperature 35°C.

5.5.2 Equilibrium sorption for 10% V-treated CMS Matrimid® (pure gas CO_2 and CH_4)

In general, molecular sieving materials follow the Langmuir sorption isotherm, where the gas molecules sorb into the pores or 'holes' of the material and sorption coefficients are determined using the parameters C_H' (Langmuir hole filling capacity) and *b* (Langmuir affinity constant). To obtain the equilibrium sorption of V-treated and untreated CMS fibers, the CMS hollow fibers were broken into small pieces to fit in a mesh filter as explained in Chapter 3. The equilibrium sorption isotherms for both the V-treated and untreated CMS pyrolysed at 600°C, and 650°C are shown in Figure 5.16, and Figure 5.17 respectively.

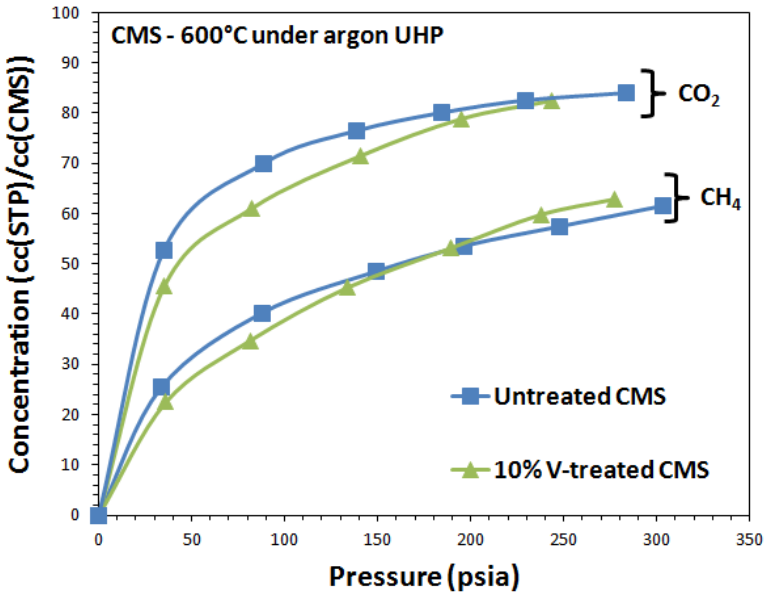

Figure 5.16: Comparison of equilibrium sorption isotherms for untreated and 10% V-treated CMS hollow fibers from Matrimid® precursor pyrolysed at 600°C under argon UHP, tested at 35°C (solid triangles denote the 10% V-treated CMS and solid squares for the untreated CMS experimental sorption data).

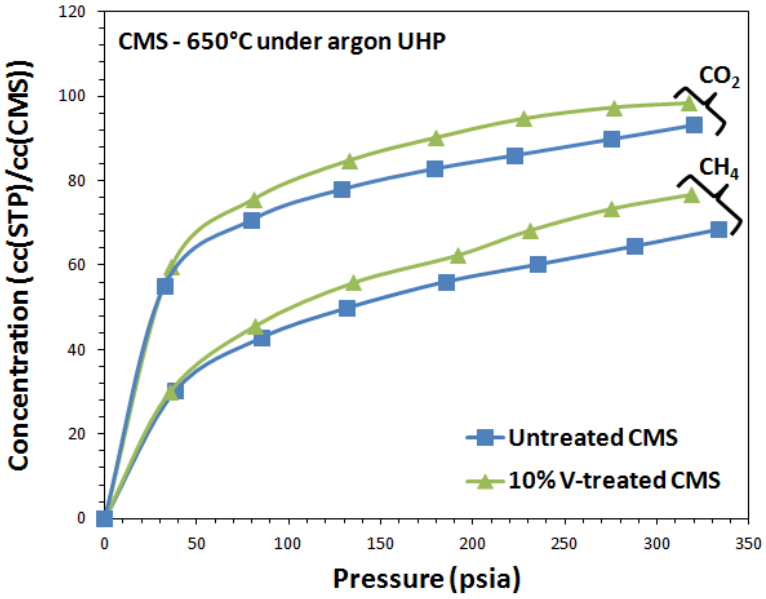

Figure 5.17: Comparison of equilibrium sorption isotherms for untreated and 10% V-treated CMS hollow fibers from Matrimid® precursor pyrolysed at 650°C under argon UHP, tested at 35°C (solid triangles denote the 10% V-treated CMS and solid squares for the untreated CMS experimental sorption data).

In the Figure 5.16 for 600°C, and Figure 5.17 for 650°C, both the untreated and 10% V-treated CMS showed similar equilibrium sorption isotherms. The small variations in the V-treated CMS isotherms can be accounted for, by considering V-treated CMS as a composite material, which is primarily composed of carbon sheets but also contains certain small amounts of glassy (organo-silica) domains from the V-treatment. The characterization analysis discussed in section 5.4 showed the presence of the glassy domains in the V-treated CMS sample mostly on the outermost CMS skin and the porous sub-structure ("struts") as explained in Figure 5.1. The Langmuir isotherm model was fit to the untreated and the 10% V-treated CMS sorption data for both the pyrolysis temperatures in Figure 5.16 and Figure 5.17. The Langmuir constant values are listed in Table 5.5.

Table 5.5: Langmuir isotherm constants for the untreated, and the 10% V-treated CMS Matrimid® hollow fibers, pyrolysed at 600°C, and 650°C under argon UHP.

Pyrolysis Temperature		C_H'(cc(STP)/cc(CMS))	b (1/psi)	Sorption selectivity
Untreated CMS from Matrimid® precursor				
600°C	CO_2	91.4	0.038	1.68
	CH_4	73.8	0.014	
650°C	CO_2	97.6	0.036	1.64
	CH_4	79.9	0.014	
10% V-treated CMS from Matrimid® precursor				
600°C	CO_2	94.6	0.024	1.67
	CH_4	89.9	0.008	
650°C	CO_2	100.1	0.045	1.64
	CH_4	95.1	0.011	

The variation in Langmuir isotherm constant values (*increase* in 'C_H'' and *decrease* in 'b') for the 10% V-treated CMS compared to the untreated CMS in Table 5.5, can be due to the presence of additional 'pores' for porous organo-silica domain. There is a possibility that the small amount of silica presence can act as an additional Langmuir sorption site which lead to differences in C_H' and b for the V-treated CMS. However, as shown in the characterization analyses in section 5.4, the presence of silica in 10% V-treated CMS is quite small and may not cause truly significant variations in sorption properties.

The sorption selectivity values in Table 5.5 for both the untreated and V-treated CMS were calculated based on the Langmuir constants and 100 psi pressures (which is the pure gas feed pressure for permeation measurements in section 5.5.1). Similar sorption selectivities were observed for the untreated CMS Matrimid® samples as reported by Rungta in her study [3].

5.5.3 Permeation results for mixed gas (CO_2/CH_4) feed

An aggressive natural gas feed composition of 50% CO_2 and 50% CH_4 was used to evaluate the separation performance of the optimized V-treated CMS hollow fibers, for a total feed pressure up to 800 psi. Fugacity coefficients were calculated to obtain the accurate gas permeance values.

A comparison of mixed-gas feed separation performance for the 10% V-treated, 100% V-treated, and untreated CMS hollow fibers from the Matrimid® precursor pyrolysed at 650°C are shown in Figures 5.18(a) and (b). Similar to the pure-gas feed separation performance, the 10% V-treated CMS hollow fiber showed around *9x* increase in gas permeance in comparison to the *3x* increase for 100% V-treated CMS hollow fiber. Both the 10% and 100% V-treated CMS fibers showed a CO_2/CH_4 selectivity ~90-100.

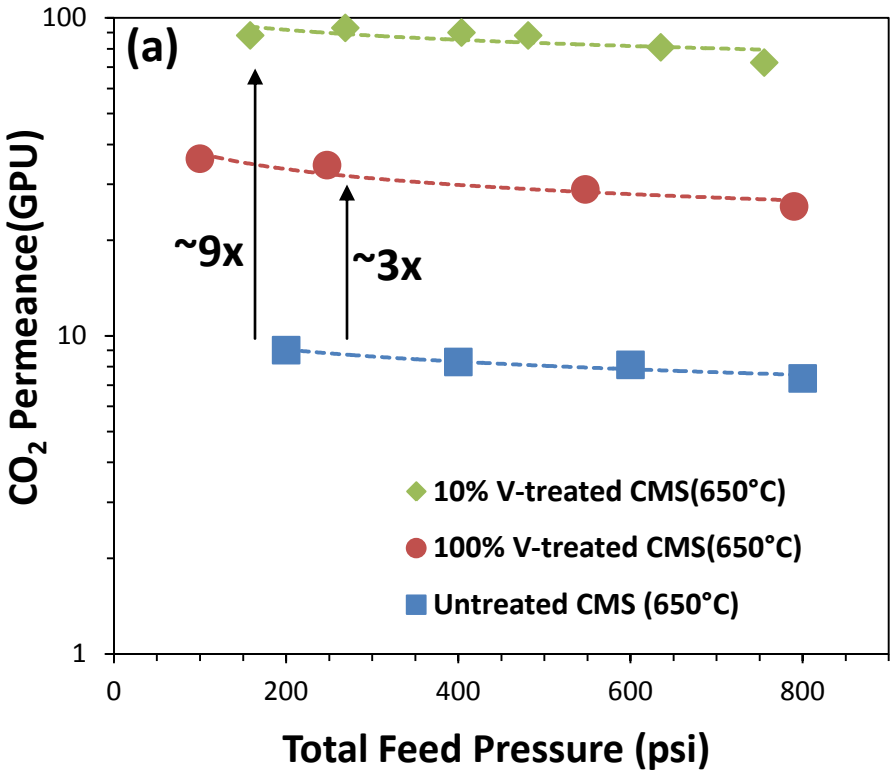

Figure 5.18(a): Comparison of CO_2 permeance for the optimized (10%) V-treated, 100% V-treated and untreated CMS hollow fibers from Matrimid® precursor pyrolysed at 650°C under argon UHP, tested at 35°C.

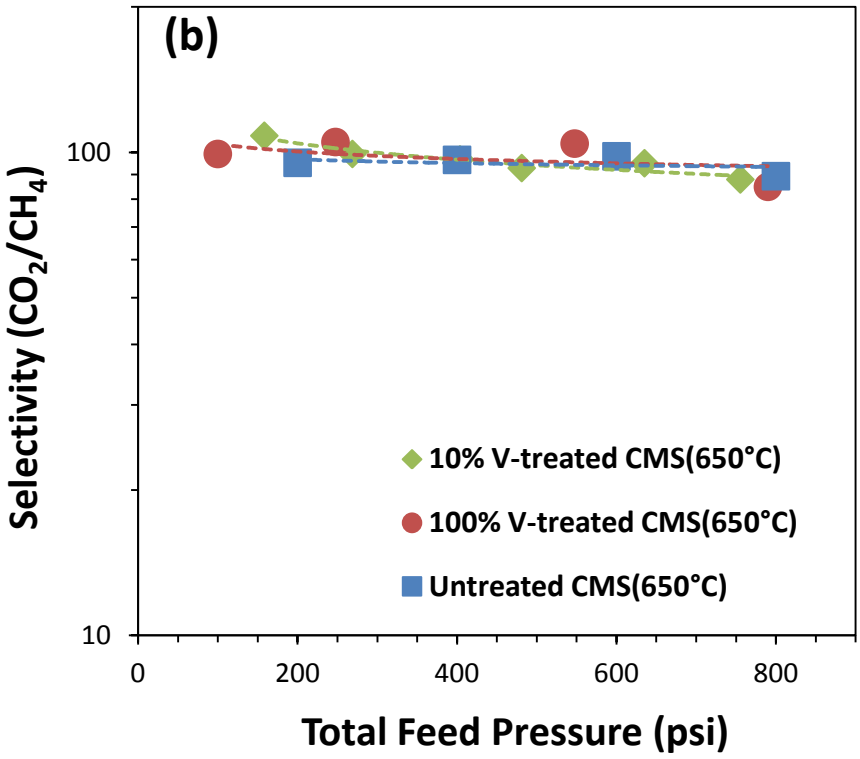

Figure 5.18(b): Comparison of CO_2/CH_4 selectivity for the optimized (10%) V-treated, 100% V-treated and untreated CMS hollow fibers from Matrimid® precursor pyrolysed at 650°C under argon UHP, tested at 35°C.

The improvement in mixed gas separation performance for the optimized V-treated CMS membranes can have broad applications to industrially relevant separations. To test the separation ability of the optimized V-treated CMS membranes for challenging gas separation fields like olefin-paraffin separation, preliminary studies were conducted and shown in section 5.6.2 and 5.6.3.

The entire V-treatment optimization studies in this chapter were focused using Matrimid® as a starting precursor material. As discussed in Chapter 4, V-treatment method has a significant potential for improving the separation performance of 6FDA based precursors by further restricting the sub-structure collapse. The potential

simultaneous etching mechanism of organo-silica during the pyrolysis of 6FDA:BPDA-DAM precursor may be a big advantage to tune the excess silica during the pyrolysis step, and is also discussed in Chapter 4. A few pure-gas permeation studies were conducted for the 6FDA:BPDA-DAM precursor using the Matrimid® based optimized (10%) V-treatment technique, and the results are discussed in Appendix D. Even though some permeance enhancement was observed, the optimization studies for the case of V-treated 6FDA:BPDA-DAM still warrant future study.

5.6 Tuning final pyrolysis temperatures for estimating the mixed-gas separation performance of CO_2/CH_4, C_2H_4/C_2H_6 and C_3H_6/C_3H_8.

5.6.1 Natural gas separation (CO_2/CH_4)

The ability to tune the pore size distribution of CMS materials by adjusting the final pyrolysis temperature is critical and can be optimized depending upon the separation application. Similar to the pure-gas feed results shown in Figures 5.14 and 5.15, the 10% V-treated Matrimid® precursor hollow fibers were also pyrolysed at 600°C under argon UHP. The mixed gas feed containing 50% CO_2 and 50% CH_4 was used to test the separation performance. The rearrangement of carbon sheets with increasing pyrolysis temperature leads to slight improvement in selectivity for the 600°C pyrolysed fibers as shown in Figure 5.19(b). The optimum pyrolysis temperature range for Matrimid® based optimized V-treated precursor is around *600°C-650°C*. Low pyrolysis temperatures (i.e. 550°C and 600°C) showed a slight competition effect due to the relatively more open structure as shown in Figure 5.19(a).

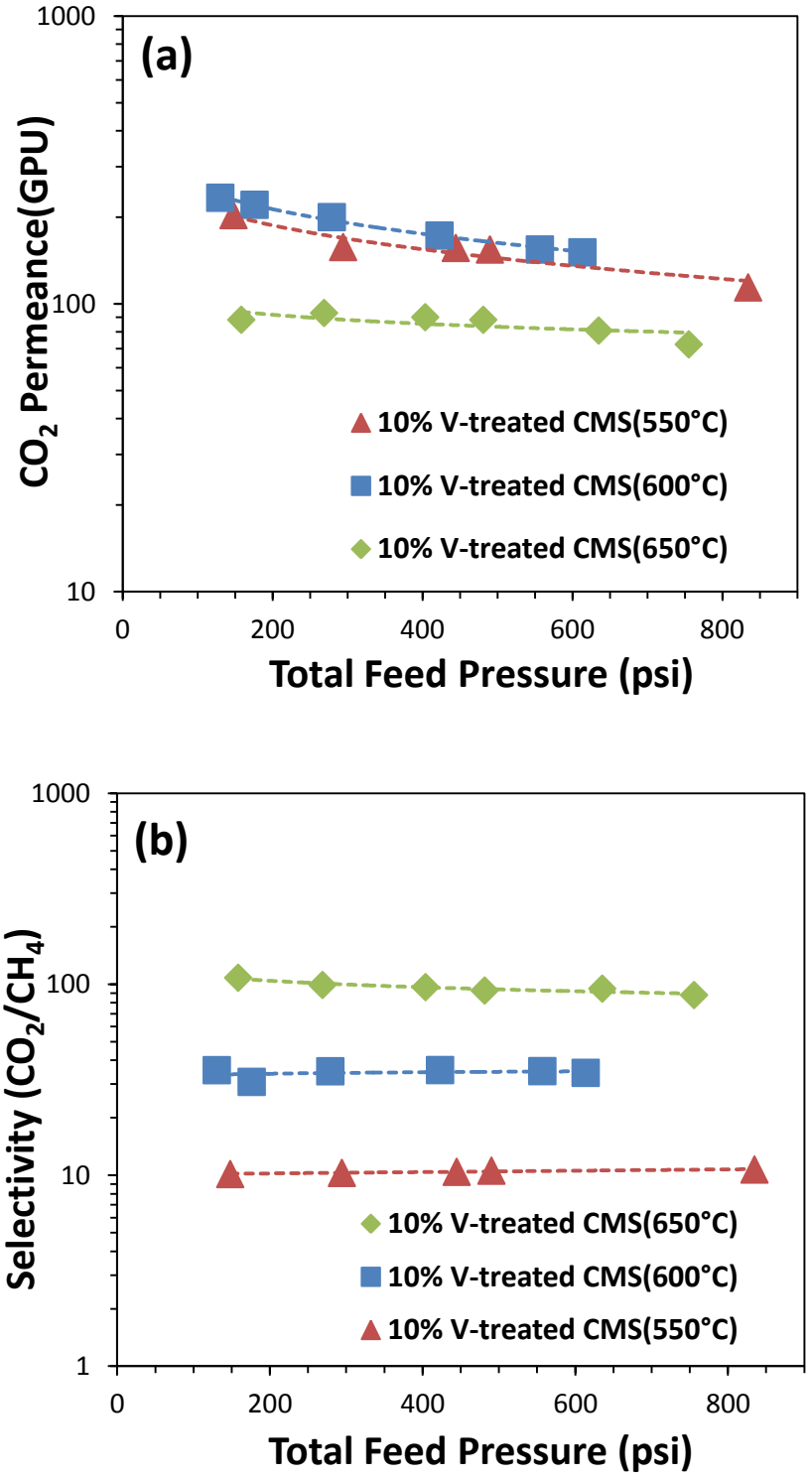

Figure 5.19: Mixed gas feed separation performance: (a) permeance and (b) selectivity for the optimized (10%) V-treated CMS hollow fibers for Matrimid® precursor pyrolysed at 550°C, 600°C and 650°C under argon UHP, tested at 35°C.

5.6.2 Ethylene/ethane (C_2H_4/C_2H_6) separation

Recent studies by Xu [4] have shown the potential of CMS hollow fiber membranes for separation of olefin/paraffins. For the case of Matrimid® based CMS hollow fibers, attractive selectivities for C_2H_4/C_2H_6 were achievable but had lower gas permeances due to sub-structure collapse. The advantage of restricting collapse by V-treatment can be translated to improve the gas permeance compared to untreated CMS hollow fibers as shown in Figure 5.20(a). The 10% V-treated CMS hollow fiber performance from Matrimid® is compared with the untreated CMS separation obtained by Xu [4] in his study. The mixed gas testing conditions were maintained similar to the previous study and the feed gas used contained 63.3% C_2H_4 and 36.7% C_2H_6, tested at 100 psi feed pressure and 35°C. A significant improvement in gas permeances for all the three pyrolysis temperatures were observed for the three different pyrolysis temperatures as shown in Figure 5.20(a),

Even though the 10% V-treatment was used, the selectivities were hampered by the silica presence in the CMS as shown in Figure 5.20(b). As the focus of this particular study was only to demonstrate the potential of V-treatment for C_2H_4/C_2H_6 separation as proofof-concept study, further optimizations were not performed.

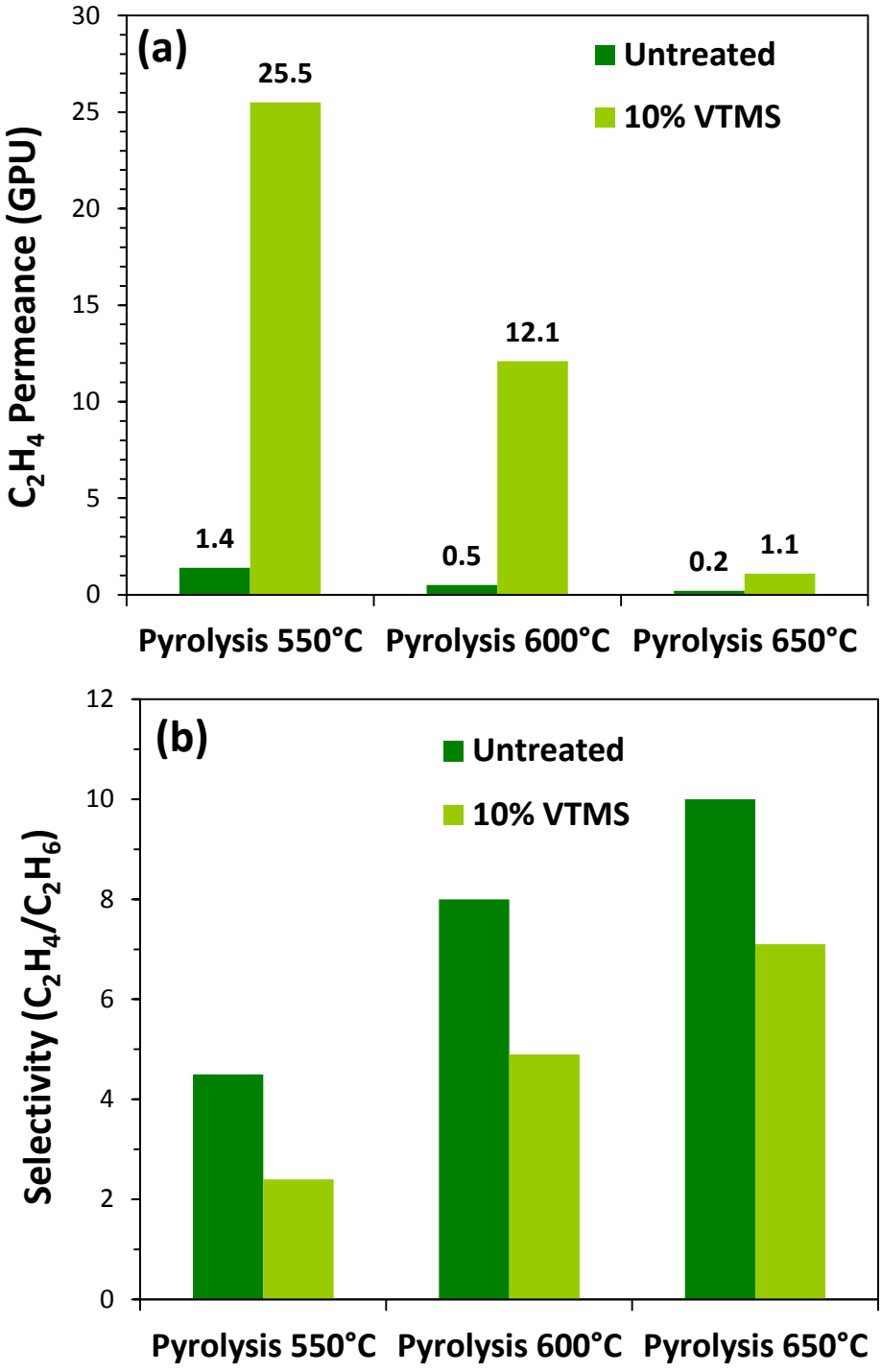

Figure 5.20: Mixed gas feed (63.3% C_2H_4 and 36.7% C_2H_6) separation performance: (a) permeance and (b) selectivity for the 10% V-treated CMS hollow fibers from Matrimid® precursor pyrolysed at 550°C, 600°C and 650°C under argon UHP, tested at 100 psi feed gas pressure and 35°C. *For the comparison, the untreated CMS hollow fiber mixed gas feed separation performance was obtained from Xu [4].*

5.6.2 Propylene/Propane (C_3H_6/C_3H_8) separation

Similar to the ethylene/ethane permeation trend, the propylene permeance after the 10% V-treated Matrimid® pyrolysis at 550°C showed an improvement in gas permeance compared to the untreated CMS hollow fiber permeance as shown in Figure 5.21(a). The separation performance was evaluated for a mixed gas feed containing 50% C_3H_6 and 50% C_3H_8 and tested at 50 psi feed pressure and 35°C.

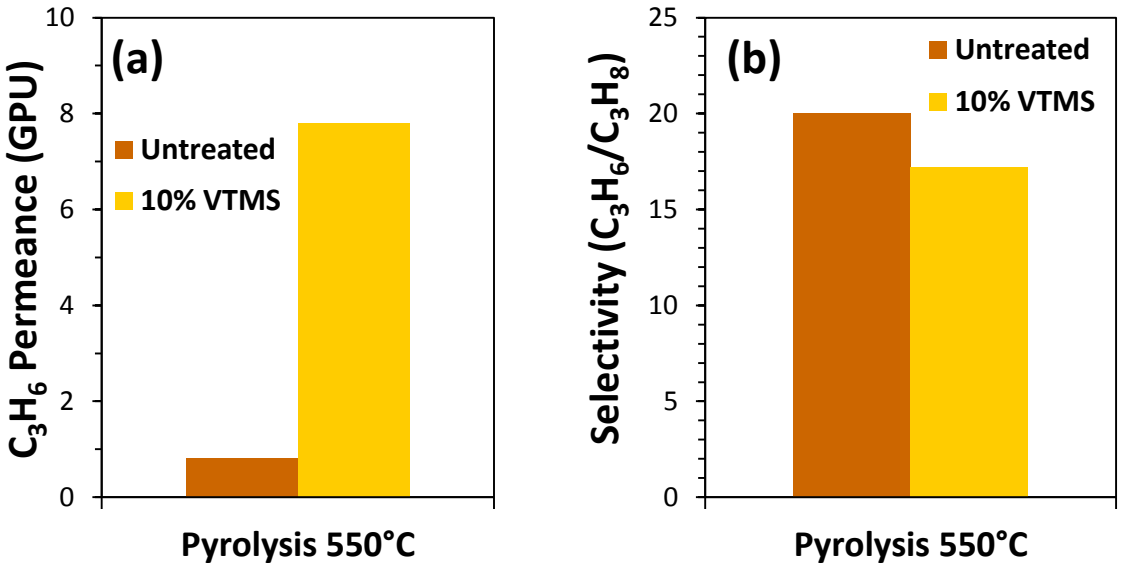

Figure 5.21: Mixed gas feed (50% C_3H_6 and 50% C_3H_8) separation performance: (a) permeance and (b) selectivity for the 10% V-treated CMS hollow fibers from Matrimid® precursor pyrolysed at 550°C under argon UHP, tested at 50 psi feed gas pressure and 35°C. *For the comparison, the untreated CMS hollow fiber mixed gas feed separation performance was obtained from Xu [4].*

The separation performance for the 10% V-treated CMS hollow fiber pyrolysed at 600°C was also evaluated, high C_3H_6/C_3H_8 selectivity of ~48 was observed but with a relatively lower gas permeance of ~2 GPU (not shown in Figure 5.21).

5.7 Summary

This chapter has presented the importance of optimization for the VTMS concentration, and the final pyrolysis temperature in V-treated asymmetric Matrimid® CMS hollow fiber membranes. After evaluating the VTMS concentration for six different concentrations, an optimum amount for the *highest* increase in CMS gas permeance was found for the 10% VTMS in hexane. The preference for hexane as a non-solvent for the VTMS-hexane combination of V-treatment is due to the existing post spinning solvent exchange process. The novelty of using hexane for V-treatment allows direct "drop in" integration into current fiber precursor processing. In addition, the importance of both organic and alkoxy functional groups were also discussed, which give the potential for further optimization of the pre-treatment process. Three different silanes with either vinyl (or) methoxy functional groups were explored, which gave the significance of vinyl group in maintaining the mechanical properties for the V-treated precursor and CMS hollow fibers. The importance of a reactive functional group (like vinyl) to form Si-C bonds during pyrolysis was suggested. The role of methoxy functional group was essential for creation of organo-silica domain via sol-gel process.

The optimized (10%) V-treated CMS membranes showed at least *9x* enhancement in gas permeance compared to the untreated CMS Matrimid® hollow fiber membranes for both pure and mixed gas feeds. The gas permeance increase correlates with the improved asymmetric CMS skin thickness, which was reduced to *~9-10x* based on the SEM images. The equilibrium sorption experiments for the 10% V-treated Matrimid® CMS further confirmed that the effects of low amounts of silica on V-treated CMS sorption properties are minimal. The XPS and elemental characterization analyses confirmed the

reduced silicon percentages in both the outermost CMS skin and the bulk CMS sample. The potential of optimized V-treatment for Matrimid® based CMS hollow fiber membrane were also evaluated for industrially relevant mixed gas pairs (CO_2/CH_4, C_2H_4/C_2H_6 and C_3H_6/C_3H_8), which consistently showed the increase in gas permeances for all cases.

5.8 References

1. Achoundong, C. S.; Bhuwania, N.; Burgess, S. K.; Karvan, O.; Johnson, J. R.; Koros, W. J., Silane Modification of Cellulose Acetate Dense Films as Materials for Acid Gas Removal. Macromolecules **2013,** 46 (14), 5584-5594.
2. Abe, Y.; Kagayama, K.; Takamura, N.; Gunji, T.; Yoshihara, T.; Takahashi, N., Preparation and properties of polysilsesquioxanes. Function and characterization of coating agents and films. Journal of non-crystalline solids **2000,** 261 (1), 39-51.
3. Rungta, M., Carbon Molecular Sieve Dense Film Membranes For Ethylene/Ethane Separations. Doctor of Philospohy, Georgia Institute of Technology, 2012.
4. Xu, L., Carbon Molecular Sieve Hollow Fiber Membranes For Olefin/Paraffin Separations. Doctor of Philospohy, Georgia Institute of Technology, 2012.

CHAPTER 6
REALISTIC EVALUATION OF V-TREATED CMS HOLLOW FIBER MEMBRANE FOR NATURAL GAS SEPARATION

6.1 Overview

This chapter evaluates critical points for the commercial viability of CMS membranes for industrial scale-ups. In addition to the improved permeances, V-treatment offers a key advantage of 'anti-stickiness' to the asymmetric CMS fibers from V-Treated Matrimid® precursor. This section also discusses time-dependent separation performance tests for V-Treated CMS membranes from Matrimid® precursor. The stability of the membranes is evaluated for aggressive feed gas conditions containing 50% CO_2/50% CH_4. The aging study is performed under three different conditions (i) active mixed gas feed (ii) stored in ambient air and (iii) CO_2 at 5-6 atm pressure.

6.2 Anti-stickiness behavior of V-treated Matrimid® hollow fiber membranes

In the pyrolysis process, when untreated Matrimid® polymer precursor fibers are pyrolysed in bundles they adhere to each other making them unusable as CMS membranes. The image of untreated CMS hollow fibers, where the untreated precursor fibers were pyrolysed by placing close to each other is shown in Figure 6.1.

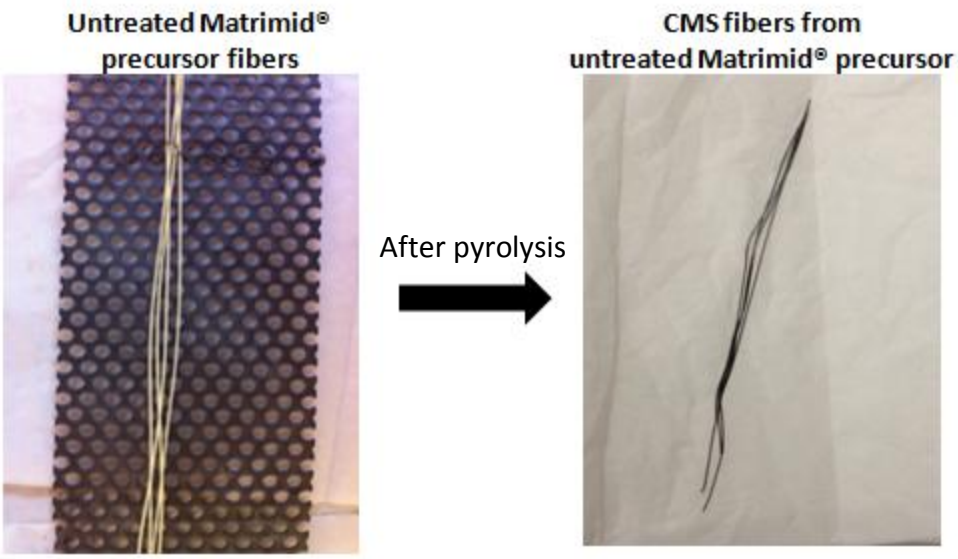

Figure 6.1: Untreated Matrimid® precursor fibers pyrolysed after placing close to each other and resultant CMS fibers unusable because of the stickiness.

For the large scale fabrication of CMS membranes, separating each fiber during pyrolysis may add additional processing, labor cost and also a time consuming process [1]. Karvan *et al*.,[1] had demonstrated the ability to produce large-scale CMS hollow fiber membranes from Matrimid® precursor and achieved 93% final recovery rate after separating each precursor fiber. The schematic of lab and pilot-scale pyrolysis systems with the fiber loading set-ups are shown in Figure 6.2.

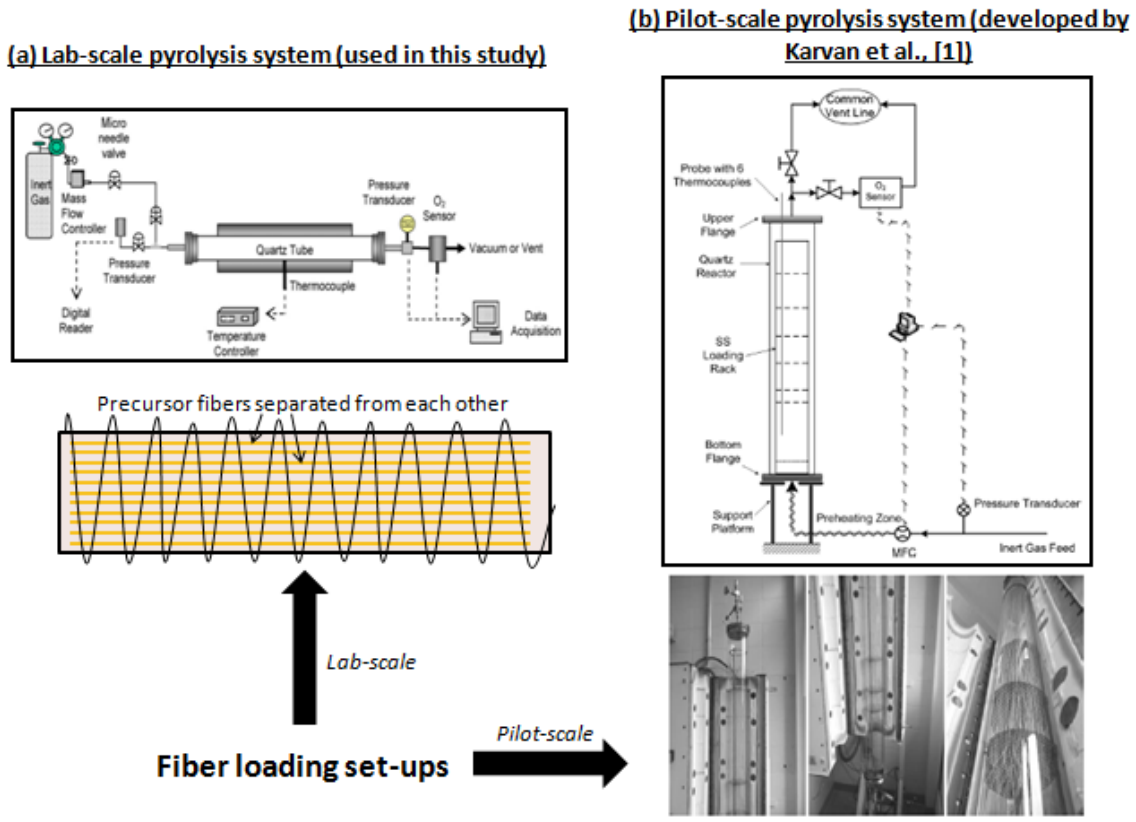

Figure 6.2: Schematic of the pyrolysis systems and fiber-loading set-ups for (a) lab-scale: used in this study, and (b) pilot-scale: developed by Karvan et al., [1].

In addition to the improved permeances, V-treatment offers a key advantage of 'anti-stickiness' to the asymmetric CMS fibers from V-Treated Matrimid® precursor. XPS characterization results discussed in Chapter 4 and 5 indicated the presence of silica on the outer layer of V-Treated fibers, which assisted in the 'anti-stickiness' of the Matrimid® precursor based CMS as shown in Figure 6.3. The bundled V-treated Matrimid® precursor fibers after pyrolysis where separable and also showed similar transport performance as compared to the non-bundled CMS V-treated Matrimid® hollow fibers. *The offset of 'stickiness' do not arise for 6FDA based precursors, as the untreated 6FDA precursor fibers were seen to be separable after pyrolysis.*

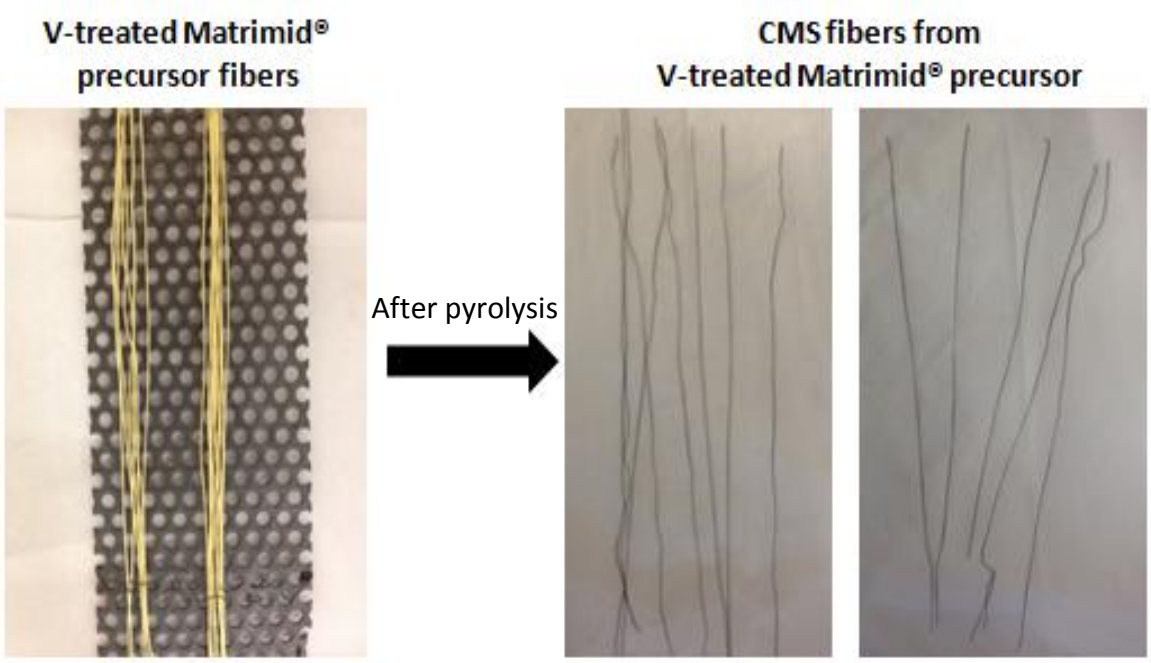

Figure 6.3: V-treated Matrimid® precursor fibers pyrolysed after placing close to each other and resultant CMS fibers which are separable after pyrolysis.

6.3 Aging stability of CMS V-treated Matrimid® hollow fiber membranes

The time dependent stability of CMS V-treated membranes under realistic feed conditions is important for the industrial application. For evaluating the stability of CMS V-treated Matrimid® hollow fiber membranes, 50% CO_2/50% CH_4 mixed gas feed was used. In addition to active feed gas testing (i.e. 6.3.1), CMS V-treated Matrimid® hollow fiber membranes stored under CO_2 (~5-6 atm pressure), and ambient air were re-tested, and are discussed in section 6.3.2, and 6.3.3 respectively.

6.3.1 Active mixed gas feed (CO_2/CH_4)

For the stability testing, mixed gas feed at 250 psi feed pressure (from shell side feed) was used. The two different final pyrolysis temperatures (i.e. 600°C and 650°C

under argon UHP) pyrolysed 10% V-treated CMS Matrimid® hollow fiber membranes were tested as a function of time and are shown in Figures 6.4 and 6.5.

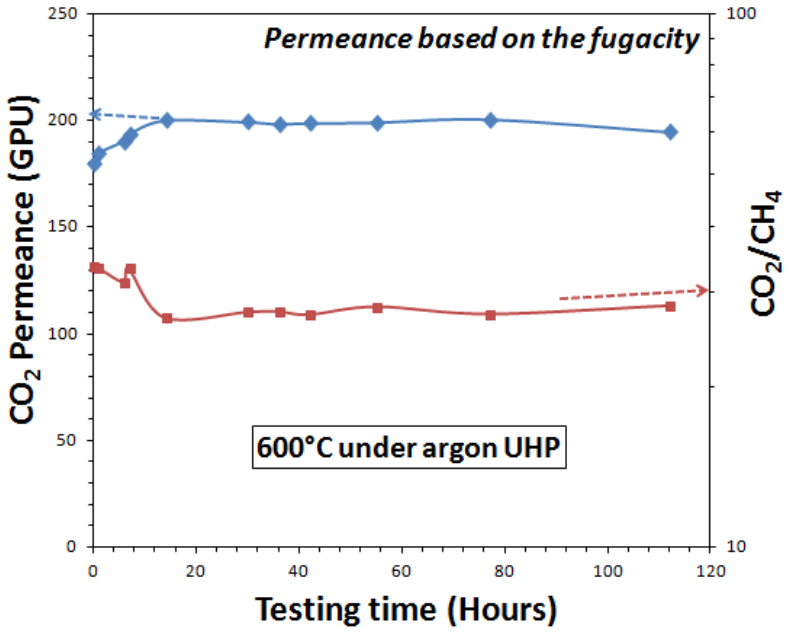

Figure 6.4: Stability testing for 10% V-treated CMS Matrimid® hollow fiber membrane module pyrolysed at 600°C under argon UHP, mixed gas feed of 50% CO_2/50% CH_4 at 250 psi feed pressure and testing temperature was 35°C.

The 600°C pyrolysed V-treated CMS hollow fibers showed a stable permeance and selectivity for over 120 hours of testing. A slight increase in permeance was observed in Figure 6.4, for the initial time duration (less than 20 hours) which later tends towards a stable CO_2 permeance. For the case of 650°C pyrolysed V-treated CMS Matrimid® hollow fiber membranes in Figure 6.5, a longer time (~220 hours) was needed to reach the stable CO_2 permeance maintaining the attractive CO_2/CH_4 selectivity. After 250 hours of continuous testing, the 650°C pyrolysed V-treated CMS was observed to reach steady permeance value similar to the 600°C pyrolysed V-treated CMS as shown in Figure 6.5.

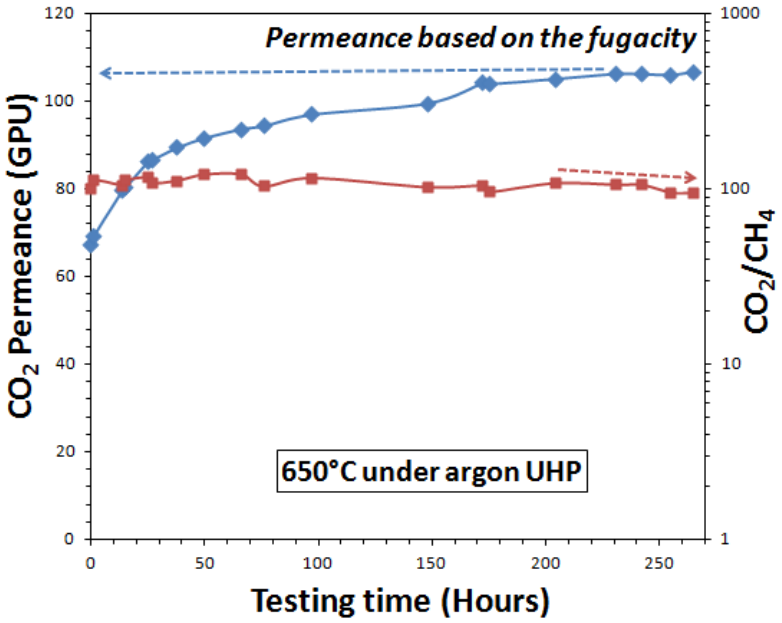

Figure 6.5: Stability testing for 10% V-treated CMS Matrimid® hollow fiber membrane module pyrolysed at 650°C under argon UHP, mixed gas feed of 50% CO_2/50% CH_4 at 250 psi feed pressure and testing temperature was 35°C.

Though the increased permeances with attractive selectivities are very much desirable, it is important to understand the initial transient transport performance of V-treated CMS membranes. The initial change in transport behavior in Figure 6.4 and 6.5, may be a more of a function of CMS sieving structure rather than the silica (from V-treatment). Similar change in initial CMS transport performance was observed in the ethylene/ethane separation study for untreated CMS hollow fibers [2]. There is a possibility that the CMS membranes posses an additional free volume which is not readily accessible by the gas molecules initially but under active feed pressure the gas molecule permeates through resulting in an increase in permeance. Depending on the pore distribution of intrinsic CMS the time taken for the stability might change, because the tightly packed CMS structure (e.g. at 650°C) will have a higher magnitude of such

additional free volumes. Xu [2] had hypothesized that due to the pyrolysis process producing a non-uniformly packed graphitic sheets, the intrinsic CMS sieving pore structure can be in a flexible intermediate state which can have a tendency to slowly re-align over the period of time.

Due to the effect of numerous parameters in the CMS formation process (as discussed in Chapter 2), it would be necessary to perform a systematic study to understand this transient behavior. The focus of this study was to emphasize on the importance of stability in V-treated CMS membranes and for further understanding of the transient behavior additional studies are required.

6.3.2 Stored under CO_2 atmosphere

For industrial application, it is important that the V-treated CMS Matrimid® hollow fibers have stable separation performance after storing modules in different atmosphere conditions. Xu [2], and Rungta [3] have hypothesized the aging phenomenon in untreated CMS membranes with a change in separation performance as a function of time, depending on the polymer precursor and storage/testing conditions. The trend of aging in CMS membranes was observed to be higher for bigger gas-pair separation (like olefins/paraffins) compared to the smaller gas-pairs (like O_2/N_2, CO_2/CH_4).

As hypothesized in the section 6.3.1, over extended period of time the intrinsic CMS pore structure is prone to re-alignment with the absence of a feed gas pressure. Hence in this section, the 10% V-treated CMS Matrimid® hollow fiber modules after the active feed gas test (in section 6.3.1) were stored in condensable pure CO_2 gas at 5-6 atm (~70-80 psi) pressure and re-tested again as shown in Figure 6.6 and 6.7. The testing

conditions were maintained similar to the active mixed feed gas test i.e., 50% CO_2/50% CH_4 at 35°C. The storage pressure was chosen based on the typical 'coke' bottle internal pressure [4], as it could be used for sealing the CMS modules to restrict the aging phenomenon.

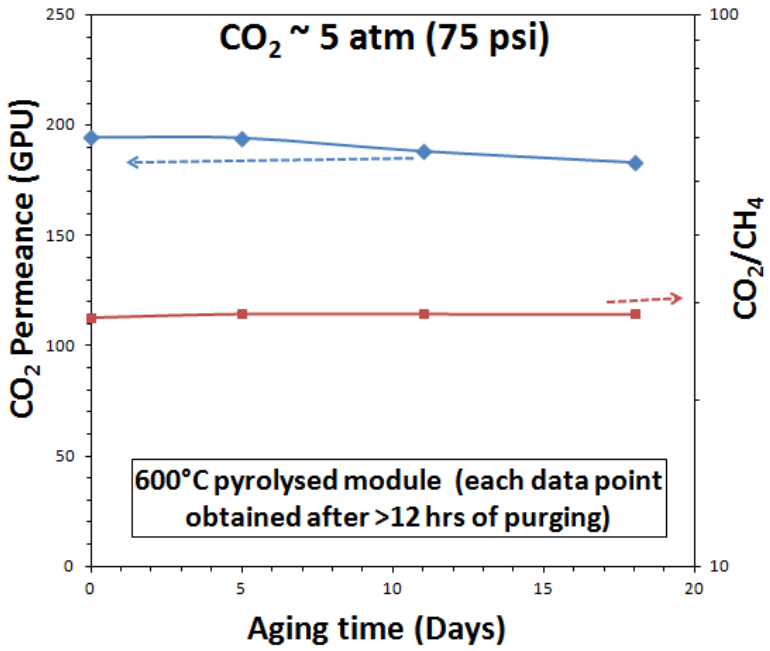

Figure 6.6: *Module stored under CO_2 at 75 psi pressure*- stability of 10% V-treated CMS Matrimid® hollow fiber membrane module pyrolysed at 600°C under argon UHP, mixed gas feed of 50% CO_2/50% CH_4 at 250 psi feed pressure and testing temperature was 35°C. (Test at 'Day 0' is after the active feed gas test in Figure 6.4)

Both the 10% V-treated CMS Matrimid® hollow fiber module pyrolysed at 600°C and 650°C showed stable separation performance for over 20 days as shown in Figure 6.6 and 6.7. Before each data-point the V-treated CMS module was purged with the feed gas for greater than 12 hours and multiple readings were taken to obtain the stable performance.

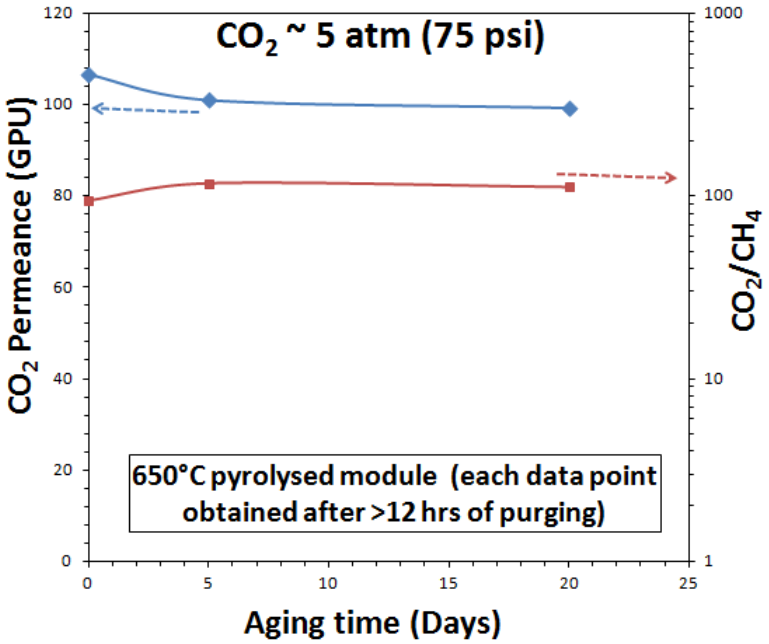

Figure 6.7: *Module stored under CO_2 at 75 psi pressure*- stability of 10% V-treated CMS Matrimid® hollow fiber membrane module pyrolysed at 650°C under argon UHP, mixed gas feed of 50% CO_2/50% CH_4 at 250 psi feed pressure and testing temperature was 35°C. (Test at 'Day 0' is after the active feed gas test in Figure 6.5)

For both pyrolysis temperatures in Figures 6.6 and 6.7, greater than *90%* of the original CO_2 permeance was retained maintaining the CO_2/CH_4 selectivity for asymmetric V-treated CMS membranes stored under condensable pure CO_2 gas.

6.3.3 Stored under ambient air

The 10% V-treated CMS Matrimid® hollow fiber membrane module pyrolysed at 650°C was re-tested after placing the modules in ambient air for extended period of time is shown in Figure 6.8.

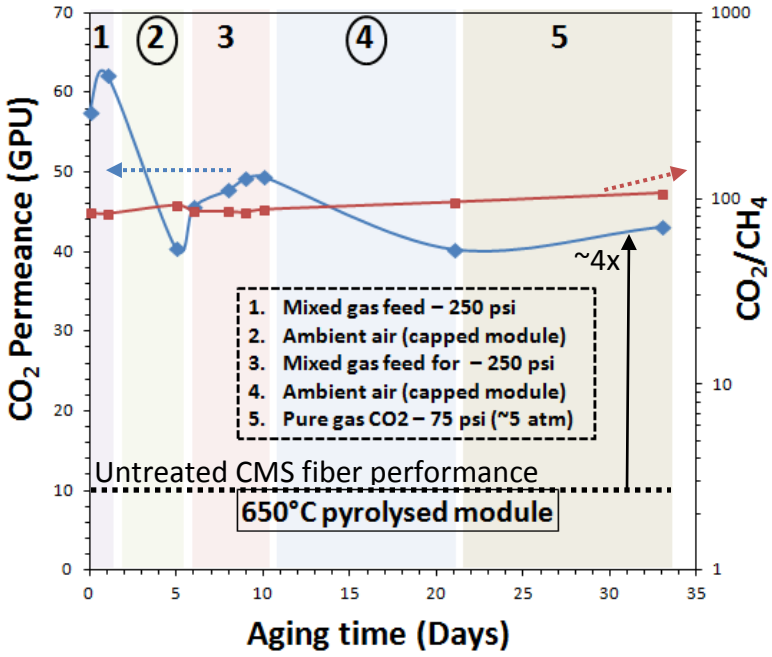

Figure 6.8: *Module stored under ambient air*- stability of 10% V-treated CMS Matrimid® hollow fiber membrane module pyrolysed at 650°C under argon UHP, mixed gas feed of 50% CO_2/50% CH_4 at 250 psi feed pressure and testing temperature was 35°C.

The test in the Figure 6.8 was performed in 5 stages, where in stage 1 the module was tested in a mixed gas feed for 24 hours to obtain the performance before aging. In stage 2, module was capped from all ends and kept in ambient air for *5 days*. After re-testing the module with mixed gas feed for another 5 days (stage 3), the drop in permeance due to ambient aging (for 5 days) was observed to be *~19%*. In stage 4, the module was re-stored for *10 days* in ambient air and later tested with the mixed gas feed after purging with CO_2 for 13 days (stage 5). The effective drop in CO_2 permeance after 15 days of ambient air aging (5 days in *stage 2* and 10 days in *stage 4*) for 10% V-treated CMS Matrimid® hollow fiber pyrolysed at 650°C was *~35%* of the original (before age) permeance. With the drop in permeance in Figure 6.8, an improvement in CO_2/CH_4 selectivity of *~20%* was observed.

From the Figure 6.8, the effect of aging under ambient air storage was observed. In comparison even after aging the 10% V-treated CMS hollow fiber (650°C pyrolysed) CO_2 permeance is 4-5x higher when compared to the untreated CMS Matrimid hollow fiber. The drop in CO_2 permeance under ambient air storage is a concern and further studies will be required for the effective development of asymmetric V-treated CMS membranes.

6.4 Summary

This chapter outlines the added advantage of V-treatment towards 'anti-stickiness' in the asymmetric CMS fibers from V-Treated Matrimid® precursor. Presence of silica on the outer layer of V-Treated fibers assists in the 'anti-stickiness' property.

For the commercial application of 10% V-treated asymmetric CMS Matrimid® membranes, the aging study was performed under three different conditions (i) active mixed gas feed (ii) stored in pure gas CO_2 at 5-6 atm pressure and (iii) stored in ambient air. The stability testing was performed with the mixed gas feed of 50% CO_2/50% CH_4 at 250 psi for two different pyrolysis temperature samples i.e. 600°C and 650°C. For the case of active feed gas test, both the V-treated CMS samples showed an increase in CO_2 permeance for initial testing duration followed with a stable performance later on. The hypothesis for the initial transient behavior in separation performance under active feed-gas and aging phenomenon in the absence of feed gas (stored in ambient air) is predicted due to the complex intrinsic CMS structure. Both the hypothesis of additional 'free volume' and the aging phenomenon require further detailed studies.

6.5 References

1. Karvan, O.; Johnson, J. R.; Williams, P. J.; Koros, W. J., A Pilot-Scale System for Carbon Molecular Sieve Hollow Fiber Membrane Manufacturing. Chemical Engineering & Technology **2013,** 36 (1), 53-61.
2. Xu, L., Carbon Molecular Sieve Hollow Fiber Membranes For Olefin/Paraffin Separations. Doctor of Philospohy, Georgia Institute of Technology, 2012.
3. Rungta, M., Carbon Molecular Sieve Dense Film Membranes For Ethylene/Ethane Separations. Doctor of Philospohy, Georgia Institute of Technology, 2012.
4. Wyeth, Nathaniel C. "Biaxially Oriented Poly (Ethylene Teflephthalate) Bottle." U.S. Patent No. 3,733,309. 15 May 1973.

CHAPTER 7

CONCLUSIONS AND RECOMMENDATIONS

7.1 Summary and conclusions

The overarching goal of the thesis dissertation is to "Establish a framework to engineer the morphology of the microporous support layer in asymmetric membranes undergoing thermal processing above the glass transition of the intrinsic polymer precursor." Due to the morphology collapse in asymmetric CMS hollow fiber membranes, the major drawback is the lower gas separation productivities. In this study, a novel treatment (V-treatment) method has been developed for the polyimide precursor hollow fiber membranes to restrict the morphology collapse during pyrolysis. The effect of V-treatment is applied on two widely studied polyimide precursors: Matrimid® and 6FDA:BPDA-DAM. The three research objectives pursued are:

1. *Methodology to restrict sub-structure collapse in asymmetric CMS hollow fiber membranes.*
2. *Optimization of V-treatment and pyrolysis parameters for superior separation performance in asymmetric CMS hollow fiber membranes.*
3. *Realistic evaluation of V-treated CMS hollow fiber membrane for natural gas separation.*

Prior to the development of V-treatment approach, several thermal and chemical pre-pyrolysis engineering routes are investigated for stabilizing the polymer precursors which are discussed in the Appendix C. Even though the methods are unsuccessful in restricting

the morphology collapse, they are essential for establishing the framework of V-treatment technique.

For the V-treatment technique, precursor hollow fibers were exposed to an organic-alkoxy silane (VTMS) and moisture to undergo a sol-gel reaction. The sol-gel crosslinking reaction induces vinyl crosslinked silica on the precursor fiber pore walls, which restricts the ability of the porous support to collapse during pyrolysis. The sol-gel reaction proposed in this study is a first-of-a-kind approach in asymmetric CMS membranes to create porous morphologies, and it can be easily integrated into the current asymmetric CMS membrane fabrication process. The V-treatment technique does not involve any chemical reaction with precursor molecular structure, which makes it a simple integral approach to restrict morphology collapse on any class of asymmetric CMS polymer precursors. This will enable low-cost facile integration into practical membrane production.

Several characterization analysis (i.e., SEM, NMR, FTIR, DMA, TGA and XPS) were performed on both the V-treated Matrimid® precursor and CMS to evaluate the reaction hypothesis and the silica structure in V-treated samples. Bulk elemental compositions showed the presence of silicon in both the V-treated precursor and CMS sample. The impact of V-treatment on asymmetric CMS sub-structure morphology and separation performance for 6FDA:BPDA-DAM based CMS hollow fiber are also studied as a 'proof-of-concept' study. A significant reduction of *5-6x* in membrane skin thickness (l) for asymmetric CMS hollow fibers from both the V-treated precursors was found. This improvement in membrane skin thickness (l) directly translated to an increase in gas permeance (P/l) by more than *3x* for asymmetric CMS V-treated Matrimid® hollow fibers

tested for both pure gases (He, CO_2, O_2, N_2 ,CH_4) and aggressive high pressure (CO_2/CH_4) mixed gas feeds. Similar improvement in permeance for asymmetric CMS V-treated 6FDA:BPDA-DAM hollow fibers by more than *4x* for both pure and mixed gas (CO_2/CH_4) feed was observed.

XPS characterization on the 100% VTMS treated CMS Matrimid® hollow fiber indicated higher concentration of silica on the outermost skin layer of the V-treated CMS hollow fiber. Due to the presence of excess silica on the intrinsic CMS separation skin, the potential permeance increase for the 100% V-treated CMS hollow fiber was not achieved. The optimization of the V-treatment process was crucial for obtaining even better separation performance. The V-treatment optimization in terms of modifying the VTMS concentration, and the final pyrolysis temperature for V-treated asymmetric Matrimid® CMS hollow fiber membranes were performed. After evaluating the VTMS concentration for six different concentrations, an optimum amount for the *highest* increase in CMS gas permeance was found for the 10% VTMS in hexane. The preference for hexane as a non-solvent is due to the existing post spinning solvent exchange process that utilizes hexane, therefore the optimized V-treatment allows for direct "drop in" integration into current fiber precursor processing.

In addition, the importance of both organic and alkoxy functional groups on the silane are also discussed, which gives the potential for further optimization of the pre-treatment process. Three different silanes with either vinyl (or) methoxy functional groups are explored, where vinyl group significance towards maintaining the mechanical properties of the V-treated precursor and CMS hollow fibers are observed. The importance of a reactive functional group (like vinyl) to form Si-C bonds during

pyrolysis is suggested. The role of methoxy functional group is essential for creation of organo-silica domain via sol-gel process.

The optimized (10%) V-treated CMS membranes showed at least *9x* enhancement in gas permeance compared to the untreated CMS Matrimid® hollow fiber membranes for both pure and mixed gas feeds. The gas permeance increase correlates with the improved asymmetric CMS skin thickness, which was reduced to approximate *~9-10x* based on the SEM images. The equilibrium sorption experiments for the 10% V-treated Matrimid® CMS further confirmed that the effects of low amounts of silica on V-treated CMS sorption properties are minimal. XPS and elemental characterization analyses further confirmed the reduced silicon percentages in both the outermost CMS skin and the bulk CMS sample. The potential of optimized V-treatment for Matrimid® based CMS hollow fiber membrane were also evaluated for industrially relevant mixed gas pairs (CO_2/CH_4, C_2H_4/C_2H_6 and C_3H_6/C_3H_8), which consistently showed the increase in gas permeances for all the gas separation pairs.

In addition to the increased permeances, another advantage of V-treatment is towards the 'anti-stickiness' of the asymmetric CMS fibers from V-Treated Matrimid® precursor. Presence of silica on the outer layer of V-Treated fibers assists in the 'anti-stickiness' property. The offset of 'stickiness' do not arise for 6FDA based precursors, as the untreated 6FDA precursor fibers were separable after pyrolysis.

For the commercial application of 10% V-treated asymmetric CMS Matrimid® membranes, the separation performance stability under three different conditions (i) active mixed gas feed (ii) stored in pure gas CO_2 at 5-6 atm pressure and (iii) stored in

ambient air is evaluated. The stability testing was performed with the mixed gas feed of 50% CO_2/50% CH_4 at 250 psi for two different pyrolysis temperature samples i.e. 600°C and 650°C. For the case of active feed gas test, both the V-treated CMS samples showed an increase in CO_2 permeance for initial testing duration followed with a stable performance later on. The hypothesis for the initial transient behavior in separation performance under active feed-gas and aging phenomenon in the absence of feed gas (stored in ambient air) is predicted due to the complex intrinsic CMS structure. Both the hypothesis of additional 'free volume' and the aging phenomenon require further detailed studies.

The impact of V-treatment in restricting the sub-structure collapse leading to an improvement in gas permeance of asymmetric CMS hollow fiber membranes can have a broad separation application. The goal of this study was achieved by developing a technique (V-treatment) for improving the attractive separation performance of CMS membranes for industrial application. There are several areas which will require further studies for the effective development of CMS membranes for industrial scale-up (like time-dependent stability and aging phenomenon).

7.2 Future recommendations:

The research goal of the thesis was achieved by the development of V-treatment technique for restricting sub-structure collapse and improving the gas permeances. For the future directions, some key areas are observed during the course of the work:

7.2.1 V-treated asymmetric CMS hollow fiber membranes for challenging gas-pair separations

Intrinsic CMS membranes have the potential to achieve attractive gas separation selectivities over polymer membranes for difficult gas-pairs (such as H_2S/CH_4, N_2/CH_4, olefin-paraffin debottlenecking). So far the drawback in untreated asymmetric CMS hollow fibers separation performance for these separations has been the low gas permeances. The ability to restrict collapse (with low % of VTMS) can have a potential in improving the flux of V-treated asymmetric CMS membranes for the challenging gas separation-pairs.

7.2.2 Applying V-treatment on different polymer precursor membranes

The current V-treatment technique is majorly focused on Matrimid® based asymmetric CMS membranes with 6FDA:BPDA-DAM based asymmetric CMS as a proof-of-concept study. Based on these two precursors and V-treatment reaction mechanism, following class of precursors can be pursued:

7.2.2.1 6FDA based precursors

Compared to Matrimid® precursor even though the 6FDA based precursors have seen to collapse to a lower content, there is still a significant order of collapse observed in 6FDA precursor based CMS. The V-treatment technique for asymmetric CMS hollow fiber membranes can further improve the gas permeances of the intrinsically open 6FDA precursor based CMS membranes.

During the course of study, the V-treated 6FDA:BPDA-DAM based CMS showed significantly lower silicon percentages compared to the V-treated Matrimid® based CMS. The hypothesis for the lower silica content is predicted due to the possibility of self-etching from fluorine based volatile gases (CHF_3 and HF) during pyrolysis. Though the exact mechanism of silica-fluorine etching during pyrolysis is not completely understood, further studies would be required for V-treated 6FDA precursors to optimize during the pyrolysis step. Similar to the V-treatment Matrimid® optimization in Chapter 5, future studies on optimization of V-treatment on 6FDA:BPDA-DAM based precursor is worth pursuing. Few preliminary studies using 10% VTMS is performed and discussed in Appendix D.

7.2.2.2 Composite asymmetric polymer precursors

For the commercial application to reduce the cost of polymer precursors in CMS membranes, a combination of V-treatment with composite hollow fiber membrane precursors can be a future path to pursue. A typical composite hollow fiber precursor may comprise of a low-cost core layer (higher degree of collapse) precursor, with a more intrinsically open 6FDA based precursor as a sheath layer. The V-treatment on these membranes may lead to a significantly higher transport flux membranes.

7.2.2.3 Crosslinkable polymer precursors

V-treatment may also be applied for the crosslinkable polymers as CMS membrane precursors (which consists of reactive functional groups like alcohol, acid groups). The reaction mechanism may proceed with the V-treatment agent (like VTMS)

to react with the functional groups and lead to robust asymmetric structure after pyrolysis.

7.2.3 Further optimization of the V-treatment technique

In the current study, impact of V-treatment optimization for Matrimid® precursor towards further improving the gas permeances is observed. Hence, in addition to exploring V-treatment on new polymer precursors it will be critical to study the optimization for each precursor individually. The important frameworks which can be followed to pursue the optimization path are:

7.2.3.1 V-treatment recipe

In addition to VTMS concentration, the moisture exposure amount and time duration at the pre-pyrolysis step can be used for tuning the excess silica from outermost skin layer. Future studies towards 'advanced optimization of V-treatment' being developed by Shweta Karwa at Koros research group, Georgia Tech can further improve the V-treatment CMS performance.

7.2.3.2 Use of different morphology stabilizers

The main focus in this study has been on VTMS as a starting 'morphology stabilizer' for restricting the micro support collapse. The advantage of sol-gel reaction mechanism and a reactive hydrocarbon group for pre-pyrolysis treatment is necessary for exploring different silane agents. The pore-structure of the resulting 'crosslinked silica scum' can be controlled by the choice of reactive hydrocarbon groups (like vinyl in this

case). To control the extent of sol-gel formation, di-alkoxy functional groups instead of tri-alkoxy groups can also be explored.

7.2.3.3 XPS characterizations on the optimized CMS membranes

XPS with depth profiling can be a useful characterization for obtaining the surface composition and surface bonding of each element on the asymmetric CMS membranes. As studied for the V-treated asymmetric CMS Matrimid® membranes, the silica depth profiling showed the transition of silicon from the outer skin layer into the intrinsic CMS. Deconvolution of XPS-depth profiling peaks could showing the change in the silicon bonding going from outermost surface into the intrinsic CMS skin.

Similar characterizations could be performed to probe the changes in surface compositions of CMS, while performing chemical modifications either prior (or) after pyrolysis. To get a better understanding and advanced optimization of different V-treatment recipes, it can be important to perform the XPS analysis.

7.2.4 Aging stability of V-treated asymmetric CMS membranes

The studies has majorly focused on the fundamental development of V-treatment and trying to translate the intrinsic CMS separation capability to asymmetric CMS hollow fiber membranes. For the industrial scale-up, it is equally important to understand the separation performance behavior as a function of time for CMS membranes stored under different atmosphere conditions.

The transient behavior seen in the intrinsic CMS V-treated Matrimid® for mixed gas CO_2/CH_4 feed requires careful understanding. It may be useful to conduct similar studies with higher condensable gases like ethylene, propylene as a function of time to confirm the 'addition free volume' hypothesis. Fundamental studies for understanding intrinsic CMS structure will have a greater importance as it is expected to influence both the transient and aging behavior.

The aging stability of CMS membranes is an ongoing study at Koros research group, Georgia Tech. The higher impact of aging is observed for the tail-end (bigger-size) gas molecules separation-pair compared to the smaller size molecules. The prediction for re-alignment of carbon sheets as a function of different storage conditions and precursor molecule is important to understand. In the case of V-treated CMS Matrimid® aging, CMS modules stored under CO_2 (5-6 atm pressure) was seen to restrict aging for CO_2/CH_4. The influence of silica (SiO_2) on the outermost CMS skin layer towards aging may also be important to control as the silica membranes are prone with react with moisture. The control studies for reducing excess silica may have an additional importance in terms of aging phenomenon too.

APPENDIX A

GAS COMPRESSIBILITY FACTORS

The compressibility factors (Z) were taken into consideration for to account for the non-ideality of the gases. The calculation is as follows:

$$Z = \frac{pV}{RT} \tag{B.1}$$

where, p is the gas pressure, V is molar volume, T is the absolute temperature, and R is the universal gas constant. The deviation from ideal gas behavior is observed to be higher at higher gas pressures, and that has to be accounted for in the calculations.

The pressure dependent compressibility equations is given in equation B.2

$$Z = 1 + (A)p + (B)p^2 + (C)p^3 + ... \tag{B.2}$$

where, A, B, C are constants and higher order terms negligible.

The compressibility constant values are obtained from National Institute of Standards and Technology (NIST). They are shown in Table A.1 below:

Table A.1: Compressibility factor equations with p, pressure in psi

Gas	Temperature	Compressibility Equation
CO_2	35°C	$Z = 1 - (3.07E-04)p - (5.35E-08)p^2 - (5.03E-11)p^3$
CH_4	35°C	$Z = 1 - (1.06E-04)p + (6.06E-09)p^2 + (3.28E-12)p^3$

APPENDIX B

ELEMENTAL ANALYSIS PROCEDURES

This appendix gives a detailed elemental analysis procedure used by ALS labs, Tuscon, AZ to obtain the elemental composition for both the precursor and CMS samples.

B. 1 Micro CHN analysis (ASTM D5373 / D5291 – *reference code for ALS labs*):

- The instrument used in this method is a Perkin Elmer 2400 Series II CHN Analyzer. With this instrument, samples were combusted at 935°C followed by a secondary combustion through the furnace at 840°C for further oxidation and particulate removal. The gas derived from the combustion was transferred by a carrier gas, homogenized and purged through an IR detector. This detector measured carbon as a CO_2 gas and hydrogen as H_2O. The nitrogen was detected by thermo conductivity in which the NO_2 gas from the resulting combustate was measured as nitrogen. The CHN results were then reported as a weight percent.
- Approximately 2-5 mg of sample was weighed out on a micro-balance, with 0.0001 mg capability. The amount of sample used derives from the sample matrix. The sample was then placed into a pre weighed, combustible tin capsule and dropped into the furnace of the instrument for analysis.
- The instrument was calibrated for the specific matrix of the sample and the capsule used.

B.2 Oxygen analysis (ASTM D5373, modified):

- The instrument used in this method was a LECO TruSpec Oxygen Analyzer. The sample was put into a capsule and weighed out on a micro balance with 0.001 mg capability. The capsule was dropped into the furnace which operates at 1300°C. In a reduction tube, monoatomic oxygen (O) was combined with carbon black in the furnace. All CO_x components were flowed through copper oxide and were converted to CO_2. The resulting gas was analyzed for oxygen by IR detection.
- The instrument was calibrated for the specific matrix of the sample and the capsule used in combustion.
- The amount of sample used in this method was typically 1-10 mg, depending on the matrix of the sample. The results were reported in weight percent of oxygen in the sample.

B.3 Silicon analysis (total dissolution):

- The samples were first digested with acids (HCl, HNO_3, HF) in a microwave, then reacted with boric acid to neutralize HF, and finally brought up to final volume with nanopure water.
- Analysis was done using *inductively coupled plasma-atomic emission spectroscopy* (ICP-OES).

B.4 Halogens by flask/bomb preparation and IC (EPA 5050/9056, ASTM 4809)

- The total halogen concentrations were determined using Schöniger oxygen flask or oxygen bomb techniques [1], where the prepared organic samples were analyzed using ion chromatography (IC). For the flask combustion technique, a sample weighing between approximately 2 to 10 mg was wrapped in a filter paper wick and secured in a platinum basket attached to a flask stopper. The flask was purged using oxygen to create a high

oxygen content atmosphere. The wick was ignited and inserted into the flask along with a Na_2CO_3 scrubber solution.

- For the oxygen bomb (trace analysis) combustion method, the sample weight has to be between 50 and 250 mg. The sample was weighed into a steel combustion capsule and mixed with approximately 500 mg of mineral oil. Appropriate care has to be taken to avoid exceeding 1.0 g of total combustible material as this could damage the bomb. The capsule was loaded into the combustion bomb ignition system and then charged with oxygen before igniting in a bomb calorimeter.
- In both the wick and oxygen bomb analysis the samples were burned, converting the halogens present in the sample into a gaseous state. This gaseous mixture was absorbed by the Na_2CO_3 scrubber solution present in both the flask and bomb, where the halogens were converted into their ionic form. The resultant halogen solution was then diluted to 100 mL and analyzed for halogens, sulfur, and phosphorous (in sulfate and phosphate forms) by IC.

B.5 References:

1. Third Supplement to the Fourth Edition of The International Pharmacopoeia.; http://apps.who.int/phint/en/p/docf/].

APPENDIX C

TECHNIQUES ATTEMPTED TO RESTRICT SUB-STRUCTURE COLLAPSE IN CMS HOLLOW FIBER MEMBRANES

C.1 Use of 'puffing agents' (polyethylene glycol – PEG)

The chemical species referred as "puffing agents", are compounds which can decompose into large volatile by-products upon heating and leave void volume in the carbon after decomposition. One such puffing technique is the use of polyethylene glycol (PEG) [1]. PEG can have an "unzipping effect" upon heating at higher temperatures. Essentially all of the PEG molecules can be seen to unzip at ceiling temperatures of ~350°C. By puffing PEG (Molecular weight 3400) in the pores before pyrolysis, it was attempted to prevent the collapse near the Matrimid® T_g (~305°C). The comparison of both the TGA curves for Matrimid® and PEG (Mol wt: 3400) is shown in Figure C.1(a).

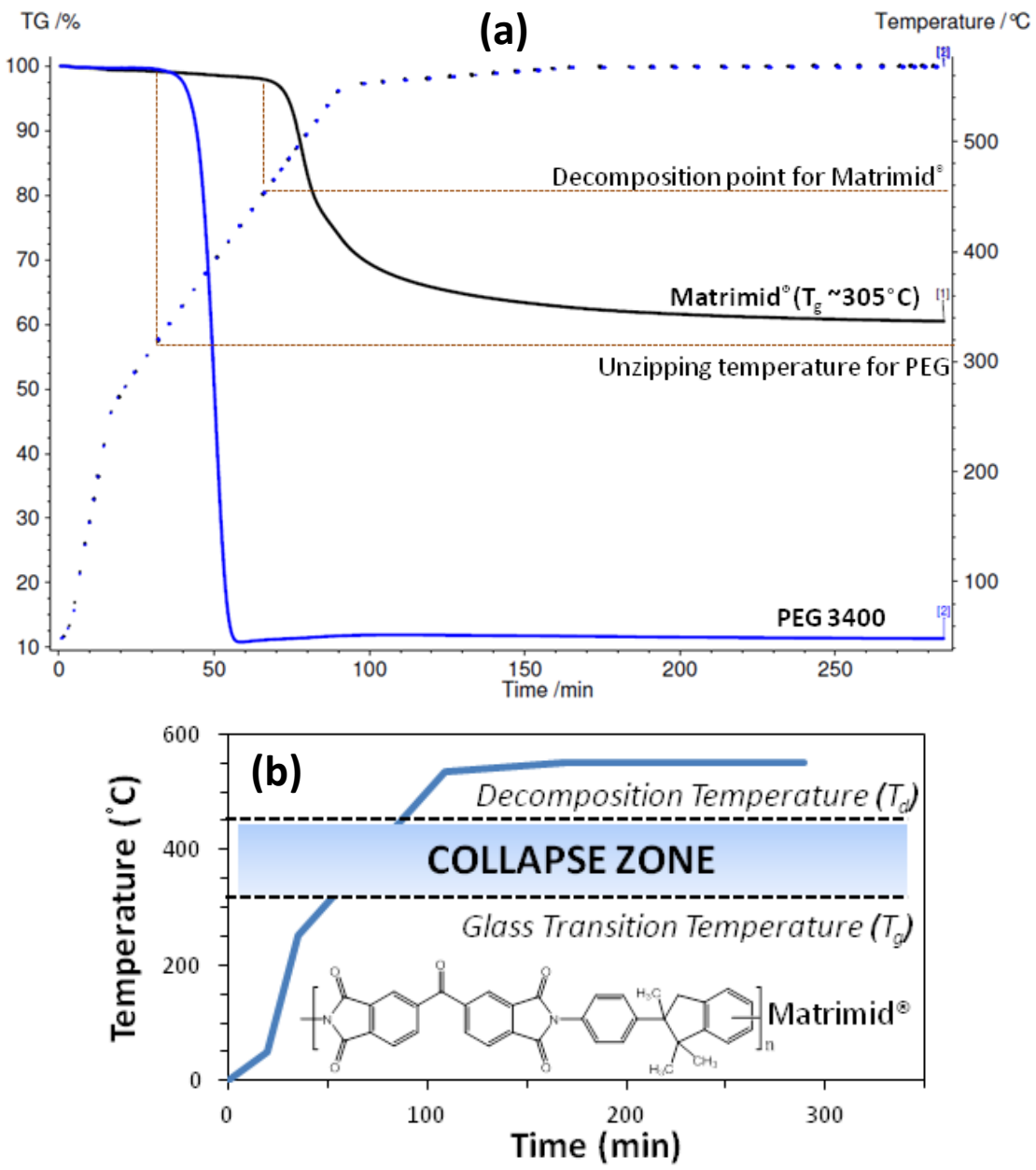

Figure C.1 (a) TGA weight loss plot for Matrimid® precursor and PEG and (b) Illustration of a temperature 'collapse zone' for Matrimid® precursor.

Nevertheless, substructure collapse still occurred even after PEG puffing as shown in Figure C.2. The inability of PEG puffing to stop collapse is because of the wide temperature range between glass transition (T_g ~305°C) and decomposition point (~425°C), referred as 'collapse zone' shown in Figure C.1(b).

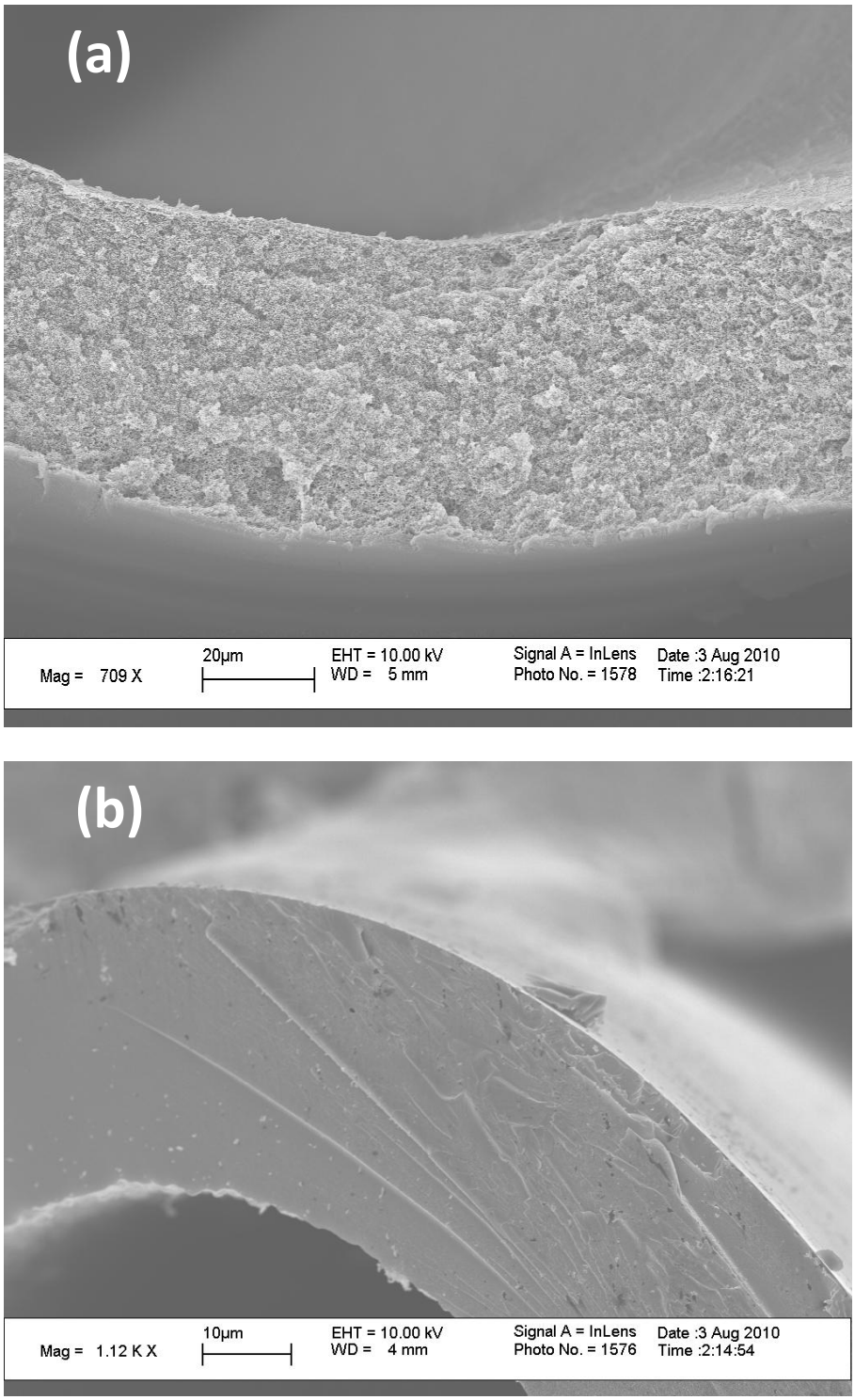

Figure C.2: SEM images of Matrimid hollow fiber wall (a) precursor after soaked in PEG 3400 (20 wt%) and (b) CMS after pyrolysis of PEG-puffed precursor fiber at 550°C

C.2 Thermal stabilization (below T_g)

One of the approaches to pre-stabilize and suppress the polymer chain movements is based on the thermal annealing, where the polymer precursors are treated at temperatures close to T_g for inducing intermolecular charge transfer complexes (CTC) between imide-aromatic rings [2-4]. Though the thermal annealing approach is advantageous for suppressing plasticization behavior, it is observed to reduce the gas permeabilities of Matrimid® dense films [5]. To explore thermal annealing for restricting sub-structure collapse in Matrimid® based asymmetric hollow fibers, precursors were heated to 270°C and stayed for 48 hours under argon and vacuum atmosphere. The thermal annealing temperature was based such that CTC's formation was started [5], but still remained lower than the T_g (~305°C). The morphology of thermally annealed precursor fiber and CMS from thermally annealed fiber is shown in SEM images: Figure C.3(a) and (b) respectively.

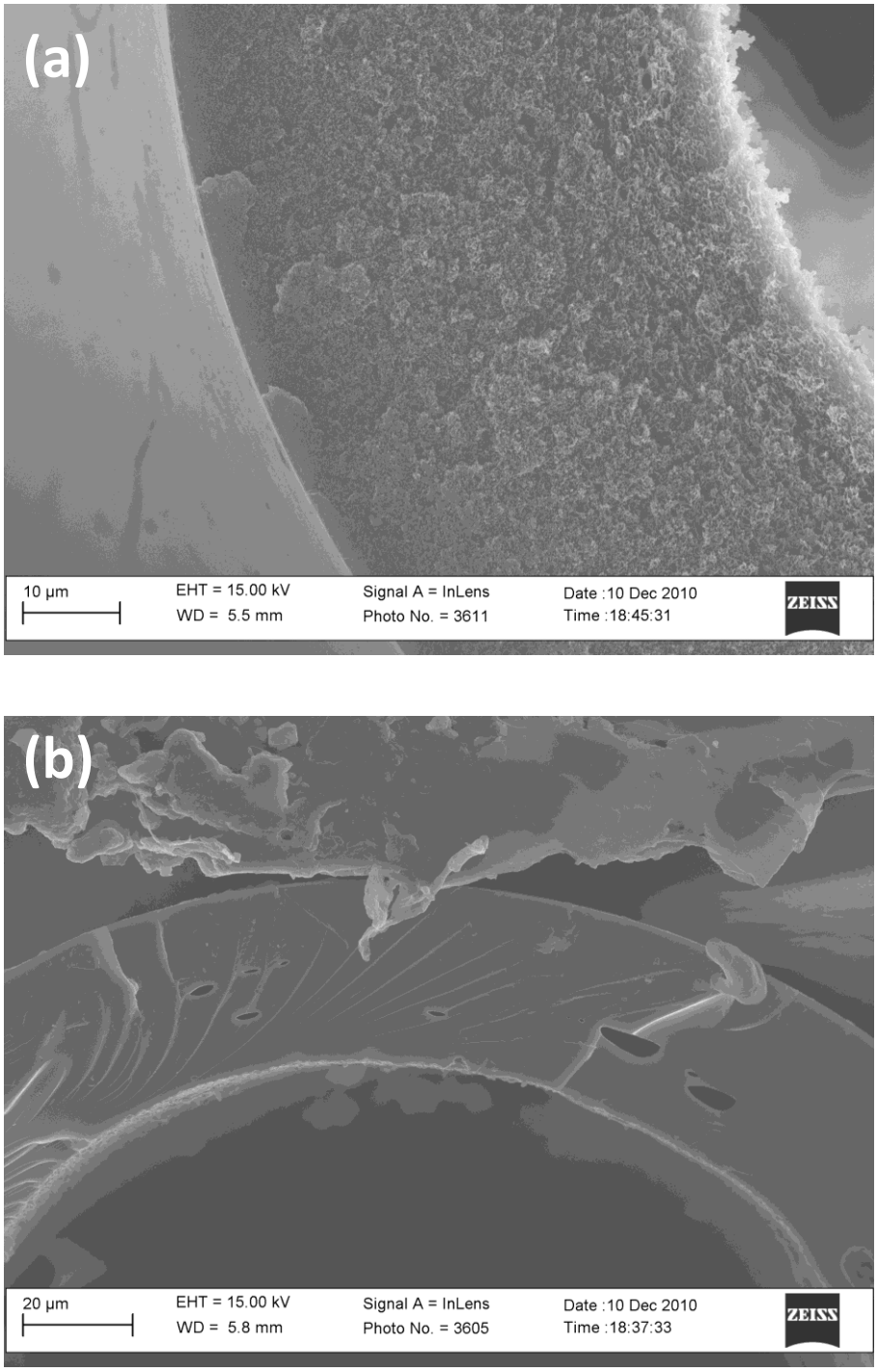

Figure C.3: SEM images of Matrimid® hollow fiber wall (a) precursor after thermal annealing at 270°C-48hrs under argon atmosphere and (b) CMS after pyrolysis of thermal annealed precursor at 550°C.

As seen in the Figure C.3(b) in spite of CTC's formation, thermal annealing is unable to restrict the collapse in asymmetric CMS membranes. The thermal stability of polymer precursor chains reverses back to the original state as temperature crosses the glass-rubber transition point. The results indicate that there is need for stronger stabilization techniques which can restrict the bulk polymer flow throughout the 'collapse zone' of pyrolysis. Hence, chemical crosslinking was attempted.

C.3 Chemical crosslinking using diamine linkers

The common technique for polymer membranes crosslinking are through the reactive functional groups (like alcohol (–OH), acid (-COOH)), existing in the backbone. Due to the absence of reactive groups in Matrimid® precursor, limited room exists to chemically modify the precursor. One approach that has been applied to crosslink polyimides is the use of diamine linkers, where the diamine reacts with imides to open the ring and form an amide bond as shown in Figure C.4 [6, 7].

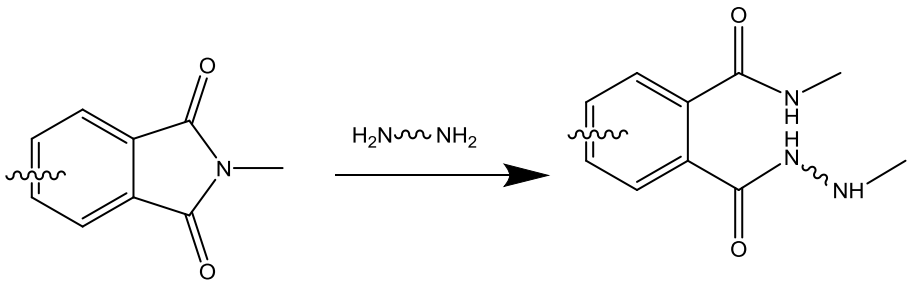

Figure C.4: Reaction mechanism of diamine-imide crosslinking of polyimides

For this study, 10 (w/v)% p-xylenediamine reaction approach [8] was used on asymmetric Matrimid® precursor hollow fiber. The reacting conditions used were similar to the dense film study carried out by Tin *et-al.*[8]. For confirmation of crosslinking,

diamine treated Matrimid® precursor fiber was immersed in hot NMP at 100°C and observed to be insoluble. Inspite of having the cross-linked precursor, the asymmetric CMS showed a collapsed morphology as shown in Figure C.5(b).

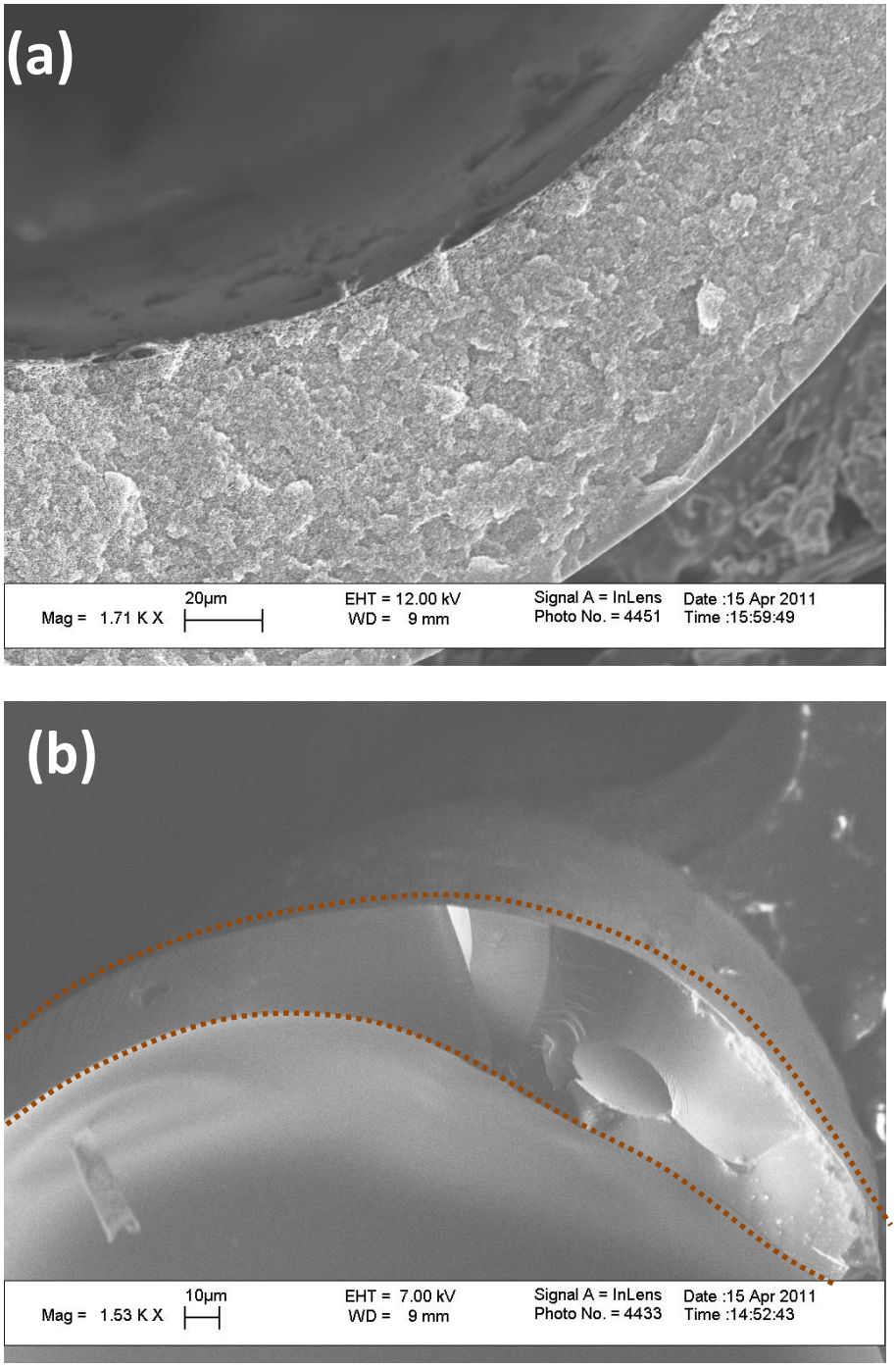

Figure C.5: SEM images of Matrimid® hollow fiber wall (a) precursor after chemical crosslinking using 10 (w/v)% p-xylenediamine and (b) CMS after pyrolysis of diamine-crosslinked precursor at 550°C.

Diamine crosslinking does not work for restricting collapse due to the instability of the peptide (-CONH) bond at higher temperatures [9]. The study by Powell *et-al.*, have

shown reverse reaction mechanism for diamine-crosslinked polyimides as the materials are heated at higher temperatures greater than T_g. The TGA analysis in Figure C.6 of diamine-crosslinked Matrimid® precursor, showed an early decomposition (~400°C) indicating the decrease in thermal stability.

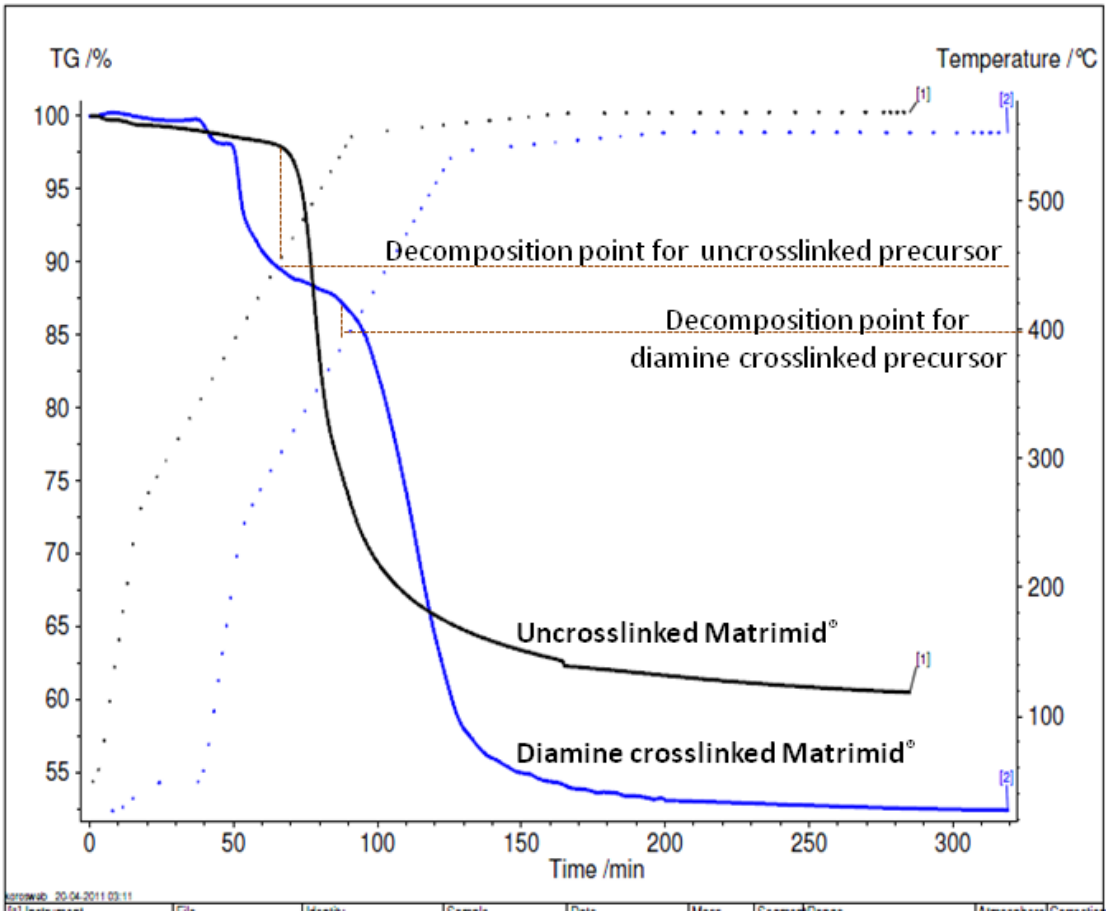

Figure C.6: TGA analysis for uncrosslinked and diamine crosslinked Matrimid® precursor fiber at 550°C.

The early onset at 100°C corresponds to the removal of solvents absorbed during the crosslinking process.

C.4 Hydrogen abstraction crosslinking

Free radical initiated-hydrogen abstraction technique is commonly used in plastics industry for crosslinking polyethylene [10]. The crosslinked polyethylene shows better mechanical and thermal properties compared with the uncrosslinked polymer. The agents used for hydrogen abstraction crosslinking is peroxide (initiator) and vinyltrimethoxy silanes (crosslinking agent), undergoing a two-step crosslinking method [10]:

(i) Grafting: Abstraction of hydrogen using Dicumyl peroxide (DCP) and grafting of vinyltrimethoxy silane (VTMS) on to the polymer backbone.

(ii) Hydrolysis and condensation of methoxy functional groups to crosslink within the silanes, in presence of Tin catalyst.

The overall reaction can be interpreted as shown in Figure C.7:

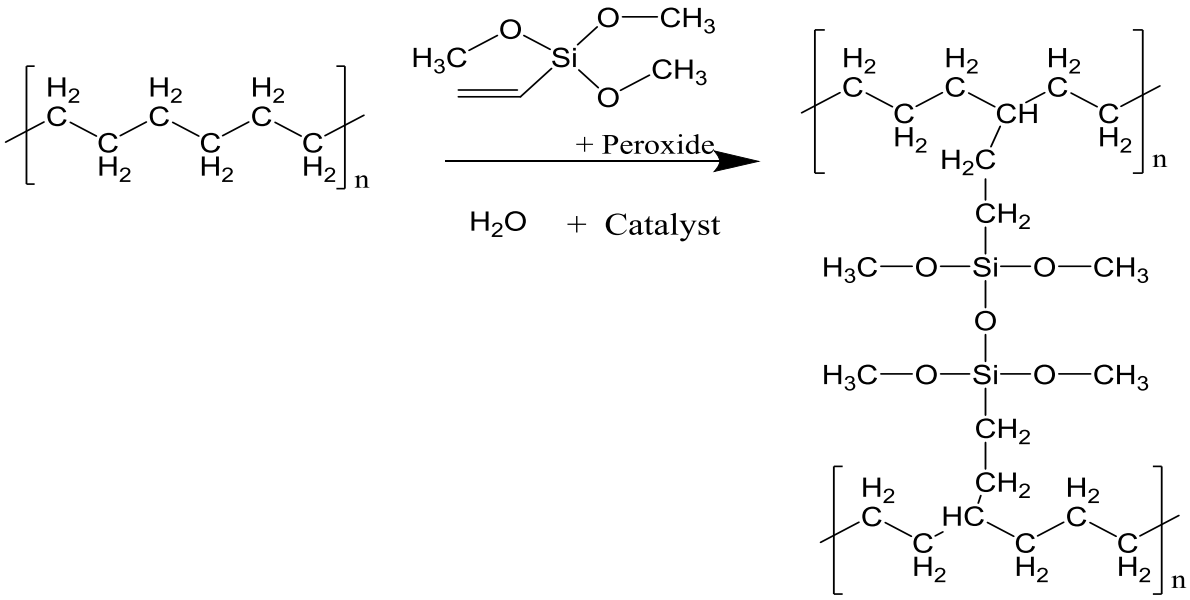

Figure C.7: Mechanism of crosslinking polyethylene using hydrogen abstraction technique.

To apply the hydrogen abstraction technique' for Matrimid® precursor, certain modifications in reaction conditions had to be made. Unlike polyethylene crosslinking

where the polymer is in powder state, in this case the crosslinking had to be done on asymmetric hollow fibers. To uniformly distribute the grafting mixture throughout the hollow fiber, an equimolar mixture (1:1) of grafting compound (dicumyl peroxide-DCP and VTMS) was added to the hollow fibers. The entire components in a closed cell were heated to 170°C, isothermal for 15 mins. After cooling the cell to room temperature, silane treated fibers were immersed in a water & catalyst mixture (99.8% and 0.02% respectively) at 85°C for 8 hours. The catalyst used was Di n-butyltin dilurate (DTBDL). After the grafting reaction step, treated fibers lack the mechanical stability and were brittle for gas transport characterization. Inspite of the transport testing limitations, SEM images of the pyrolysed fibers from silane crosslinked precursor showed an improvement in the asymmetric morphology (Figure C.8).

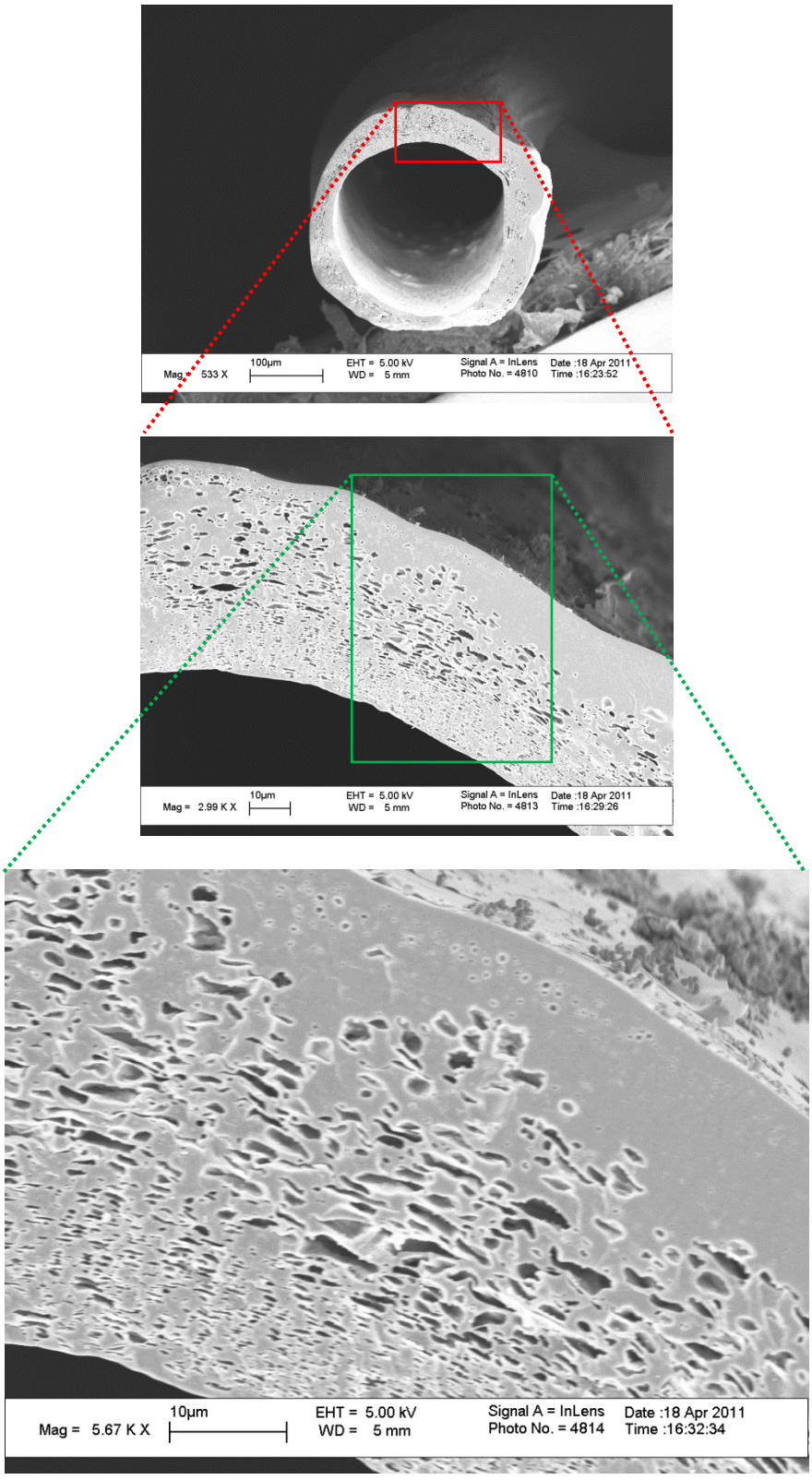

Figure C. 8: SEM images of pyrolysed fiber from silane treated Matrimid® precursor

The extreme peroxide % was found to be undesirable for the mechanical properties of the hollow fiber. Hence, the grafting reaction mixture (i.e. DCP and VTMS) both were reduced by using a non-solvent substituent methanol. For grafting, different compositions of Silane(S):Peroxide(P):Methanol(M) was attempted specifically for maintain the low peroxide & silane concentration. After crosslinking the fibers with new grafting compositions, it had the better mechanical stability to be pyrolysed and tested for separation performance (Figure C.9).

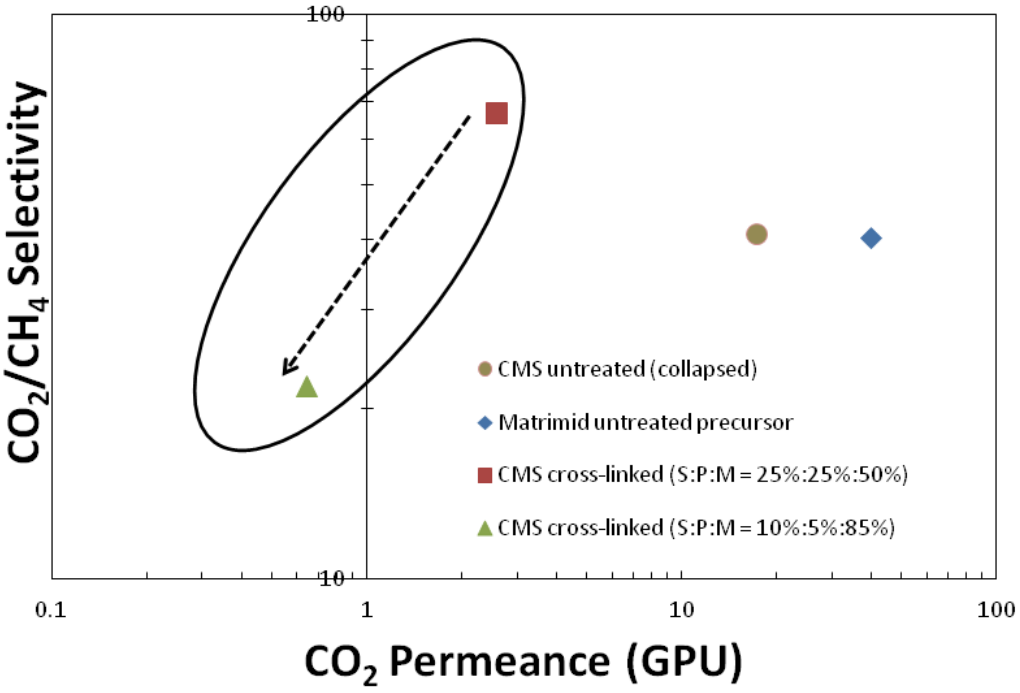

Figure C.9: Comparison of the CMS hollow fiber transport performance from cross-linked (with methanol) and uncross-linked CMS hollow fiber. For all the CMS, pyrolysis was done at 550°C at 100 psi feed pressure, 35 ^{0}C permeation temperature. (**Cross-linked fiber from S:P:M = 10:1:89 was also pyrolysed and tested under same conditions; CO_2 permeance was observed to be low ~ 0.02 GPU, CH_4 permeance was below the leak rate of the testing module* – **not shown in the graph**)

The CMS permeance result in Figure C.9, after addition of methanol in reaction mixture showed even lower fluxes than compared with the untreated CMS hollow fiber

permeance. The observation that the permeance kept on decreasing as we kept increasing the methanol ratio (Figure C.9) indicated that the methanol is unfavorable for the silane crosslinking reaction. Initially, the role of methanol in grafting reaction was anticipated to be of a non-solvent not effecting the reaction (or) precursor morphology. The boiling point of methanol (65^0C) is lower than the reaction temperature of 170^0C. The methanol would vaporize out of the fiber pore, allowing the peroxide-silane mixture to graft onto Matrimid®. SEM images (Figure C.10) of the CMS fibers from methanol *containing* silane-peroxide cross-linked precursors showed a different morphology (closed-foam) when compared to the CMS from *without* methanol silane-peroxide cross-linked precursors (Figure C.8).

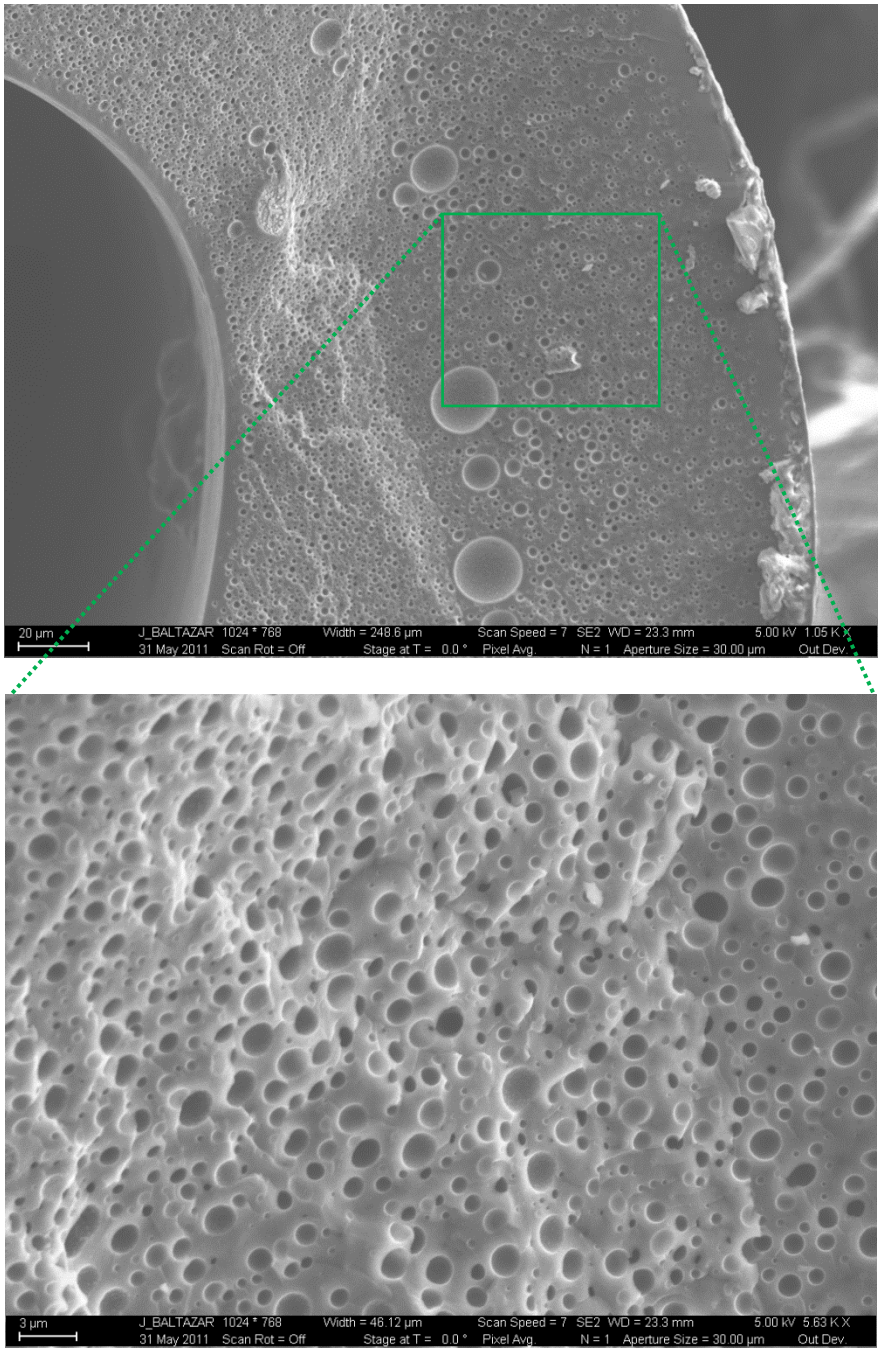

Figure C.10: CMS morphology from the cross-linked precursor *with methanol* in grafting.

The pores in Figure C.10 resembled collapsed bubbles which are not connected to each other i.e., closed cell foam, which could relate to the permeance drop with the increase in methanol concentration.

While exploring the controls for each of the grafting reaction mixture (i.e., silane, peroxide and methanol) separately on the CMS asymmetric morphology, the plain silane (without any peroxide) showed a much better CMS morphology. The plain VTMS treated precursor also exhibited better mechanical stability compared to the VTMS & peroxide combination. This control was crucial for the development of V-treatment process in Chapter 4.

C.5 Tuning of pyrolysis temperature profile

The Figure C. 1(b) illustrated a 'collapse temperature range' for the Matrimid® precursor, which is between the glass transition (T_g) and decomposition point (T_d). By using higher-ramp rates for pyrolysis between the T_g and T_d, it would reduce the time duration for precursor to be in that collapse zone. The use of extreme high ramp-rates was limited by the temperature controller of pyrolysis system and also caused significant stress in polymer precursors at extreme high-ramp rates. For the study, higher ramp-rate of 25°C/min was used at two different final pyrolysis temperatures 550°C and 650°C as shown in the Figure C.11.

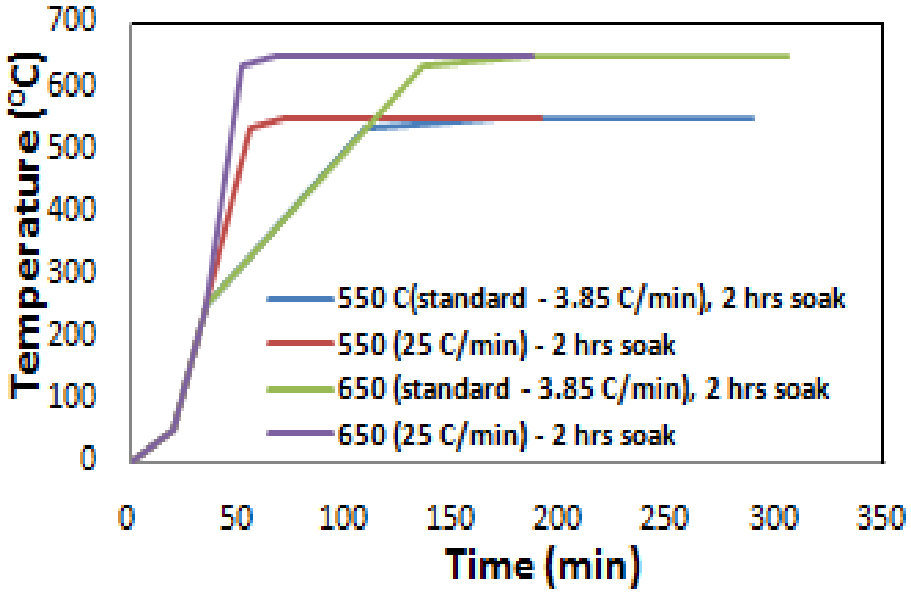

Figure C.11: Temperature profiles for standard and high ramp-rate pyrolysis

Slight improvement in permeance was observed by using higher ramp-rates at both temperatures as shown in Figure C.12. Though it was still not a significant approach, as the substructure collapse would still occur in the high-ramp rate pyrolysed CMS fibers.

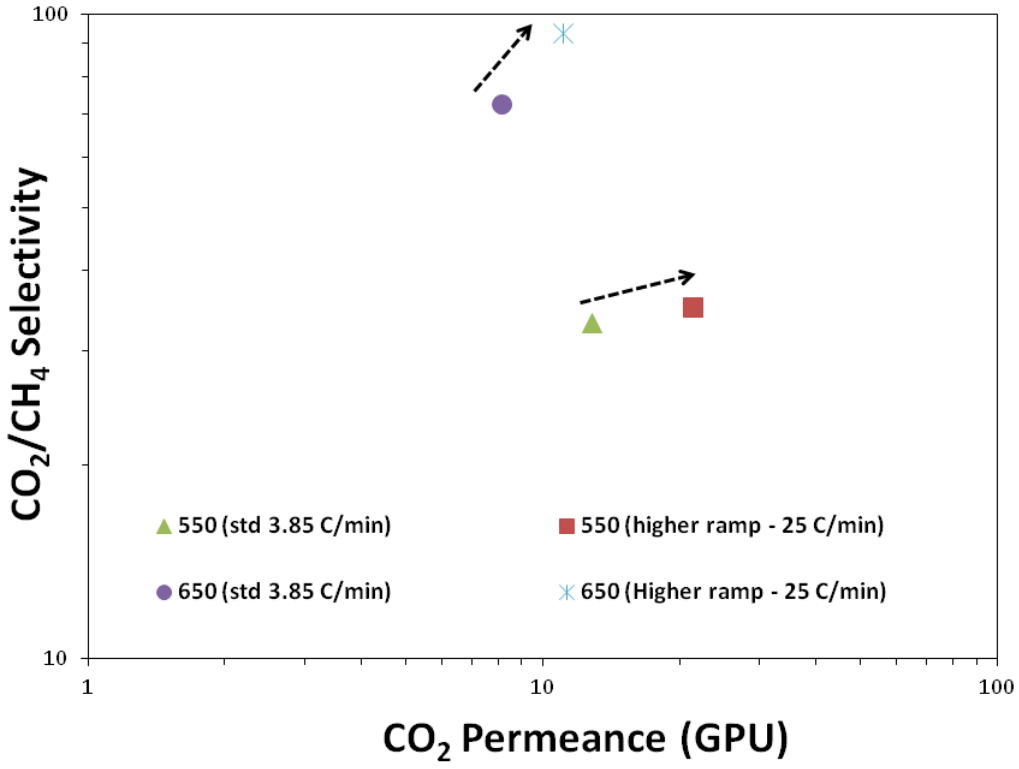

Figure C. 12: Separation performance of CMS hollow fibers from Matrimid® precursor's pyrolysed at higher ramp-rates between (T_g and T_d). Tested for pure gas feed at 100 psi, 35°C.

C.6 References:

1. Lafyatis, D.S., J. Tung, and H.C. Foley, Poly(furfuryl alcohol)-derived carbon molecular sieves: dependence of adsorptive properties on carbonization temperature, time, and poly(ethylene glycol) additives. Industrial & Engineering Chemistry Research, 1991. **30**(5): p. 865-873.
2. Vaughn, J. T.; Koros, W. J.; Johnson, J. R.; Karvan, O., Effect of thermal annealing on a novel polyamide–imide polymer membrane for aggressive acid gas separations. J Membrane Sci **2012,** 401–402 (0), 163-174.
3. Krol, J.J., M. Boerrigter, and G.H. Koops, Polyimide hollow fiber gas separation membranes: preparation and the suppression of plasticization in propane/propylene environments. Journal of Membrane Science, 2001. **184**(2): p. 275-286.
4. Barsema, J. N.; Klijnstra, S. D.; Balster, J. H.; van der Vegt, N. F. A.; Koops, G. H.; Wessling, M., Intermediate polymer to carbon gas separation membranes based on Matrimid PI. J Membrane Sci **2004,** 238 (1–2), 93-102.
5. Zhou, F. and W.J. Koros, Study of thermal annealing on Matrimid® fiber performance in pervaporation of acetic acid and water mixtures. Polymer, 2006. **47**(1): p. 280-288.
6. Zhao, H.-Y.; Cao, Y.-M.; Ding, X.-L.; Zhou, M.-Q.; Yuan, Q., Effects of cross-linkers with different molecular weights in cross-linked Matrimid 5218 and test temperature on gas transport properties. J Membrane Sci **2008,** 323 (1), 176-184.
7. Xiao, Y.; Low, B. T.; Hosseini, S. S.; Chung, T. S.; Paul, D. R., The strategies of molecular architecture and modification of polyimide-based membranes for CO2 removal from natural gas--A review. Progress in Polymer Science **2009,** 34 (6), 561-580.
8. Tin, P. S.; Chung, T.-S.; Kawi, S.; Guiver, M. D., Novel approaches to fabricate carbon molecular sieve membranes based on chemical modified and solvent treated polyimides. Micropor Mesopor Mat **2004,** 73 (3), 151-160.
9. Powell, C. E.; Duthie, X. J.; Kentish, S. E.; Qiao, G. G.; Stevens, G. W., Reversible diamine cross-linking of polyimide membranes. J Membrane Sci **2007,** 291 (1-2), 199-209.
10. Barzin, J., H. Azizi, and J. Morshedian, Preparation of silane-grafted and moisture cross-linked low density polyethylene: Part I: Factors affecting performance of grafting and cross-linking. Polymer-Plastics Technology and Engineering, 2006. **45**(8): p. 979-983.

APPENDIX D

LOWER VTMS CONCENTRATION (10%) V-TREATMENT ON 6FDA:BPDA-DAM PRECURSOR HOLLOW FIBER MEMBRANES

D.1 10% V-treatment on 6FDA:BPDA-DAM precursor

In chapter 4, the potential of V-treatment using the 100% VTMS was evaluated for reducing sub-structure collapse in the 6FDA:BPDA-DAM precursor based CMS hollow fiber membranes. The V-treated 6FDA:BPDA-DAM CMS hollow fiber had showed more than *4x* increase in CO_2 permeance, which was even higher when compared to 100% V-treated Matrimid® CMS hollow fibers (~*3x*) permeance increase. The improvement in gas permeance increase was postulated to be due to the simultaneous etching mechanism of organo-silica during the pyrolysis of 6FDA:BPDA-DAM precursor. Such a hypothetical silica-etching behavior of 6FDA based precursors represents a big advantage for tuning the excess silica during the pyrolysis step. Further characterization analyses would be required in the future, to accurately predict the etching behavior and to quantify the silica-fluorine etched gaseous species evolving during the pyrolysis.

In this appendix, the results for the 10% V-treated 6FDA:BPDA-DAM CMS hollow fiber pyrolysed at 550°C under argon with 30 ppm of oxygen are discussed. The pyrolysis conditions for the permeation studies were chosen based on a CMS dense film study to obtain better separation performance for CO_2/CH_4[1]. The SEM images for untreated, 100% V-treated and 10% V-treated 6FDA:BPDA-DAM CMS hollow fiber are shown in the Figure D.1. Similar reductions in CMS separation skin (~3-*4x*) for both the

100% and 10% V-treated CMS hollow fiber were observed when compared to the untreated CMS fiber, as shown in the SEM images (Figure D.1).

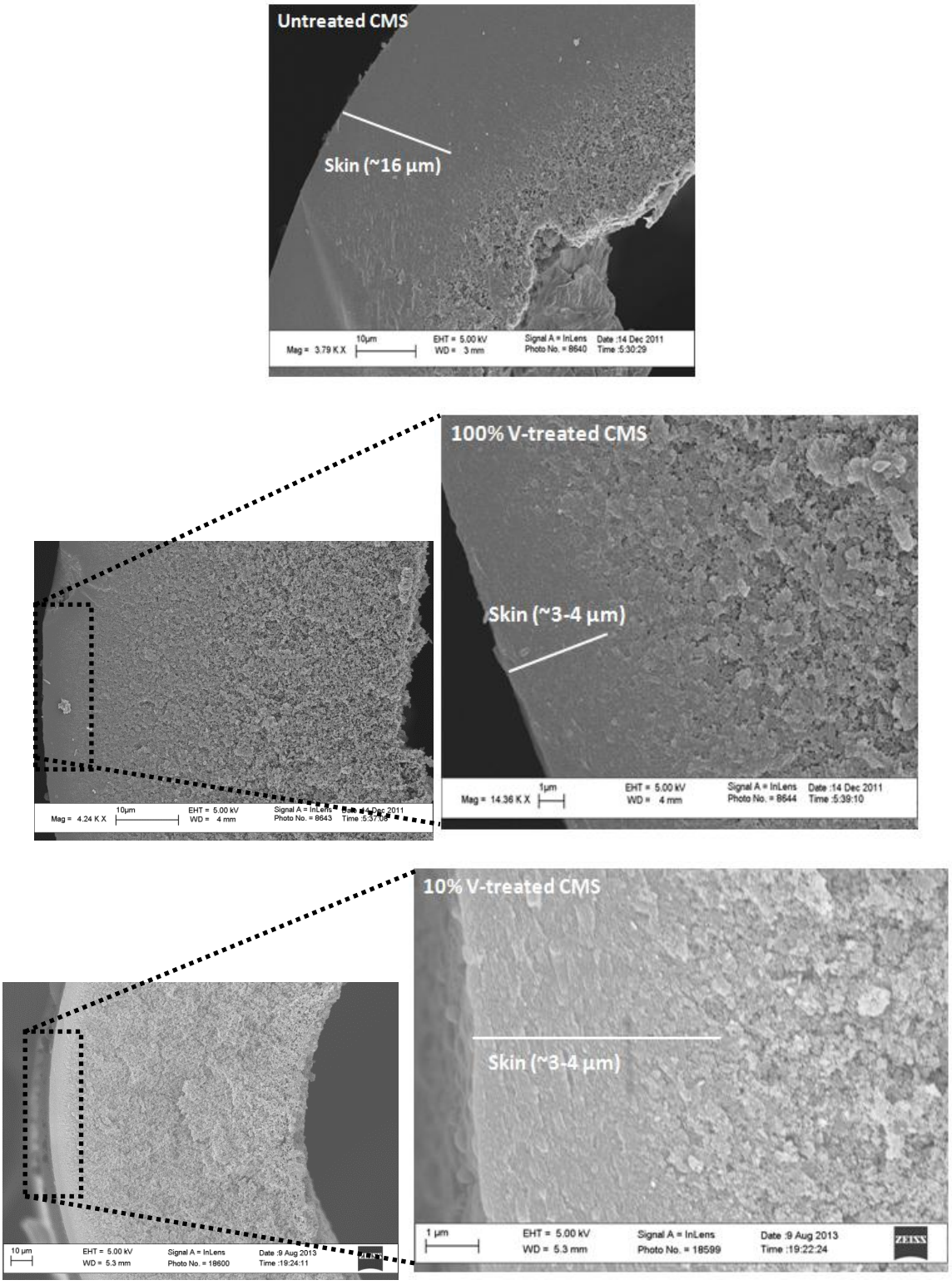

Figure D.1: Comparison of the CMS separation skin thickness for untreated, 100% V-treated, and 10% V-treated CMS hollow fiber membrane from 6FDA:BPDA-DAM precursor pyrolysed at 550°C under argon with 30 ppm of oxygen.

Despite reducing the VTMS concentration from 100% to 10% for V-treatment, V-treated CMS 6FDA:BPDA-DAM hollow fiber showed similar CMS separation skin (Figure D.1) and gas permeance (Table D.1), unlike the situation for the V-treated Matrimid® case (as discussed in Chapter 5).

Table D.1: Separation performance comparison for untreated, 100% V-treated, and 10% V-treated CMS hollow fibers from 6FDA:BPDA-DAM precursor pyrolyzed at 550°C under argon with 30 ppm of oxygen, pure gas feed was used for testing at 100 psi and 35°C.

State	$P(CO_2)$ (GPU)	CO_2/CH_4
Untreated CMS	52	50
100% V-treated CMS	250	52
10% V-treated CMS	266	49

To understand this behavior, elemental analysis[8] was obtained for the untreated and V-treated (10% and 100%) CMS 6FDA:BPDA-DAM, indicated in Table D.2. First, it was evident that a much lower silicon wt% was present in the 100% V-treated 6FDA:BPDA-DAM CMS pyrolysed at 550°C under argon UHP, compared to the 100% V-treated Matrimid® CMS sample pyrolysed at the same conditions. Similarly for the 10% V-treatment case also, V-treated 6FDA:BPDA-DAM CMS sample had lower silicon% vs. 10% V-treated Matrimid® CMS sample.

Another observation from Table D.2 is the decrease in silicon% going from 100% VTMS to 10% VTMS for V-treatment in 6FDA:BPDA-DAM CMS case was *~1.8x*

[8] As discussed in Chapter 3-5, the elemental analysis for CMS represents for the bulk sample obtained after grinding the CMS sample to powder. The accuracy of the technique (using untreated precursors) was obtained to be +/- 1%.

which is lower than the silicon% decrease for the case of V-treated Matrimid® CMS (*~2.9x*). The difference could be due to the fact that when 100% V-treated 6FDA:BPDA-DAM precursor was pyrolysed it already had a reduced silica content when compared with the 100% V-treated CMS Matrimid® sample. As hypothesized earlier the likely reduction in silica for the 6FDA based precursor could be due to the strong silica-etching behavior of CHF_3 and HF gases evolved during pyrolysis [2-5].

Table D.2: Combined elemental analysis for untreated, 100% VTMS and 10% VTMS treated CMS Matrimid® and 6FDA:BPDA-DAM (Pyrolysed at 550°C under argon UHP)

		Carbon	Hydrogen	Nitrogen	Oxygen	Fluorine	Silicon
Matrimid® based CMS							
Untreated	(wt%)	87.4	3.1	4.8	4.8	---	---
	(At%)	66.1	28.1	3.1	2.7	---	---
V-treated (100% VTMS)	(wt%)	76.1	3.2	4.0	5.2	---	11.6
	(At%)	56.2	35.6	2.3	2.4	---	3.6
V-treated (10% VTMS)	(wt%)	85.6	3.4	3.9	3.0	---	4.2
	(At%)	64.2	30.3	2.5	1.7	---	1.3
6FDA:BPDA-DAM based CMS							
Untreated	(wt%)	82.5	3.1	7.4	7.0	---	---
	(At%)	60.6	27.0	4.7	3.9	---	---
V-treated (100% VTMS)	(wt%)	78.9	2.8	6.9	8.8	0.2	2.4
	(At%)	62.4	26.8	4.7	5.2	0.1	0.8
V-treated (10% VTMS)	(wt%)	81.2	3.0	7.0	7.3	0.2	1.3
	(At%)	63.0	27.6	4.6	4.3	0.1	0.4

There is of course, a possibility that the V-treatment optimization value (10% VTMS) for Matrimid® precursor does not hold for the V-treated 6FDA:BPDA-DAM. The 10% VTMS might not be the optimum amount for 6FDA based precursors and possibly an even lower VTMS concentration could be better in terms of separation performance. As the purpose this study has been to develop a fundamental concept for restricting collapse and to demonstrate its potential in achieving superior gas permeances, only Matrimid® precursor has been the focus of V-treatment optimization. Hence, further studies following optimization of V-treatment for 6FDA based precursors can lead to a bigger impact for different industrially relevant challenging gas separations.

D.2 References

1. Kiyono, M., P.J. Williams, and W.J. Koros, Effect of pyrolysis atmosphere on separation performance of carbon molecular sieve membranes. Journal of Membrane Science, 2010. **359**(1-2): p. 2-10.
2. Coburn, J. and H.F. Winters, Plasma etching—A discussion of mechanisms. Journal of vacuum Science and Technology, 1979. **16**(2): p. 391-403.
3. Pan, W.S. and A. Steckl, Reactive ion etching of SiC thin films by mixtures of fluorinated gases and oxygen. Journal of the Electrochemical Society, 1990. **137**(1): p. 212-220.
4. Dhar, S.; Seitz, O.; Halls, M. D.; Choi, S.; Chabal, Y. J.; Feldman, L. C., Chemical properties of oxidized silicon carbide surfaces upon etching in hydrofluoric acid. J Am Chem Soc **2009,** 131 (46), 16808-16813.
5. Williams, P.J., Analysis of factors influencing the performance of CMS membranes for gas separation. Doctor of Philosophy, Georgia Institute of Technology, 2006.